SOME CHEMISTRY OF POLY (FLUOROALUMINIUM - PHTHALOCYANINE), $[Al(Pc)F]_n$

Thesis submitted to the University of Glasgow in fulfilment

of the requirement of the degree of Doctor of Philosophy.

by

ADNAN HADI FZEA

Department of Chemistry

University of Glasgow

May , 1992

ProQuest Number: 11011483

ProQuest 11011483

ProQuest LLC.
789 East Eisenhower Parkway
P.O. Box 1346
Ann Arbor, MI 48106 – 1346

DEDICATION.

I would like to dedicate this work to my parents.

CONTENTS

CHAPTER FOUR - REACTIONS OF POLY(FLUOROALUMINIUM-PHTHALOCYANINE) WITH THE HEXAFLUORIDES OF URANIUM, MOLYBDENUM AND TUNGSTEN AND WITH THE NO$^+$ CATION.

CHAPTER FIVE - REACTIONS OF THIN FILMS OF $[Al(Pc)F]_n$ WITH THE HALOGENS, Cl_2, Br_2 AND I_2, AND WITH THE PENTAFLUORIDES, PF_5, AsF_5 AND IF_5

CHAPTER SIX - TRANSMISSION ELECTRON MICROSCOPY STUDY OF THE $[Al(Pc)F]_n$ POLYMER REACTED WITH MoF_6, WF_6, Br_2, I_2 and CF_3COOH

Acknowledgements.

I would like to express my sincere thanks to my supervisors, Dr. J.M. Winfield and Dr. J.R. Fryer for all their help, guidance and encouragement throughout this work.

Many thanks are due to my colleagues in the department, Dr. J. Thomson, Mr. L.McGhee and Mr. P. Stevenson for their help, discussions and assistance during the course of this work.

I would also like to thank Mr. S. Abdulrassak and Mr. R. Munro for their help with the diagrams, Mr. G. McCulloch for the infrared service, Mr. W. McCormack for the glass blowing assistance, Mr. J. McIver for the n.m.r. service and Mr. D. Thom for help with the electron microscopy.

Thanks to Mrs. L. Hughes for her efficient typing of this thesis.

My very special thanks go to every member in my family for their continual support and encouragement and all my friends for their good company.

Finally, I would like to acknowledge the scholarship awarded to me by the Ministry of Higher Education, Republic of Iraq.

- i -

SUMMARY

This thesis describes a study of partial oxidation or protonation of the compound poly(fluoroaluminium-phthalo-cyanine), $[Al(Pc)F]_n$, by different types of oxidising agents and strong protonic acids.   Oxidation reactions were carried out in the presence of acetonitrile, in the absence of a solvent and by exposing thin films of the $[Al(Pc)F]_n$ polymer deposited on KCl and silica substrates, to the vapours of the oxidants.

Chapter one summarises previous studies made of the hexafluorides, UF_6, MoF_6, WF_6 or $NOPF_6$, the halogens, Cl_2, Br_2 or I_2 and the pentafluorides, PF_5, AsF_5 or IF_5 which were all used in the present work.   It is concerned with the preparations, structures and redox chemical behaviour under different conditions and in different solvents.   Previously reported studies involving several metal-phthalocyanine complexes and analogous organic compounds are also described in this chapter.

Chapter two describes the methods used to prepare and purify the reagents used in the reactions and the main experimental techniques, vibrational and electronic spectroscopy and transmission electron microscopy, which were used in the investigation of reaction products.

In chapter three, investigations of the solubility of the $[Al(Pc)F]_n$ polymer in several organic solvents and its interactions with the strong protonic acids CF_3SO_3H, H_2SO_4 and CF_3COOH are reported.   On the basis of the observations made, it has been concluded that the $[Al(Pc)F]_n$ polymer

behaves as a base and dissolves in the strong protonic acids through the protonation of the outer nitrogen atoms of its phthalocyanine (Pc) rings. However, the degree of protonation and, hence, the solubility of this polymer depends on the strength of the acid used as determined by its Hammett acidity value (Ho). In some cases evidence for depolymerization of $[Al(Pc)F]_n$ was obtained from the electronic spectra of the products formed, indicating that protonation and depolymerization are related.

In chapter four, the reactions between $[Al(Pc)F]_n$ and binary hexafluorides MF_6 (where M = U, Mo and W) or the NO^+ cation in the presence of MeCN, in the absence of a solvent, or by using thin films of the polymer on silica and KCl substrates are described and discussed. The products isolated from these reactions were characterised by infrared and u.v./visible spectroscopy and in some cases by transmission electron microscopy. In all cases the products had different colours and different vibrational and electronic spectra than those of $[Al(Pc)F]_n$. Unlike pristine $[Al(Pc)F]_n$, the oxidised products were very soluble in acetonitrile. The anions MF_6^- (M = U, Mo and W) and PF_6^- were identified by vibrational spectroscopy.

In chapter five the reactions between thin films of $[Al(Pc)F]_n$ deposited on silica substrates and non-metal pentafluorides or halogen vapours, AF_5 (where A = P, As or I) and X_2 (where X = Cl, Br or I) are described and discussed. The films after the reactions were examined by electronic spectroscopy; several spectral changes involving phthalocyanine electronic transitions in the region 1000-200 nm were observed.

Chapter six deals with a study of the lattice structure of the epitaxial thin films of $[Al(Pc)F]_n$ on KCl substrates using transmission electron microscopy. A comparison is made between the present study and previous work reported in the literature. Results from the examination of selected samples from the reactions described in chapters 3-5 indicated that in all cases the oxidation or protonation of $[Al(Pc)F]_n$ introduced distortion into the structure of the polymer. It appeared likely that the polymeric chains were broken during the reactions.

In chapter seven, comparisons among the spectroscopic results obtained from the reactions described in chapters 3-6 are made. The conclusions from all the reactions carried out in the present study and future work were also described in this chapter.

CHAPTER ONE

INTRODUCTION

1.1 Aims of the present work.

Conjugated polymers can become viable electronic conductors only in the presence of certain additives, which remove or add electrons from the polymer system. The quantities of additives should be in chemical proportion to the monomer units which are oxidised or reduced. It has been found that the conductivity of the oxo- or halo-bridging metal-phthalocyanine polymers can be increased when they are partially oxidised by oxidants such as the NO^+ cation or diiodine. When the doping is successful, a charge transfer occurs between the polymer and the dopant causing an increase in the number of delocalised charges on the polymer chains and therefore an increase in the electronic conductivity of the polymer.

In this work, the compound poly[μ-fluoro(phthalo-cyaninato)aluminium(III)], $[Al(Pc)F]_n$ which can be also named poly(fluoroaluminium-phthalocyanine) has been studied. It can be prepared using the method described in the literature [1]. The information reported about its structure, physical and chemical properties and particularly its behaviour as a semiconductor make the compound an attractive candidate for oxidative doping. The NO^+ cation [2] and diiodine [3] have been used most often, but the use of binary high oxidation state fluorides has also been briefly reported [4]. The ready availability, intense colour and apparent thermal and hydrolytic stability of this polymer, enable its reactions with oxidising agents to be carried out both in solution and in the solid state. From earlier work using transmission and scanning electron microscopy [5], it has been shown that

epitaxial thin films of the polymer can be grown on KCl single crystal substrates. It has also been shown that the polymer chains lie vertically on the KCl substrate, while on the mica substrate they lie horizontally. In the present work this approach has been extended to prepare thin films of the polymer on substrates such as silica, $LiNbO_3$ and mica, and in selected cases to expose the films to the vapour of volatile oxidising agents. It is also possible to protonate the $[Al(Pc)F]_n$ polymer using strong protonic acids such as H_2SO_4, CF_3SO_3H, FSO_3H and CF_3COOH, and these reactions have been studied. In all cases the reactions have been investigated by vibrational and electronic spectroscopy or by transmission electron microscopy.

The remainder of this chapter deals with some of the properties of the elements and compounds, for example, the halogens and high oxidation state fluorides that were used in this work and some of the concepts that underlie the work. The chapter concludes with an account of polymeric conducting materials and metal–phthalocyanines.

1:2 <u>The Halogens</u> :

The members of the halogen family of elements are fluorine, chlorine, bromine, iodine and astatine. They occupy group 17 of the Periodic Table and are characterized by their high electronegativities. Since the halogen atoms are only one electron short of the noble gas configuration, the elements readily form the anion X^- or a single covalent bond. The molecules of all the halogens are diatomic at room temperature and thus differ from the elements of groups 15 and 16 in which the first elements, nitrogen and oxygen alone are diatomic under these conditions. The chemistry of the halogens is non-metallic and in general, the properties of the elements and their compounds change progressively with increasing size. Table 1:1 shows the more common physical properties of the halogens. It can be seen that most of their properties change regularly when the elements are arranged in the order of their atomic numbers.

Their ionisation energies are generally high, but fall markedly when the atomic number increases. The electron affinities show a maximum at chlorine and then decreases as the atomic number increases, in accord with the increasing number of inner orbitals and the size of the atoms. The small size and high electronegativity of the F atom account for many of the differences between fluorine and other halogens.

Table(1:1).Some physical properties of the halogens[6-9].

Properties	Fluorine (F_2)	Chlorine (Cl_2)	Bromine (Br_2)	Iodine (I_2)	Astatine (At)
Atomic number	9	17	35	53	85
Melting point, K	40	170	265.8	386	----
Boiling point, K	155	238.4	331.7	457	----
Electron affinity of X atom, kJ mol^{-1}	-340	-356	-342	-303	-298
Ionisation energy of X atom, kJ mol^{-1}	1514.7	1107.5	1016.8	895.3	----
Electronegativity	4.1	2.85	2.75	2.2	1.95
Ionic radius X$^-$, Å	1.19	1.70	1.87	2.12	0.62
Colour of vapour	Pale-Yellow	Greenish-Yellow	Reddish-Brown	Violet	----
Energy of dissociation of X$_2$, kJ mol^{-1}	155	243	193	151	⁻116

The last member of the halogen group is astatine, which exists only as very short-lived radioactive isotopes. The longest lived of the 21 isotopes of astatine which have been defined are ^{210}At ($t_{1/2}$ = 8.3 h) and ^{211}At ($t_{1/2}$ = 7.21 h) [6]. Work has been carried out using either ^{210}At or ^{211}At, and the very high activity necessitates working in 10^{-14} mol dm^{-3} solutions, and following reactions by coprecipitation with iodine compounds [6].

1:2:1   Occurrence.

Because of their high reactivity, none of the halogens occur in the elemental state in nature.   Fluorine occurs widely in nature as fluorspar (CaF_2), Cryolite (Na_3AlF_6), and fluorapatite [$3Ca_3(PO_4)_2Ca(F\ Cl)_2$] [7].   Fluorine in the combined state constitutes 0.078% of the earth's crust and is more abundant than chlorine (0.055%) [8].   Most natural water contains traces of fluorides and in some cases the amounts are comparatively large.   The element was first isolated in 1886 by Moissan, who pioneered the chemistry of fluorine and its compounds [9].

Chlorine occurs in nature mainly as sodium chloride in seawater and in various inland salt lakes.   Isolated bodies of water in arid regions are frequently found to be high in chlorine content.   Industrially unimportant with regard to chlorine content or as a source of chlorine, are the ores of certain heavy metals which occur as chlorides, for example $AgCl$, $CuCl$, and $PbCl_2$.   Chlorine was first prepared by Scheele [10] in 1774 from the reaction between hydrogen chloride and manganese dioxide.

Bromine is found in brines, bitterns, seawater and saline deposits as bromides derived originally from the dissolution of alkali, alkaline earth and magnesium salts. The bromide content is much smaller than the chloride content in all of these sources.   Average seawater contains about 0.015% bromine [11].   The discovery of bromine was made by Balard in 1824 [12].   He obtained it from the mother liquor of the Montpellier bitterns, which are high in magnesium bromide.

Iodine occurs naturally in oil-well brines and in some types of marine life, such as oysters, seaweeds and certain fishes. The greatest concentration of iodine in the human body is found in the thyroid gland. The element was first isolated in 1812 by the French chemist Courtois [13]. After seaweed had been ashed and the soda removed, Courtois discovered that sulphuric acid reacted with the hot mother liquor to liberate the new element in the form of its violet vapour.

The discovery of astatine in nature was claimed by many chemists, for example Allison in 1931 [6] and Carson in 1940 [13]. Later information [6] about the short half-life of all the isotopes of this radioactive element make doubtful any claims that this element might exist in nature. In spite of the studies which were carried out on the isotopes of astatine using tracer methods, the chemistry of this element and its properties are not well known compared to the other members of the halogen family.

1:2:2   Preparation.

Although free fluorine was first isolated by Moissan as a product of the electrolysis of anhydrous liquid hydrogen fluoride containing some potassium hydrogen fluoride (KHF_2), significant improvements have been made in the development of cells, electrodes, and electrolytes [9]. Developments in the small-scale preparation of the element which followed led to large-scale operations and the production of fluorine in commercial quantities [14]. Because of the volatility of

hydrogen fluoride, it is difficult to avoid the contamination of the product. This problem is reduced materially by the use of fused potassium hydrogen fluorides over which the vapour pressure of hydrogen fluoride is comparatively low [15]. As a consequence, only operations at medium and high temperatures have proved to be effective. Corrosion problems are reduced by use of metals such as nickel, copper or Monel, which are covered with protective fluoride coatings, graphite and unreactive plastics such as Teflon [$(CF_2)_n$ polymer]. Preparation of fluorine by purely chemical means is not particularly successful because of the difficulty of oxidising the fluoride ion. Numerous claims have been advanced for the liberation of fluorine as a result of thermal decomposition of high-valence metal fluorides for example Pb(IV), Ag(II) and Mn(III) [10]. Compounds such as AgF_2, MnF_3, PbF_4 and CeF_4 are effective fluorinating agents, and they may release fluorine under appropriate conditions. Many other claims have been made that fluorine can be formed from the thermal decomposition of fluorides of the other halogens (the interhalogens). For example, fluorine may be prepared from chlorine trifluoride, since this dissociates completely into fluorine and chlorine monofluoride at a temperature of about 973 K [15] (equation 1-1)

$$ClF_3 \rightleftharpoons ClF + F_2 \qquad \dots\dots\dots\dots (1-1)$$
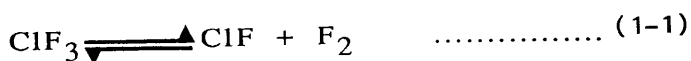
Chlorine monofluoride (b.p. 169.2K), and any undissociated chlorine trifluoride (b.p. 285 K), can be separated from fluorine (b.p. 85 K) by cooling the mixture gases in liquid oxygen (b.p. 90 K). All the above mentioned fluorinating agents which have been used in the preparation of fluorine are usually prepared by reactions involving elemental

fluorine so that their utilities as inexpensive sources would be limited. The first purely chemical generation of elemental fluorine in significant yield and concentration has been reported by Christe [16]. In this method, fluorine has been formed by a simple displacement reaction between starting materials that can be prepared in high yields without the use of elemental fluorine as in the following equations (equations 1-2, 1-3 and 1-4).

$$2KMnO_4 + 2KF + 10HF + 3H_2O_2 \xrightarrow{50\% HF(aq)}$$
$$2K_2MnF_6 + 8H_2O + 3O_2 \ldots (1-2)$$
$$SbCl_5 + 5HF \longrightarrow SbF_5 + 5HCl \ldots (1-3)$$
$$K_2MnF_6 + 2SbF_5 \longrightarrow 2KSbF_6 + MnF_3 + \frac{1}{2}F_2 \ldots (1-4)$$
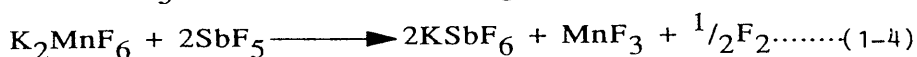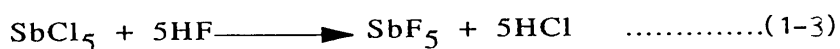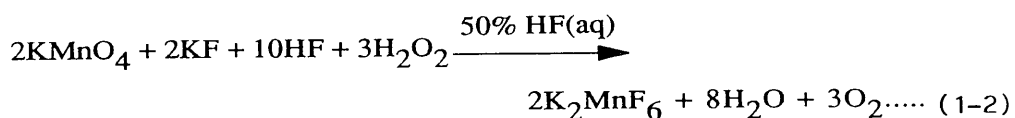
On a laboratory scale, chlorine is normally prepared by the chemical oxidation of chloride ion employing hydrochloric acid or a metal chloride and sulphuric acid with a suitable oxidant such as manganese(IV)oxide. The direct oxidation of HCl by concentrated nitric acid results in the formation of chlorine and nitrosyl chloride (equation 1-5)[17].

$$3HCl + HNO_3 \longrightarrow Cl_2 + NOCl + 2H_2O \ldots (1-5)$$
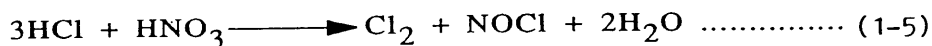
The HCl and HNO_3 may be generated by the addition of concentrated sulphuric acid to an alkali or alkaline earth chloride and nitrate. The addition of nitric acid to a mixture of MnO_2 and HCl increases the efficiency of chlorine production (equation 1-6)

$$MnO_2 + 2HNO_3 + 2HCl \longrightarrow Mn(NO_3)_2 + 2H_2O + Cl_2 \ldots (1-6)$$
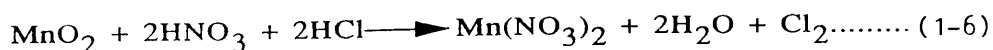
All methods of bromine production depend on the oxidation of the bromide ion. There are no naturally occurring oxygen salts of bromine which act as a source of

the element. Bromine can be formed by the oxidation of bromide ion by manganese dioxide in the presence of sulphuric acid (equation 1-7) [12].

$$MnO_2 + 4H^+ + 2Br^- \longrightarrow Br_2 + Mn^{2+} + 2H_2O \quad \dots \dots \dots \quad (1-7)$$
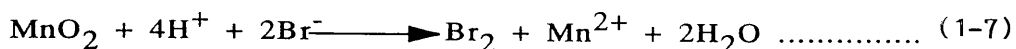
Concentrated sulphuric acid, however is a sufficiently good oxidising agent itself to oxidise the bromide ion to bromine. For this reason the usual displacement of the more volatile hydrohalide from its salt by sulphuric acid cannot be used for the preparation of anhydrous hydrogen bromide (equation 1-8)

$$2H^+ + H_2SO_4 + 2Br^- \longrightarrow Br_2 + SO_2 + 2H_2O \quad \dots \dots \dots \quad (1-8)$$
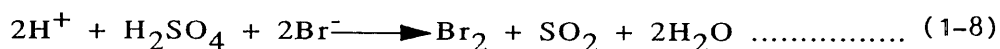
Bromine and iodine are normally prepared on a laboratory scale by methods comparable with those used for chlorine as well as by oxidation of the halide ion with chlorine. Oxidation of halide ions is used commercially for the production of both halogens. Bromine is recovered technically from seawater [13] by chlorination at pH 3.5 and removal with air. The bromine is then stripped from the air by absorption in sodium carbonate to give bromide and bromate. Acidification then yields bromine which can be purified by distillation.

Iodine is liberated from iodides in salt well brines by oxidation with nitrite and is removed by adsorption on charcoal. Iodine is also displaced from solutions of iodides by chlorine. This process is essentially the same as that employed for the preparation of bromine. The quantity of chlorine used is critical since, if insufficient chlorine is used, there is not only a loss of available chlorine but some of the iodine dissolves in the brine

through the reaction, (equation 1-9)

$$I_2 + I^- \longrightarrow I_3^- \quad \dots \dots \dots \dots \quad (1\text{-}9)$$
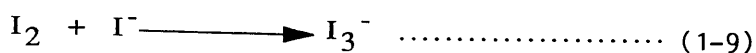
If too much chlorine is used, iodine is lost through the reaction, (equation 1-10)

$$I_2 + Cl_2 \longrightarrow 2ICl \quad \dots \dots \dots \dots \quad (1\text{-}10)$$
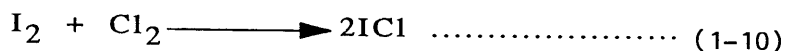
or through the formation of IO_3^- [13].

1:2:3 <u>Reactivity and Chemical Properties of the Halogens.</u>

Chemical reactivity of the halogen elements decreases from fluorine to iodine. Fluorine has the greatest electronegativity of any of the elements and therefore it is considered to be a good oxidising agent. It forms compounds with all elements except helium, neon and argon; and it will usually replace chlorine from its compounds [18].

Chlorine and bromine also combine directly, though less vigorously with most elements, while iodine is less reactive and does not react with some elements such as sulphur [19].

The great reactivity of fluorine is in part attributable to the low dissociation energy (155 kJ mol^{-1}) of the F-F bond, and the fact that reactions of atomic fluorine are strongly exothermic [18]. The weakness of the bond in F_2 is generally due to the repulsion between the pairs of unshared electrons on each F atom, while the X-X bond in Cl_2, Br_2 and I_2 is stronger possibly because of the hybridisation of p and d orbitals in these molecules. In spite of their lower dissociation energies (see Table 1:1) bromine and iodine are weaker oxidising agents than chlorine; this is due to

their smaller electron affinities and smaller hydration energies. Fluorine, particularly, and chlorine to a lesser extent, often oxidise both metals and non-metals to higher oxidation states than do bromine and iodine. Thus both fluorine and chlorine oxidise phosphorus and arsenic to the +5 oxidation state compounds such as PCl_5 and AsF_5 [19]. Sulphur can be converted to SF_6 by fluorine, to SCl_4 by chlorine and to S_2Br_2 by bromine [19].

Many reactions of elementary fluorine with most other elements are exothermic because of the formation of a short and strong bonds between its atoms and those elements. When ionic crystalline fluorides are formed their lattice energies are high because the F^- ion is comparatively small.

Halogens with a formally positive oxidation state occur in complexes in which the coordination numbers range from 2 to 7 and the other element present is either oxygen, or another halogen which is more electronegative than the first. These complexes are usually ions, but in some cases, for example I_2O_5 or Cl_2O_7, they are neutral molecules. In complexes with oxygen, the halogen atom is surrounded by oxygen atoms; in interhalogen compounds the larger halogen is surrounded by the smaller halogen atoms. The number of bond pairs around the central atom can be increased by either the use of some of its electrons to form π bonds with surrounding atoms or by the promotion of some of its electrons to nd levels followed by the formation of δ bonds with the surrounding atoms. All the molecules and ions employing four electron pairs are basically tetrahedral, those employing five pairs are trigonal bipyramidal and those with six pairs are octahedral.

When a halogen atom forms a bond to another atom or group more electronegative than itself, the bond will be polar with a partial positive charge on the halogen [7]. Examples are the Cl atoms in SF_5OCl, CF_3OCl and FSO_2OCl, the Br atoms in O_3ClOBr and FSO_2OBr, and the iodine atom in $I(ONO_2)_3$.

1:3 The Interhalogens.

The differences in electronegativity among members of the halogen family make possible the combination of one halogen with another to form an interesting series of compounds known as the interhalogens. In these compounds the halogens combine exothermally with one another and the product depends on the combination conditions. For instance equi-molar quantities of F_2 and Cl_2 react to give the ClF compound, while if excess quantity of F_2 is used in this reaction, the product is ClF_3 compound [18] (equations 1–11 1–12).

$$F_2 + Cl_2 \xrightarrow{470K} 2ClF \quad \cdots\cdots\cdots\cdots\cdots (1-11)$$

$$3F_2 + Cl_2 \xrightarrow{550K} 2ClF_3 \quad \cdots\cdots\cdots\cdots (1-12)$$
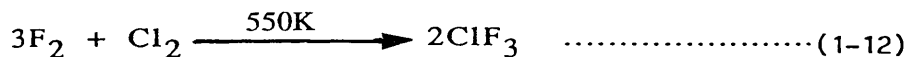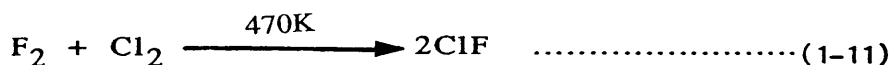
Bromine vapour diluted with nitrogen reacts with a limited quantity of fluorine to give mainly BrF_3. If an excess of F_2 was used, the main product will be BrF_5. Except for BrCl, ICl, ICl_3 and IBr, the interhalogens compounds are all halogen fluorides. Chemically, the interhalogens are all rather reactive. They are even more reactive than the elements (except F_2) because the bond energy of two different

halogens (A-X) is less than the bond energy of two similar halogens (X-X), (X being the more electronegative element involved) [7]. For example, BrCl (D of Br-Cl = 218 kJ mol^{-1}) is more reactive than Cl_2 (D of Cl-Cl = 243 kJ mol^{-1}). Iodine trichloride, ICl_3, is formed by treatment of liquid chlorine with the stoichiometric quantity of iodine, or with a deficiency of iodine followed by evaporation of the excess of chlorine [20]. Of the AX_3 compounds, ClF_3 is the most reactive, but BrF_3 is more useful in preparative work and it is a valuable fluorinating agent. It converts many metals, metal oxides and many metal chlorides, bromides and iodides to fluorides [20]. Bromine pentafluoride is the most reactive among the AX_5 compounds, and it is too violent to be used undiluted for the preparation of fluorides. Liquid IF_5, on the other hand, is a good conductor (equation 1-13)

$$2IF_5 \rightleftharpoons IF_4^+ + IF_6^- \quad \dots\dots\dots\dots\dots\dots (1-13)$$
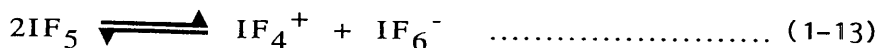
and it reacts with KI at its boiling point to give KIF_6 [21]. The only example of AX_7 type is iodine heptafluoride, which can be made by heating IF_5 with F_2 at 520-540 K.

A characteristic property of most halogen fluorides is their amphoteric character, that is, with strong bases, such as alkali metal fluorides they can form anions, and with strong Lewis acids such as SbF_5 they can form cations [22].

1:4 High Oxidation State Binary Fluorides.

High oxidation binary fluorides find a great use as oxidising agents in non-aqueous media for metals and non-metals to generate solvated cations.   The main advantage in their use is that they can be obtained and used in rigorously anhydrous conditions.   The chemistry of the high oxidation binary fluorides of the second and third series of the transition metals has been dominated over the past years by the study of their oxidising properties.

The hexafluorides of uranium, molybdenum and tungsten which have been used in the present work, are members of the 5f, 4d and 5d series respectively.   Uranium and molybdenum have four binary fluorides, the hexafluoride, pentafluoride, tetrafluoride and trifluoride, while tungsten has three well characterised binary fluorides, the hexafluoride, pentafluoride and tetrafluoride [23].

1:5 Preparation and Physical Properties of Uranium, Molybdenum and Tungsten Hexafluorides.

The hexafluorides of uranium, molybdenum and tungsten can be prepared by various methods [24,25].   However, the reaction between metals and elemental fluorine in flow systems at high temperature is the most satisfactory method. In this method, active NaF which absorbs HF, enables Pyrex glass apparatus to be used to collect the product [26]. Uranium hexafluoride has great technological importance in the separation of the fissile [235]U isotope from natural

uranium by gas diffusion [25]. Because of this, UF_6 has been the subject of extensive research compared with MoF_6 or WF_6 and numerous methods for the synthesis have been developed [27]. Summaries of the preparative methods leading to UF_6, MoF_6 and WF_6 are presented in figures 1:1, 1:2 and 1:3 respectively.

The physical properties of the transition metal fluorides change regularly when the oxidation states change. In general, the volatilities of the fluorides of an element increase when the oxidation state of the element increases. Some of the hexafluorides are very reactive and corrosive substances and they must be handled in Nickel or Monel apparatus. The stability of the transition metal hexafluorides decreases with respect to dissociation into F_2 and lower fluorides varies in the order $WF_6 > ReF_6 > OsF_6 > IrF_6 > PtF_6$, and $RuF_6 > RhF_6$ [7] and the volatility of the compounds also decreases as the mass increases.

Uranium, molybdenum and tungsten hexafluorides have relatively high vapour pressures at room temperature. The boiling points for UF_6, MoF_6 and WF_6 are 329, 308 and 290 K respectively [7]. These properties make their use and manipulation in a vacuum system possible.

1:6 Structure and Electron Affinities of the Hexafluorides of Molybdenum, Tungsten and Uranium.

1:6:1 The Structure.

There has been a great deal of interest in binary
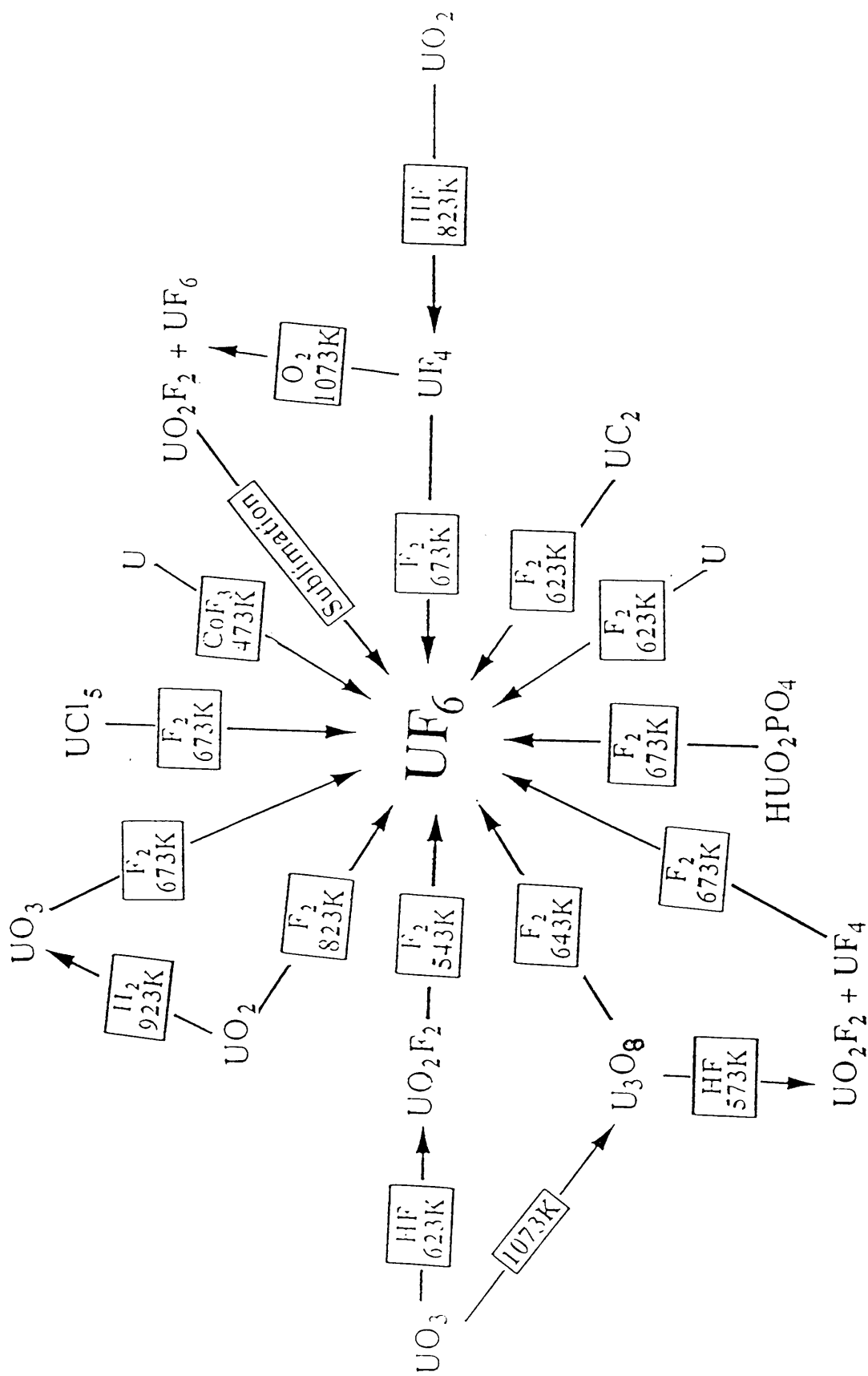
Figure(1:1).Preparation of uranium hexafluoride[27].
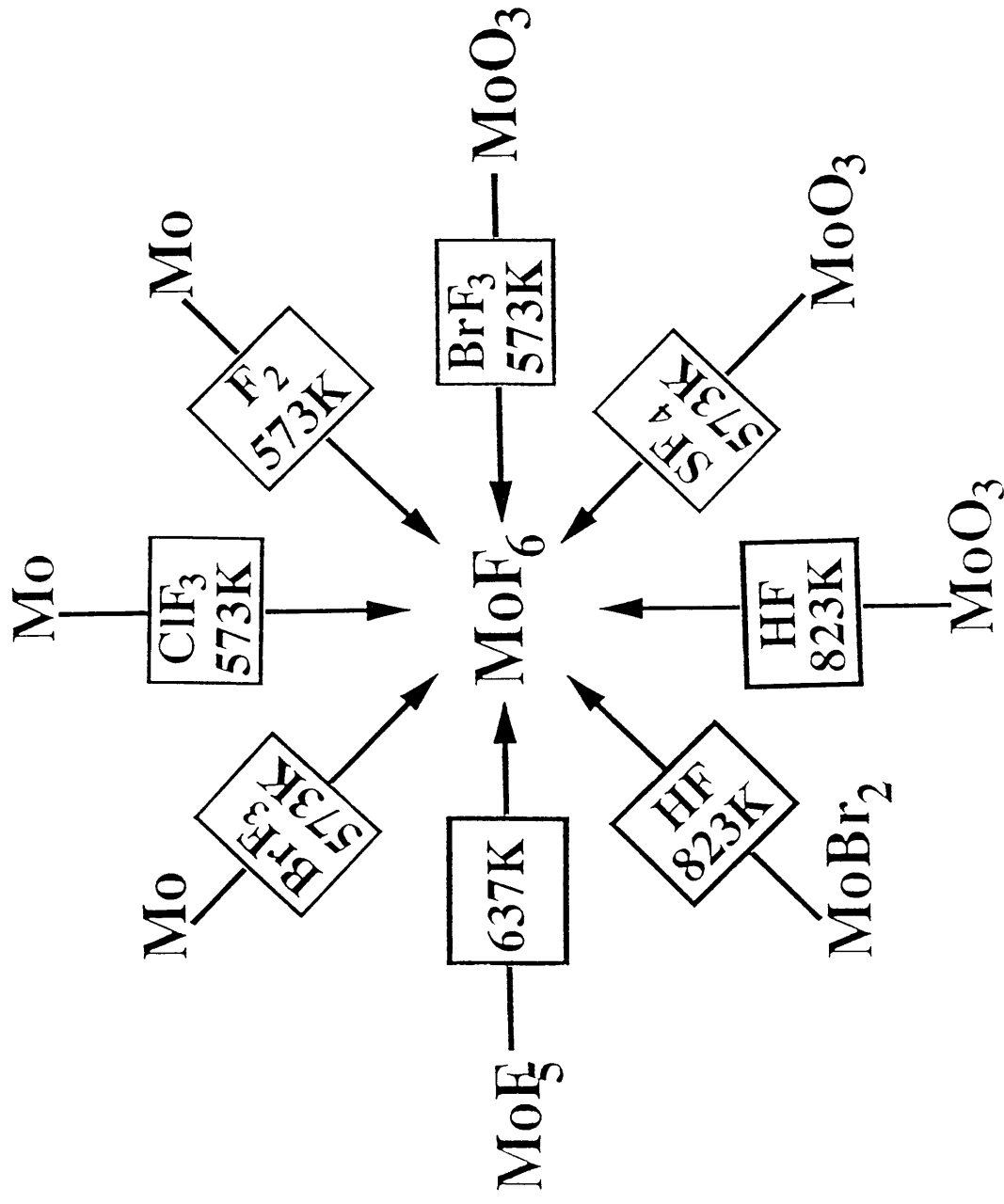
Figure(1:2).Preparation of molybdenum hexafluoride[24,25].
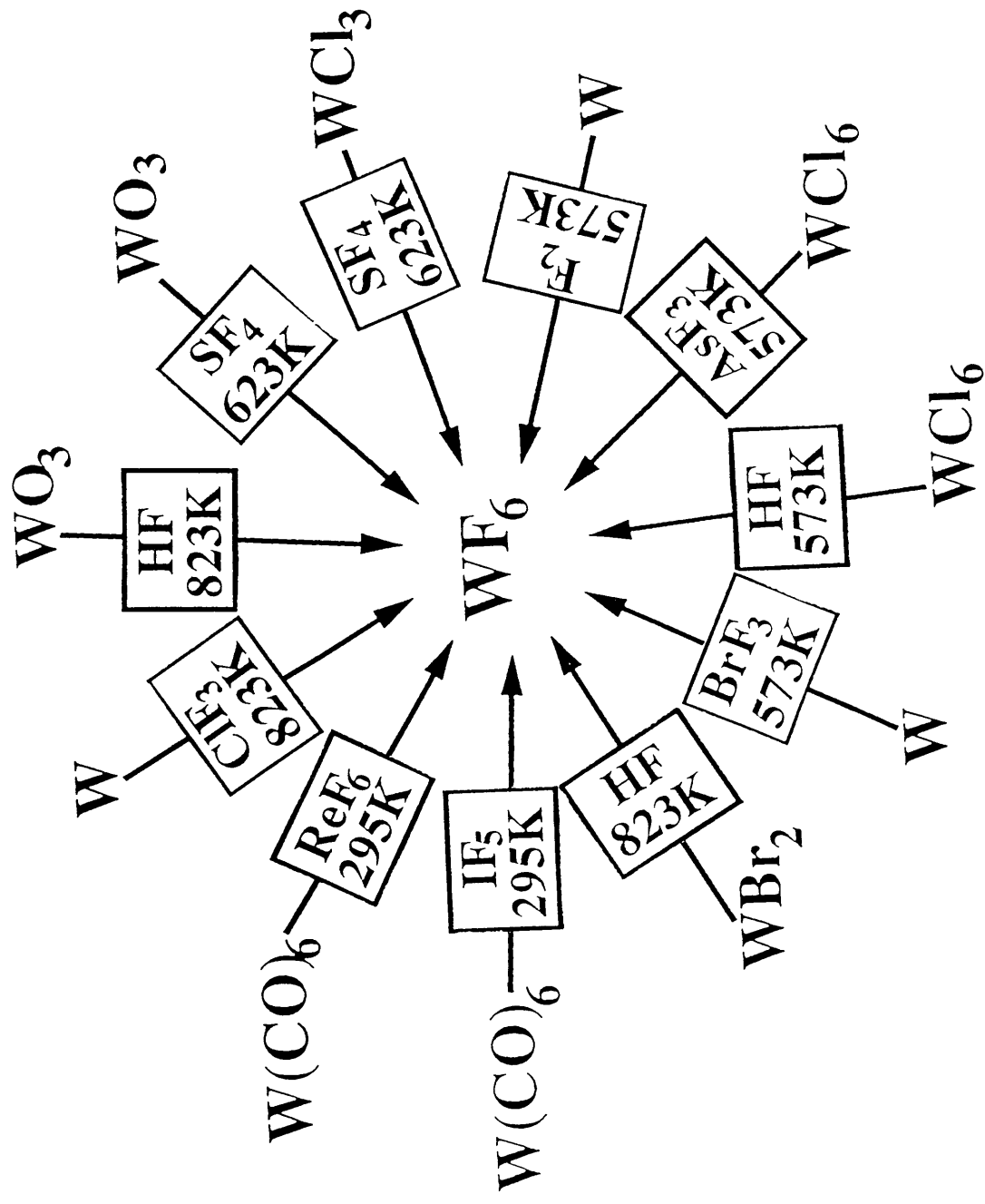
Figure(1:3).Preparation of tungsten hexafluoride[30,31]

transition metal fluorides from the structural point of view. The metals of the second and third transition series form hexafluorides which, structurally as a group, are the most closely related of all the transition metal fluorides. All of these hexafluorides are dimorphic, with a high temperature cubic form and a low temperature orthorhombic form [23].

The hexafluorides of uranium, molybdenum and tungsten in the vapour phase are monomeric having an octahedral arrangement in which six fluorine atoms surround the central metal atom. In the solid state, MoF_6 and WF_6 undergo a phase transition from a low temperature ortho-rhombic form to a high temperature cubic form at 264.3 and 264.8 K respectively [28]. It has been determined that the average metal-fluorine bond distances are 1.820 Å (MoF_6) and 1.832 Å (WF_6) [29]. Furthermore, the molecular volumes of MoF_6 in the orthorhombic (103.9 Å^3) and cubic (120.4 Å^3) phase of the solid are significantly smaller than those of WF_6 (105.5 Å^3 for orthorhombic, 123.8 Å^3 for cubic) [29]. However the Mo-F and W-F bonds are much shorter than that of U-F bond (2.00 Å) [30]. Neutron powder diffraction studies on UF_6, MoF_6 and WF_6 have been carried out by T.H. Levy et al [30] at 77 K. The results of these studies have shown that MoF_6 and WF_6 exist as more compact and spherically shaped molecules than UF_6 in the solid state. Molecular vibrations are greater in MoF_6 and WF_6 than in UF_6 since their molecules have less tendency to interlock [23].

1:6:2   The Electron Affinities.

The electron affinity (EA) of a molecule or atom is defined as the difference in energy between the neutral

molecule or atom in its ground state, E^O and ion in its ground state E^-, i.e. $EA = E^O - E^-$ [31]. The number of compounds whose electron affinities are accurately known is few. Measurement of electron affinities is difficult because of the complexity of molecular negative ions.

The electron affinities of the hexafluorides of uranium molybdenum and tungsten hexafluorides have been determined by many workers using different methods. Burgess et al [32] have estimated the electron affinities of MoF_6 and WF_6 as 517 ± 6 and 490 ± 5 kJ mol^{-1} respectively by measuring the heat of hydrolysis of the alkali metal hexafluoromolybdates (V) and hexafluorotungstates (V) with aqueous solution of hypochlorite. Dispert and Lacmann [33] have determined the electron affinity of WF_6 as 352 kJ mol^{-1} by the reaction of an alkali metal atom beam with tungsten hexafluoride. Another measurement has been carried out by Mathur et al [34] who reported the electron affinities of UF_6, MoF_6 and WF_6 as 471, 432 and 413 kJ mol^{-1} respectively. Beauchamp [35] used the ion cyclotron resonance technique to calculate the EA of UF_6. In his experiment he measured the threshold for the reaction (equation 1-14)

$$ UF_6^- + BF_3 \longrightarrow BF_4^- + UF_5 \quad \dots\dots\dots\dots (1\text{-}14) $$
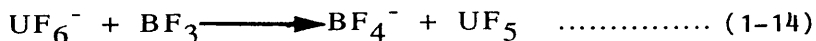
and he reported the value of EA (UF_6) = 470 ± 48 kJ mol^{-1}. The electron affinity of MoF_6 has been determined by Sidorov et al [36] as 345 kJ mol^{-1} using an effusion technique. The latest determination of the electron affinity of UF_6 has been carried out by Pyatenko et al [37] who reported the value of EA(UF_6) = 532 kJ mol^{-1} which is the average value obtained from their experiment and some previously determined values.

Although there is some disagreement among the values of the electron affinities for these hexafluorides obtained by different workers who used different methods, it appears that the electron affinity of UF_6 or MoF_6 is larger than that of WF_6. For example, studies involving the third transition series hexafluorides have demonstrated [38] that a hexafluoride must have an electron affinity of at least 452 kJ mol^{-1} if it is to intercalate into graphite spontaneously and oxidatively. Hence due to its relatively low electron affinity, 338 kJ mol^{-1} [39], WF_6 does not oxidise graphite [40].

1:7 Chemical Reactivity of The Hexafluorides.

The oxidising properties of the transition metal hexafluorides have been studied both in solution and in the gas phase. From the early work [41] including the reaction chemistry with simple one electron reductants, e.g. NO and O_2 [29] it has been established that the oxidising abilities of d-block hexafluorides in the absence of a solvent increase from left to right across a row in the periodic table. It has been also reported [42] that the hexafluorides of 4d elements are stronger oxidising agents than their 5d analogues. Comparison studies have been made between f- and d-block hexafluorides in which relationships between their oxidising abilities were established [41]. For example, the oxidising abilities increase in the order WF_6 < MoF_6 and OsF_6 < PuF_6 < RuF_6 [43,44]. It has been recognised that the hexafluorides of Mo, U, Os Ir and Pt oxidise graphite with concomitant intercalation of the hexafluoroanions [40]. It

has been shown that graphite intercalated with a hexafluoride exhibits high electrical conductivity [45]. Similarly, polyacetylene is oxidised by several hexafluorides, including WF_6 and ReF_6, which do not oxidise graphite [46].

The hexafluorides of U, Mo and W were used in the present work both in solution and in the gas phase. The oxidising properties of UF_6, MoF_6 and WF_6 have been investigated in various solvents. For example, in acetonitrile they are capable of oxidising a variety of transition and post-transition metals to give solvated metal cation salts of the corresponding MF_6^- anion [47,48]. In some cases the oxidation state of the metal depends on the hexafluoride used. This is illustrated by the example of thallium which is oxidised to Tl(III) by UF_6 and MoF_6 and to Tl(I) by WF_6 showing the relatively low oxidising ability of the latter as compared with UF_6 and MoF_6 [47]. It has been demonstrated that molecular iodine is oxidised by UF_6 and MoF_6 in MeCN to give solvated, mononuclear I^+, isolated as $[I(NCMe)_2][MF_6]$, (M=U, Mo), but WF_6 does not have sufficient oxidising ability to form I_2^+ [49]. However in iodine pentafluoride only UF_6 oxidises I_2 to I_2^+ [48]. The difference in behaviour between the hexafluorides in the two solvents emphasises the role played by MeCN in solvation. In MeCN, WF_6 is differentiated from UF_6 and MoF_6, both by its weaker oxidising power and by its ability to accept an F^- ion from WF_6^- to form WF_7^- [50,51]. The role played by the solvent in the behaviour of the hexafluorides is illustrated further by the example of sulphur dioxide in which MoF_6 and WF_6 have been shown to oxidise iodide anion to diiodine with

reduction to the corresponding hexafluorometallate (V) (equation 1-15)

$$2MF_6 + 2I^- \longrightarrow I_2 + 2[MF_6]^- \quad \ldots\ldots\ldots\ldots\ldots (1\text{-}15)$$
(M = Mo, W)
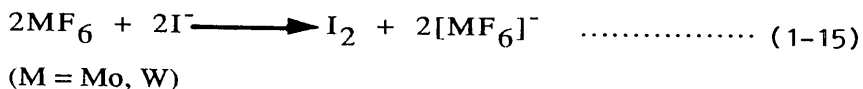
It has been established from the cyclic voltammetry and redox chemistry studies of the hexafluoride used in the present work that the order of their oxidising ability in MeCN is $UF_6 > MoF_6 > NO^+ > WF_6$ [50]. Unstable oxidation states of some cations can be stabilised by oxidation with the hexafluorides using a suitable solvent. For instance, Cu metal can be oxidised by MoF_6 or WF_6 in acetonitrile to form the stable complexes $[Cu(NCMe)_4][MoF_6]$ or $[Cu(NCMe)_4][WF_6]$ respectively [47]. In the gas phase it has been shown that nitric oxide is oxidised by UF_6 and MoF_6 to give products which contain $[NO^+]$ cation and where the central atom is reduced to a pentavalent state [53,54,55]. However WF_6 shows no oxidising ability towards NO even at 373 K [53,54].

1:8 Chemistry of the Pentafluorides of Phosphorus, Arsenic and Iodine.

Phosphorus pentafluoride and arsenic pentafluoride are colourless gases at room temperature and atmospheric presure, while iodine pentafluoride is liquid at the same conditions. In early investigation [56] it has been established that both PF_5 and AsF_5 are strong Lewis acids. Various statements have been made [57,58,59] on the order of their Lewis acidity, and it has been shown that this order depends on the individual medium as well as on which criterion for acidity

is used. In liquid HF, for instance, it has been reported that AsF_5 is stronger Lewis acid than PF_5 [60].

Iodine pentafluoride has an amphoteric character; that is with strong bases such as alkali metal fluorides, it forms anions, and with strong Lewis acids such as AsF_5 it forms cations [67] (equations 1-16 and 1-17)

$$IF_5 + AF \longrightarrow A^+IF_6^- \quad \cdots\cdots\cdots\cdots\cdots\cdots \quad (1\text{-}16)$$
$$A = \text{alkali metal}$$

$$IF_5 + AsF_5 \longrightarrow IF_4^+AsF_6^- \quad \cdots\cdots\cdots\cdots\cdots \quad (1\text{-}17)$$
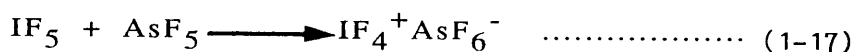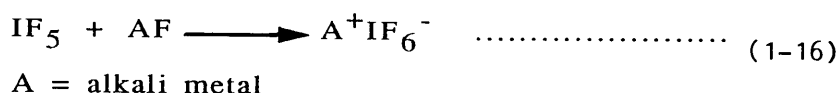
The molecular structures of phosphorus pentafluoride, arsenic pentafluoride and iodine pentafluoride have been determined by X-ray and electron-diffraction studies [56,61,62]. From these studies, it has been shown that PF_5 and AsF_5 molecules have a structure of trigonal bipyramid, while IF_5 molecule has a structure of square pyramidal; these structures and the lengths of P-F, As-F and I-F bonds are described in figure 1:4.

Phosphorus and arsenic pentafluorides form stable non-ionic six-coordinate complexes with organic donor molecules such as ethers, sulphoxides, amides, esters and in particular MeCN [63]. The vibrational spectra of AsF_5.NCMe have been studied in detail [64] and have shown that the arsenic atom is in an octahedral environment. Although it has not been possible to isolate adducts of PF_5 with MeCN [69], [19]F [65,66] and [31]P [65,67] n.m.r. spectroscopic studies have shown that rapid exchange takes place between free and complexed PF_5. The crystal structure of PF_5.py (py =
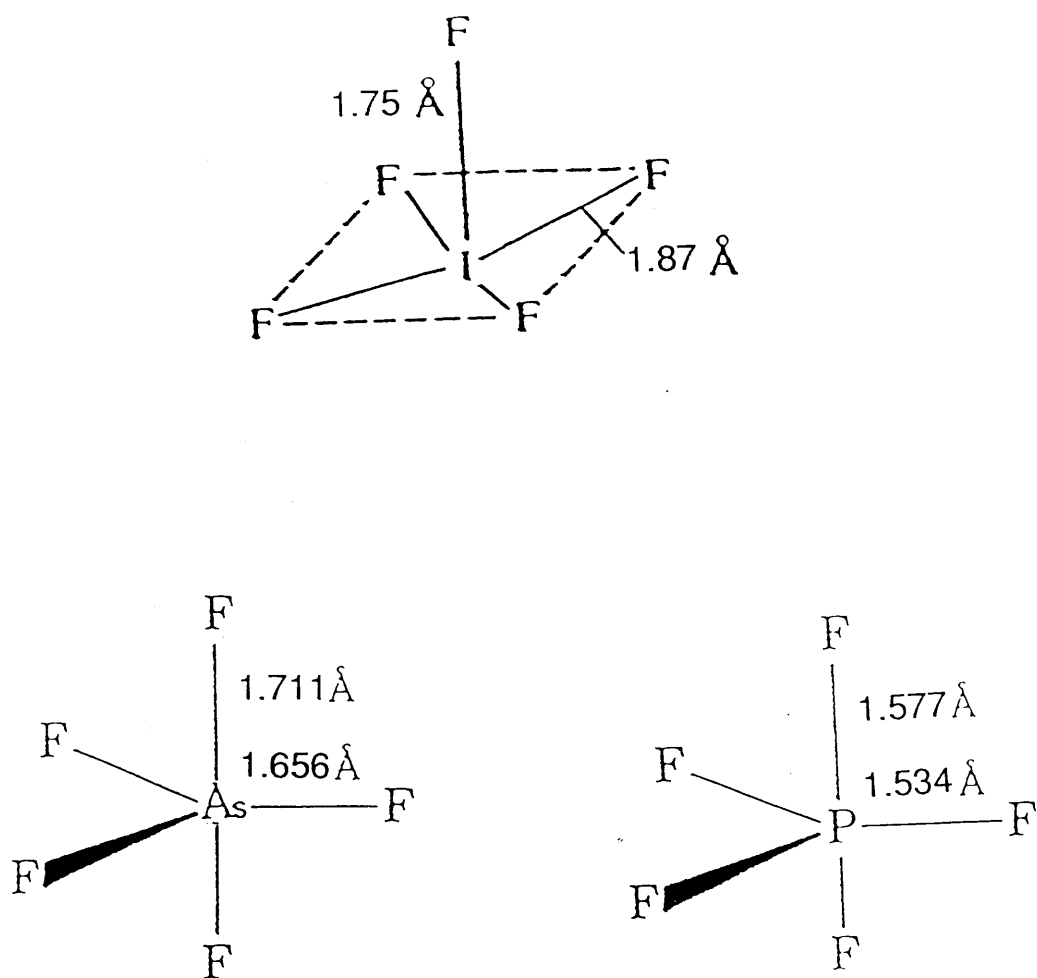
Figure(1:4).Structures of the pentafluorides of iodine, arsenic and phosphorus[56,61,62].

pyridine) [68] and $PF_5.NH_3$ [69] have shown that in either case the phosphorus atom is in an octahedral environment.

With fluoride ion donors such as selenium tetrafluoride [70], sulphur tetrafluoride or tellurium tetrafluoride [71], PF_5 and AsF_5 form adducts in which the cations SeF_3^+, SF_3^+ or TeF_3^+ and the corresponding anion are linked by fluorine bridges.

The Lewis acid-base properties of iodine pentafluoride and its fluorinating ability towards organic compounds have been well documented [72,73]. Reactions between IF_5 and the organosilicon compounds $Me_3Si(OMe)$ or $Me_2Si(OMe)_2$ have been carried out by G. Oates et al [74] at 293 K; the products of these reactions were $IF_4(OMe)$ and the corresponding fluoro(methyl)silane. Iodine pentafluoride has been used as a strong acidic solvent in the oxidation of iodine to form the polynuclear cations I_2^+, I_3^+ and I_5^+ [75]; these cations are not formed in the basic solvent, MeCN.

The oxidising properties of PF_5 and AsF_5 have been demonstrated in many ways. In sulphur dioxide AsF_5 has been used to oxidise copper and nickel metals to give $CuAsF_6$ and $Ni(AsF_6)_2.2SO_2$ respectively [76]. In MeCN copper metal is also oxidised by PF_5 although slowly to give solvated copper (I) hexafluorophosphate but AsF_5 shows no oxidising ability towards Cu under the same conditions [65]. In the presence of fluorine PF_5 and AsF_5 have been shown to intercalate oxidatively in graphite [77] to give C_8MF_6 (M=P or As) salts. When M=As the salt exhibits a conductively comparable to that of aluminium metal [78]. An excess of arsenic pentafluoride has been reacted with graphite fluorosulphate to form the

intercalation compound $C_{14}^+[AsF_5(SO_3F)]^-$ which is found to exhibit high electrical conductivities [79].

1:9 Oxidation Reactions of NO^+.

A number of oxidation reactions involving the use of NO^+ cation have been established. For example, solvated cations of the first row transition metals have been prepared by the oxidation of metals with $NOClO_4$ [80] or $NOBF_4$ [81] as oxidising agents. The metals react with suspensions of nitrosyl perchlorate or nitrosyl tetrafluoroborate in acetonitrile, according to the following equations:

$$M_{(s)} + 2NOClO_{4(s)} \xrightarrow{\text{MeCN}} M^{2+}_{(solv)} + 2ClO_4^-{}_{(solv)} + 2NO_{(g)}$$
$$\longrightarrow [M(NCMe)_x][ClO_4]_{2\ (s)} \cdots\cdots\cdots (1\text{-}18)$$
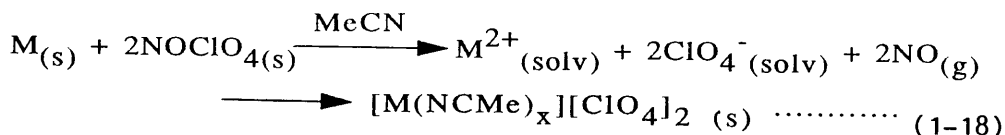
M = Co,, Mn, Cu and Zn.

X = 4 for Mn, Cu and Zn, and 6 for Co.

$$M_{(s)} + 2NOBF_{4\ (s)} \longrightarrow M^{2+}_{(solv)} + 2BF_4^-{}_{(solv)} + 2NO_{(g)}$$
$$\longrightarrow [M(NCMe)_x][BF_4]_{2\ (s)} \cdots\cdots\cdots (1\text{-}19)$$
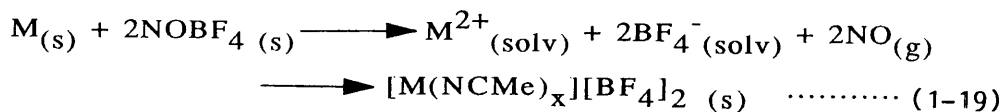
M = Fe, Co, Mn, Ni, Cu and Zn

X = 4 for Mn, Cu and Zn and 6 for Fe, Co and Ni.

All the above solvated metal cations are obtained in the +2 oxidation states except copper, where a mixture of Cu(II) and Cu(I) species is formed. Excess nitric oxide reacts rapidly

with gaseous uranium or molybdenum hexafluoride at temperatures from 298-333 K to give the solid ionic compounds $No^+[UF_6]^-$ and $NO^+[MoF_6]^-$ respectively [53].

G.M. Anderson et al [50] have studied the redox properties of $NOPF_6$ salt in acetonitrile at 298 K by cyclic voltammetry. These workers have reported that the half-wave potential, $E_{1/2}$, for the couple NO^+/NO is +0.87 V vs. Ag^+ (0.1 mol dm^{-3})/Ag^o, and the peak-to-peak separation, ΔEp, is 0.10 V at a scan rate 0.10 V s^{-1}. Furthermore, they have compared the redox properties of $NOPF_6$ with the redox couples MF_6/MF_6^- (where M = U, Mo and W) and Cu^{II}/Cu^I using cyclic voltammetry, and by carrying out appropriate redox reactions in acetonitrile. As a result of that comparison, the order of oxidising ability in MeCN established is UF_6 > MoF_6 > NO^+ > solvated Cu^{2+} > WF_6 [50].

1:10 General Acid-Base Definitions.

The early studies of acids and bases were restricted to aqueous solutions. For instance, the ionic acid-base definition which evolved from the theory of ionic dissociation was first proposed by Arrhenius in 1887 [82]. Arrhenius defined an acid as a substance that gives the hydrogen ion (H^+) as one of the products of its ionic dissociation in water, (equation 1-20) and a base as a substance that gives the hydroxide ion (OH^-) as one of the products of its ionic dissociation in water (equation 1-21)

$$H_xB \rightleftharpoons XH^+ + B^{x-} \quad \dots\dots\dots\dots \quad (1-20)$$
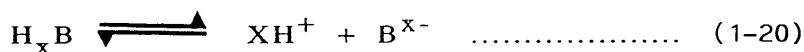
(B^{x-} is the corresponding counterion or anion)

$$M(OH)_y \rightleftharpoons M^{y+} + YOH^- \quad \dots\dots\dots \quad (1-21)$$
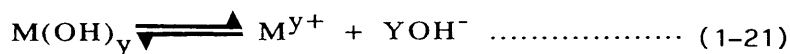
(M^{y+} is the corresponding counterion or cation)

The Arrhenius definition is solvent dependent in the sense that it probably applies only to ionic dissociation in aqueous solution, hence the limiting of the definition of base to include only hydroxides which are soluble in water. It did not answer the crucial question of why some hydrogen compounds were acidic (e.g. HCl) whereas others were not (e.g. CH_4). This definition does not express present views about aqueous solutions and cannot be applied to solutions in solvents other than water.

The definition of acids and bases by Arrhenius was extended by Brønsted and Lowry in 1923 [83,84] to include reactions taking place in solvents other than water. They defined an acid as a molecule or ion with a tendency to

donate a proton, and a base as a molecule or ion with tendency to gain a proton. This definition can be represented by the reaction of gaseous ammonia and hydrogen chloride to produce ammonium chloride (equation 1-22)

$$NH_3 + HCl \longrightarrow NH_4^+Cl^- \quad \ldots\ldots\ldots\ldots \quad (1\text{-}22)$$
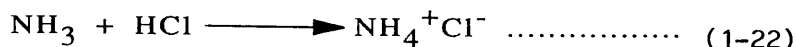
When an acid loses its proton it does so to a base. The acid is thereby converted to its conjugate base and the base to its conjugate acid, as exemplified in the following equation (equation (1-23)

$$\underset{\text{acid}}{CH_3COOH} + \underset{\text{base}}{H_2O} \rightleftharpoons \underset{\text{base}}{CH_3COO^-} + \underset{\text{acid}}{H_3O^+} \quad \ldots\ldots \quad (1\text{-}23)$$
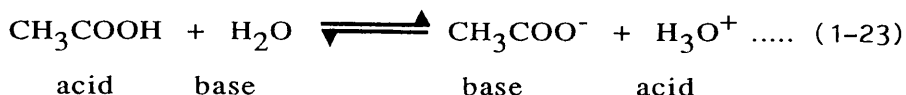
The disadvantage of this definition is that it applies only to acids containing hydrogen.

Another definition worth mentioning has been made by Franklin [85] also known as the solvent system definition. According to this concept, the acid is defined as any substance that yields either by direct dissociation or by interaction with solvent, the cation characteristic of that solvent. A base is defined as any substance that yields by direct dissociation or by interaction with the solvent, the anion characteristic of the solvent. One of the solvent system deficiencies is that it restricts acid-base behaviour to the liquid phase. It emphasises the importance of ionic dissociation phenomena and consequently cannot be applied to non-ionising solvent systems (e.g. benzene).

A more general concept of acids and bases has been developed by G.N. Lewis in 1923 [86]. Lewis defined a base as an atom, molecule or ion with at least one pair of electrons not shared in a covalent bond, and an acid as a species in which some atom, the acceptor atom, has a vacant orbital which can accommodate a pair of electrons. This definition was, in turn, based on Lewis' hypothesis of the shared electron-pair bond which he first proposed in 1916 [87]. Before Lewis made his definition of acids and bases, Langmuir [88] had used this hypothesis to suggest that within the context of the proton definition, bases must act as electron-pair donors. The formation of a chemical bond required the presence of a shared electron pair, and the transferred proton had no valence electrons. Therefore the base must logically be the electron-pair source. This definition includes the Brønsted-Lowry definition as a special case, since the proton can be regarded as an electron-pair acceptor and the base as an electron-pair donor. The Lewis definition covers a great many systems of reactions, for example the reaction between trimethylamine as Lewis base and boron trifluoride as Lewis acid (equation 1-24)

$$BF_3 + :NMe_3 \longrightarrow F_3BNMe_3 \quad \cdots\cdots\cdots\cdots\cdots \quad (1-24)$$

A number of complexes with the general formula, $[M(CH_3CN)_n][SbCl_6]_2$, (M=Fe, Co, Mn, Ni, Cu, Zn and n=4 or 6) have been synthesised by the reaction of $SbCl_5$ with metal chlorides in acetonitrile [89]. In these reactions, metal chlorides act as Lewis bases and $SbCl_5$ as Lewis acid.

Heterogeneous Lewis acid-base reactions involving covalent high oxidation state fluorides as Lewis acids and

metal binary fluorides as Lewis bases, have been used to generate solvated metal cations in acetonitrile. For example anhydrous CuF_2 or TlF react with WF_6 in MeCN forming the soluble Cu(II) or Tl(I) heptafluorotungstates [47]. The solid salts isolated are $[Cu(NCMe)_5][WF_7]_2$ and $TlWF_7$ respectively. Similar reactions involving the pentafluorides of phosphorus, arsenic and tantalum as Lewis acids and CuF_2 as Lewis base, in acetonitrile, result in the formation of solvated Cu(II) hexafluoroanion salts [65] (equation 1-25)

$$CuF_{2\ (s)} + 2MF_{5\ (solv} \longrightarrow Cu^{2+}_{(solv)} + 2MF_6^-{}_{(solv)} \cdots (1\text{-}25)$$
(M = Ta, P, As)
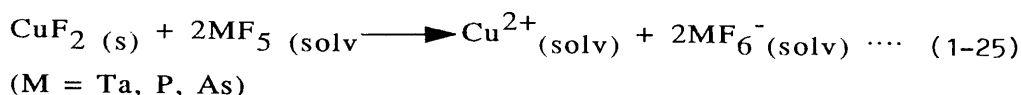
These reactions suggest that MeCN has good solvating properties and that the pentafluorides have strong tendency to accept the fluoride ion. Copper(II) fluoride, in the same way, reacts with UF_5 in acetonitrile at room temperature to give the solvated copper(II) hexafluorouranate(V) salt [90].

1:11 Electrical Conduction in Polymers.

One way of classifying materials is on the basis of their electrical properties. Materials can be classified as metals, semiconductors or insulators depending upon the way in which their electrical resistivity changes with temperature. With metals the resistivity increases with temperature, while with semiconductors and insulators the resistivity decreases exponentially with temperature. It has been reported in early work [91] that polymers in general are usually insulators or semiconductors.

The main property of most polymers, which distinguishes them from metals is their inability to carry electricity. Good conductors such as copper (with conductivity 6 x 10^5 ohm^{-1} cm^{-1}) conduct because there are electrons available to transmit the current when an electrical potential is applied. This is not the case with most common polymers since the electrons are tightly bound in covalent bonds. Polar polymers such as polyvinyl chloride have higher conductivities than non-polar polymers because of the electric dipole which is present. Nevertheless, polar polymers are essentially non-conductors and they are widely used in low voltage insulation. They are also useful as dielectric materials where their polarity and insulating character enable small capacitors of high storage capability to be manufactured. Especially useful in this area are poly(vinyl fluoride) and poly(vinylidene difluoride) in film form [91].

The most common method of making polymers electrically conductive is by incorporating a conductive material such as

carbon or metal powders in the polymer [92]. Polymers with conjugated double bonds are found to be more conductive than non-conjugated polymer structures. For example, in polyacetylene (Fig. 1:5a) in which the single and double bonds alternate along the polymer chain, the conduction is due to the delocalization of the π electrons of the double bonds. Polyphenylene sulphide (Fig. 1:5b) shows conductive capability due to delocalization involving the aromatic ring and the sulphur atom.

-CH=CH-CH=CH-CH=CH-CH=CH-

(a)   (b)
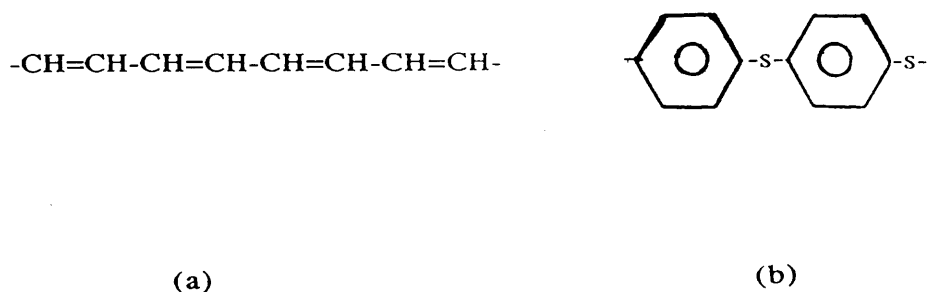
Figure(1:5).(a).Polyacetylene and (b).Polyphenylene sulphide.

Delocalization in itself however, does not significantly improve the conductive nature of the polymer but if the polymer is doped with additives (electron donors or acceptors) conductivity values of up to $10 \text{ ohm}^{-1} \text{ cm}^{-1}$ can be achieved depending on the additive, its concentration, and the polymer. The effect of the dopant is to provide electrons or positive holes (due to the removal of electrons) available for conduction. Other methods of releasing electrons to improve the conductive nature of polymers

include the use of heat, light or mechanical stress. In fact, the insulating properties of polymers are a significant advantage for many applications of plastics. Electrical wires for example, are protected from shorting by a coating of insulating polymer.

The discovery of the first organic conductor from the reaction between the electron donor tetrathiofulvalene (TTF) and the electron acceptor tetracyano-p-quinodimethane (TCNQ) in 1973 [93] has led to the realization that under certain conditions, organic materials may exhibit electrical conductivity. With the development of microelectronics during the same period there has been an increasing effort to utilize these materials as the basis for microelectronic components, especially since they exhibit the whole range of conducting properties, from semiconductivity to photo- and superconductivity [94]. During the past 15 years, a new class of organic polymer has been devised with the remarkable ability to conduct electrical current. Some of these 'Synthetic Metals' are under development for practical applications, such as rechargeable batteries and electrolytic capacitors. A major obstacle to the rapid development of conductive polymers is the lack of understanding of how electrical current passes through them and a lack of detailed structural information in many cases. A basic research goal in this field is to understand the relationship between the chemical structure of the repeating unit of the polymer and its electrical properties.

The polymers, polyacetylene, polyaniline, polypyrrole, polythiophene, poly(phenylenesulfide) and poly(phenylene-vinylene) have been studied most intensively. Polyaniline

was the first polymer to be prepared when H. Letheby [95] in 1962 anodically oxidised aniline in sulphuric acid. However, the conductive polymer that actually launched this new field of research, was polyacetylene $[(CH)_n]$. In 1977, Shirakawa in Japan and Heeger in America [96] discovered that partial oxidation with iodine or other reagents made polyacetylene films 10^9 times more conductive than they were originally. The process for transforming a polymer to its conductive form via chemical oxidation or reduction is called doping. The doping process that transforms polyacetylene to a good conductor of electricity is ordinary oxidation, termed p-doping. Reductive doping, called n-doping, is also possible using for example alkali metals, but it has been explored much less because the resulting conductive polymers are more sensitive to air than the undoped polymers. The two types of doping (p-type and n-type) are illustrated by the following examples [97], (equations 1-26 and 1-27)

$$(CH)_n + {}^3/_2 I_2 \longrightarrow (CH)_n^+ (I_3^-)_{0.33} \quad \cdots\cdots \quad (1\text{-}26)$$

$$(CH)_n + XNa \longrightarrow (Na^+)_x [(CH)_n]^{x-} \quad \cdots\cdots \quad (1\text{-}27)$$
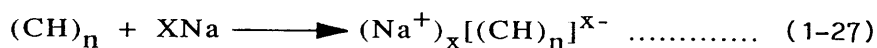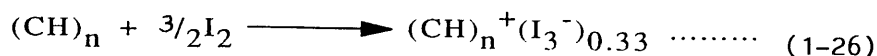
In the doped form, the polymer backbone is either positively or negatively charged and the small counterions such as I_3^- or Na^+ act as simple bystanders that do not effect the electrical properties directly. Conductive polymers can be doped and undoped (changed from the conductive to the insulating state) by applying an electrical potential, which causes the dopant ions to diffuse in and out of the structure.

Three other polymers studied extensively since the

early 1980's are polypyrrole, polythiophene and polyaniline. Art. F. Diaz has found that polypyrrole could be obtained as a film by electrochemically oxidising pyrrole in acetonitrile [97]. In 1982 Tourillon and Garnier made polythiophene by the anodic oxidation of thiophene [97]. Because this electrochemical method allows the oxidation potential of the polymerisation to be controlled, the quality of the polymer can be optimized. In this method films in the doped state can be made, and it is now the most widely used technique for the synthesis of conductive polymers. Many studies were carried out on polyaniline including the description of its structure and electrical properties [98]. These studies showed that polyaniline consists of more than 1000 repeating units and it has electrical conductivities varying from 10^{-11} $ohm^{-1}cm^{-1}$ to more than 10 $ohm^{-1}cm^{-1}$. Different compositions of polyaniline have different colours and electrical properties. Only one form of polyaniline however, the emeraldine salt, is electrically conductive [98]. Mechanically flexible, dark blue films of conductive polyaniline have been also achieved by protonic doping of emeraldine films cast from N-methylpyrroldinone solutions [98]. Protonic doping can be achieved by the dipping of emeraldine films in acid or passing a gaseous acid over them; it protonates the imine nitrogen atoms in the backbone of the polymer. The conductive emeraldine salt becomes the emeraldine base when treated with aqueous alkali. Because protonic doping does not change the number of electrons, the conductivity of the polymer in this case will depend on the pH of the solution which it is treated with.

1:12 Metal-Phthalocyanine Complexes.

Metal-phthalocyanine complexes have been the subject of many physical and chemical studies with regard to their photoconducting, semiconducting and conducting properties [3]. Because of their thermal and hydrolytic stability, intense colours and ready availability, they are of considerable interest as new candidates for optical, electronic, photoelectronic, and electrochemical applications Since the first discovery of iron(II) phthalocyanine in 1928 [99] thousands of patents and publications concerning the phthalocyanines have appeared. Phthalocyanine complexes are all intensely coloured, purple blue or green compounds. Most of them are thermally stable and many can be sublimed unchanged at 673 K/10^{-6} Torr. Copper phthalocyanine for example, is stable with respect to decomposition at 1173 K in vacuo [100]. The phthalocyanine complexes often exist in two or more polymeric modifications, which may be distinguished by infrared and x-ray diffraction techniques. Although phthalocyanines in which the central metal ion has an oxidation state of 2 are the most common, complexes are known with metals in all oxidation states from 0 to 6. Manganese phthalocyanine complexes for instance, exist with Mn in oxidation states 0,1,2,3 and 4 [101].

1:12:1   Structure of Phthalocyanine Complexes.

The classic studies elucidating the structure of the phthalocyanines were carried out in the early 1930's under the direction of Sir Patrick Linstead [99]. These studies showed that metal-free phthalocyanine (abbreviated PcH_2) contained a ring system of four isoindole units linked by aza nitrogen atoms (Fig. 1:6a) The two central hydrogen atoms of the phthalocyanine are replaceable by a wide range of metals and metalloids. Linstead's study offered no explanation for the equal lengths of the C-N bonds in the   macro-ring and C-C bonds linking it with the benzene nuclei.   He also did not explain the homogeneity of the oxidation products and the absence of isomeric forms of the metal derivatives.

Further structural studies of phthalocyanine compounds were carried out by Robertson in 1935 [102].   On the base of x-ray analysis, Robertson showed that the phthalocyanine and its complexes are planar molecules.   The planarity of the molecule follows from the classical formula in figure 6a taking possible resonance structures into account. Structural studies carried out with metal-free [103] nickel [104] and platinum [104]phthalocyanines have shown that the metal atoms are in square planar environment and that the entire phthalocyanine molecules are square.   The studies carried out by Robertson on metal-free, beryllium, manganese (II), iron (II), cobalt (II), nickel (II) and copper (II) phthalocyanines showed that these complexes form long, flat, ribbon-like monoclinic crystals, the surface of the ribbon being the (001) plane and the axis (010) [104]. An alternative presentation of the metal-free phthalocyanine is given in Fig. 1:6b [101] in which the dots represent the 16 π
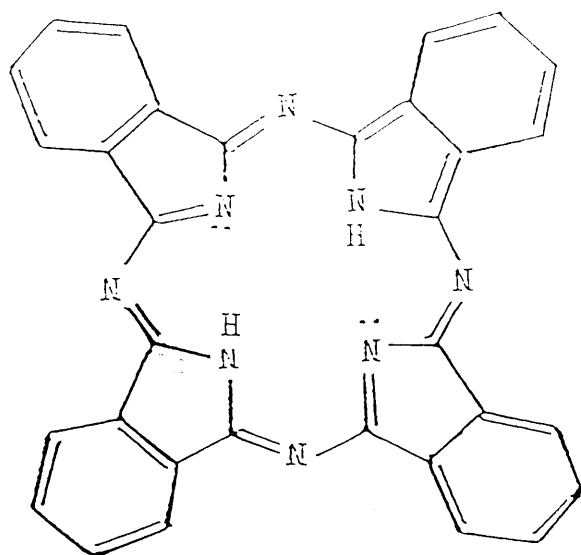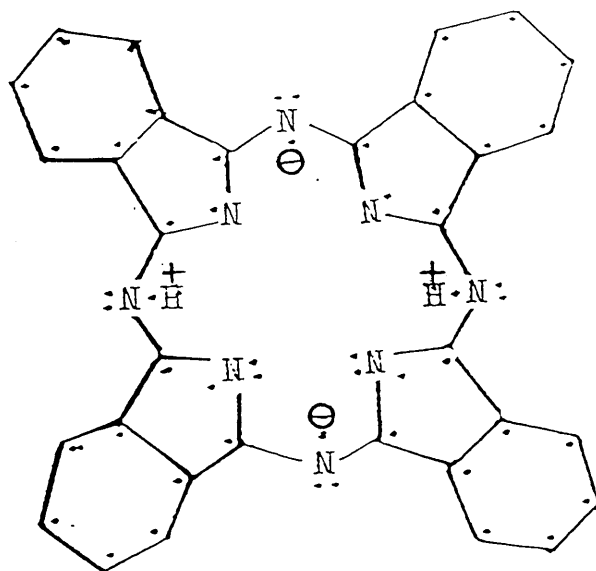
Figure(1:6).Structure of metal-free phthalocyanine proposed by R.P.Linstead(a) and B.D.Berezin (b).

electrons of the macro-ring and the 24 π electrons of the benzene rings, and two circles represent the electrons resulting from internal ionization of the two imino-hydrogen atoms of H_2Pc. As a consequence each proton is in the electrostatic field generated by three nitrogens. The sextets of π electrons of the benzene rings form stable π-electron shells participating in a very weak interaction with the π electrons of the macro-ring. The last 18 π electrons constitute an aromatic system independent of the benzene rings and obeying Huckel's rule (4n + 2 = 18).

The π electrons of the macro-ring together with the two ionization electrons occupy nine bonding molecular orbitals (ψ_π) of the macro-ring. The lowest-energy orbital corresponds to even distribution of the electron pairs among all C-N bonds.

1:12:2   Methods of Preparation.

Metal phthalocyanine complexes may be prepared by various methods. Usually they are formed from molecular fragments of phthalocyanine, for example phthalonitrile, phthalimide, phthalic anhydride or diiminoisoindoline in the presence of a metal ion source which may be a chloride, acetate, oxide or the free metal. Preparation methods are illustrated by the following equations [105].

$$PcH_2 + MX_2 \xrightarrow[\text{b.p.}]{\text{solvent (e.g. quinoline)}} PcM + 2HX \ \text{.......} \ (1\text{-}28)$$

M = metal, X = halogen.

$$4 \quad \text{(benzene ring with CN, CN)} + M \xrightarrow[\text{dry or solvent}]{573 \text{ K}} PcM \ \text{..................} \ (1\text{-}29)$$

$$4 \quad \text{(benzene ring with CONH}_2\text{, CN)} + M \xrightarrow[\text{dry}]{573 \text{ K}} PcM + 4H_2O \ \text{...............} \ (1\text{-}30)$$
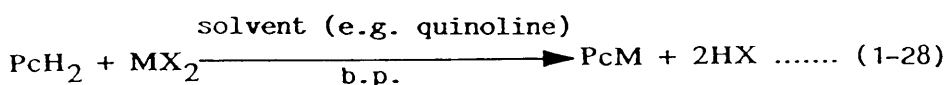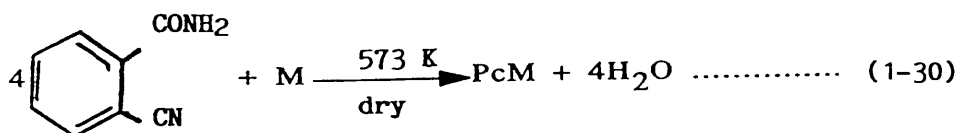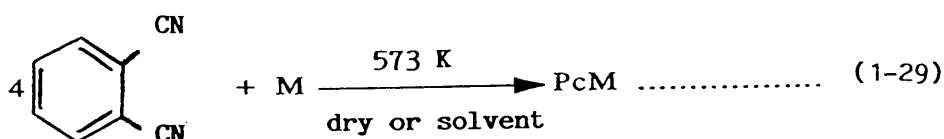
Reactions (1-29) & (1-30) may also be carried out with metal salts or oxides.

$$4 \quad \text{(isoindoline with NH, NH, NH)} + MX_2 \xrightarrow{\text{formamide}} PcM + 4NH_3 \ \text{..........} \ (1\text{-}31)$$

$$PcLi_2 + MX_2 \xrightarrow[\text{room temp.}]{\text{solvent}} PcM + 2LiX \ \text{..................} \ (1\text{-}32)$$
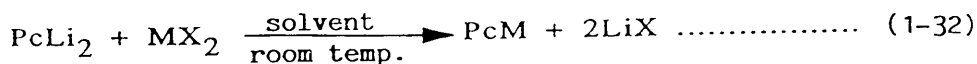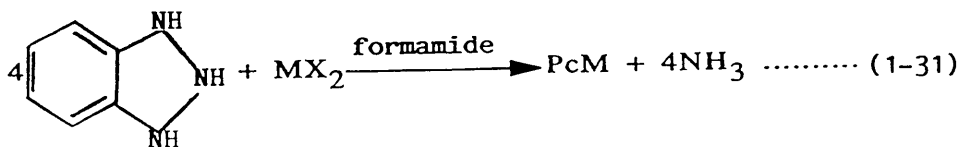
The reactions between phthalonitrile and metals are usually very vigorous at 523-573 K.   Sufficient heat is generated to maintain the reaction temperature.   Even more surprising are the observations that palladium black and gold will dissolve in molten phthalonitrile [105].

1:13 Polymeric Metal-Phthalocyanines and their Structures.

An important aspect of metal-phthalocyanines chemistry is to determine the relationships among monomeric and polymeric species that are characteristically found for these complexes. Their insolubility in most solvents and the wide variety of crystalline forms, ribbon, linear, branched, cross-linked, three dimensional make the determinations difficult. One procedure that has been used successfully [106] is a spectroscopic method. This involves making a comparison between electronic absorption spectra of monomers and polymers using concentrated H_2SO_4 (98%) as solvent. The method has been applied to complexes of Cu, Zn, Os, Mo and Ga phthalocyanines [101]. It appears that phthalocyanine polymers differ widely from the monomers by the low intensities of the bands in the electronic absorption spectrum. Characteristically the position of the bands remains practically the same. This means that the state of the electronic energy levels of the phthalocyanine chromophore in a monomer and a polymer is the same also. Such a behaviour of spectra in the transition of monomeric phthalocyanine to the polymeric state suggests that the decrease in intensity of the bands and the invariability of their position as the polymer chain grows are inversely proportional to the degree of polymerization and result from the impossibility of excitation of two or more chromophores of the conjugated polymer chain of phthalocyanine at the same time [107]. In the determination of the degree of polymerization (n) using spectroscopic method, polymers with a small value of (n) are usually formed. The mean statistical value of (n) does not exceed 3-14 for various metal-phthalocyanines [107].

The degree of polymerization of $[Ru(Pc)(HSO_4)]_n$ and $[Os(Pc)(SO_4)]_n$ polymers have been determined using the method of acid-base titration of the side groups $(CO)_2NH$ in a 1N solution of KOH [101] The results established from the titration method have shown [101] that polymeric osmium phthlocyanine is a ribbon polymer with $n \simeq 7\text{-}8$ and contains 13 side groups $(CO)_2NH$, while in polymeric ruthenium phthalocyanine, $n \simeq 3$ and the side groups are eight; the values of n are in good agreement with the spectral data.

It has been shown [108] that the spectral method of determining the value of n is also applicable to bridged polymers of metal phthalocyanines, particularly to poly-(phthalocyaninesiloxane), $[Si(Pc)O]_n$. The method of vacuum dehydration of $[Si(Pc)(OH)_2]$ produces an oligomer with $n = 3$, whereas heating of dihydroxysilicon phthalocyanine in nitrobenzene with $ZnCl_2$ at 448 K yields a polymer with $n = 11$ [101].

Fluorine-bridged metal phthalocyanines such as $[Fe(Pc)F]_n$ [109] $[Al(Pc)F]_n$ and $[Ga(Pc)F]_n$ have been studied using different methods. The results from the use of infrared and mass spectroscopy, electron microscopy, thermogravimetric analysis, conductivity measurements and x-ray diffraction have suggested that these complexes are polymeric and have a $(M\text{-}F)_n$ backbone, involved in fluorine linkages between the phthalocyanine units and it seems likely that these backbones have symmetrical, linear M-F-M bridges [1].

1:14 Electrical Conductivities of Metal-Phthalocyanine Polymers.

The interest in polymeric phthalocyanines arises from their stability in ambient atmosphere and their ionization potential, which depends on the metal; and they can be oxidised by a large variety of oxidants. Phthalocyanine polymers containing terminal cyano groups undergo polymerization on heating via the $-C \equiv N$ bonds, leading to highly conducting polymers [110]. Thermal treatment of a nickelphthalocyanine polymer having terminal carboxyl groups results in the formation of highly conjugated structures and mobile radical defects, which cause an increase in the room-temperature electrical conductivity [111]. The fluorine-bridged metal phthalocyanines $[M(Pc)F]_n$, (M=In or Ga) have been reacted with nitrosonium salts NO^+Y^-, (Y=BF_4 or PF_6) to give products with conductivities as high as $10 \, ohm^{-1} \, cm^{-1}$ [2]. It has been reported that the ionization potential of $[Al(Pc)F]_n$ is 4.55 eV [112], and this polymer can be doped by oxidants such as O_2, NO_2 and Cl_2 [112]. Iodine has been used as a vapour and in solution in heptane or pentane for the doping of $[Al(Pc)F]_n$ and $[Ga(Pc)F]_n$ to give products of $[Al(Pc)FI_x]_n$ and $[Ga(Pc)FI_x]_n$ [3]. Doping with iodine results in increases in conductivity by factors as high as 10^9 with the highest conductivity $(5 \, ohm^{-1} \, cm^{-1})$ being observed for the stoichiometry $[Al(Pc)FI_{3.4}]_n$. Conductive thin films of nickel phthalocyanine, NiPc treated with iodine at elevated temperatures have also been examined, with a view to their ultimate use as improved photosensitisors for optoelectronic devices [113]. Work on bridged-stacked phthalocyanines, $[M(Pc)O]_n$, (where M=Si, Ge, Sn) has shown that the presence of a central atom-oxygen bridge does not

prevent high conductivity [114].   In other reported work on conduction properties of phthalocyanines, it has been claimed that the polymer $[M(Pc)F]_n$ with M=Al or Ga can be partially oxidised by AsF_5 [115], IF_5 [116], MoF_6 [4], WF_6 [4] and UF_6 [4] to produce highly conducting compositions with thermal and chemical stabilities.

CHAPTER TWO

EXPERIMENTAL

2:1 Experimental Techniques:

Most of the starting materials and the products obtained in the present work were moisture sensitive. Therefore, in order to ensure anhydrous and oxygen free conditions, all experiments and manipulations were carried out using conventional high vacuum techniques. A Pyrex vacuum line and a nitrogen atmosphere glove box were used throughout this work.

2:1:1 Vacuum Line:

The vacuum line was made from Pyrex glass and consisted of a mercury diffusion pump (Jencons), a rotary oil pump (Edwards high vacuum) and standard glass joints. This system could achieve a vacuum of 10^{-4} Torr, which was checked approximately using a mercury vacustat. The standard glass joints were greased with Apiezon N or Voltalef Kel-F high vacuum greases. Apiezon black wax was used for sealing the semi-permanent joints. Polytetrafluoroethylene (P.T.F.E) Pyrex stop-cocks (Rotaflo or J. Young) were used when they were necessary. Most reactions were carried out in double limbed vessels (Fig. 2:1) fitted with the above mentioned stop-cocks. Similar vessels with one limb replaced by a Spectrosil cell for electronic spectroscopy or by an n.m.r. tube were also used. All the glassware and reaction vessels were evacuated and flamed out using a gas-oxygen torch before use.
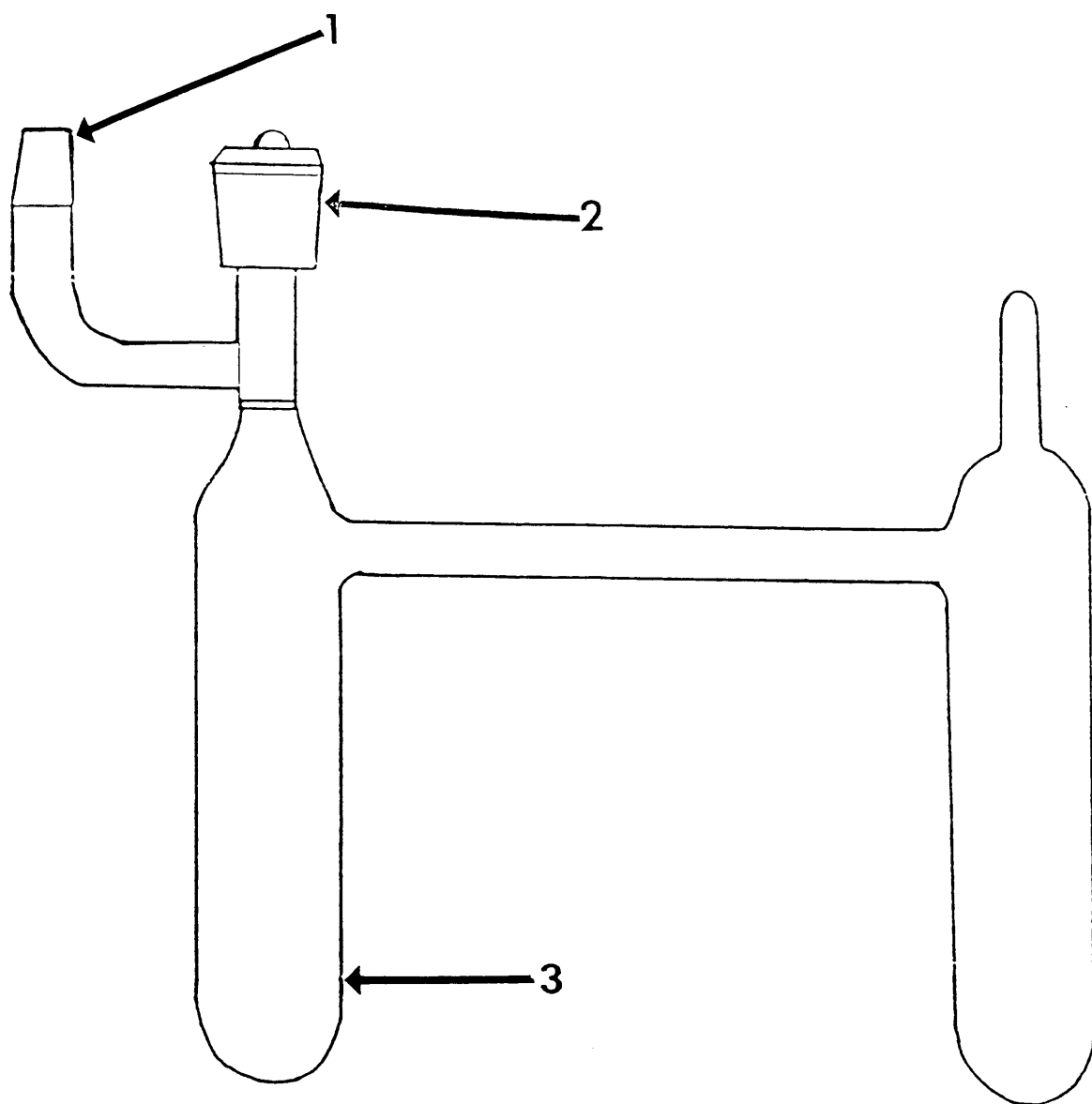
1. B-14 Ground glass cone
2. Rotaflo stopcock
3. Reaction vessel

Figure(2:1).Double-limbed reaction vessel.

2:1:2   The Glove Box

The non-volatile materials which were moisture sensitive, were handled in a N_2-atmosphere glove box (Lintott Engineering) in which the moisture level was kept below 10 p.p.m.   An evacuable airlock was attached on one end of the glove box as a transfer port.   This permitted the apparatus and material to be introduced into the box without affecting the dry atmosphere condition inside the box.

2:2 Electronic Absorption Spectroscopy [117, 118]

Electronic absorption spectroscopy is a useful method for the identification of electronic transitions from one state to another in a molecule or metal ion.   The electronic absorptions usually occur in the visible and ultraviolet regions (10,000 - 50,000 cm^{-1}).   In a molecule, electrons occupy different types of orbitals, which can be described as σ-bonding, non-bonding and π-bonding, with different energies in the ground state.   Electrons from these different orbitals can be excited to higher energy molecular orbitals by absorbing radiation, thus giving rise to many possible excited states.   Electronic transitions occur according to well defined selection rules.   During a transition from the ground state to an excited state, the number of unpaired electrons must be unchanged.   If the transitions involve redistribution of elecrons within a given set of orbitals they are described as Laporte forbidden.   That means, in a centro-symmetric molecule, the g -> u and u -> g transitions are allowed while g -> g and u -> u transitions are forbidden.   The electronic transitions p -> p and d -> d,

for example, are Laporte forbidden, while s -> p and p -> d transitions are allowed.   Due to this Laporte rule, d -> d transitions are not allowed, so many transition metal complexes should not be coloured.   However, if a transition metal ion does not have a centre of symmetry or vibrates causing the symmetry to be destroyed, mixing of d and p orbitals can occur through hybridization.   As a result, electronic transitions between d levels with different amounts of p character can occur.   The intensity is relatively proportional to the extent of mixing of the orbitals.

2:2:1   Charge-transfer Transitions [119]

Because of the close approach of a metal atom and a set of ligands in a complex or molecule it is often possible for transitions to occur between a metal-based level and a ligand-based level.   As these formally involve transfer of an electron from metal to ligand or from ligand to metal they are called charge-transfer transitions.   These are specially important for the transition metal complexes of the second- and third-row, where they tend to dominate the spectra. Weak d-d transition bands and even intra-ligand bands are obscured by the much stronger charge-transfer bands.

Charge-transfer bands are usually responsible for some of the strongest colours, even for first-row transition metals.   For example, in the permanganate ion, MnO_4^-, the central atom is in the +VII oxidation state and therefore carries a high formal positive charge.   The charge-transfer transitions responsible for the intense purple colour in

which transfer of electrons from essentially oxygen ligand-based orbitals to metal-based orbitals. This is an example of a ligand to metal charge-transfer and may be regarded as an internal redox reaction. The reverse, metal to ligand charge transfer, is possible as for example, in organic amine complexes of low-valent metals such as $[TiCl_3(bipy)]$.

Charge-transfer bands may overlap with d-d bands, and with bands corresponding to excitation within ligands themselves, and assignments in this case are often very difficult.

2:2:2 **Sample Preparation**

(i) Solution Samples.

Sample solutions required for electronic spectroscopy were prepared in a one-limb reaction vessel provided with a 10 mm Spectrosil cell. This vessel was specially designed for handling solutions which are sensitive to air and moisture (Fig. 2:2). The reactions were carried out in the vessel, and the coloured solution was decanted into the cell.

(ii) Thin Film Samples:

An evacuable gas cell fitted with a Young's tap, a B-14 cone and Spectrosil-B windows was designed (Fig. 2:3). The wafer was held in reproducible position for each sample examined by means of a P.T.F.E. holder (Fig. 2:3). This cell enabled the spectra of films supported on wafers to be recorded before and after the addition of the oxidising agents.
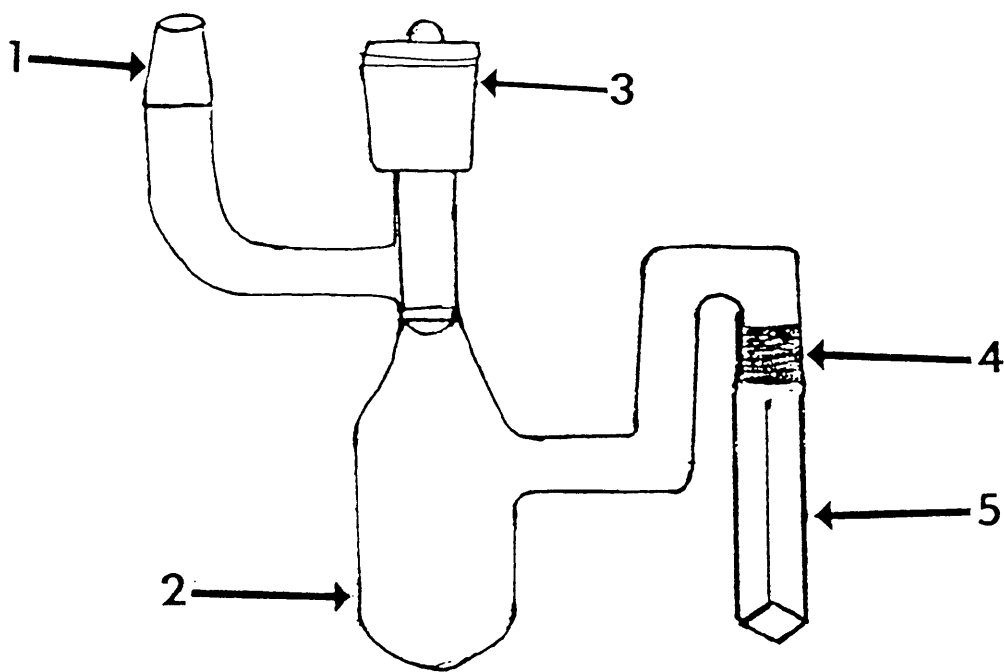
1.B-14 Ground glass cone

2.Reaction vessel

3.Rotaflo stopcock

4.Quartz Pyrex graded joint

5.10mm Quartz cell

Figure(2:2).Single-limbed reaction vessel provided with a 10mm
Spectrosil cell.
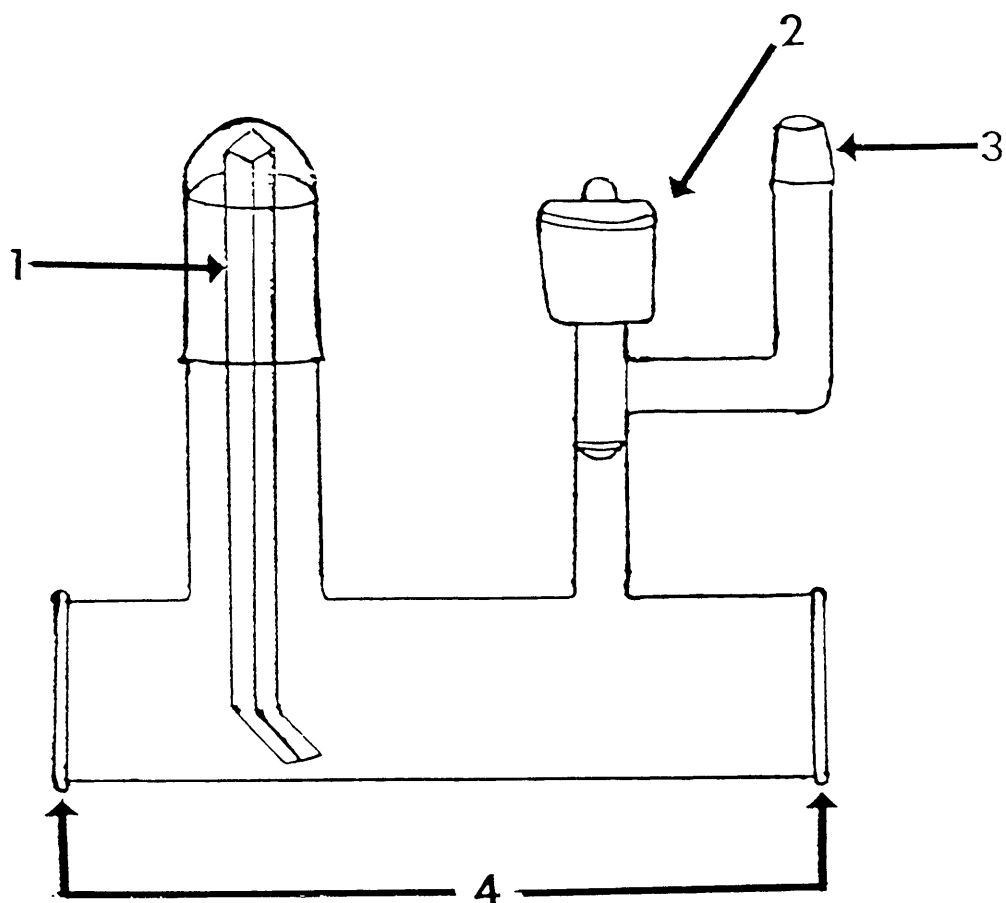
1. Sample holder
2. Rotaflo stopcock
3. B-14 Ground glass cone
4. Spectrosil-B windows

Figure(2:3).An evacuable reaction gas cell.

A Perkin-Elmer Lambda 9 spectrophotometer was used to record the spectra for both the solution and thin film samples over the region 1000-185 nm. In the case of the solution samples obtained from the reaction of $[Al(Pc)F]_n$ with UF_6 in MeCN, the spectra was recorded in the near infrared region (1400-1200 nm).

2:3 Vibrational Spectroscopy [120, 121]

Vibrational spectroscopy has been extensively used by organic and inorganic chemists for many years. Infra-red and Raman spectroscopy have proved to be useful for identifying the structures of complexes and for quantitative analysis in some cases. Infra-red spectroscopy was used frequently in the present work. This was very helpful for the identification of the presence of coordinated ligands (for example MeCN) and fluoroanions in the reaction products.

When molecules absorb radiation from the infra-red region of the spectrum, they are raised to higher energy excited vibrational states. Infrared light is absorbed when the oscillating dipole moment of the molecular vibration interacts with the oscillating electric vector of the infra-red beam. A simple rule for deciding whether this interaction occurs or not is that the dipole moment at one extreme of a vibration must be different from the dipole moment at the other extreme of the vibration.

The importance of these selection rules is that in a molecule with a centre of symmetry those vibrations symmetrical about the centre of symmetry are Raman active and

inactive in the infra-red. Those vibrations which are not centrosymmetric are inactive in the Raman and usually active in the infra-red. For example, in octahedral molecules or ions, such as MF_6 or MF_6^- (where M = U, Mo or W) the two vibrational modes of symmetry T_{1u}, which are antisymmetric with respect to the centre of symmetry, are infra-red active, while vibrational modes of symmetry A_{1g}, E_g and T_{2g}, which are symmetric with respect to the centre of symmetry, are Raman active.

2:3:1 Sample Preparation:

Samples for infra-red spectroscopy can be prepared and examined as gases, liquids, solids or solution. In the present work, the samples studied were solids and thin films.

(i) Solid Samples:

Solid samples were prepared as mulls. Nujol (liquid paraffin) or Fluorolube (a fluorocarbon oil) were used as mulling agents; their absorption bands were distinguished readily from those of the sample. The solid sample (about 1mg) was first ground to a fine particle size using an agate mortar and pestle, and then two drops of the mulling agent were added. After the sample was dispersed to form a homogeneous mixture, it was pressed between silver chloride plates, which were then mounted in a suitable holder ready for examination.

(ii) Thin Film Samples:

The procedure used to record the electronic spectra of the thin films on silica substrates was repeated here.

A Pyrex gas cell similar to the one in Fig. 2:3, but fitted with silver chloride windows, was used to record the vibrational spectra of the thin films on KCl substrates.

For both the solid samples and the thin films samples the vibrational spectra were recorded over the range 4000-400 cm^{-1} using Perkin Elmer 580 or 983 spectrophotometers.

2:4 Nuclear Magnetic Resonance Spectroscopy [122,123,124]

N.m.r. spectroscopy can provide extremely useful information about the chemical environment of the different nuclei in a compound. For example, the spectra enable quantitative measurements of nuclear concentrations to be made or chemical shifts and coupling constants to be observed and hence structures determined.

The property of a nucleus known as its spin is the basis of nuclear magnetic resonance spectroscopy. For every isotope of every element there is a ground state nuclear spin quantum number, I, which has a value of n/2 (where n is an integer). Isotopes having atomic and mass numbers that are both even such as ^{12}C, ^{28}Si and ^{56}Fe, have I value equal to zero, therefore these nuclei have no n.m.r. effect.

Isotopes with odd atomic numbers but even mass numbers such as ^{2}H, ^{10}B and ^{14}N have n even, while those with odd mass numbers such as ^{1}H, ^{19}F, ^{13}C and ^{55}Mn have n odd. Some of this last group have values of I equal to $^1/_2$, and these are the nuclei most commonly studied by n.m.r. spectroscopy.

When I is non-zero, the nucleus has a magnetic moment, μ, which is given by the following equation:

$$\mu = v\hbar \; [I(I + 1)]^{1/2} \quad \ldots\ldots\ldots\ldots\ldots (2\text{-}1)$$

where h is Planck's constant and v is the magnetogyric ratio, which is a constant characteristic of the particular isotope. In the presence of a strong magnetic field, B_0, the spin axis orientation is quantized, with magnetic quantum numbers, m, taking values of I, I-1, I-2 .....-I. Irradiation at an appropriate frequency causes transitions, with a selection rule $\Delta m = -1$, and it is these transitions that were observed in the n.m.r. spectroscopy.

If a nuclei with I = $^1/_2$ is placed in a magnetic field, it may take up either a low-energy orientation in which the nuclear magnet is aligned with the field or a high-energy orientation in which it is aligned against the field. When the system is at equilibrium, the lower level will have a higher population (N_1) than the upper level (N_2). The energy difference (ΔE) between the two levels is given by the following equation.

$$\Delta E = \hbar v B_0 \quad \ldots\ldots\ldots\ldots (2\text{-}2)$$

The n.m.r. signal is due to the net absorption of radio-frequency radiation (i.e., more transitions from E_1 to E_2 than from E_2 to E_1 because $N_1 > N_2$). N.m.r. spectroscopy is less sensitive than optical spectroscopy because the ΔE, and hence ΔN values are much larger for infra-red or uv-visible spectroscopy than for n.m.r.

In the present work ^1H, ^{13}C and ^{19}F n.m.r. spectroscopy were employed to identify products of reactions.

2:4:1   Sample Preparation:

Samples for n.m.r. spectroscopy were prepared in single-limbed Pyrex vessels fitted with 5 mm precision n.m.r. tubes. The tubes were sealed in vacuo using a gas/oxygen flame. Generally $[^2H]$-hydrogen labelled acetonitrile, CD_3CN, was used as a solvent. In some reactions, $[^2H]$-hydrogen labelled trifluoroacetic acid, CF_3COOD, was used as a solvent. For ^{13}C spectra, $^{13}C/D$ signals were used as an internal reference, while for ^1H spectra, the residual ^1H in the respective CD_3CN solvent was used as an internal reference. For ^{19}F n.m.r. spectra, trichlorofluoromethane was used as an external reference. The spectra were recorded using Bruker AM200 and WP200SY spectrometers.

2:5 Electron Microscopy [124, 125]

Electron microscopy techniques were used in the present work for the study of the thin films of $[Al(Pc)F]_n$ polymer before and after reactions. A thorough examination of the thin film surfaces can be made due to the high magnification obtainable. Furthermore, internal crystallographic structure including defects in the lattice can be detected and analysed in detail.

The electron microscope uses a beam of electrons rather than a beam of visible light. The most common source of the electron beam is an electrically heated thin tungsten wire which acts as a cathode. The wavelength of an electron beam is only 0.037 $\overset{\circ}{A}$, thus the resolution of the microscope is not limited by the wavelength. It is in fact, limited by aberrations in the magnetic lenses.

The beam is accelerated into the condenser lens by an anode at earth potential and then focussed onto the specimen. The objective lens follows which forms the image which is in turn magnified by the intermediate and projector stages. Finally the electrons hit a fluorescent screen and an image is formed. This image can be recorded by replacing the fluorescent screen with a photographic plate. To minimise the scattering of the beam the entire column of the micro-scope is under high vacuum.

The operational instructions and other details of the electron microscope are described in Chapter 6.

2:5:1   Specimen Preparation:

Some of the thin films described later in this chapter were coated with a thin layer of carbon using Polaron E5000 coating unit.   The carbon coated films were then floated off the substrate (KCl or mica) onto distilled water.   The sample was then picked up on specimen grids of copper or gold (Agar Scientific Limited) and left in an oven at approximately $30^{o}C$ to dry.   The characterization of the sample was carried out using the transmission electron microscopes, Jeol 100C and Jeol 1200 Ex.

2:6   Preparation of Poly(fluoroaluminium-phthalocyanine), [Al(Pc)F]$_n$.
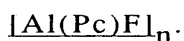
The [Al(Pc)F]$_n$ polymer was prepared using the procedure established by Kenney et al [2].   This procedure consists of the following three steps.

(i) Preparation of chloroaluminium phthalocyanine, [Al(Pc)Cl]

A mixture of 1,2-dicyanobenzene (phthalonitrile) (Aldrich Chemical Co. Ltd.; 10g, 78 mmol), freshly sublimed aluminium trichloride (Fluka AG; 5g, 37.5 mmol) and quinoline (Aldrich Chemical Co. Ltd; distilled twice at 463 K and atmospheric pressure and then deoxygenated with nitrogen, 50 cm^3) was refluxed for 1 h.   Initially a pale yellow solution was obtained; the colour changed through dark green to blue during the reaction.   After cooling to approximately 273 K the solution was filtered and a dark blue solid was isolated.

The solid material was washed successively with benzene, carbon tetrachloride and acetone and was dried to $110^{o}C$ (yield 5.6g, 9.75 mmol, 50%).

(ii) Preparation of (hydroxy)aluminium-phthalocyanine, [Al(Pc)OH.H_2O]:

A mixture of [Al(Pc)Cl] (4.25g, 7.4 mmol), ammonia (aq) (Aldrich Chemical Co. Ltd.; sp.gr. 0.880, 85 cm^3) and dried pyridine (B.D.H., Analar, 42.5 cm^3) was refluxed at 393 K and atmospheric pressure for 7 h. The resulting solution was filtered, and the filter cake was washed with pyridine, concentrated ammonia (aq) and hot water. The solid material was dried at 383 K (yield 2.48g, 4.32 mmol, 58.5%).

(iii) Preparation of poly(fluoroaluminium-phthalocyanine), [Al(Pc)F]$_n$

A mixture of [Al(Pc)OH.H_2O] (2.1g, 3.6 mmol) and two separate portions of 48% hydrofluoric acid, (HF aq) (B.D.H. Analar, 18 cm^3 each time) was evaporated to dryness on a steam bath. The resulting blue solid was washed with water, methanol, pyridine and acetone and dried at 283 K (yield 1.7g, 2.84 mmol, 83%).

Infrared spectrum of the [Al(Pc)F]$_n$ product was recorded in the region 4000-400 cm^{-1} as Nujol and Fluorolube mulls (Fig. 2:4). This was compared to that obtained by Djurado et al. [115]
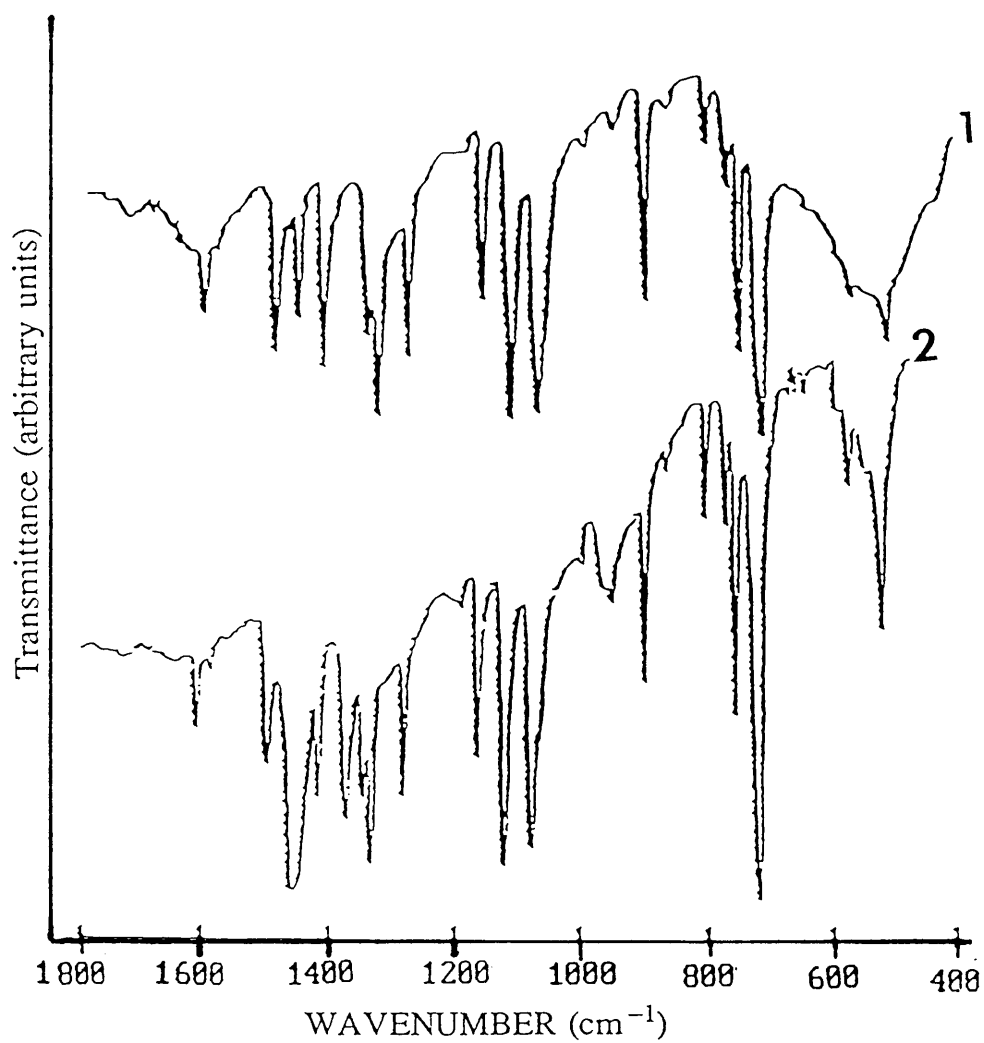
Figure(2:4).Infrared spectra of [Al(Pc)F]$_n$ (Nujol mull),
(1)from ref.[115],(2)from the present work.

2:7 Preparation of Thin Films of Poly(fluoroaluminium-phthalocyanine), $[Al(Pc)F]_n$.

It has been established that metal-phthalocyanine complexes form crystalline thin films with columns of parallel stacks of planar molecules [126]. For example thin films of copper-phthalocyanine, CuPc, were prepared by epitaxial growth on KCl cleavage face through vacuum evaporation [125].

This concept was used in the present work for preparing thin films of $[Al(Pc)F]_n$ polymer supported on different kinds of wafers. The wafers used, and their suppliers are described in the following:

I. KCl (100) (Hilger Analytical)

II. $LiNbO_3$ (z-cut) (Barr and Stroud Ltd, Pilkington electro-optic materials), mechanically polished on both faces to an optically smooth finish (using Syton W15 submicron powder), [127].

III. Silica, a large piece of polished Spectrosil-B (Multi-lab Ltd) was cut using a diamond saw into 20 x 10 x 1 mm rectangular wafers.

IV. Mica (Agar Scientific Ltd).

$LiNbO_3$ and silica wafers were degreased and carefully cleaned by soaking in 1,1,1-trichloroethane, methanol, and acetone successively, with 5 min ultrasonic agitation in each case. Finally the wafers were washed with isopropyl alcohol and dried in an oven at approximately $30^{\circ}C$. This cleaning

procedure was adopted to ensure clean surfaces of the wafers before use.   Mica and KCl wafers were freshly cleaved by a clean razor blade and used directly.

The preparation method of the films was carried out using an Edwards high vacuum coating unit (Fig. 2:5).   A measured quantity of $[Al(Pc)F]_n$ powder was placed in a molybdenum boat.   The single crystal wafers were clamped onto the furnace and placed above the molybdenum boat.   The system was pumped out until a presure of 10^{-6} Torr was obtained. The furnace was heated to a temperature of 493 K in order to obtain dry and clean wafer surfaces.   The boat was then heated until the $[Al(Pc)F]_n$ powder sublimed onto the wafer face.   The furnace was maintained at 493 K throughout for a further 30 min to ensure that the nucleation and growth of the phthalocyanine molecules align uniformly on the wafer surface.   After cooling to room temperature, the wafers were removed and stored in a warm oven ready for examination by transmission electron microscopy, vibrational and electronic spectroscopy.

2:7:1   Thickness of the films:

It is very important when preparing thin films to be able to control to some extent the thickness of the films since the structure and properties depend on the thickness. The film thickness was calculated to an order of magnitude, using the following equation .

$$T = \frac{3M \times 10^7}{16\pi r^2 d} \quad \dots\dots\dots\dots\dots\dots (2-3)$$

To high vacuum pumps
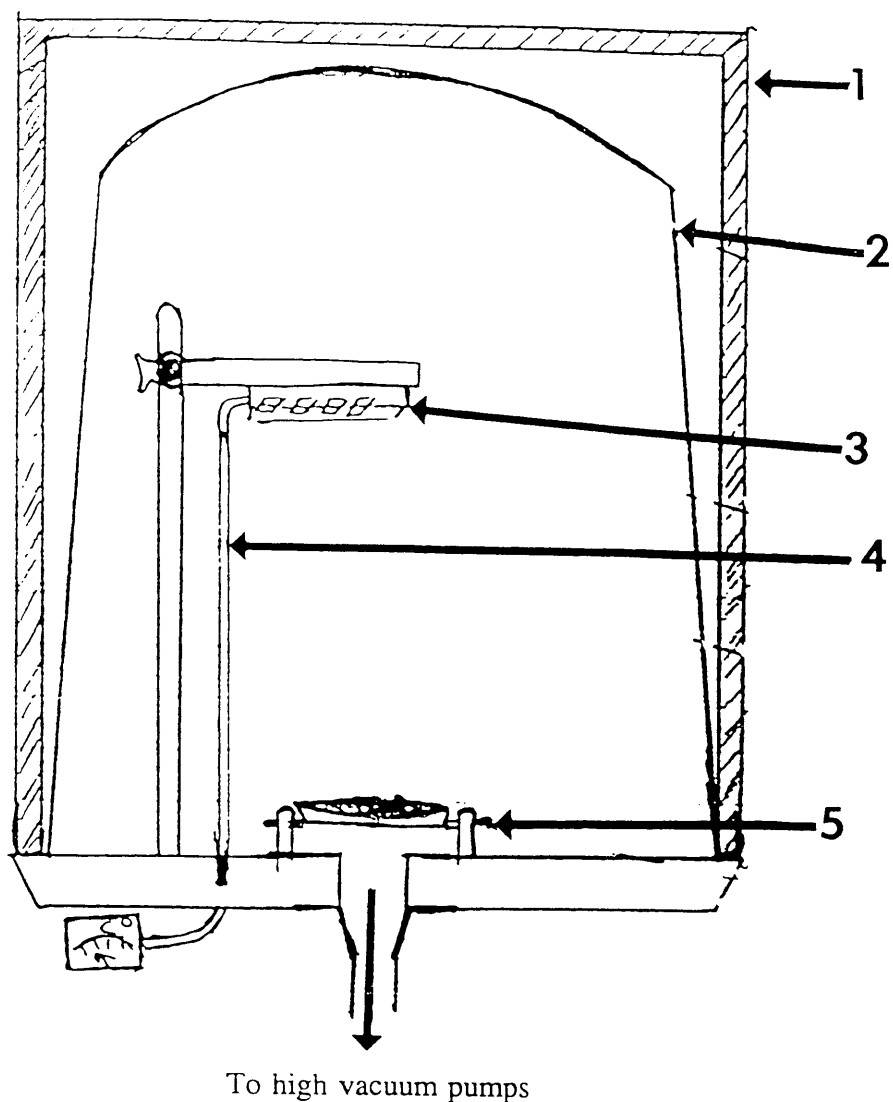
1. Protective shield
2. Glass bell jar
3. Furnace with KCl plate
4. Thermocouple
5. Mo boat with $[Al(Pc)F]_n$ powder.

Figure(2:5).Edwards high vacuum coating unit.

where M = mass of the material (g)

    r = source to substrate distance (cm)

    d = density of material (g cm^{-3})

    T = thickness of the film formed (nm)

2:8 Preparation and Purification of Molybdenum and Tungsten Hexafluorides [38, 45]

The hexafluorides of molybdenum and tungsten can be prepared by several methods. Examples of some preparative methods are given in Chapter 1. The method employed at this department consists of direct fluorination of pure molybdenum or tungsten metal powders with elemental fluorine at 573-632 K.

The procedure and apparatus used for the preparation of molybdenum hexafluoride and tungsten hexafluoride in the present work were identical. Here, the preparation of molybdenum hexafluoride is described. Like most transition metal hexafluorides, molybdenum hexafluoride (m.p. = 17.4°C, b.p. = 35°C) is a toxic and highly hygroscopic material. Therefore, it must be handled in a clean and dry high vacuum system. The preparation apparatus (Figs. 2:6 and 2:7) consisted of a 60 cm long nickel tube equipped with Swagelok couplings, glass apparatus and a small nickel boat.

The molybdenum powder (5g) was placed in the small nickel boat and spread as much as possible. The boat containing the molybdenum metal was then placed inside the nickel tube and the Swagelok coupling was replaced. The tube
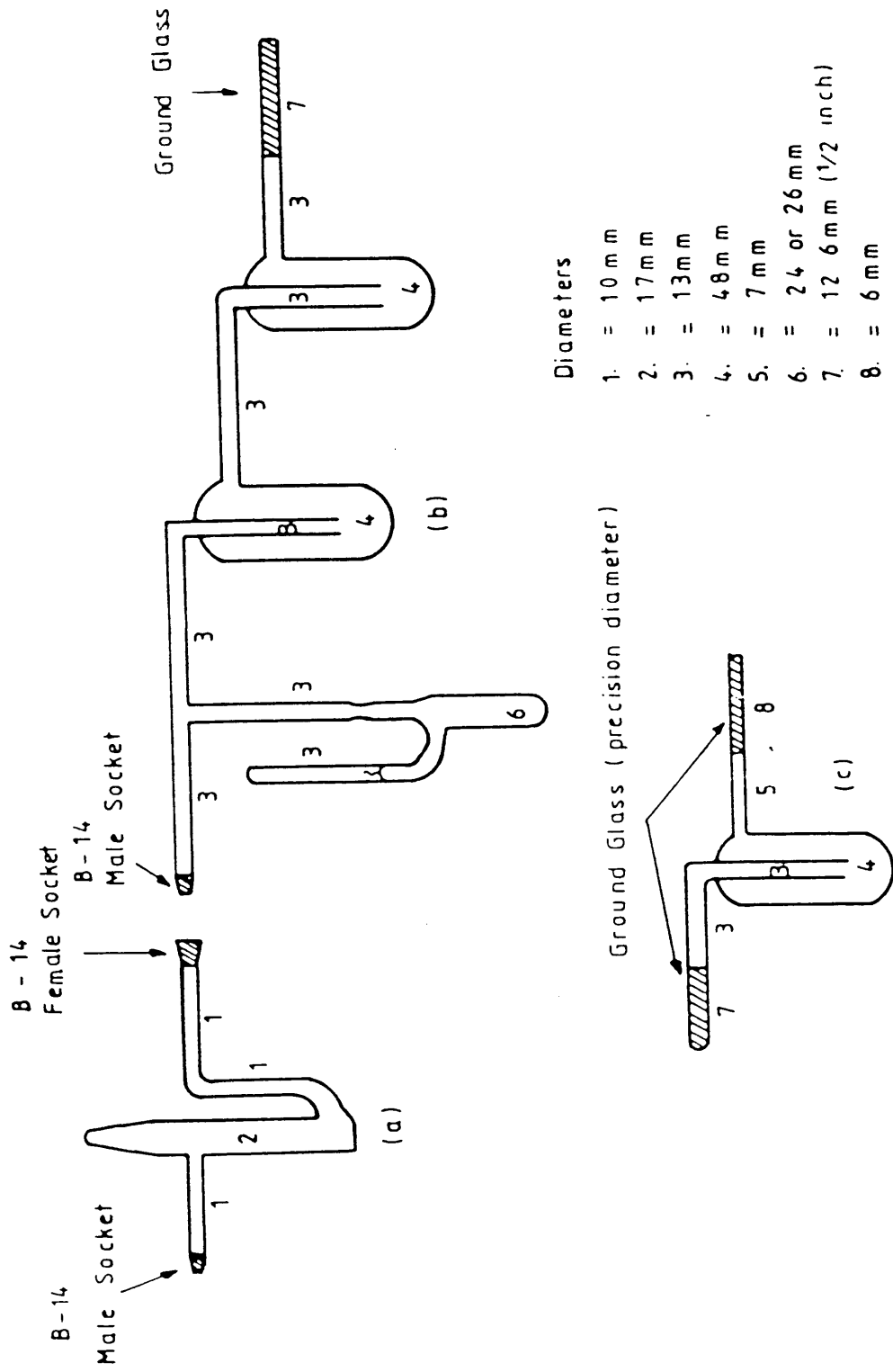
Figure(2:6).The glass apparatus used in the preparation of MoF_6.

3/4 inch nickel pipe

Male Connector
(3/4 inch NPT pipe
thread to 1/2 inch
tube)

nickel boat

Female Connector
(3/4 inch tube to 3/4
inch NPT pipe thread)
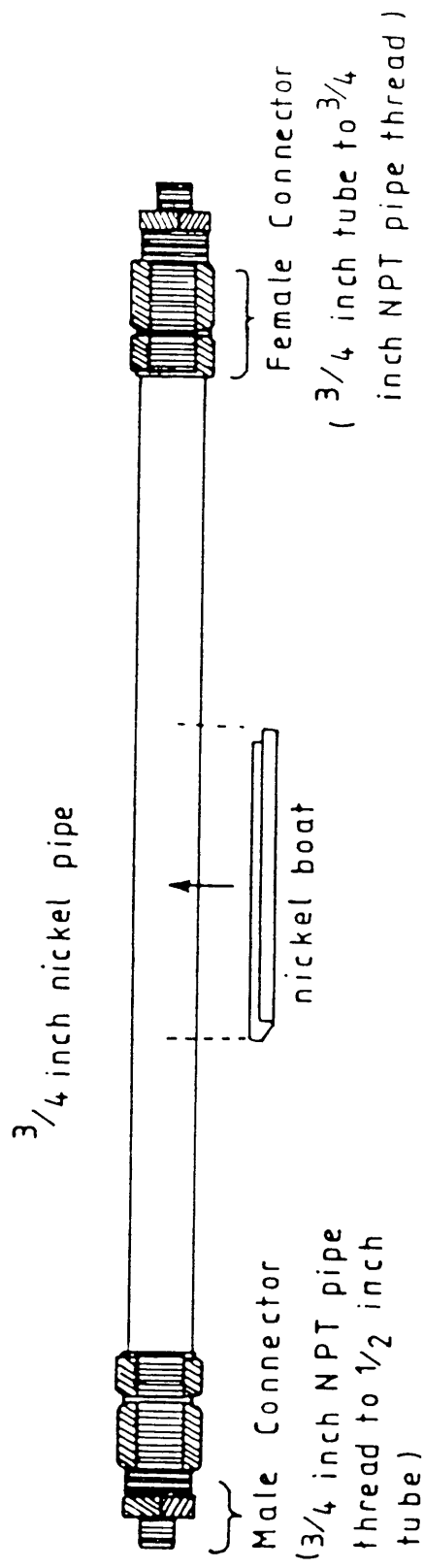
∴ BOTH CONNECTORS ARE STAINLESS STEEL.

Figure(2:7).Nickel tube & boat.

was placed in a furnace and glass apparatus, which contained sodium fluoride in traps E, F, G and I (Fig. 2:8) which were connected to the tube using the Swagelok couplings and P.T.F.E. ferrules. The apparatus was then attached to the fluorine gas cylinder on one side and connected to a vacuum line using Kel-F grease via B-14 sockets on the other side.

The apparatus was evacuated (10^{-2}Torr) and the glass section of the apparatus was degassed several times over a period of 2 hours. The traps containing NaF were flamed out three times using a medium flame from a gas oxygen torch. After the apparatus was cooled to room temperature, the stopcock A was closed and nitrogen gas was admitted very slowly into the system in order to bring it to atmospheric pressure. The joint B was disconnected and N_2 flow (70 cm^3 min^{-1}) was allowed to continue through the system for approximately 12 hours.

At this stage the furnace was switched on before the admission of fluorine in order to reach a reaction temperature of about 623 K. At the same time, cold traps were placed around trap C (for trapping moisture from the air), traps F and G (for collecting product MoF$_6$), and trap I (for trapping traces of HF). The traps were cooled to 193 K using dry ice/dichloromethane slush baths.

The fluorine cylinder was then opened, and the cylinder head pressure gauge was adjusted to 40 psi. Fluorine was passed through the system diluted with N_2 to give a 1:2 ratio by volume of fluorine/nitrogen and a total flow rate of 100 cm^3 min^{-1}. After about 5 minutes of fluorine/nitrogen flow, the furnace was switched off as the reaction is
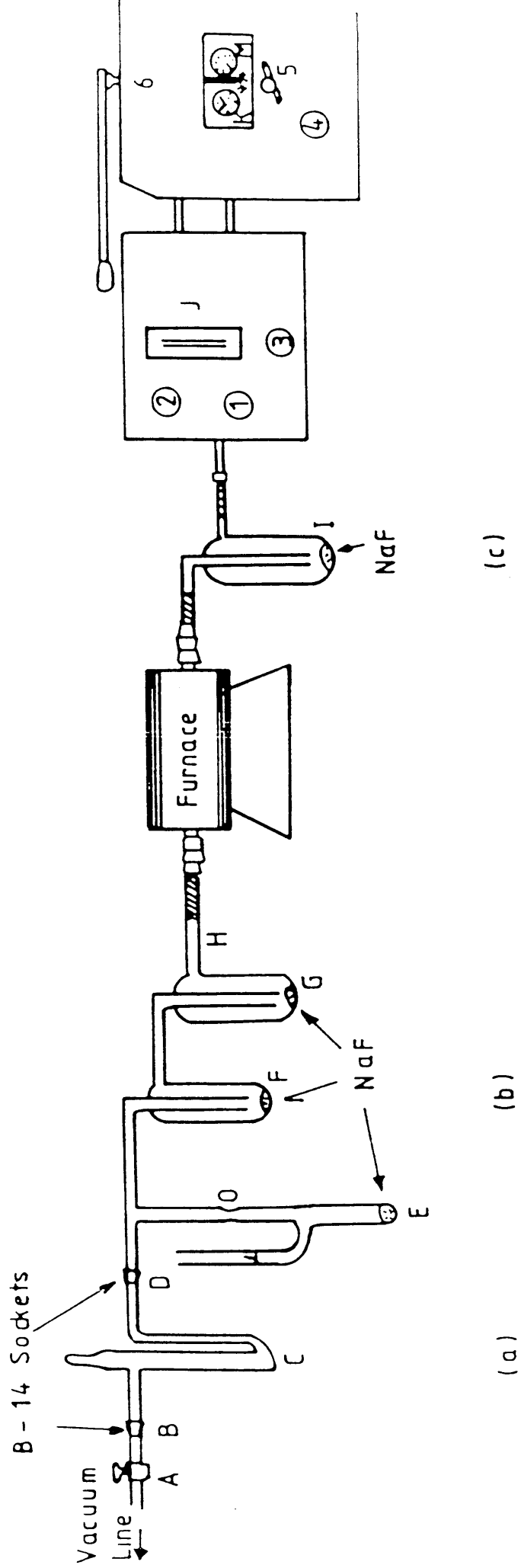
Figure(2:8).Fluorination system for MoF$_6$.
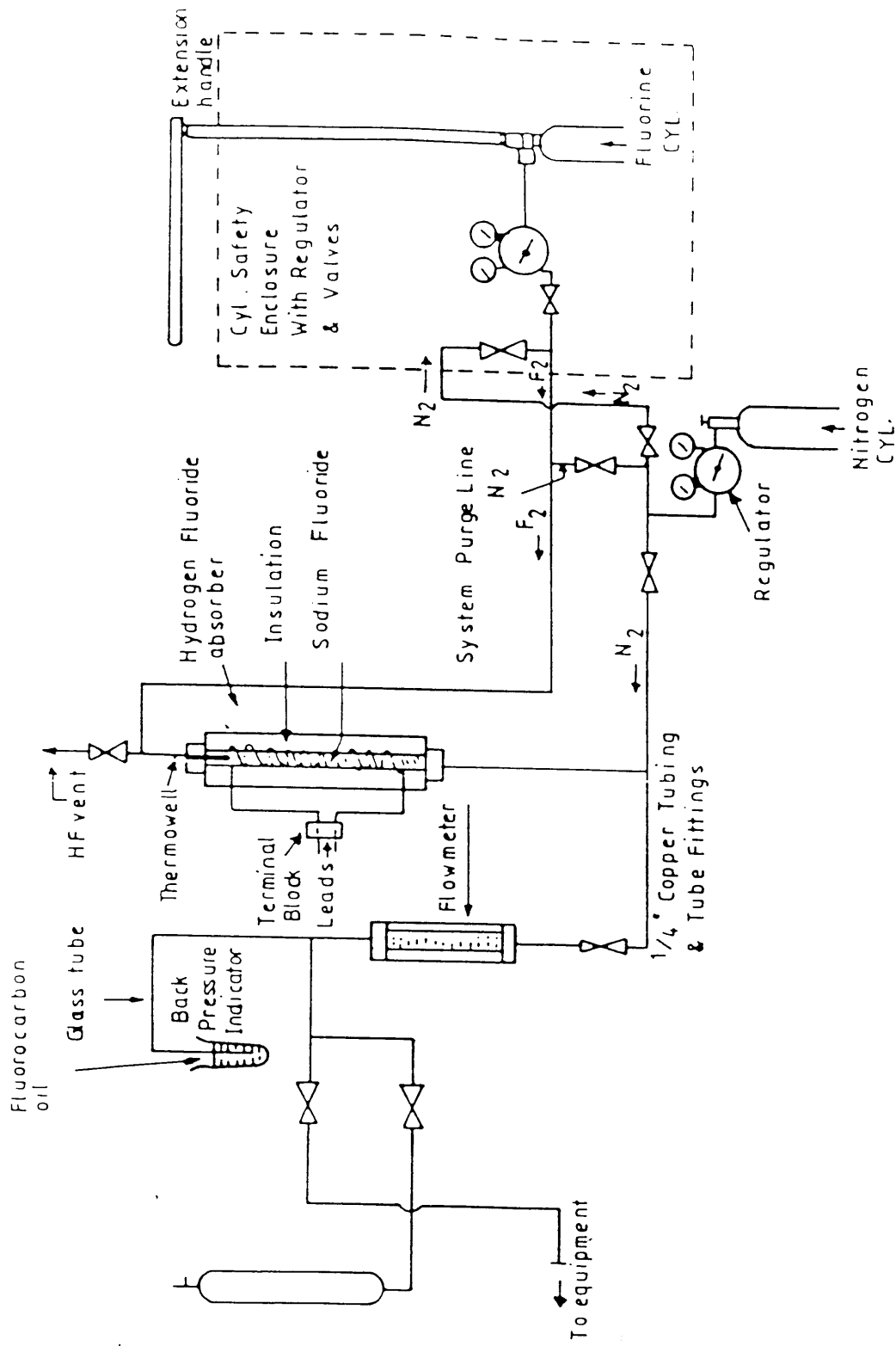
Figure(2:9).Fluorination laboratory set-up schematic.

exothermic. The reaction was completed within approximately one hour. Testing for F_2 at the exit of the apparatus was carried out by the use of moist potassium iodide/starch indicator paper.

When the reaction was completed, the main valve of the fluorine cylinder 6, was closed. After the cylinder pressure gauge had dropped to zero, valves 5 and 4 were closed. Nitrogen flow was then continued through the system for about 15 minutes.

The glass apparatus was sealed at point H, the collection train (b) was disconnected from trap (a) and attached immediately to a vacuum line. The collection train (b) containing the MoF_6 product frozen at 77 K was evacuated. Purification of the product was achieved by trap to trap vacuum distillation from G to F and then to E at 77 K. To obtain a pure product, a slow distillation was necessary at this stage, from 193 K to 77 K. The main impurity was usually $MoOF_4$ which is less volatile than MoF_6. Finally, the product was sealed in E at the point O and stored at 77 K.

2:9 Purification of Uranium Hexafluoride.

Uranium hexafluoride (British Nuclear Fuels, Plc) was purified by trap to trap vacuum distillation over activated NaF at 77 K to reduce any hydrogen fluoride impurity. The purified UF_6 was finally transferred into a previously flamed out break-seal vessel containing activated NaF at 77 K, and stored at this temperature until required.

2:10 <u>Purification of Acetonitrile.</u>

Acetonitrile has proved to be a useful solvent for solution reactions involving high oxidation state fluorides, for example the reactions described in Chapter 1. Before it can be used however, it has to be rigorously purified in order to remove moisture and impurities such as acrylonitrile and benzene. The purification of MeCN has been carried out by different workers using different methods. The method applied in this department [128], is an extension of the method established by Walter and Ramalay [129]. It consisted of a series of refluxes of MeCN (HPLC Grade, Rathburn Chemicals Ltd) followed by rapid distillation in a Pyrex still equipped with a 0.75 m vacuum-jacketed separating column, which was protected from atmospheric moisture by silica-gel drying tubes. The following sequence of reagents was used, quantities and times are given in parentheses:

(i)   Anhydrous $AlCl_3$ (15g dm^{-3}; 60 min)

(ii) $KMnO_4$ + Li_2CO_3 (10g dm^{-3} each; 15 min)

(iii) $KHSO_4$ (15g dm^{-3}; 60 min)

(iv) CaH_2 (20g dm^{-3}; 60 min)

(v) and (vi) P_2O_5 (1g dm^{-3}; 30 min)

The solvent was distilled rapidly and topped and tailed by approximately 3% after each reflux. At the final stage the distilled acetonitrile was collected in vessels containing activated Al_2O_3 (neutral 60 mesh) without exposure to atmospheric moisture, and degassed twice <u>in vacuo</u>. The MeCN was then transferred to a storage vessel containing previously activated 3A molecular sieves by vacuum

distillation at 77 K (200 cm^3). Acetonitrile purified in this way had an absorbance of less than 0.05 (H$_2$O reference) at 200 nm and an apparent u.v. cut-off at about 175 nm.

2:11 Purification of The Halogens.

As stated earlier in this chapter, most of the materials and reagents used in the present work are sensitive to oxygen and atmospheric moisture. The starting materials had therefore to be purified and dried thoroughly before use.

The purification of halogens used in the present work was carried out using the following procedure.

A quantity of dichlorine (Matheson) or dibromine (B.D.H. Analar) was vacuum condensed from the metal cylinder into a Pyrex vessel fitted with a Rotaflo stop cock at 77 K. The vessel was opened up to the vacuum line and pumped for approximately 5 min. The halogen was distilled into a previously evacuated and flamed-out vessel. The vessel was allowed to warm up to 193 K using slush bath (mixture of dichloromethane and ice) and left at this temperature for 5 min. The vessel was then pumped for a short time on the vacuum line in order to remove trace air and HBr (in the case of Br$_2$). At this stage the halogen was vacuum distilled from 193 K to 77 K; this process was repeated twice. Finally, the halogen was degassed and vacuum distilled into a vessel containing freshly sublimed phosphorus pent oxide and stored at 77 K ready for use. Diiodine was purified by subliming the solid (B.D.H. Analar) under vacuum into a

previously evacuated and flamed out Pyrex single-limbed vessel at 77 K. The purified diiodine was stored in vacuo at room temperature ready for use.

The purification of difluorine was carried out during the preparation of molybdenum hexafluoride which is described earlier in this chapter. Difluorine was diluted with N_2 and passed over traps containing activated NaF to remove any hydrogen fluoride which may be present as an impurity.

2:12 Purification of the Pentafluorides of Phosphorus, Arsenic and Iodine.

The pentafluorides of phosphorus, arsenic and iodine from the cylinder usually contain impurities such as POF_3, AsF_3 and I_2 respectively. Hydrogen fluoride impurity may also be present with the above pentafluorides. In order to remove any of these impurities, the pentafluorides used in the present work (PF_5, AsF_5 and IF_5) were purified using the following method:

A quantity of phosphorus pentafluoride (Fluorochem Ltd), arsenic pentafluoride (Matheson) or iodine pentafluoride (Fluorochem Ltd) was vacuum condensed from the metal cylinder into a Pyrex glass vessel fitted with a Rotaflo stop-cock at 77 K. The vessel was opened up to the vacuum and degassed for approximately 3 min. The pentafluoride (PF_5, AsF_5 or IF_5) was trap-to-trap vacuum distilled over activated NaF and finally transferred into a break-seal vessel at 77 K where it was stored over NaF at this temperature ready for use.

2:13 Purification of Aluminium(III) Chloride:

Aluminium(III) chloride was purified by sublimation using an all glass manifold (Fig. 2:10);the following method was used in the present work.

Aluminium(III) chloride (anhydrous. > 99% pure, Fluka AG, 5g) along with a piece of aluminium wire (99.99% pure, Fluka AG/Balzers) was loaded into a previously evacuated and flamed-out break-seal vessel fitted with a B-14 cone and Rotaflo stop cock in the glove box. The vessel was re-evacuated and sealed off at point D using a gas-oxygen torch before being joined to the manifold. The manifold was flamed-out under vacuum, the seal broken open using a glass sealed metal bar, and tap S closed. Aluminium(III) chloride was then sublimed under vacuum (10^{-4} Torr) at 393 K using an electrical furnace fitted with a thermocouple. The sublimate was collected in the u-shaped tube at 77 K. The tube was sealed at points L and N and transferred to the glove box where the sublimate was transferred to a previously flamed-out and evacuated vessel. Finally the vessel was attached to the vacuum line, re-evacuated and stored under vacuum until required.

To vacuum

S

L

N

(77 k)

2

D

1

6

3

4

5

1. Break-seal vessel contains $AlCl_3$

2. Glass sealed metal bar

3. B-14 Ground glass cone

4. Rotaflo stopcock

5. Liquid N_2

6. Electric furnace fitted with a thermocouple
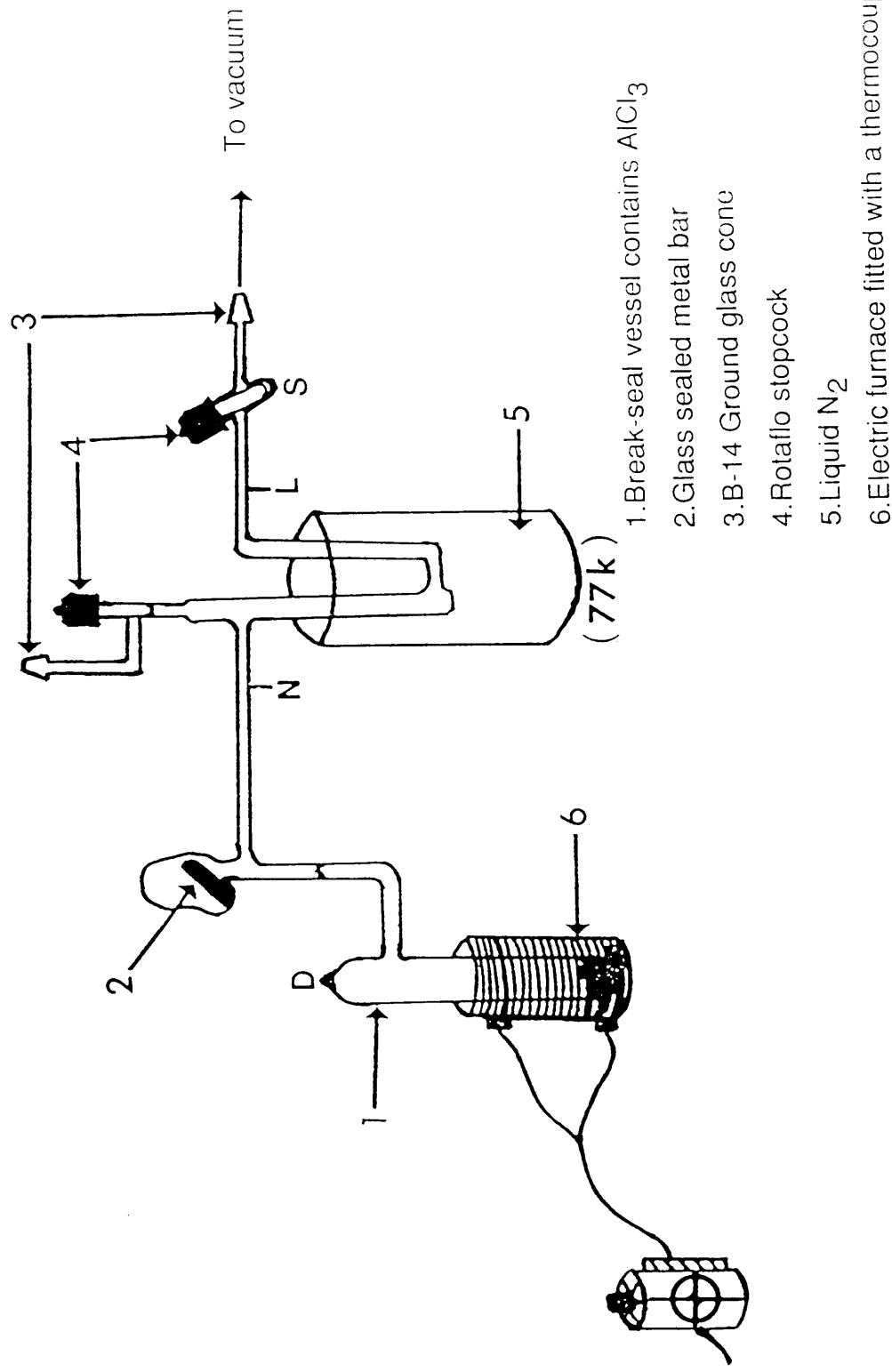
Figure(2:10). The apparatus used in the purification of aluminium(III) chloride.

CHAPTER THREE

SOLUBILITY OF POLY(FLUOROALUMINIUM-PHTHALOCYANINE), $[Al(Pc)F]_n$.

3:1 - Introduction

The majority of chemical reactions and many spectroscopic measurements are carried out in solution. Therefore, the physical and chemical properties of the solvent can play an important role in determining the success of many organic and inorganic reactions in solution.

In most chemical interactions between the solute and solvent molecules the solvation process takes place through the formation of hydrogen-bond complexes or donor-acceptor complexes. Hydrogen-bond complexes are usually formed when a hydrogen atom in a compound such as R-O-H is bound in a covalent fashion to one of the electronegative atoms of another compound such as R-O-R as in the following equation (equation 3-1)

$$R-O-H \ + \ R-O-R \longrightarrow R-OH....\overset{\underset{|}{R}}{O}-R \quad .... \ (3-1)$$
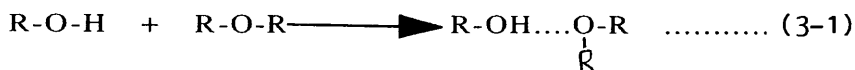
While donor-acceptor complexes are formed as a result of the chemical interaction between a molecule or ion that has at least one electron pair that can be so donated (Lewis base) such as Et_2O and metal ions or molecules with incomplete valence electron shells (Lewis acids) such as BF_3 as in the following equation (equation 3-2)

$$Et_2O \ + \ BF_3 \longrightarrow \ \overset{Et}{\underset{Et}{>}}O - \overset{F}{\underset{F}{B}} - F \quad .... \ (3-2)$$
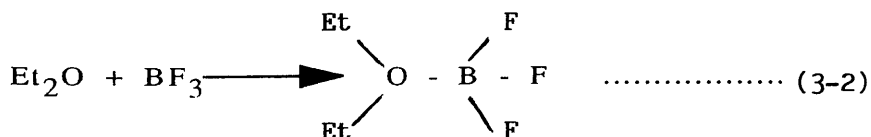
Many compounds can be formed by carrying out reactions in aqueous media, however, problems often occur because of

the acidities and basicities available in water. When extremely acidic or basic media are used, unusual cationic or anionic species can be formed, the stabilities of which depend on the availability or the non-availability of basic or acidic species in the solvent. However, handling of these reagents is not so easy and presents a number of difficulties. The use of superacids presents problems due to their highly corrosive properties. Acidic solvents like sulphur dioxide or bases such as liquid ammonia require low temperatures and specially designed apparatus to work with them safely. Some of these difficulties can be prevented by using an appropriate organic solvent.

A great number of protonic and aprotic solvents could be used for studying the chemistry of cations in non-aqueous media. Protonic solvents such as liquid ammonia or sulphuric acid, usually suffer self-ionization through the transfer of a proton from one molecule of the solvent to another. This results in the formation of a solvated proton and a deprotonated anion. Aprotic solvents which do not involve the transfer of a proton may conveniently be divided into three groups [130]. The first group includes solvents such as benzene and cyclohexane, which are non-polar, do not suffer self-ionization and therefore generally behave as non-solvating agents. Solvents that are polar and do not ionise to an appreciable extent, form the second group. Examples of this type are, acetonitrile, acetone, pyridine, dimethyl-sulphoxide (DMSO) and sulphur dioxide. These are good coordinating solvents because of their polarity which ranges from low in the case of SO_2 to extremely high in the case of (DMSO). Most of the solvents belonging to this group are Lewis bases. The third group consists of solvents which are

highly polar and auto-ionising such as bromine trifluoride and iodine pentafluoride; these two solvents are Lewis acids.

The choice of a solvent for inorganic or organic synthesis is obviously large. Each solvent has its own merits, but ease of handling, non-corrosive properties, convenient liquid range, useful volatility range, useful for spectroscopic work and ease of purification are general criteria which make a solvent attractive for synthesis.

The solubility of a complex in the polymeric form in most common solvents is generally low compared to its monomeric form [92]. The process of dissolving such a polymer in any solvent involves three fundamental steps, the penetration of the solvent, the separation of the polymer chains and the solvation of the chains. For separation of the chains to occur, the solvent must be able to overcome the inter-chain forces which vary in strength from weak dispersion forces to strong chemical bonds. Since the inter-chain forces are determined by the chemical nature of the polymer, the chemical nature of the solvent in relation to the polymer is very important. In addition to separating the chains, the solvent must be able to solvate the polymer chains in order to reduce the free energy of the separated chains so that dispersion of the chains in the solvent can take place.

The properties of a polymer such as its structure or polarity can significantly affect its solubility. For instance, non-polar polymers generally tend to dissolve in non-polar solvents. Polymers with cross-linked structures, in general, are not soluble in most ideal solvents [92]; this

is due to the covalently linked atoms in these polymers and consequently the polymer chains are permanently tied together. Penetration of the solvent may take place in the cross-linked polymers, but dispersion of the chains is not possible. Polymers with low molecular weight usually dissolve more readily than high molecular weight polymers. Polymeric fluorine-bridged complexes, in general, are difficult to dissolve in most common solvents, for example the compound $[Ru(CO)_3F_2]_4$ [131].

Metal-phthalocyanines and their numerous stable complexes are practically insoluble in water and organic solvents because they are hydrophobic and have high molecular lattice energies. Even in supersolvents such as sulpholane and DMFA they are not soluble, in quinoline and α-chloro-naphthaline, their solubility does not exceed 10^{-5} mol dm^{-3} [132]. Berezin et al [133] have shown that phthalocyanine complexes do not react with aqueous solutions of most strong mineral acids and do not pass into solution. However, these workers have reported that the most effective and practically the only solvent for phthalocyanines is concentrated sulphuric acid. The solubility of all stable phthalocyanines is high in sulphuric acid and may vary widely with its concentration. Many reactions involving metal-free phthalocyanine or its metal derivatives with highly acidic solvents have been described by Moser et al [126]. For example the reactions of thin films of metal-free phthalocyanine with gaseous hydrogen chloride and hydrogen bromide; the reactions of iron(II) phthalocyanine with concentrated aqueous hydrochloric and hydrobromic acids have been also reported [126]. These workers have suggested that the above reactions involved protonation of one of the

bridging nitrogen atoms in the phthalocyanine molecule. In order to obtain reliable values for the degree of protonation of several phthalocyanine complexes in highly acidic media, the same workers [126] have reacted metal-free phthalocyanine and its copper derivative with chlorosulphuric acid. They have made conductometric measurements on the solutions obtained from the above reactions and concluded that all of the bridging nitrogen atoms in the phthalocyanine molecule were protonated; it is noteworthy that HSO_3Cl is more acidic than H_2SO_4 [133]. However detailed information about the species present in solutions of these compounds in highly acidic solvents is lacking.

An improvement in the solubility of metal phthalocyanine complexes has been achieved by attaching substituents such as chloro, amino, hydroxy and sulphonate groups to the benzene rings of phthalocyanine ligands [101]. This approach has been applied to phthalocyanines of group 1 and 2 elements; the derivatised compounds are soluble in most spectroscopically transparent and electrochemically useful solvents when chloro or sulphonate groups were attached to their benzene rings through chlorination or sulphonation reactions [134]. Metal-phthalocyanine derivatives of the general type $MPc(SO_3H)_n$ (where M=Cu, Fe and Co; n = 2-4) are of interest as water-soluble compounds [101,135].

In the present work, various organic and inorganic solvents (table 3:1) were used in an attempt to determine the optimum conditions required to dissolve the $[Al(Pc)F]_n$ polymer. In earlier work [2,3] using this polymer it has been reported that nitromethane and 1,2-dichlorobenzene could be used as solvents in the solution reactions of the polymer

Table(3:1)[a]. The solvents used in the present work with their relative permittivities and vapour pressure values.

Solvent	Relative Permittivity at 298 K	Vapour Pressure Torr at 298 K
1. Acetone	20.7	166.6
2. Benzene	2.274	100
3. Acetonitrile	38	89
4. 1-Chloronaphthalene	2.54	<1
5. Chlorobenzene	5.6	10
6. Quinoline	9	<1
7. Toluene	2.38	33.3
8. Pyridine	12.3	23
9. Conc. H_2SO_4 (98%)	107	<1
10. Trifluoroacetic acid[b]	39	72
11. Trifluoromethane-sulphonic acid[c]	120	<1

a Ref 137   b Ref 138   c Ref 7

with $NOPF_6$ and diiodine respectively. However, in all the solution reactions of this polymer studied to date, there is no information about its solubility properties or the ability of the solvents used to dissolve it. The aim of the present work was to obtain as much information as possible about the solubility properties of this polymer using the solvents in table 3:1. The present study was also carried out to select a suitable solvent for performing reactions in solution between the $[Al(Pc)F]_n$ polymer and various oxidising agents; these reactions are reported in chapters 4 and 5.

The solvents in table 3:1 were chosen according to the information obtained from the study of the molecular structure [5], physical and chemical properties, and the acid-base behaviour expected from $[Al(Pc)F]_n$. The physical and chemical properties of each solvent are very important. For instance, the solvents should have reasonable vapour pressures at room temperature in order to use them in vacuum line work. The nature and chemical reactivity of the solvent are also important to avoid any undesirable reactions which could occur during the solvation process.

Two important features of metal-free and metal-phthalocyanine complexes are their electronic and vibrational spectra. The electronic spectra of all metal-free and metal-phthalocyanine complexes contain several bands in the u.v. and visible regions. In most of the reported work involving metal phthalocyanines in general [3], the bands in the visible region have been labelled as Q bands; those in the u.v. region were labelled as B bands. This nomenclature was first used for the transition bands in the electronic spectra of porphyrin complexes [138]. Because of the

similarity between the structures and the spectra of phthalocyanine and porphyrin complexes, the same names (Q and B) have been used in the descriptions of the electronic spectra of phthalocyanine complexes. In order to simplify the discussion of the spectra obtained in the present work the bands in the B region (traditionally called the Soret region) are labelled from low to high energy, as B_1, B_2 and B_3. Both electronic and vibrational spectra of these complexes are treated in detail in chapter 4.

3:2 Experimental

The experimental methods used throughout the course of the present work were very similar. Table 3:1 shows that some of the solvents (solvents No. 1,2,3,7,8 and 10) have high vapour pressures and are readily volatile at room temperature; these solvents were suitable for vacuum line work. Other solvents in the table, (solvents No. 4,5,6,9 and 11) have low vapour pressure and were used on the open bench. Trifluoroacetic acid and trifluoromethanesulphonic acid were purified by trap-to-trap vacuum distillation at 77 K in order to remove dissolved oxygen and to reduce any impurities such as hydrogen fluoride which may have been present . This purification process was repeated several times until the acids were colourless. Due to the very low vapour pressure of trifluoromethanesulphonic acid at room temperature , its purification process was lengthy, far longer than that of CF_3COOH. To purify 8 cm^3 of the acid took approximately seven hours.

For the solvents with high vapour pressures the

following method was used to study solubility of $[Al(Pc)F]_n$. A flamed out u.v. cell (Fig. 2:2) was loaded with $[Al(Pc)F]_n$ powder (9 mg, 0.016 mmol) in the dry box. The cell was attached to the vacuum line and re-evacuated and the solvent (8 cm^3) was added to the cell by vacuum distillation at 77 K. The mixture was allowed to warm up to room temperature and coloured solutions and suspensions were obtained as the solvents showed different abilities to dissolve the $[Al(Pc)F]_n$ polymer (table 3:2). Each mixture was shaken for 3 h and then left to stand overnight to allow the suspension to settle. For the solvents with low vapour pressures, the polymer (9 mg, 0.016 mmol) was mixed with the solvent (8 cm^3) in the u.v. cell on the open bench. The solutions and suspensions formed from both of the above methods were examined by electronic spectroscopy in the region between 1000-185 nm. Solutions of $[Al(Pc)F]_n$ in trifluoroacetic acid were also examined using nuclear magnetic resonance spectroscopy. In some cases the solids isolated from solutions were also examined by vibrational spectroscopy. Thin films of $[Al(Pc)F]_n$ deposited on KCl and silica substrates were exposed to the vapour of CF_3COOH and examined by i.r. and electronic spectroscopy respectively. The results of these reactions were compared with those obtained from the solution reactions.

3:3 Results and Discussion

In an attempt to give an explanation of the results obtained, the discussion will be based on the acid-base behaviour of both the polymer and the solvent. Previously obtained information about the acidic or basic properties of metal-phthalocyanine complexes in general and the solvents

used in the present work was taken into account in the
interpretation of each result.

3:3:1 - <u>Results.</u>

The solvents used in the present work could be classified into three groups according to their abilities to dissolve the $[Al(Pc)F]_n$ polymer:

I. Solvents with no ability to dissolve the $[Al(Pc)F]_n$ polymer:

These solvents included acetone and benzene. Although they have relatively high vapour pressures at room temperature which make them ideal solvents for vacuum line work, they failed to show any ability to dissolve the polymer. The mixtures of these solvents with the polymer were colourless and did not show any absorption in the u.v. and visible regions.

II. Solvents with weak abilities to dissolve the $[Al(Pc)F]_n$ polymer:

These solvents included acetonitrile, 1-chloronaphthalene, chlorobenzene and quinoline; they appeared to dissolve a very small quantity of the polymer (~ 1mg) and formed pale blue solutions. However most of the solute remained undissolved. Similar behaviour was observed using pyridine and toluene. Mixtures of these solvents with the polymer resulted in pale blue suspensions unaffected even after they were left for several days to settle. The electronic spectra of the above solutions and suspensions showed several electronic absorption bands in the region between 700-200 nm (Fig 3:1). Owing to the low solubility of the $[Al(Pc)F]_n$ polymer in these solvents it was not possible to determine
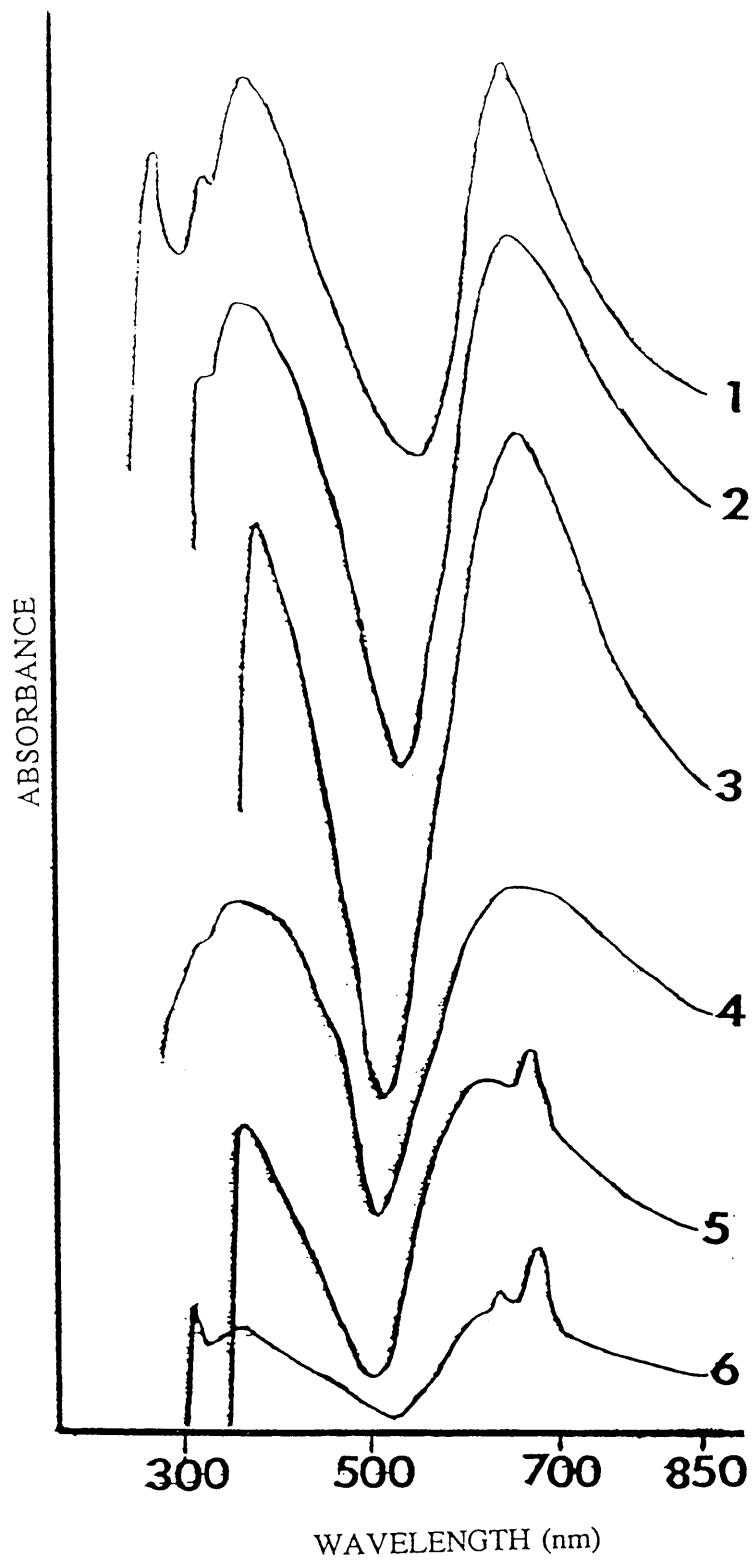
Figure(3:1).Electronic spectra of the mixtures of [Al(Pc)F]$_n$
with (1).acetonitrile,(2).1-chloronaphthalene ,
(3).chlorobenzene,(4).toluene,(5).quinoline and
(6).pyridine.

the concentrations of the solutions or suspensions obtained. Therefore, the molar extinction coefficient values (ε) of the bands observed in the spectra were not calculated. These bands along with other properties observed are illustrated in table 3:2.

III. Solvents with high ability to dissolve the $[Al(Pc)F]_n$ polymer:

These solvents included sulphuric acid (with various concentrations), trifluoroacetic acid and trifluoromethane-sulphonic acid.

A. Solubility of $[Al(Pc)F]_n$ in different concentrations of sulphuric acid:

The concentrations of H_2SO_4 used ranged from 0.2-16.2 mol dm^{-3}. These concentrations were prepared by the dilution of measured volumes of 98% H_2SO_4 (18 mol dm^{-3}) with distilled water in volumetric flasks.

At low molarities of H_2SO_4 solution ($c = 0.2$-4 mol dm^{-3}) the $[Al(Pc)F]_n$ was not dissolved. The mixtures were colourless and their electronic spectra did not show any absorption in the u.v./visible regions. Increasing the concentration of H_2SO_4 resulted in the formation of coloured solutions as the $[Al(Pc)F]_n$ started to dissolve. The colours of these solutions were dependent on the concentration of H_2SO_4 used as shown in tables 3:3 and 3:4. These experiments indicated that the higher concentrations of H_2SO_4 used the more $[Al(Pc)F]_n$ polymer became soluble. When the concentration of H_2SO_4 ranged from 4.6-11 mol dm^{-3} some

Table(3:2)[*].Electronic spectra (λmax,nm) and other properties observed from the mixtures of $[Al(Pc)F]_n$ with the solvents in group (II).

Solvent	solubility of $[Al(Pc)F]_n$	Colour of mixture	λ_{max} (nm)
Acetonitrile	low	Pale Blue	621 332 287 231
Cloronaphthaløne	low	Pale Blue	634 348
Chlorobenzene	low	Pale Blue	631 229
Quinoline	low	Pale Blue	677 625 370
Toluene	very low	Pale Blue	637 318
Pyridine	very low	Pale Blue	670 631 345

[*] Due to the low solubility of $[Al(Pc)F]_n$ in these solvents the concentrations of Al^{III} in the mixtures were not determined, therefore, the ε values of the absorption bands observed in the spectra were not calculated.

Table(3:3)[*].Electronic spectra (λmax,nm) and the colours of the solutions of $[Al(Pc)F]_n$ in different concentrations of sulphuric acid (4.6-11 mol dm^{-3}).

Concentration of H_2SO_4 (mol dm^{-3})	Colour of solution	λ_{max} (nm)
4.6	Pale Blue	645 330 205
5.5	Pale Blue	645 315 235 195
6.4	Pale Blue	645 335 275 200
7.3	Pale Blue	695 375 295 210
8.3	Pale Green	730 305 235 195
9.2	Pale Green	705 390 300 205
10	Pale Green	700 395 295 210
11	Pale Green	740 705 390 295 210

[*] Due to the low solubility of $[Al(Pc)F]_n$ when the concentration of H_2SO_4 ranged from 4.6-11 mol dm^{-3} the concentrations of Al^{III} in the mixtures formed were not determined and,hence,the ε values of the bands observed were not calculated.

Table(3:4).Electronic spectra (λmax,nm) and the coloures of the solutions of [Al(Pc)F]$_n$ in different concentrations of sulphuric acid (12-16.2 mol dm^{-3}).

Concentration of H_2SO_4 (mol dm^{-3})	Colour of solution	λ_{max} (nm)	ε (mol^{-1} dm^3 cm^{-1})
12	Dark Green	785	8500
		755	9000
		680	9000
		405	7500
		305	9000
		210	9000
12.85	Dark Green	790	5500
		755	6500
		680	5000
		415	5500
		305	6500
		190	7000
13.8	Dark Green	785	27000
		756	27000
		720	11500
		680	10000
		430	8500
		305	16500
		205	17500
		195	14500
		190	12000
14.7	Dark Green	830	30000
		460	31500
		410	26500
		335	31500
		255	29500
		250	26500
		200	31500
		195	19500
		190	18000
16.2	Yellow	----	----

quantity of the polymer remained undissolved in the bottom of the cell. Therefore it was not able to determine the exact concentration of Al^{III} in these solutions. As concentration of H_2SO_4 ranged from 12-16.2 mol dm^{-3}, all the quantity of $[Al(Pc)F]_n$ used was dissolved and dark green and yellow solutions were formed. The concentration of Al^{III} in these solutions was determined as ca 0.02 mol dm^{-3}.

All the above solutions were examined by electronic spectroscopy in the region 1000-185 nm. The spectra indicated that several changes involving the bands in the Q and B regions had occurred following the increase in the concentration of H_2SO_4. The Q band was shifted to longer wavelength (lower energy), broadened and split into several components during the gradual increase in the concentration of H_2SO_4 (tables 3:3 and 3:4). The B1, B2 and B3 bands were shifted to longer wavelength and increased in intensities. Typical spectra showing the spectral changes in the Q and B bands when the concentration of H_2SO_4 was 11-12.85 mol dm^{-3} are shown in figure 3:2. When the concentration of H_2SO_4 was 16.2 mol dm^{-3} the solution was yellow and it was not possible to record its electronic spectrum because all the absorption bands were off scale. This solution was diluted several times with distilled water in which the colour changed from yellow through green to pale blue. The electronic spectrum of the diluted solution showed a decrease in the intensities of all absorption bands; the positions of these bands remained constant.

In most reported studies involving metal-phthalocyanine complexes it has been found that the spectral region between 500 nm and 200 nm is complicated and generally not well known
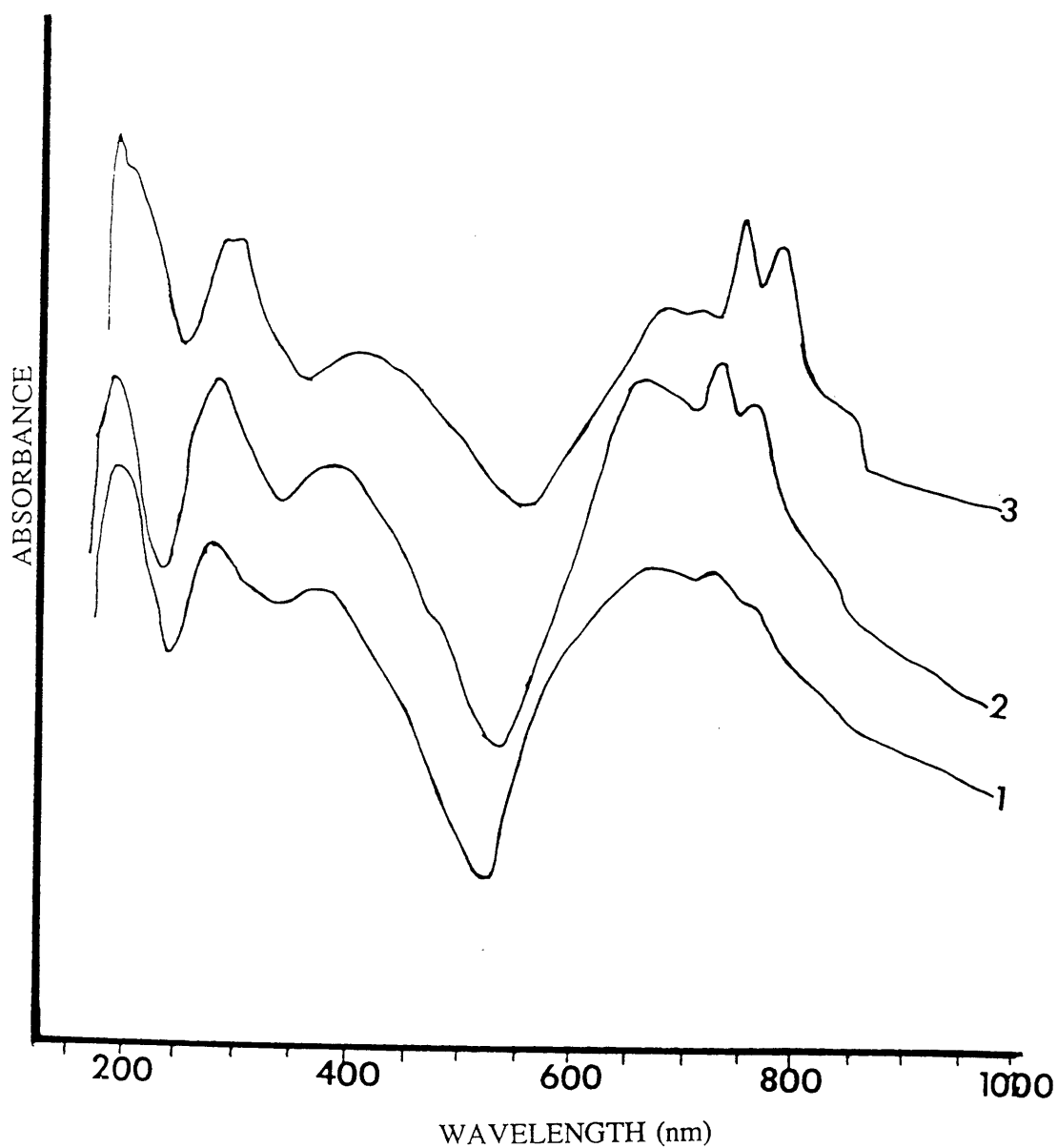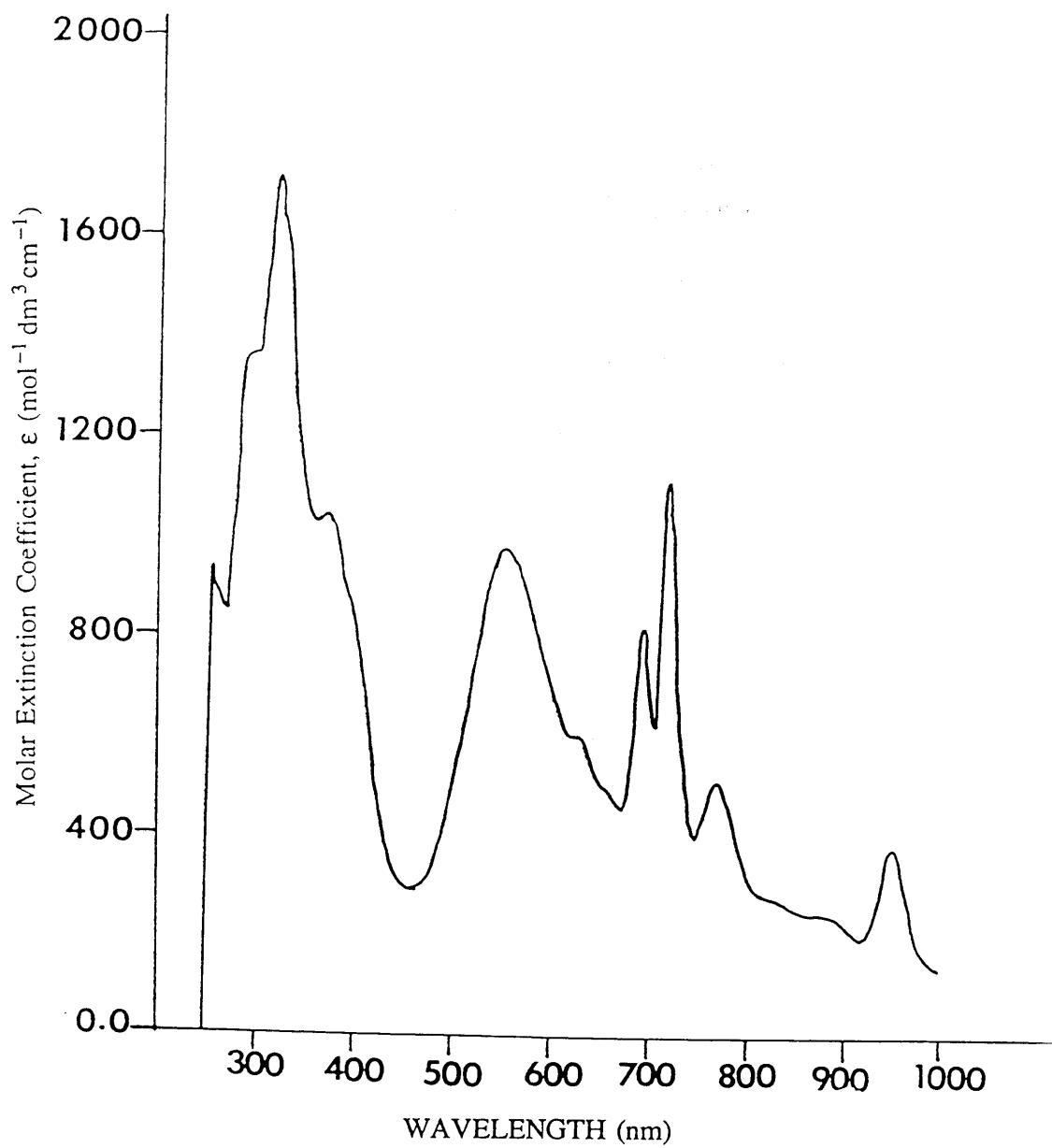
Figure(3:2).Electronic spectra of $[Al(Pc)F]_n$ in H_2SO_4 with concentration (1).11 mol dm^{-3} , (2).12 mol dm^{-3} and (3).12.85 mol dm^{-3}.

[139]. This $_{\wedge}^{is}$ probably attributed to the limited solubility of these complexes in most spectroscopic solvents known. Thus, the interpretation of the spectral changes in this region is much more difficult.

B. Solutions of $[Al(Pc)F]_n$ in trifluoroacetic acid:

The high vapour pressure of CF_3COOH at room temperature (see table 3:1) enabled these experiments to be performed using the vacuum system. This solvent showed relatively high ability to dissolve the polymer (~ 5 mg dissolves in 8 cm^3 of the solvent) and produced an intense purple coloured solution. The electronic spectrum of this solution ($\underline{ca}$ ~ 0.01 mol dm^3) contained several absorption bands in the u.v./visible regions (the Q and B regions) (Fig. 3:3). A characteristic feature of this spectrum was the band at 945-950 nm (Fig. 3:3); this band has not been observed in any of the other $[Al(Pc)F]_n$/solvent systems examined in the present work. All the absorption bands observed in this spectrum and their molar extinction coefficient values (ε) are listed in table 3:5; the ε values were estimated by assuming that all the quantity of $[Al(Pc)F]_n$ used was dissolved in the acid. In order to examine the reproducibility of the band at 945-950 nm, different solutions with concentrations ranging from 6×10^{-4} to 3×10^{-2} mol dm^{-3} were prepared and examined by electronic spectroscopy. From the spectra obtained for these solutions; it was concluded that the band at 945-950 nm only appeared when the concentration of the solution was $c \geq 1 \times 10^{-2}$ mol dm^{-3}.

The pale blue and purple solutions formed from dissolving the $[Al(Pc)F]_n$ polymer in MeCN and CF_3COOH respectively were examined by ^1H, ^{13}C and ^{19}F n.m.r. spectroscopy. Owing to the low solubility of this polymer

Figure(3:3).Electronic spectra of [Al(Pc)F]$_n$ in CF$_3$COOH solution(ca 1x10^{-2} mol dm^{-3})

Table(3:5).Electronic spectra (λ max,nm) and molar extinction coefficient (ε,mol^{-1}dm^{3}cm^{-1}) of the solution of [Al(Pc)F]$_n$ in (a).CF$_3$COOH (concentration of the solution ca 0.001 mol dm^{-3}).(b).CF$_3$SO$_3$H(concentration of the solution ca 0.02 mol dm^{-3}).

(a)		(b)	
λ_{max} (nm)	ε^* (mol^{-1} dm^3 cm^{-1})	λ_{max} (nm)	ε^* (mol^{-1} dm^3 cm^{-1})
950	400		
890 sh.	---		
770	550	800	2350
720	1150	715	350
695	850		
660 sh.	---		
630 sh.	---		
550	1000	455	250
395 sh.	---		
370	1050		
320	1750	305	550
295 sh.	---		

sh. = shoulder

* the ε values were estimated by assuming that all the quantity of [Al(Pc)F]$_n$ used was dissolved in the acid.

in MeCN, no n.m.r. signals assigned to the polymer were observed. The spectra of the solution of $[Al(Pc)F]_n$ in CF_3COOH showed only signals assigned to the solvent.

The vibrational spectra of the purple solid products isolated from the reactions of $[Al(Pc)F]_n$ with CF_3COOH as Nujol and Fluorolube mulls were recorded in the region 4000-400 cm^{-1}. In all cases the spectra of the products were similar to that of untreated $[Al(Pc)F]_n$.

The electronic spectrum of a thin film of the polymer on a silica substrate exposed to the vapour of CF_3COOH showed several absorption bands in the u.v. and visible regions. (Fig. 3:4) This spectrum was compared with that obtained from the solution reaction. The band at 945-950 nm was not observed in the spectrum of the thin film and the Q band was split into two broad peaks (Fig. 3:4). The vibrational spectrum of a thin film of $[Al(Pc)F]_n$ on a KCl substrate exposed to the vapour of CF_3COOH was compared with that of unreacted film. From that comparison, it found that the intensities of the bands were increased and new broad bands at 1790, 1185, 1030 and 645 cm^{-1} appeared in the spectrum of the reacted film (Fig. 3:5). Assignments of these new bands were made by comparing the spectrum in figure 3:5 with that of pure CF_3COOH vapour (Fig. 3:6).

The vibrational spectrum of CF_3COOH in the vapour phase has been studied previously [140] and the broad band at 1788 cm^{-1} has been assigned to $\nu_{c=o}$ str. in the dimer $(CF_3COOH)_2$. Hence, the band at 1790 cm^{-1} observed in the spectrum of the reacted film could be also assigned to $\nu_{c=o}$ str. of the $(CF_3COOH)_2$ dimer retained in the film. The broad band
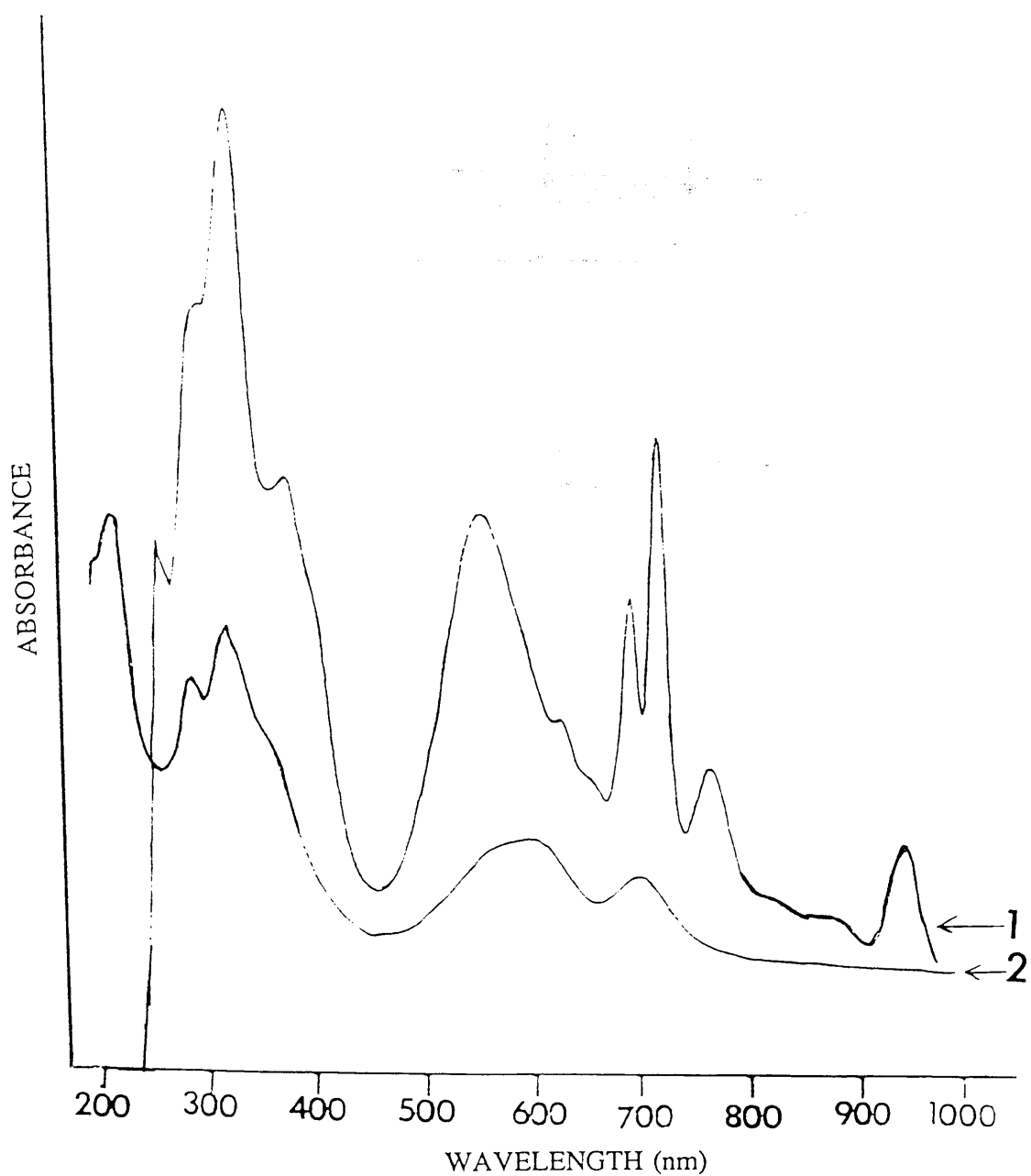
Figure(3:4).Electronic spectra of [Al(Pc)F]$_n$ reacted with
CF$_3$COOH , (1).in solution (ca 0.01 mol dm^{-3})
and (2).as thin film on a silica substrate.
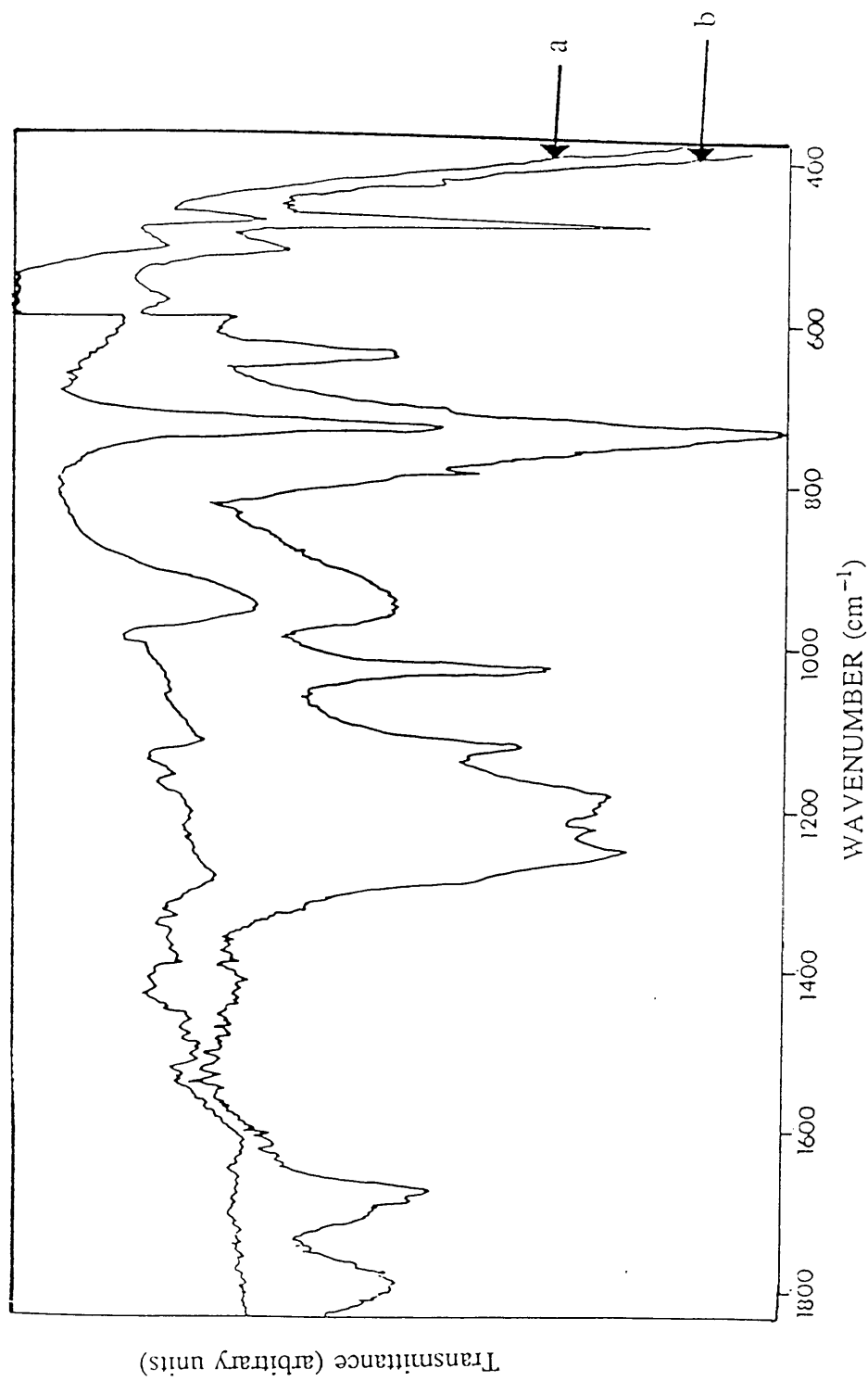
Figure(3:5).Infrared spectra of (a).thin film of $[Al(Pc)F]_n$ on a KCl substrate(thickness=55nm) and (b).the film exposed to the vapour of CF_3COOH.
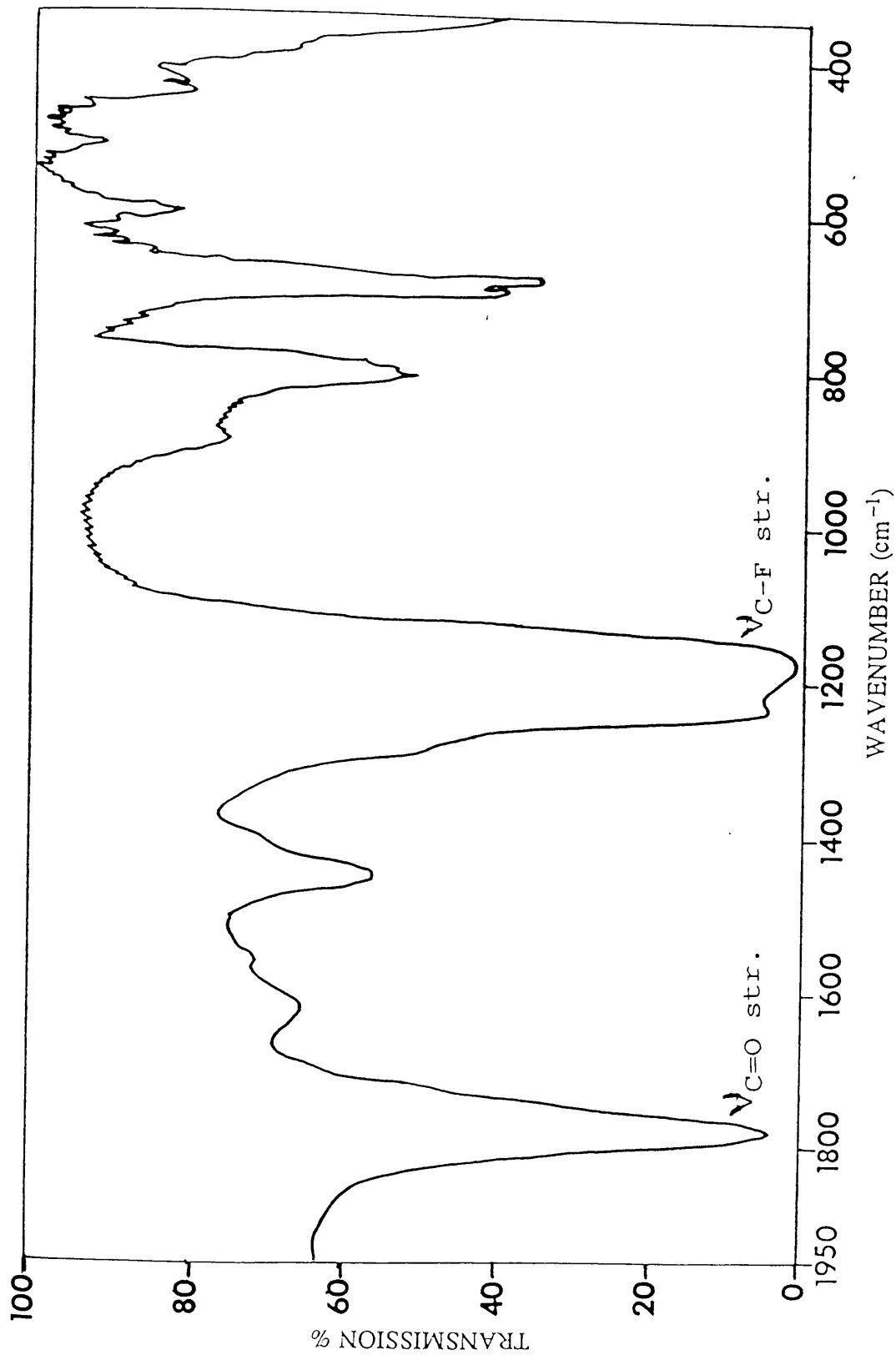
Figure(3:6).Infrared spectrum of CF_3OOH vapour.

in the region 1150-1240 cm^{-1} observed in the spectrum of the acid is assigned to the v_{C-F} str. [141]; this band was also observed in the region 1170-1260 cm^{-1} in the spectrum of the reacted film. The band at 690 cm^{-1} found in the spectrum of the acid may be assigned to v_{C-F} def. as this band usually appeared in this region [141]. This was shifted to 645 cm^{-1} in the spectrum of the reacted film. All the bands observed in the spectra of CF_3COOH, $[Al(Pc)F]_n$ film on a KCl substrate and the reacted film are illustrated in table 3.6.

In order to follow the changes occurring during the apparent reactions of $[Al(Pc)F]_n$ with CF_3COOH, the electronic spectra of a solution (c = 6 x 10^{-4} mol dm^{-3}) were recorded every 1 h for a period of 5 h. It was observed that the colour of this solution which was initially blue, changed successively to purple then to pale green and finally became dark green. During this period the intensities of all the bands in the Q and B regions were increased as shown in figure 3:7 and table 3:7.

Removal of solvent from the solution of $[Al(Pc)F]_n$ in CF_3COOH gave a purple solid. This was re-dissolved in MeCN giving a blue solution. The electronic spectrum of this solution was compared with that of $[Al(Pc)F]_n$ in CF_3COOH. The comparison showed that the band at 945-950 nm had disappeared, the number of bands in the Q region was reduced from four to two and they were shifted to shorter wavelength; the intensities of these bands were decreased (Fig. 3:8). The bands in the B region were also shifted to shorter wavelength, but their intensities increased (Fig. 3:8).

Table(3:6).Infrared absorptions (cm^{-1}) of thin film of [Al(Pc)F]$_n$ on KCl before and after the reactions with CF_3COOH vapour.

CF_3COOH	[Al(Pc)F]$_n$	[Al(Pc)F]$_n$/CF_3COOH
1788 s		1790 b
		1680 b
1630 w		
1500 b		
	1335 w	
	1285 w	1255 b
1185 b	1160 w	1190 b
	1120 w	
		1030 s
	955 b	950 b
810 b		
703 w	725 s	735 s
690 s		645 s
603 m		
515 w	515 w	520 w
	480 m	480 s

s=strong; m=medium; w=weak; and b=broad
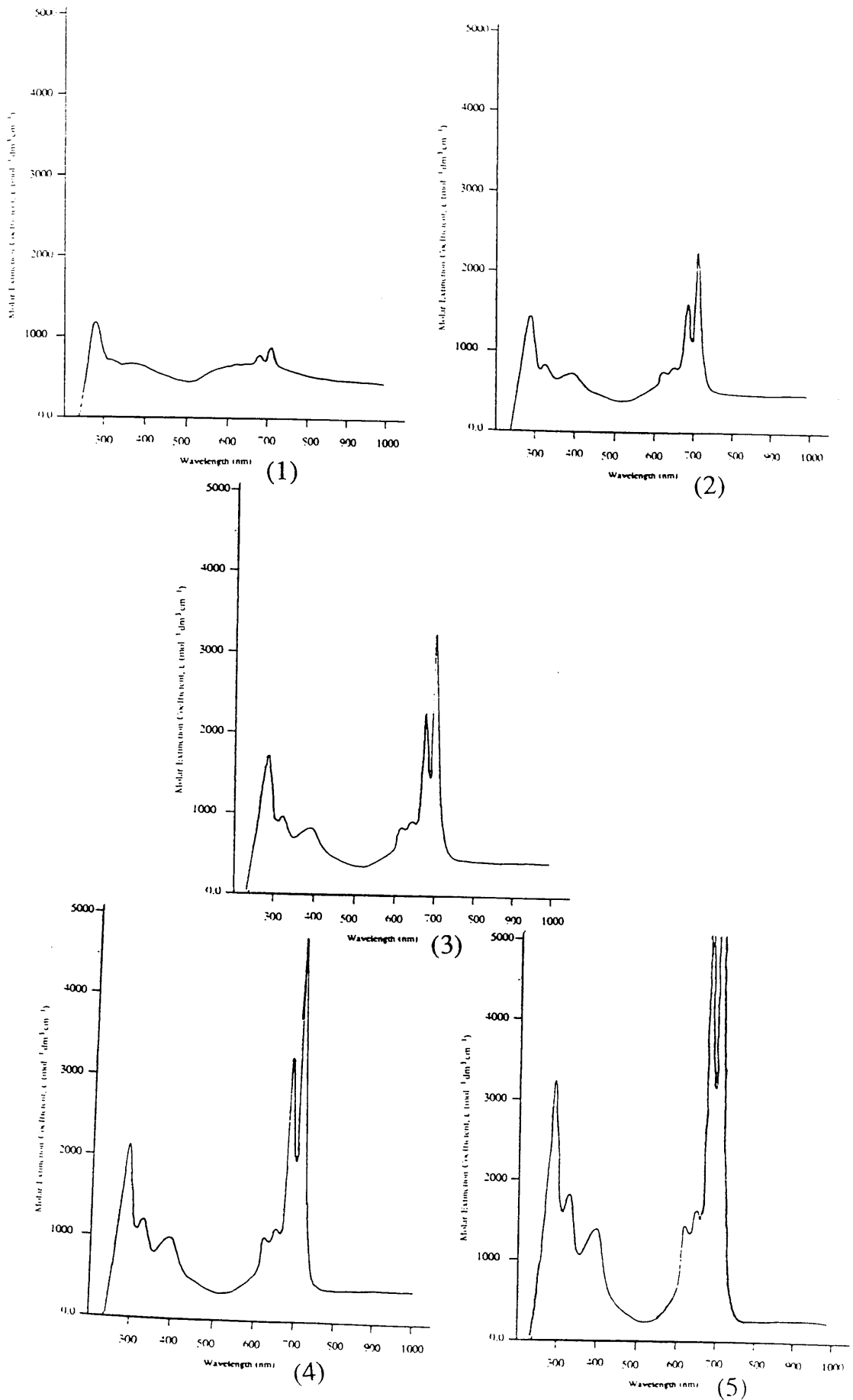
Figure(3:7).Electronic spectra of [Al(Pc)F]$_n$ in CF$_3$COOH
solution (ca 6x10^{-4} mol dm^{-3}) after (1).1h,
(2).2h,(3).3h,(4).4h and (5).5h.

Table(3:7)[*].Electronic spectra(λmax,nm) and molar extinction coefficient(ε,mol^{-1}dm^{3}cm^{-1}) of [Al(Pc)F]$_n$ in CF$_3$COOH (concentration of the solution $\underline{ca}$ 6x10-4 mol dm^{-3}) for a period of a.1h, b.2h, c.3h, d.4h and e.5h

a		b		c		d		e	
λ_{max}	ε	λ_{max}	ε	λ_{max}	ε	λ_{max}	ε	λ_{max}	ε
715	900	715	2300	715	3300	715	4800	715	6900
700	800	700	1650	700	2310	700	3300	700	5650
655	700	655	850	655	950	655	1150	655	1650
625	700	625	800	625	900	625	1050	625	1450
400	650	400	750	400	850	400	1000	400	1400
330	700	330	800	330	1000	330	1250	330	1800
285	1200	290	1450	290	1750	290	2150	290	3200

[*] The ε values were estimated by assuming that all the quantity of [Al(Pc)F]$_n$ used was dissolved in the acid.
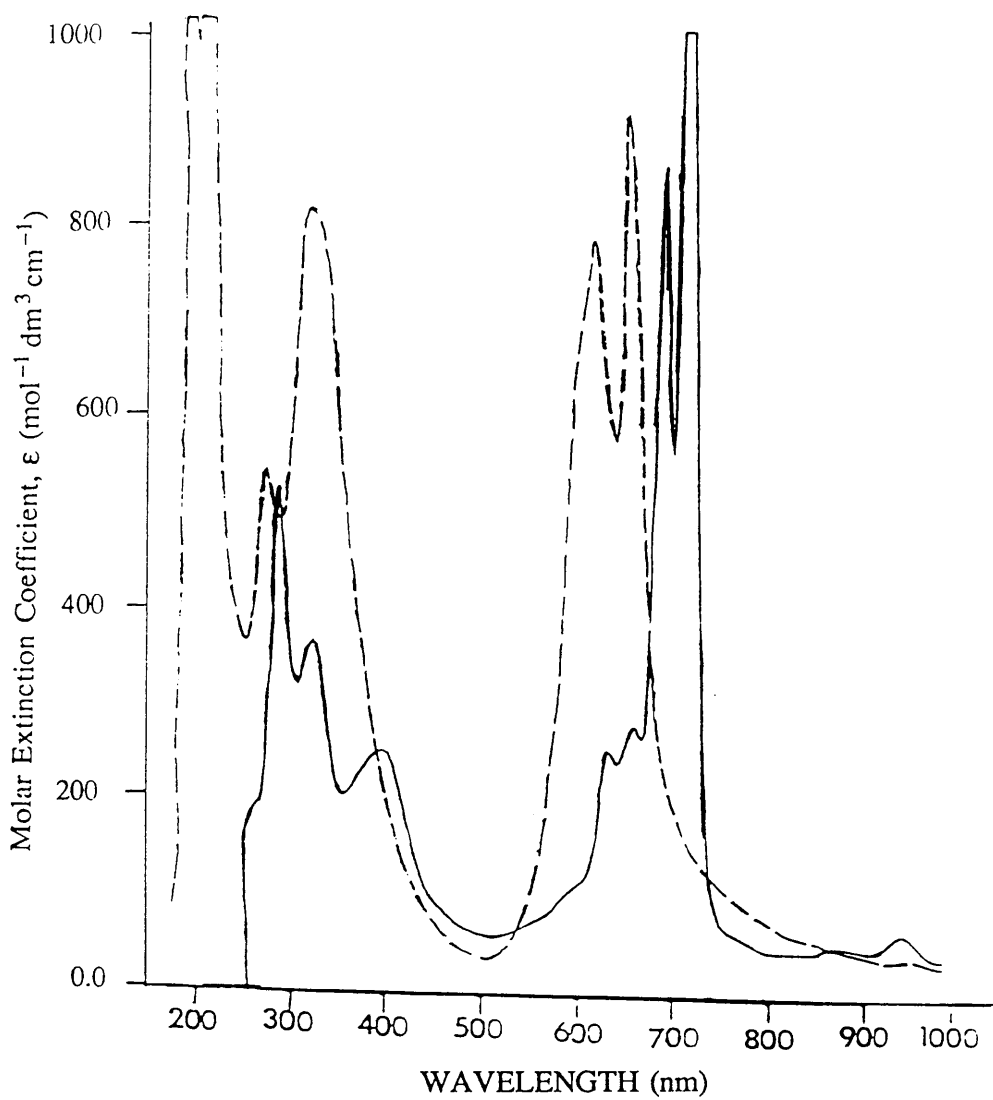
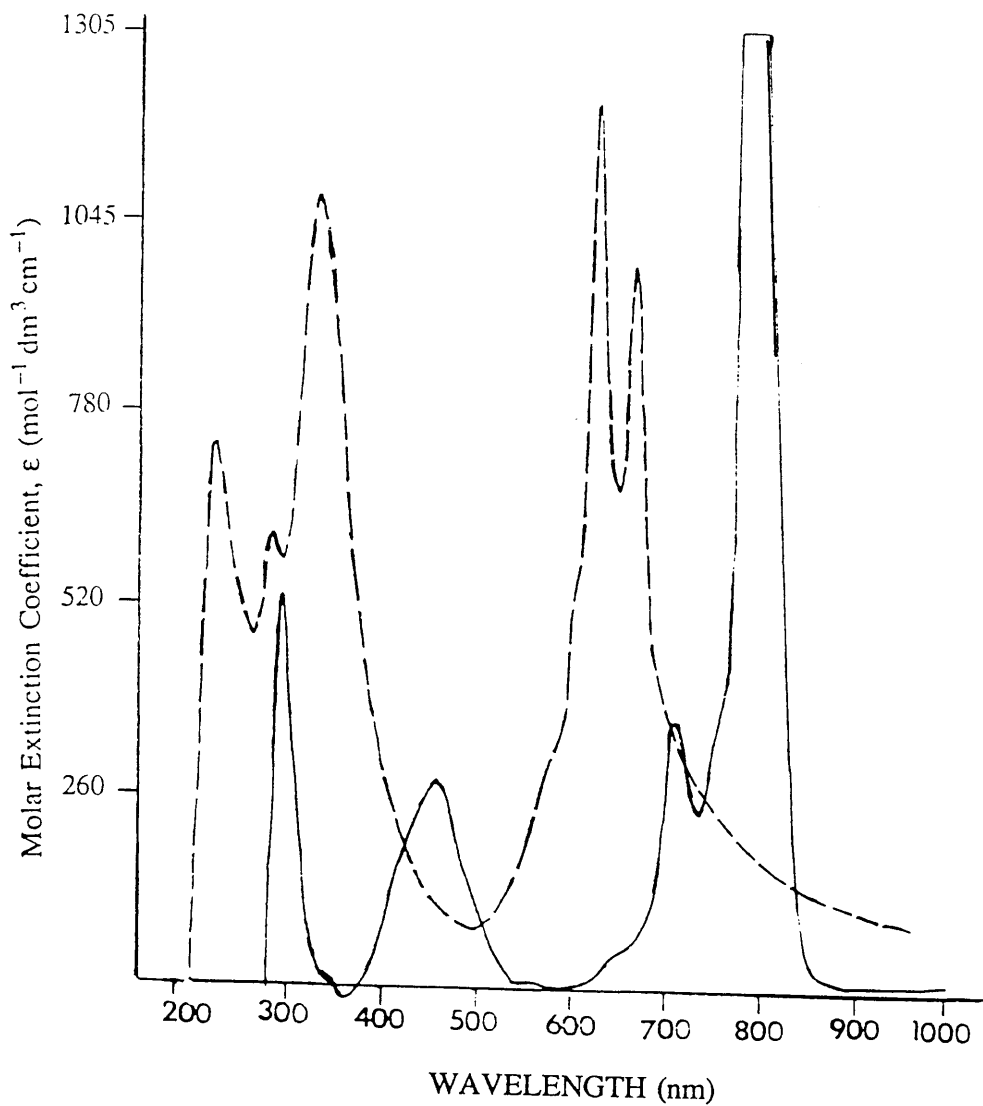Figure(3:8).Electronic spectra of $[Al(Pc)F]_n$ in CF_3COOH (the solid line) and the solid product dissolved in acetonitrile(the dotted line).

C.   Solutions of [Al(Pc)F]$_n$ in trifluoromethanesulphonic acid.

This solvent showed the highest ability (among the solvents in table 3:1) to dissolve the [Al(Pc)F]$_n$ polymer and produced a yellow solution.   The electronic spectrum of this solution (ca ~ 0.02 mol dm^{-3}) showed strong absorption bands in the Q and B regions (Fig. 3:9).   Greenish-yellow solid was isolated from this solution and re-dissolved in MeCN in which a blue coloured solution was formed.   The electronic spectrum of this solution was compared with that of [Al(Pc)F]$_n$ in CF$_3$SO$_3$H (Fig. 3:9).   The comparison showed that the two bands in the Q region were shifted to shorter wavelengths and the intensity of the one on the low energy side decreased while the high energy band increased.   The bands in the B region were increased from two to three bands, their intensities increased and they were shifted to shorter wavelengths (see table 3:5 and figure 3:9).

Figure(3:9).Electronic spectra of [Al(Pc)F]$_n$ in CF$_3$SO$_3$H (the solid line) and the solid product dissolved in acetonitrile(the dotted line).

3:3:2 Discussion

Although reactions in solution involving a number of phthalocyanine complexes have been reported, examples are given in the introduction of this chapter, details about the solvation process of these complexes in the solvents used are lacking. However, the parent compound metal-free phthalocyanine, PcH_2 (were Pc = phthalocyanine = $C_{32}H_{18}N_8$) (Fig. 1:6) has been reported [101] to behave as an amphoteric compound. For example this compound may lose the two inner imino protons to form the anion Pc^{2-}, whilst possible protonation sites are the inner basic nitrogen atoms and the four bridging nitrogen atoms. In the case of the $[Al(Pc)F]_n$ polymer (Fig. 3:10), each central aluminium atom is bonded to four nitrogen atoms of a phthalocyanine molecule and two fluorine atoms. The four outer bridging nitrogen atoms in each phthalocyanine molecule in the polymer have unshared pairs of electrons; these atoms can give the polymer basic properties because they are possible protonation sites. The formation of donor-acceptor complexes between the polymer and the solvents in table 3:1 is not possible because of the unavailability of an empty orbital in the central aluminium atom to accommodate electron pairs from the solvent molecules. The formation of hydrogen bonded complexes between the polymer and the solvents in groups (I) and (II) is also difficult because of the absence of active hydrogen atoms in these solvents towards the formation of a hydrogen bond. Hence most attention will be devoted to the acid-base interaction between the polymer and the solvents in table 3:1, and in particular to that involving the donation of protons from some solvents to the polymer.

The non-ability of group (I) solvents or weak ability
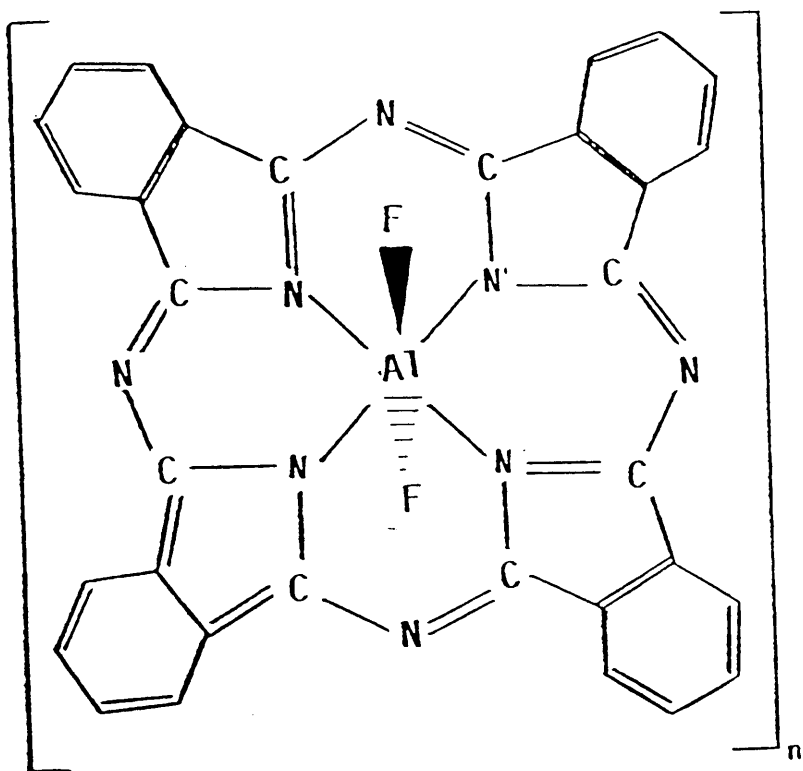
Figure(3:10).Structure of the [Al(Pc)F]$_n$ polymer.

of group (II) solvents to dissolve the $[Al(Pc)F]_n$ polymer can be related to the different acidic or basic behaviour of these solvents towards the polymer. For example the insolubility of the polymer, considered as a base, in acetone (a strong base compared to some basic solvents in groups I and II) may be attributed to the repulsion between the molecules of these two bases. While acetonitrile, although it is well known as a Lewis base, has a weak ability to dissolve the polymer because of the relatively high polarity it possesses. The pale blue solution formed from mixing the polymer with acetonitrile may be resulted from an electrostatic interaction between the polymer molecules and the molecules of this solvent.

The formation of coloured solutions from the reactions of $[Al(Pc)F]_n$ with H_2SO_4, CF_3COOH and CF_3SO_3H suggested that a strong acid-base interaction has taken place between the polymer and these solvents. This may be attributed to the attachment of one or more protons donated from these acids to the outer nitrogen atoms of the polymer.

The attachment of protons to the outer nitrogen atoms of the phthalocyanine molecules causes electron movement from the Al-F bonds towards the phthalocyanine ring in order to stabilise the electron density on it. Hence, these bonds will be weakened and the polymer chain can be severed to give soluble mixtures of monomers, dimers, trimers, etc., as shown in figure 3:11. The protonation process can be represented by the following equation (equation 3-3).

Breaking Point

Phthalocyanine Ring

HX

$[Al(Pc)HF]^+X^-$
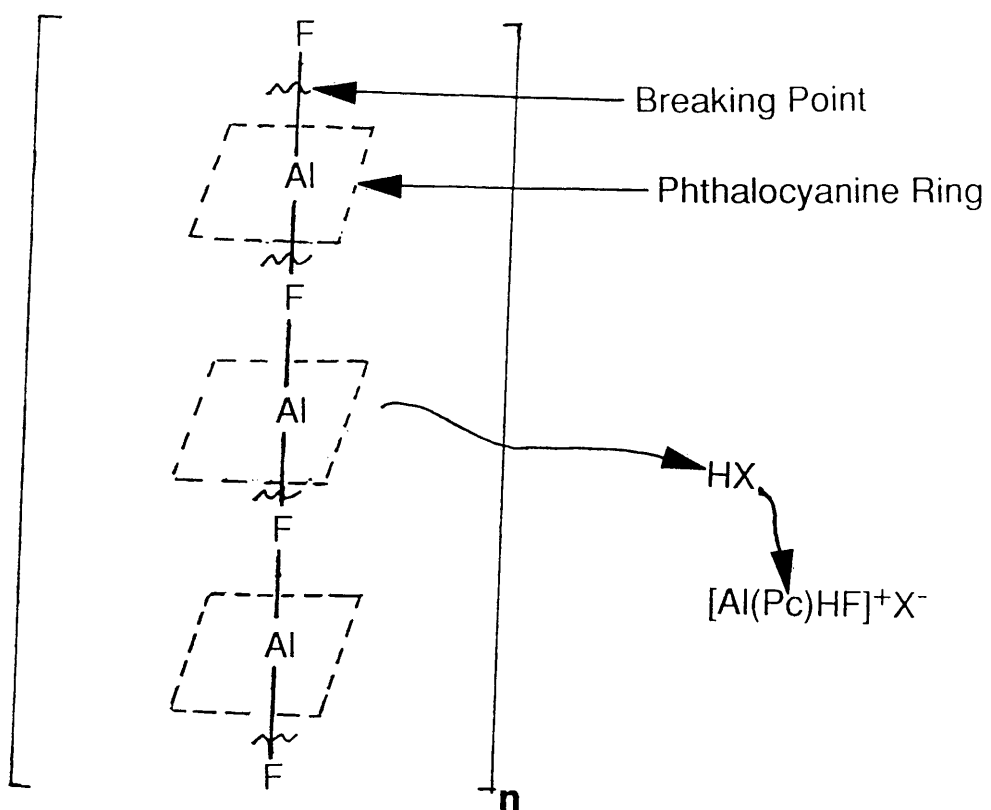
HX=strong protonic acid (i.e CF_3SO_3H, 98%H_2SO_4 or CF_3COOH).

Figure(3:11).Schematic representation of the interaction between one molecule of $[Al(Pc)F]_n$ with one molecule of a strong protonic acid.

$$[Al(Pc)F]_{n(s)} \xrightarrow{HX} [Al(Pc)FH]_n^+ X^- \xrightarrow{HX} [Al(Pc)FH_2]_n^{2+} 2X^-$$

$$\xrightarrow{HX} [Al(Pc)H_3]_n^{3+} 3X^- \xrightarrow{HX} [Al(Pc)FH_4]_n^{4+} 4X^- \quad ...(3-3)$$
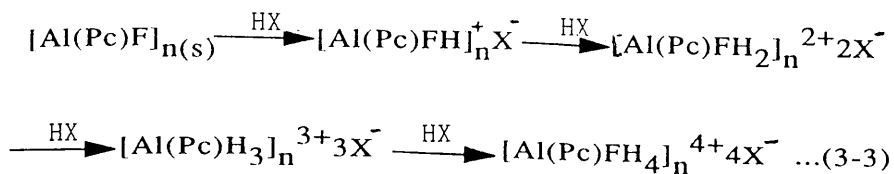
where $HX = CF_3SO_3H$, H_2SO_4 or CF_3COOH.

The electronic spectrum of a solution of $[Al(Pc)F]_n$ in an organic solvent such as acetonitrile and in H_2SO_4 differed to such extent that one can speak of a strong chemical interaction (Fig. 3:12). However, the spectra of $[Al(Pc)F]_n$ in H_2SO_4 remained unchanged with time, this suggests that no reactions like sulphonation or oxidation were taking place in the solution and the acid only protonated the outer bridging nitrogen atoms of the phthalocyanine molecules. This suggestion can be supported by the fact that H_2SO_4 is a strong protonic acid. The variation in colour and spectra of the solutions of $[Al(Pc)F]_n$ in different concentrations of H_2SO_4 suggested that increasing the concentration of H_2SO_4 resulted in providing more protons in the solution and hence increasing the protonation process of the nitrogen atoms of the phthalocyanine molecules.

The changes in the colour and the spectrum of $[Al(Pc)F]_n$ in H_2SO_4 when this solution was diluted with distilled water possibly resulted from the deprotonation of the phthalocyanine rings when water was added.

In the case of the reactions of $[Al(Pc)F]_n$ with CF_3COOH and CF_3SO_3H the same suggestion can be made to interpret the results obtained. These acids are also strong protonic acids and they interacted with the $[Al(Pc)F]_n$ polymer through the protonation of the nitrogen atoms in the phthalocyanine molecules.
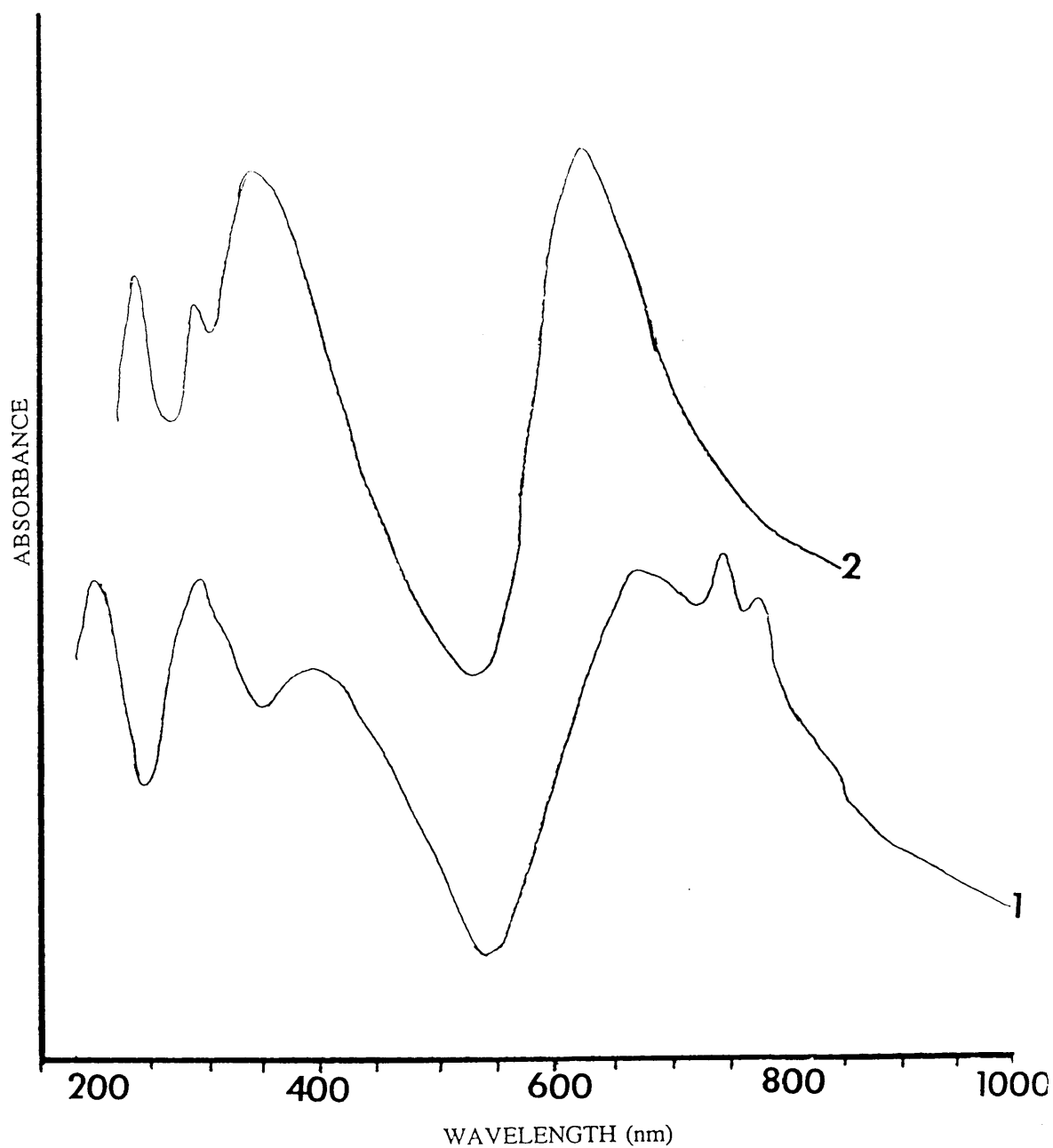
Figure(3:12).Electronic spectra of [Al(Pc)F]$_n$ in (1).12M H$_2$SO$_4$
and (2).acetonitrile.

The comparison between the colours and electronic spectra of the solutions of $[Al(Pc)F]_n$ in CF_3SO_3H, 98% H_2SO_4 and CF_3COOH showed that the protonation of the phthalocyanine rings was dependant on the strength of the acid used. According to the Hammett acidity values, Ho reported for these acids [7,14] the order of their strength can be arranged as CF_3SO_3H (Ho = 15.1) > 98% H_2SO_4 (Ho = 12) > CF_3COOH (Ho = 2.77 - 4.4). Therefore the more stronger the acid provides more protons to interact with the nitrogen atoms of the phthalocyanine molecules and hence increase the solubility of the polymer.

The electronic spectrum of $[Al(Pc)F]_n$ in MeCN was compared with the spectra obtained for the coloured solutions of this polymer in CF_3SO_3H, H_2SO_4 (12 mol dm^{-3}) and CF_3COOH. This comparison has showed that the Q band was split into several components and shifted to longer wavelength when the polymer was dissolved in these acids (see tables 3:2, 3:3, 3:4 and 3:5). This strong bathochromic spectral shift of the Q band in these acids promoted the suggestion that one (or more) proton donated from these acids is attached to the external nitrogen atoms of the $[Al(Pc)F]_n$ polymer. The attachment of the proton strongly polarises the phthalocyanine molecules and the result is a strong dipole which decreases the energy of all electronic transitions associated with the macro-ring.

The presence of the absorption band at 945-950 nm in the spectrum of the purple solution of $[Al(Pc)F]_n$ in CF_3COOH could be attributed to the formation of monomeric species from the polymer. A similar band has also been identified

in the spectra of monomeric [Mg(Pc)] oxidised by concentrated nitric acid [142].

Finally, among the solvents used in the present investigation acetonitrile has proved to be the most useful solvent for studying the reactions between the $[Al(Pc)F]_n$ polymer and the oxidising agents described in chapter 4. Despite the low solubility of this polymer in acetonitrile, the electronic spectrum of the mixture obtained was satisfactory for observing all the absorption bands in the Q and B regions; this solvent is transparent down to 175 nm (see chapter 2). While some of the spectra obtained for the mixtures of $[Al(Pc)F]_n$ with other solvents were complicated and in particular, the bands in the B region were not observed due to the solvent absorption bands. Furthermore, the nature of the reagents used for the reactions in chapter 4 required vacuum line techniques and MeCN is a useful solvent for this approach (see table 3:1).

CHAPTER FOUR

REACTIONS OF POLY(FLUOROALUMINIUM-PHTHALOCYANINE),

$[Al(Pc)F]_n$ WITH THE HEXAFLUORIDES OF URANIUM,

MOLYBDENUM AND TUNGSTEN AND WITH THE NO^+ CATION.

4:1 Introduction

The use of transition metal fluorides as oxidising agents in inorganic chemistry is well established, both in solution and in the gas phase. Many examples illustrating this aspect of transition metal pentafluoride and hexafluoride chemistry have been described in chapter one.

Oxidative fluorination of organic compounds by transition metal fluorides, for example cobalt(III) fluoride [143] or VF_5 [144], is a well-known route to fluorocarbon species. Molybdenum and tungsten hexafluorides have both been used to fluorinate carbonyl groups in organic molecules [145,146]. Uranium hexafluoride has also been used as a selective oxidant for organics [147]; in this case oxidation is sometimes achieved without concomitant fluorination.

The electrical conductivity of many polymeric phthalocyanine complexes increases markedly when they are doped with certain doping agents; examples are given in chapter one. When the doping is successful the result is a crystal composed of segregated, partially oxidised phthalocyanine stacks and partial arrays of counterions (i.e. donors and acceptors in different columns.

As a result of the above observations, several studies have been reported in which the reactions of polymeric phthalocyanines with oxidants such as those mentioned in chapter one and others like XeF_2 [148], O_2 and NO_2 [112] have been examined. In most cases, methods such as x-ray powder diffraction, thermogravimetric analysis, infrared spectroscopy and electrical conductivity measurements have

been employed in the characterization of the products formed. Particular attention has been devoted to the study of magnetic and electrical properties of the conducting materials obtained. However, it is well known that such electrical conductivity properties of a material depend upon its electronic structure. Hence, as far as the doping process of polymeric phthalocyanine complexes is concerned, the electronic structure of these compounds will depend on the type of dopant used. For instance, the changes in the electronic structure of the phthalocyanine molecules will vary depending on the size, the shape, the electron affinity and the quantity of the doping molecules inserted. An additional reason particularly important in studying the electronic structures of these complexes is to determine the effect of doping on the state of polymerization. For example, do the oxidation reactions lead to depolymerization of these complexes or not. In this context, the study of the electronic structural changes in these compounds, before and after the doping, can supply vital information for the interpretation of electrical conductivity changes.

In the present work the $[Al(Pc)F]_n$ polymer (Fig. 4:1) has been reacted with the hexafluorides of uranium, molybdenum and tungsten, and with the NO^+ cation; particular attention has been given to the choice of reaction conditions. It is noteworthy that uranium, molybdenum and tungsten hexafluorides are strong one-electron oxidising agents in MeCN [149] as shown below (equation 4-1).

$$MF_6 + e^- \longrightarrow MF_6^- \quad \ldots\ldots\ldots\ldots\ldots(4\text{-}1)$$
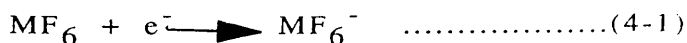
M = U, Mo or W.
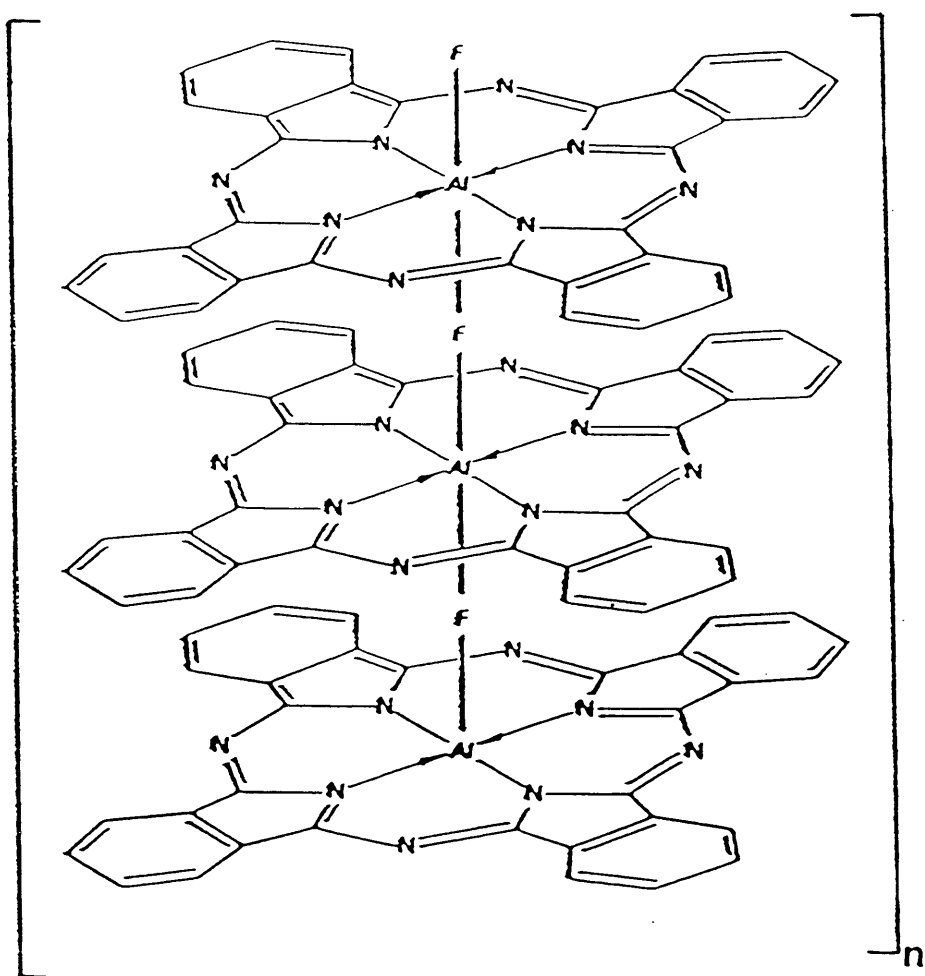
Figure(4:1).Structure of poly(fluoroaluminium-
phthalocyanine),[Al(Pc)F]n.

The reactions were carried out in the presence of acetonitrile, and by exposing thin films of the polymer deposited on silica and potassium chloride substrates to the vapours of UF_6, MoF_6 and WF_6. In some cases, reactions between polycrystalline samples of the polymer and the oxidants WF_6 and $NOPF_6$ have been performed. The products of these reactions have been examined by electronic and vibrational spectroscopy. In some cases samples from these reactions were examined by transmission electron microscopy; these are described in detail in chapter six.

4:2 Experimental

The reactions between the $[Al(Pc)F]_n$ polymer and each
oxidising agent used in the present investigation were
repeated several times at room temperature. The repetition
of experiments using carefully controlled additions of the
starting materials enabled the establishment of useful
experimental conditions in which the products formed could
be easily characterized and interesting spectroscopic data
obtained. Furthermore, appropriate stoichiometries for the
reactions performed in the presence of acetonitrile were
established. These were based on the physical properties
observed for the products, such as solubility in acetonitrile
and the colours of the resulting solutions; the
stoichiometric relationships are given in more detail in the
results section of this chapter.

The quantities of the $[Al(Pc)F]_n$ polymer used in all
experiments were determined using an electrical balance
(precision $\pm$ 0.001 g) in the dry box.

The quantities of the oxidising agents (UF_6, MoF_6 and
WF_6) were determined using a specially designed weighing
vessel fabricated from fluorocarbon polymers and shown in
figure 4:2. The vessel was evacuated, transferred to the
dry box and weighed using the electrical balance. The
vessel was re-attached to the vacuum line and filled with an
unknown quantity of the oxidising agent by vacuum
distillation at 77 K. After warming to room temperature,
the vessel containing the oxidising agent was transferred to
the dry box and re-weighed. The quantity of the oxidising
agent was determined from calculating the difference between
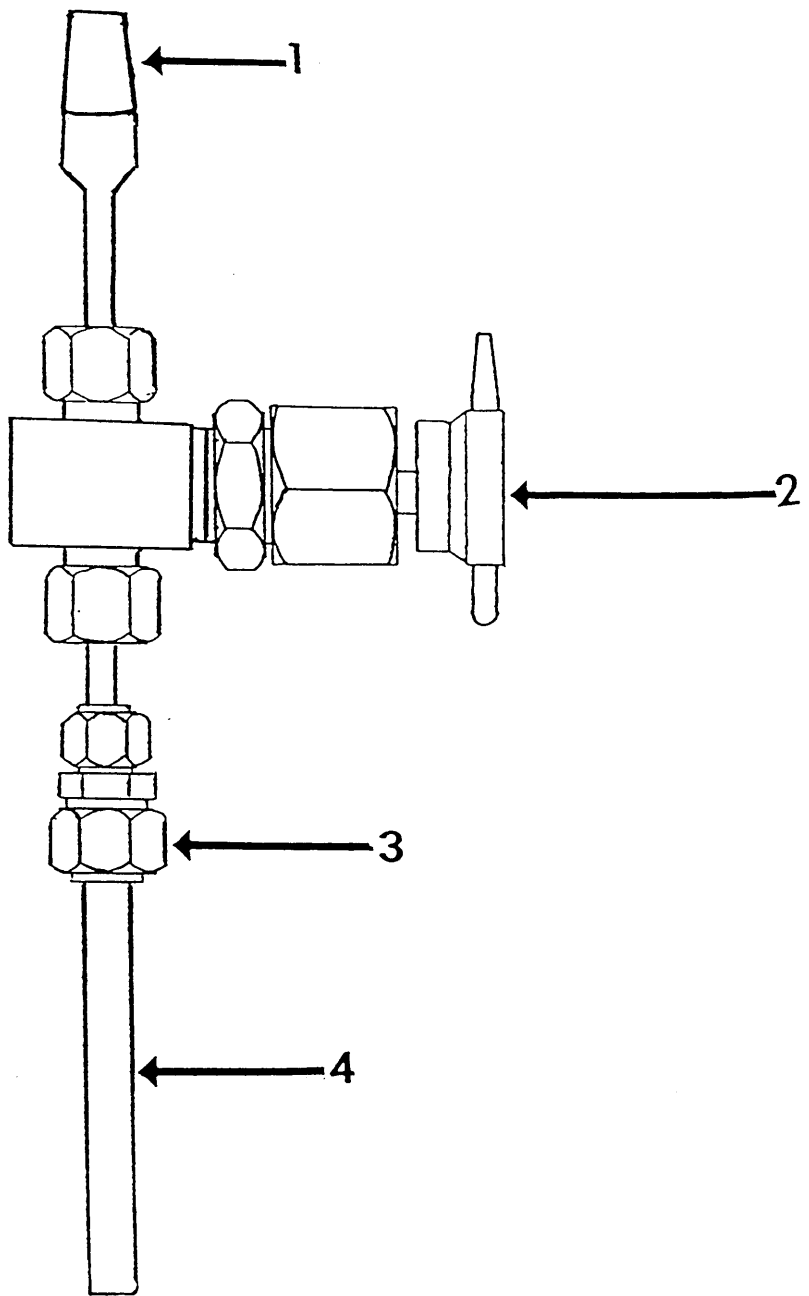
1. *B* -14 Ground glass cone
2. P.T.F.E. needle valve
3. P.T.F.E. reducing union
4. F.E.P. Tube

Figure(4:2).Single-limbed weighing vessel.

the two weights. The quantities of the $NOPF_6$ salt were weighed in the reaction double limbed vessel (Fig. 2:1) using the balance in the dry box.

All quantities of the $[Al(Pc)F]_n$ used in the repeated experiments with UF_6, MoF_6, $NOPF_6$ and WF_6 in the presence of acetonitrile are given in tables 4:1, 4:2, 4:3 and 4:4 respectively. It can be seen from the tables that the quantities of both the $[Al(Pc)F]_n$ polymer and the oxidants were different for each experiment. The quantity of acetonitrile (6 cm^3) used was the same in all experiments.

The reactions between $[Al(Pc)F]_n$ and MF_6 (M = U, Mo and W) in the presence of MeCN were carried out using an identical method, described in section A(I). The reactions of $[Al(Pc)F]_n$ with solutions of $NOPF_6$ in MeCN are described in section A(II). The experimental method used for exposing thin films of the $[Al(Pc)F]_n$ polymer deposited on silica and single crystal KCl substrates to the vapours of UF_6, MoF_6 and WF_6 was the same and is described in section B.

The reactions of polycrystalline $[Al(Pc)F]_n$ with WF_6 vapour and $NOPF_6$ salt were carried out using the experimental manipulations described in section C.

The electronic and vibrational spectra of several samples of unreacted $[Al(Pc)F]_n$ were recorded in the regions 1000-185 nm and 4000-400 cm^{-1} respectively. These spectra were used as references to make comparisons with the spectra of the products obtained from the reactions.

Table(4:1).The observations made from six experiments carried out using different quantities of [Al(Pc)F]$_n$ and UF$_6$ in acetonitrile (6 cm^3) at room temperature.

[Al(Pc)F]$_n$		UF$_6$		mole ratio	observations
mg	mmol	mg	mmol	[Al(Pc)F]$_n$: UF$_6$	
0.10	0.18	0.03	0.08	2.2 : 1.0	Blue purple solution, some undissolved [Al(Pc)F]$_n$ remained, blue solid isolated.
0.21	0.38	0.12	0.34	1.1 : 1.0	Purple solution, some undissolved [Al(Pc)F]$_n$ remained, purple solid isolated.
0.07	0.12	0.06	0.17	1.0 : 1.4*	Dark purple solution, all the [Al(Pc)F]$_n$ dissolved, purple solid isolated
0.02	0.03	0.07	0.19	1.0 : 6.3	Greenish - yellow solution, greenish - yellow jelly like solid isolated
0.18	0.32	1.26	3.57	1.0 : 11.1	Pale brown solution, brownish - yellow jelly like solid isolated.

*The mole ratio at which all the solid material isolated from the reaction was completely dissolved by adding fresh acetonitrile (6 cm^3).

Table(4:2).The observations made from five experiments carried out using different quantities of $[Al(Pc)F]_n$ and MoF_6 in acetonitrile (6 cm^3) at room temperature.

$[Al(Pc)F]_n$		MoF_6		mole ratio	observations
mg	mmol	mg	mmol	$[Al(Pc)F]_n : MoF_6$	
0.21	0.38	0.07	0.33	1.1 : 1	Purple solution, some undissolved $[Al(Pc)F]_n$ remained, purple solid isolated
0.08	0.14	0.05	0.23	1.0 : 1.6*	Dark purple solution, all the $[Al(Pc)F]_n$ dissolved, purple solid isolated
0.01	0.02	0.02	0.09	1.0 : 4.5	Greenish-yellow solution, greenish-yellow solid isolated
0.13	0.23	0.46	2.19	1.0 : 9.5	Yellow solution, yellow jelly like solid isolated
0.07	0.12	0.34	1.61	1.0 : 13.4	Pale brown solution, brownish - yellow jelly like solid isolated

*The mole ratio at which all the solid material isolated from the reaction was completely dissolved by addingfresh acetonitrile (6 cm^3).

Table(4:3).The observations made from four experiments carried out using different quantities of $[Al(Pc)F]_n$ and $NOPF_6$ in acetonitrile(6 cm^3) at room temperature.

$[Al(Pc)F]_n$		$NOPF_6$		mole ratio	Observations
mg	mmol	mg	mmol	$[Al(Pc)F]_n : NOPF_6$	
0.48	0.86	0.15	0.85	1.0 : 1.0	Blue solution, some undissolved $[Al(Pc)F]_n$ remained, purple solid isolated
0.21	0.38	0.14	0.80	1.0 : 2.1	Dark purple solution, all the $[Al(Pc)F]_n$ dissolved, purple solid isolated
0.07	0.12	0.06	0.34	1.0 : 2.8*	Dark purple solution, all the $[Al(Pc)F]_n$ dissolved, purple solid isolated
0.09	0.16	0.12	0.68	1.0 : 4.2	Greenish-yellow solution, greenish-yellow jelly like solid isolated

*The mole ratio at which all the solid material isolated from the reaction was completely dissolved by adding fresh acetonitrile (6 cm^3).

Table(4:4).The observations made from four experiments carried out using different quantities of $[Al(Pc)F]_n$ and WF_6 in acetonitrile (6 cm^3) at room temperature.

$[Al(Pc)F]_n$		WF_6		mole ratio	Observations
mg	mmol	mg	mmol	$[Al(Pc)F]_n : WF_6$	
0.03	0.05	0.01	0.03	1.6 : 1.0	Blue solution, some undissolved $[Al(Pc)F]_n$ remained, blue solid isolated
0.30	0.53	0.17	0.57	1.0 : 1.0	Blue-purple solution, some undissolved $[Al(Pc)F]_n$ remained, purple solid isolated
0.09	0.16	0.15	0.50	1.0 : 3.1*	Dark,purple solution, all the $[Al(Pc)F]_n$ dissolved, purple solid isolated
0.13	0.23	0.36	1.20	1.0 : 5.2	Greenish-yellow solution, greenish-yellow jelly like solid isolated

*The mole ratio at which all the solid material isolated from the reaction was completely dissolved by adding fresh acetonitrile (6 cm^3).
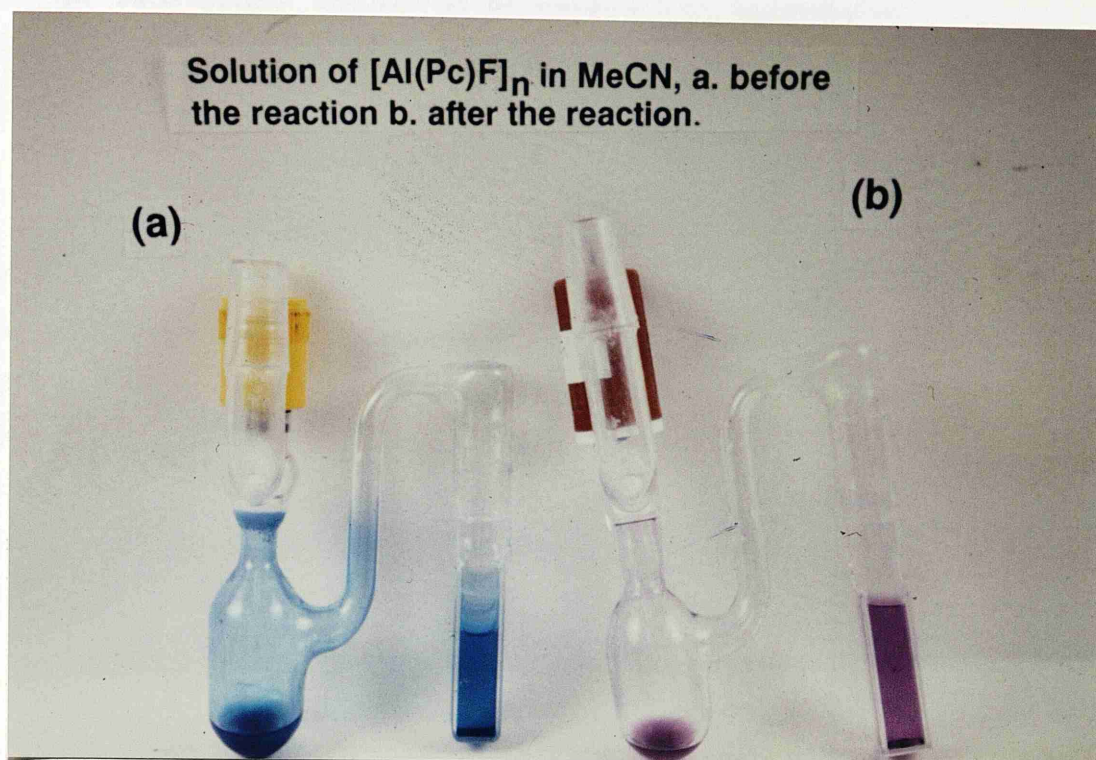
A. Reactions in the Presence of Acetonitrile.

(I). With UF_6, MoF_6 or WF_6.

A flamed-out double-limbed reaction vessel (Fig. 2:1) was transferred to the dry box. A weighed quantity of the $[Al(Pc)F]_n$ powder was loaded in one of the limbs. The vessel was attached to the vacuum line and re-evacuated. Acetonitrile (6 cm^3) was added to the vessel by vacuum distillation at 77 K. The mixture was left to warm up to room temperature and a pale blue solution was formed as a small amount (~ 1 mg) of $[Al(Pc)F]_n$ dissolved in the solvent; most of the polymer used remained undissolved. The weighed quantity of the oxidising agent (UF_6, MoF_6 or WF_6) was added to the mixture by vacuum distillation at 77 K. The reaction mixture was left to warm up to room temperature and any reaction allowed to proceed for 5 min. After this period various colours were observed depending on what mole ratio of $[Al(Pc)F]_n:MF_6$ was used (see tables 4:1, 4:2 and 4:4). The solvent and excess MF_6 were decanted to the empty limb of the vessel and solids with different colours were isolated; the colours of these solids were also dependant on the $[Al(Pc)F]_n:MF_6$ mole ratio used (see tables 4:1, 4:2 and 4:4).

The purple solids isolated from carrying out reactions using the mole ratio marked with an asterisk in tables 4:1-4:4 were examined by infrared spectroscopy in the range 4000-400 cm^{-1} as Nujol and Fluorolube mulls. These solids were highly soluble in acetonitrile. When these solids re-dissolved in fresh solvent (6 cm^3) intense purple coloured solutions were obtained (Fig. 4:3). The concentrations of Al^{III} in these solutions were estimated as follows, $[Al(Pc)F]_n:UF_6$ mole ratio $\simeq$ 1.0:1.4 ca 0.020 mol dm^{-3}; $[Al(Pc)F]_n:MoF_6$ mole ratio $\simeq$ 1.0:1.6 ca 0.023 mol dm^{-3}

Solution of [Al(Pc)F]$_n$ in MeCN, a. before the reaction b. after the reaction.

(a)

(b)

Figure(4:3).(a).A mixture of [Al(Pc)F]$_n$ in acetonitrile

(b).Solutions of [Al(Pc)F]$_n$ after reactions

with MF$_6$ (M=U,Mo,or W) or NO$^+$ cation in

acetonitrile.

$[Al(Pc)F]_n:WF_6$ mole ratio $\simeq$ 1.0:3.1 $\underline{ca}$ 0.026 mol dm^{-3}. The electronic spectra of these solutions were recorded over the range 1000-185 nm; but the solution concentrations were too high for satisfactory spectra to be obtained. In order to bring the bands on scale these solutions were diluted within the reaction cell using the following procedure.

The highly concentrated dark purple solutions were re-decanted into the Pyrex part of the cell leaving traces of the solid products in the Spectrosil limb. The solvent was then transferred to the Spectrosil limb by back distillation using a mixture of dry ice in water around the limb overnight. The mixture in the limb was warmed to room temperature and a pale purple solution was formed. This solution was examined by electronic spectroscopy.

The above procedure of obtaining diluted solutions for the examination by electronic spectroscopy was carried out without opening the reaction cell in order to avoid hydrolysis of the products. The disadvantage of this procedure was the inability to determine the concentrations of the diluted solutions. Thus, molar extinction coefficients (ε) of the absorption bands observed in the spectra after the reactions were not obtained. However this problem was overcome, to some extent, by comparing the spectra of the diluted solutions with those of the $[Al(Pc)F]_n$ thin films after the reactions with MF_6 oxidants.

(II). With $NO^+PF_6^-$

A weighed quantity of $[Al(Pc)F]_n$ powder was placed in one limb of the reaction vessel and a weighed quantity of $NOPF_6$ in the other limb in the dry box. The vessel was attached to the vacuum line and re-evacuated. The $NOPF_6$ salt was dissolved in MeCN (6 cm^3) which was added by vacuum distillation at 77 K and a colourless solution obtained. This solution was decanted into the limb containing the $[Al(Pc)F]_n$ powder. The mixture was shaken for 5 min and a purple solution was formed. During the shaking process, bubbles resulting from the formation of NO gas were evolved from the solution. The solvent and excess soluble $NOPF_6$ were decanted to the empty limb of the vessel and a purple solid was isolated (see table 4:3). This solid was highly soluble in acetonitrile and an intense purple coloured solution obtained when the solid was dissolved in fresh solvent (6 cm^3). The concentration of Al^{III} in this solution was estimated as $[Al(Pc)F]_n$:$NOPF_6$ mole ratio $\simeq$ 1.0:2.8 <u>ca</u> 0.02 mol dm^{-3}. The electronic spectrum of this solution was recorded over the range 1000-185 nm. This spectrum contained absorption bands that were off scale due to the high concentration of the solution. Therefore a diluted solution was obtained by using the procedure described earlier. This diluted solution was pale purple and was examined by u.v/visible spectroscopy.

The purple solid isolated from this reaction was examined by infrared spectroscopy as Nujol and Fluorolube mulls in the range 4000-400 cm^{-1}.

B. Thin Film Reactions.

Thin films of $[Al(Pc)F]_n$ polymer deposited on silica and single KCl crystal substrates were prepared using the method described in section 2:7 of chapter two. The films on silica substrates (thickness $\simeq$ 55 nm) were loaded (in the dry box) into an evacuable reaction gas cell fitted with Spectrosil-B windows by means of a P.T.F.E. holder (Fig. 2:3). The cell was attached to a reaction manifold on a vacuum line and re-evacuated. The tap of the cell was closed and the calibrated manifold was filled with the hexafluoride vapour (UF_6, MoF_6 or WF_6) at a measured pressure (155.6 Torr). The cell was then re-opened to the manifold, filled with the hexafluoride and closed again. The colour of the film changed rapidly from blue to purple (Fig. 4:4), and the reaction was allowed to proceed for 5 min. The residual unreacted hexafluoride was transferred to an empty vessel (attached to the manifold and evacuated previously) by vacuum distillation at 77 K. The cell was pumped for approximately 15 min to ensure the removal of any traces of unreacted hexafluoride adsorbed on the film or SiF_4 which could have resulted from trace hydrolysis in the cell. The electronic spectrum of the purple film was recorded in the region 1000-185 nm.

The quantities of the $[Al(Pc)F]_n$ polymer as thin films on silica substrates were determined by weighing the substrates before and after the deposition of the films. The silica substrates used for preparing the $[Al(Pc)F]_n$ films had identical weights, and the films were deposited on these substrates by using an identical preparation method.
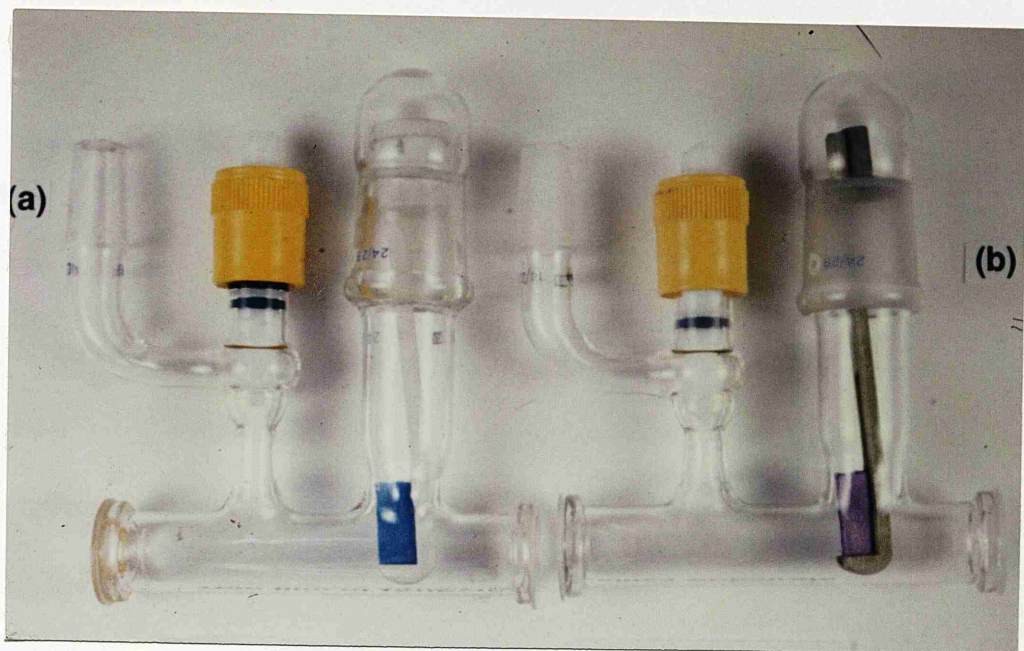
Figure(4:4).(a).Thin film of $[Al(Pc)F]_n$ on a silica substrate
(thickness=55nm).
(b).The film after reactions with MF_6
(M=U, Mo,or W) vapour.

Therefore, it was found that all the $[Al(Pc)F]_n$ films used in the above reactions had an identical weight (0.98 mg, 0.02 mmol). The reaction gas cell (Fig. 2:3) used had a measured volume of 52.9 cm^3. The pressure of the hexafluoride (UF$_6$, MoF$_6$ or WF$_6$) used in the gas cell was the same (123.3 Torr) in all reactions with the $[Al(Pc)F]_n$ films. By using the above data the quantities of the hexafluorides used in the gas cell were determined as follows, UF$_6$ (12.3 mg, 0.34 mmol); MoF$_6$ (7.3 mg, 0.34 mmol); WF$_6$ (10.4 mg, 0.34 mmol). In all these reactions the mole ratio $[Al(Pc)F]_n$:MF$_6$ (M = U, Mo or W) was estimated as 1:17. This mole ratio is higher than those established earlier for the reactions between $[Al(Pc)F]_n$ powder and MF$_6$ oxidants in the presence of MeCN (see tables 4:1-4:4); but of course it cannot be equated with the combining ratio because in reality only part of the above quantity of MF$_6$ used reacted with the $[Al(Pc)F]_n$ film. Unfortunately it was not possible to measure the quantity of the unreacted excess MF$_6$ in the cell. Thus the film reactions were carried out using a mole ratio $[Al(Pc)F]_n$:MF$_6$ far in excess than that required to react completely with the $[Al(Pc)F]_n$ present.

The reactions between thin films of $[Al(Pc)F]_n$ polymer deposited on KCl substrates (thickness $\simeq$ 90 nm) and the hexafluorides, UF$_6$, MoF$_6$ or WF$_6$ were carried out using similar experimental manipulations. In this case the reaction gas cell used was fitted with silver chloride windows. The observations made from these reactions were identical to those described above. The infrared spectra of the purple thin films were recorded in the region 4000-400 cm^{-1}.

C. Reactions of [Al(Pc)F]$_n$ with WF$_6$ and NOPF$_6$ in the Absence of Solvent.

(I). [Al(Pc)F]$_n$ with WF$_6$.

This reaction was carried out in a specially designed reaction cell fitted with silver chloride windows (Fig. 4:5) using the following experimental method.

A flamed out single limb vessel (Fig. 4:5) was loaded with a weighed quantity of [Al(Pc)F]$_n$ powder (19 mg, 0.34 mmol) in the dry box. The vessel was attached to a vacuum line and re-evacuated. The vessel was then attached to the cell which in turn was attached to the vacuum line and evacuated. The quantity of tungsten hexafluoride (14 mg, 0.47 mmol) was weighed using the weighing vessel shown in figure 4:2. The hexafluoride was distilled into the trough of the calibrated gas cell by vacuum distillation at 77 K. The WF$_6$ was allowed to warm to room temperature and a background vibrational spectrum for the unreacted gas (96 Torr) was recorded in the range 4000-400 cm^{-1}. The cell was re-attached to the vacuum line and WF$_6$ was frozen at 77 K. The cell was isolated from the pumps and a small portion of the [Al(Pc)F]$_n$ powder in the vessel was dropped onto the frozen WF$_6$ in the trough of the cell. The two reactants were allowed to mix for 2 min at room temperature. The infrared spectrum of the gaseous products was recorded in the range 4000-400 cm^{-1}. These manipulations were repeated by dropping two more portions of the [Al(Pc)F]$_n$ powder onto the portion of WF$_6$ that remained unreacted. The spectra obtained from each reaction after the addition of [Al(Pc)F]$_n$ powder are given in figure 4:6. During the mixing process of the two reactants, it was observed that the colour of the [Al(Pc)F]$_n$ powder changed from blue to purple. The total
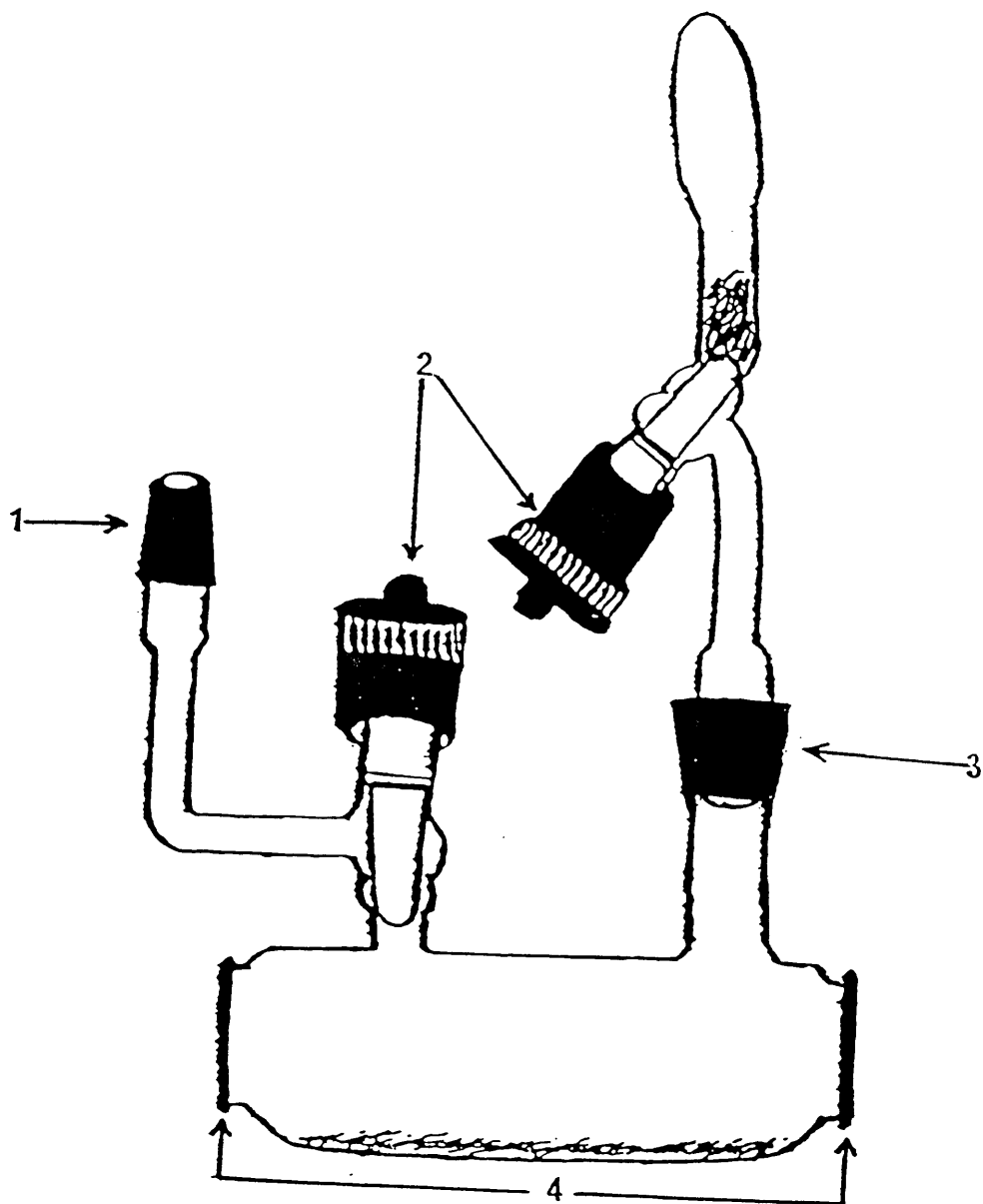
1- $B - 14$ Ground glass cone

2- Rotaflo stopcock

3- $B - 14$ Ground glass socket

4- Silver chloride windows

Figure(4:5).Reaction gas cell fitted with a single-limbed vessel.
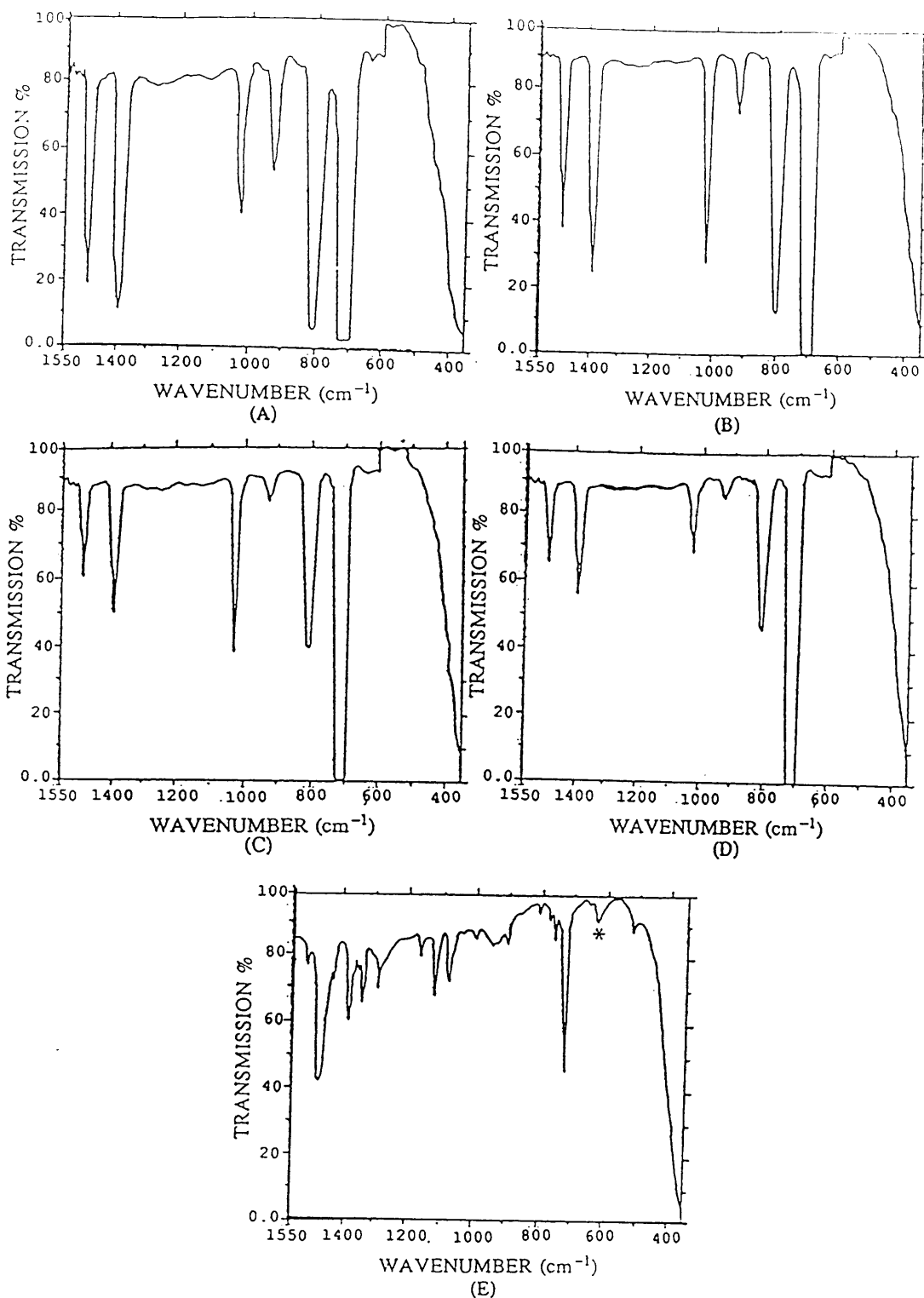
Figure(4:6).Infrared spectra of WF_6 vapour(A),from the
reaction after three additions of $[Al(Pc)F]_n$
(B),(C), and (D) and from the resultant
solid as a Nujol mull (E); the WF_6^- anion
absorption is marked with an asterisk.

amount of $[Al(Pc)F]_n$ used in this reaction was estimated as 4 mg (0.07 mmol) after weighing the quantity of the unused powder left in the single limb vessel. The interpretation of the spectra obtained before and after the additions of $[Al(Pc)F]_n$ powder is given in the results section of this chapter.

(II). $[Al(Pc)F]_n$ with $NOPF_6$.

This reaction was carried out using the gas cell and single limb vessel used above (Fig. 4:5). The vessel was flamed out under vacuum and transferred to the dry box. It was then loaded with a weighed quantity of $NOPF_6$ (0.27 g, 1.54 mmol), attached to the vacuum line and re-evacuated. The gas cell vessel was attached to the vacuum line, evacuated and transferred to the dry box. A weighed quantity of $[Al(Pc)F]_n$ powder (37 mg, 0.66 mmol) was placed in the trough of the cell which in turn was attached to the vacuum line and re-evacuated. A background infrared spectrum was recorded in the range 4000-400 cm^{-1} before the two reactants were mixed. The $NOPF_6$ salt was dropped onto the $[Al(Pc)F]_n$ powder and the mixture was shaken for approximately 15 min. The colour of the mixture changed from blue to purple during the shaking process. The design of the reaction gas cell enabled the solid reactants to be kept out of the i.r. beam and the spectrum was recorded for the gaseous products in the region 4000-400 cm^{-1} (Fig. 4:7). Details of the assignments of the absorption bands obtained in the spectrum of the products are given in the results section of this chapter.
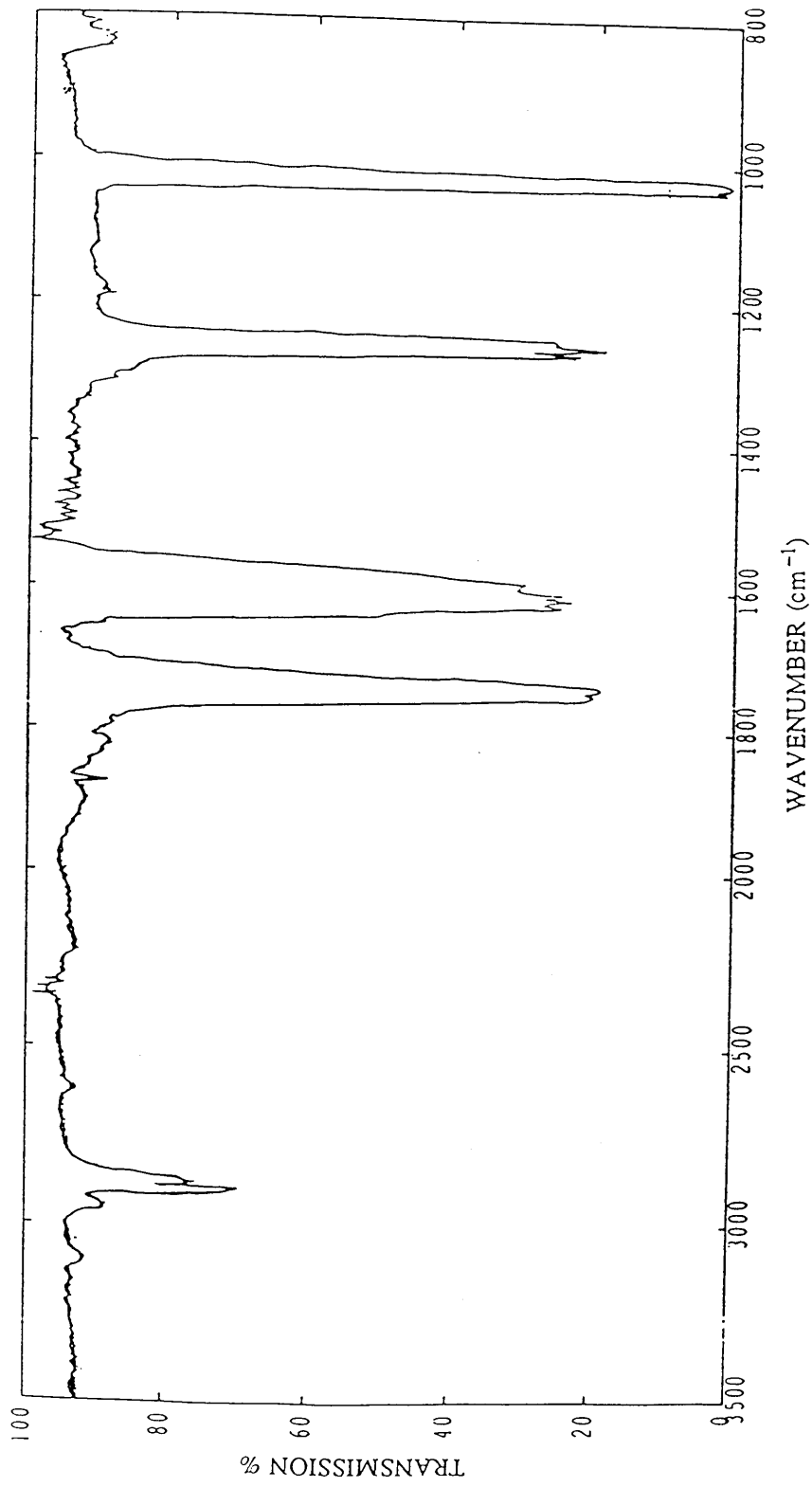
Figure(4:7).Infrared spectrum of the gaseous products evolved from the solid state reaction between [Al(Pc)F]$_n$ and NOPF$_6$ salt; the weak absorption band at 1875 cm^{-1} is assigned to NO gas.

4:3 Results and Discussion

Despite the reports of the vibrational spectra of the $[Al(Pc)F]_n$ polymer that have been reported previously [115], assignments of the bands observed in the spectra have not been mentioned. Similarly, the electronic spectra of this polymer have not been reported in the literature. The $[Al(Pc)F]_n$ polymer and its reactions with the MF_6 (M = U, Mo or W) and $NOPF_6$ oxidants were studied in the present work, mainly by infrared and u.v/visible spectroscopy. It was therefore necessary to make comparisons between the spectroscopic results obtained in the present work and that of other metal-phthalocyanine complexes reported in the literature in order to simplify the discussion of these results and to give useful interpretation.

In the early studies involving several metal-phthalocyanines (MPc's), it has been found that these complexes have closely similar vibrational and electronic spectra [139, 150-153]. Many groups [151, 154-156] have studied the vibrational spectra of various MPc's using Nujol (or halocarbon) mulls and potassium chloride (or bromide) disks. In most of these studies the absorption bands in the spectra have been assigned to the phthalocyanine ring vibrations such as C-H out-of-plane deformation, C-C benzene-ring skeletal vibrations (stretching and deformation) and C-N stretching. The vibrational spectra of $[Al(Pc)F]_n$ as a Nujol mull and as thin film deposited on a KCl substrate were similar and showed several bands in the region 1800-400 cm^{-1} (Fig. 4:8). The most characteristic feature of the spectra was the band at 520 cm^{-1} which was previously assigned to Al-F stretching vibration [1]. The rest of the bands in the
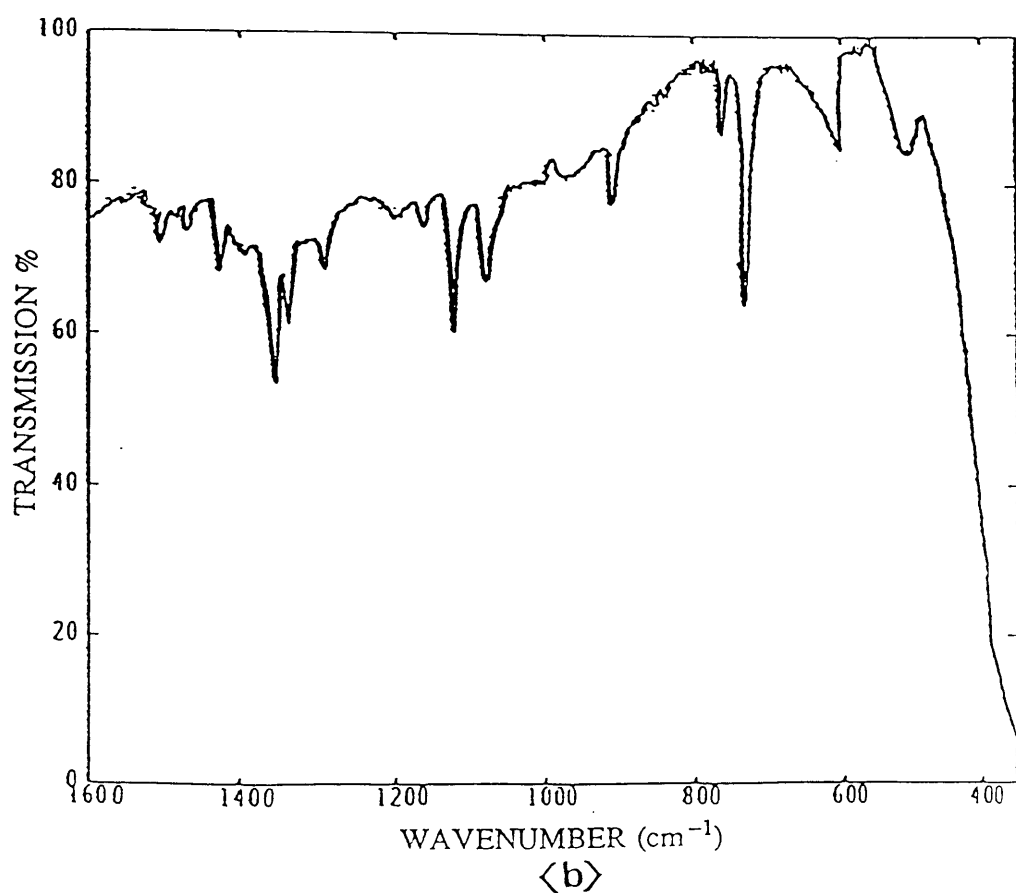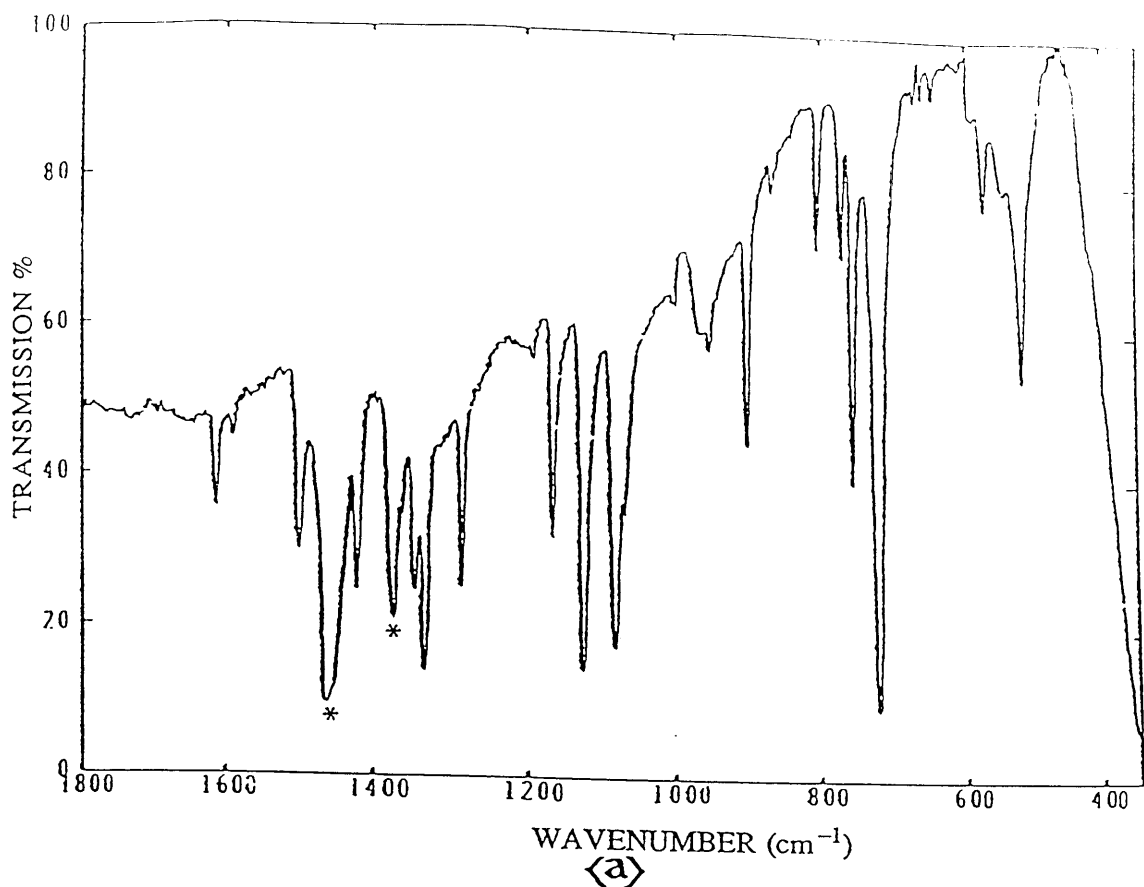
Figure(4:8).Infrared spectra of [Al(Pc)F]$_n$,(a) as Nujol mull and (b) as a thin film deposited on a KCl substrate (thickness=90nm). Nujol bands are marked with an asterisk.

spectra were assigned by comparisons with several reported studies [151, 154-156] involving other MPc complexes.

Despite the large number of optical spectra that have been published for PcH_2 and MPc complexes, there have been few assignments reported for the absorption bands observed. In particular, the construction of the bands in the B region 400-200 nm (traditionally called the Soret region) is generally not well-known [139]. The initial observations from the electronic spectra of several MPc complexes can be understood through the work of Gouterman and co-workers [152, 157, 158]. These workers have described that the electronic spectra of most MPc complexes arise primarily from π-π^* transitions within the delocalized phthalocyanine rings as shown in figure 4:9. They have concluded that the electronic spectra of most MPc complexes consist of five absorption bands in the region 800-200 nm. These bands have been labelled by the above workers, ranging from low to high energy, as Q, B, N, L and C. The Q band appears in the visible region (the Q region) near 700-600 nm, while the rest (B, N, L and C bands) appear in the ultraviolet region (the B region) between 400-200 nm [152]. Assignments of the first four bands (Q,B,N and L) are shown in figure 4:9 [152]. In addition to these bands, shoulders on the lower energy side of the B band have been observed in the spectra of many MPc complexes [159]. These shoulders have been tentatively assigned to the n-π transition from peripheral (bridging) aza links [159]. Except for those indicated above, no Pc-localized electronic spin-allowed transitions are expected energetically below the B band [159]. However, where empty metal d orbitals lie inside the HOMO-LUMO gap, low molecular

$2\,eg$ —————— (π^*)

$1\,b_{2u}$ —————— (π^*))

$1\,b_{1u}$ —————— $(\pi^*)^*$

$1\,eg$ —————— (π^*)

Q B N L

$1\,a_{1u}$ —————— (π)

$1\,a_{2u}$ —————— (π)

$1\,eg$ —————— (π)

$1\,b_{1u}$ —————— (π)

$2\,a_{1u}$ —————— (π)

$2\,eg$ —————— (π)
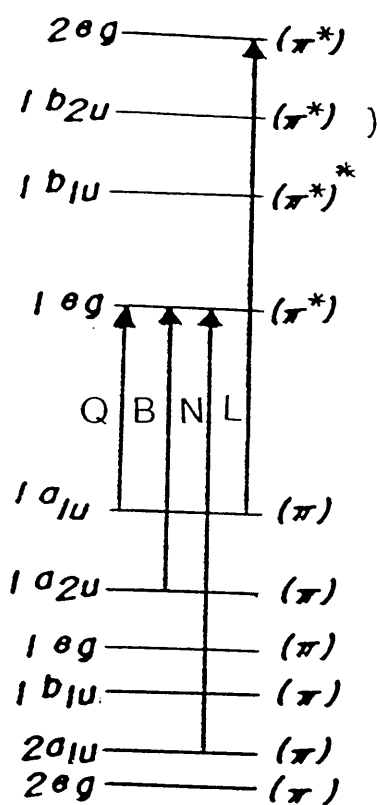
Figure(4:9).Molecular orbitals of the phthalocyanines,
the order of the orbitals has been adopted
from ref.[139,159].

charge transfer (LMCT) transitions of the general type Pc(π) -> d may be anticipated [159]. These can occur in the near i.r. region or in the region between the Q and B bands [159]. The electronic spectra of several MPc complexes have been studied by many other groups recently. Stillman et al [139] have reported the electronic spectra of ZnPc before and after the photo-and electrochemical oxidation with imidazole (Im) in methylene chloride (containing 0.05 M tetraethylammonium perchlorate). These workers have also identified the above stated absorption bands (Q,B,N,L and C) in the spectra of the unoxidised ZnPc [139]. Furthermore, they have reported additional absorption bands centred at 822, 511 and 424 nm in the spectra of the oxidised [ZnPc(-1)(Im)]$^{.+}$ species [139]. These bands have been assigned as π-π transitions from low-lying π MO's into the a_{1u} HOMO [139]. The studies of the electronic spectra of NiPc by Melson et al [150] and MgPc by Ough et al [160] have described observations similar to that reported by Gouterman [152, 157, 158] and Stillman [139].

In the present work, the electronic spectra of the [Al(Pc)F]$_n$ polymer as a pale blue mixture in MeCN and as thin film deposited on a silica substrate were relatively similar. Both spectra showed four characteristic absorption bands in the Q (visible) and B (ultraviolet) regions (Fig. 4:10); a shoulder on the lower energy side of the B1 band (near 380-390 nm) was also observed in the spectra. The absorption maxima (λ max) and assignments of these bands are given in table 4:5. Assignments of the bands were made by comparisons with the previously reported studies of other MPc complexes which were described earlier in this section. Note that the bands in the B region which have been labelled
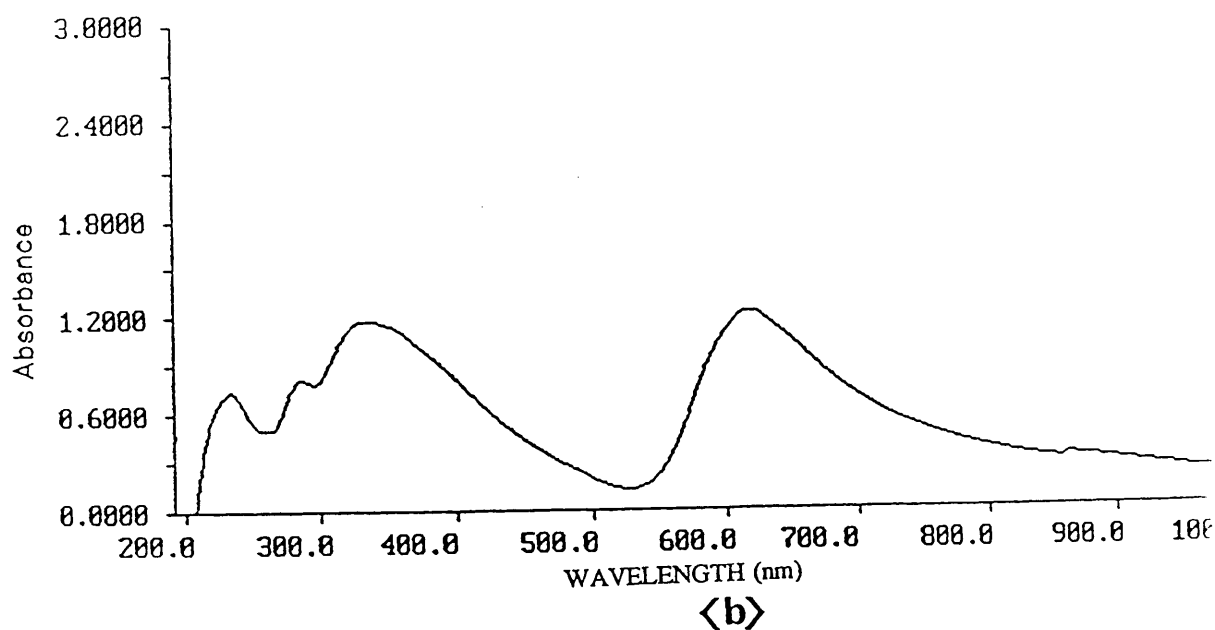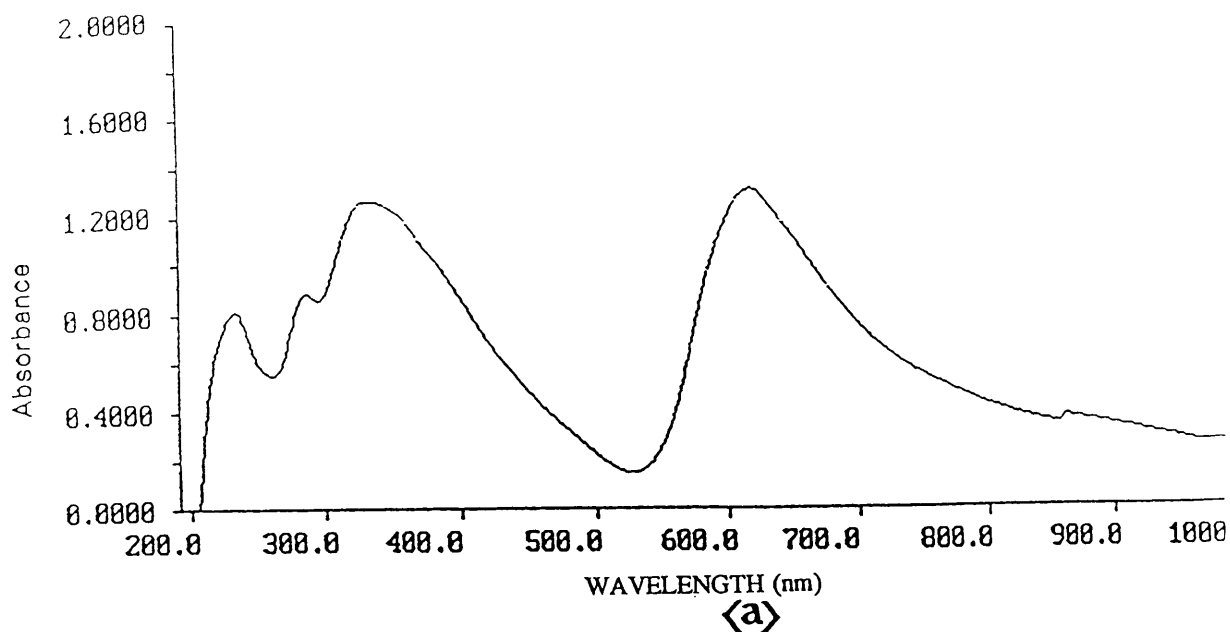
Figure(4:10).Electronic spectra of [Al(Pc)F]$_n$,(a) as a
mixture in acetonitrile (ca 0.003 mol dm^{-3})
and (b) as thin film deposited on a silica
substrate(thickness=55nm).

Table(4:5).Electronic spectra(λmax,nm) of the $[Al(Pc)F]_n$ polymer,(a).as a mixture in acetonitrile and (b).as a thin film on silica(thickness–55nm).

(a)   (b)

$[Al(Pc)F]_n$ (mixture in MeCN)	$[Al(Pc)F]_n$ (thin film)	Bands[c] label	Assignments[d]
620	620	Q	$1a_{1u}(\pi) \text{--->} 1e_g(\pi^*)$
385sh.	385sh.	---	------------------
330	330	B1	$1a_{2u}(\pi) \text{--->} 1e_g(\pi^*)$
285	285	B2	$2a_{1u}(\pi) \text{--->} 1e_g(\pi^*)$
235	235	B3	$1a_{1u}(\pi) \text{--->} 2e_g(\pi^*)$

sh=shoulder

c.The bands B1, B2 and B3 have been traditionally called B, N and L respectively.

d.Assignments of the bands were made by comparisons with previous studies carried out on other metal-phthalocyanine complexes[1,40,47,151-162].

in the literature as B, N and L are re-named in the present work as B1, B2 and B3 respectively; these new names were also used earlier in chapter three.

It is important to mention that the vibrational and electronic spectra of $[Al(Pc)F]_n$ in figures 4:8 and 4:10 respectively were reproducible when several samples were examined. In the case of the electronic spectrum of $[Al(Pc)F]_n$/MeCN mixtures, it is not certain whether the B3 band (near 300-200 nm) belongs to the polymer or to the solvent; although this band also appears in the spectrum of the film on silica substrate.

4:3:1 Results

A. Reactions in the Presence of MeCN.

The $[Al(Pc)F]_n$ polymer reacted with UF_6, MoF_6, $NOPF_6$ and WF_6 in the presence of acetonitrile rapidly at room temperature. In each case coloured solutions were formed. The colours of these solutions were dependent on the mole ratio $[Al(Pc)F]_n$:MF_6 (where M = U, Mo and W) or $[Al(Pc)F]_n$: $NOPF_6$ used. In all cases when the mole ratio $[Al(Pc)F]_n$:MF_6 (or $[Al(Pc)F]_n$:$NOPF_6$) was greater than one, the colour of the solutions formed was blue and part of the $[Al(Pc)F]_n$ remained undissolved in the bottom of the reaction vessel (see tables 4:1 - 4:4). Increasing the quantity of the oxidising agent resulted in changing the colour of the solutions from blue through purple to greenish-yellow. The quantity of the solid $[Al(Pc)F]_n$ remaining undissolved appeared to decrease also. The rate of a reaction as estimated by the time

taken for changes in colour to be observed and the quantity of solid remaining after the reaction was dependent on the oxidant used. For example a gradual increase in the quantity of UF_6 used resulted in colour changes from blue (with the mole ratio $[Al(Pc)F]_n:UF_6>1$) to dark purple (mole ratio ca 1.0:1.4), to greenish yellow (mole ratio ca 1.0:6.3) and finally pale brown when the mole ratio was ca 1.0:11.1. The formation of blue solutions together with the remaining undissolved solids and the absence of spectral changes in their spectra suggested that the reactions of $[Al(Pc)F]_n$ with MF_6 or $NOPF_6$ were incomplete.

The formation of greenish-yellow solutions when the mole ratio $[Al(Pc)F]_n:MF_6$ was 1.0:6.3, M = U; 1.0:4.5, M = Mo; 1.0:5.2, M = W and 1.0:4.2 in the case of $[Al(Pc)F]_n:NOPF_6$ were attributed to the depolymerization of $[Al(Pc)F]_n$ as well as oxidation. This speculative conclusion is based on comparison with the green and yellow solutions formed from the reactions of $[Al(Pc)F]_n$ polymer with strong protonic acids such as 98% H_2SO_4 and CF_3SO_3H which were described earlier in chapter three.

The formation of pale brown solutions when the mole ratio $[Al(Pc)F]_n:MF_6$ was 1.0:11.1 (M = U) and 1.0:13.4 (M = Mo) could be attributed to the presence of unreacted excess MF_6 which induced a polymerization process involving the solvent molecules. The solids isolated from these solutions had yellowish-brown colours, of a gel-like consistency and were insoluble in fresh MeCN. On the basis of the observations made above, it was concluded that the most favourable mole ratios for studying these reactions were those which produced dark purple solutions.

The purple solid products isolated from carrying out the reactions using the stoichiometries marked with an asterisk in tables 4:1 - 4:4 were highly soluble in MeCN, were easily isolated and were stable _in vacuo_ for a long time. These solids and their solutions in acetonitrile were examined by infrared and u.v/visible spectroscopy respectively; the spectra obtained were compared with that of the unreacted $[Al(Pc)F]_n$ polymer.

The vibrational spectra of the solid products indicated that the number of the phthalocyanine bands in the region 1600-400 cm^{-1} was reduced; many of the bands were relatively broad (Fig. 4:11). The spectra also showed new bands at 845, 635, 565 and 555 cm^{-1} depending on the oxidizing agents used (Fig. 4:11). The bands at 845 and 555 cm^{-1} were assigned to v_3 and v_4 of the PF_6^- anion by comparison with the i.r. spectrum of KPF_6 [161]. The bands at 635 and 565 cm^{-1} were assigned to v_3 (MoF_6^-) and $v_3(UF_6^-)$ respectively by comparison with the i.r. spectra of $[I(NCMe)_2][MF_6]$ (M = Mo or U) [149]. The band at 605 cm^{-1} was tentatively assigned to v_3 (WF_6^-) by comparison with the band at 595 cm^{-1} identified in the reported i.r. spectrum of $[Cu(NCMe)_4][WF_6]$ [47]. It was also observed that an additional band in the region 1050-1065 cm^{-1} had appeared in the spectra of the products isolated from the reactions with UF_6, MoF_6 and $NOPF_6$ in the presence of MeCN (Fig. 4:11). This band has been also observed in the i.r. spectra of [Mn(Pc)] doped with I_2 or Br_2 [162], and it has been tentatively attributed to the appearance of a positive charge on the phthalocyanine ligand. Furthermore, it has been reported [163] that the i.r. spectra of several protonated metal-phthalocyanine complexes exhibit
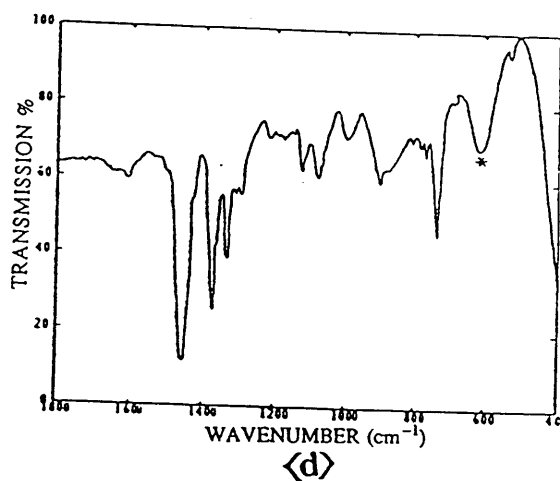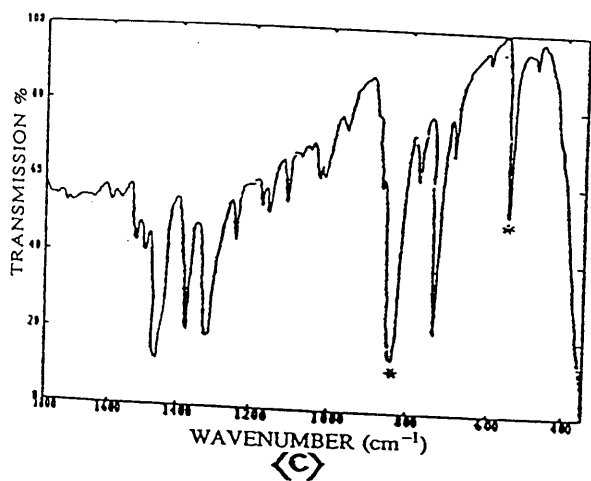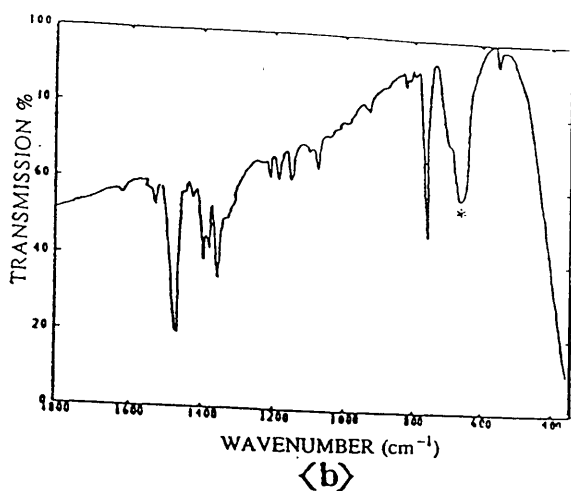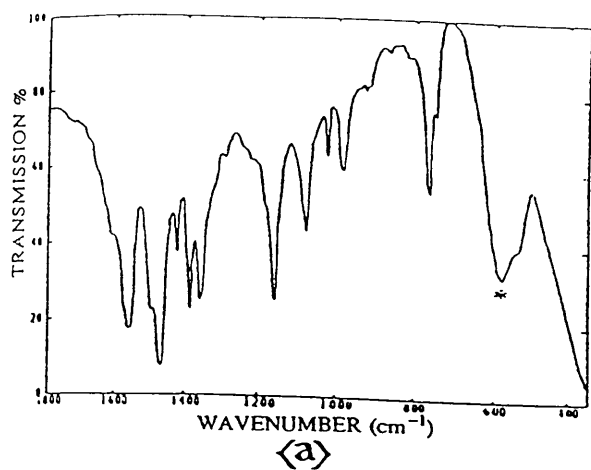
Figure(4:11).Infrared spectra of [Al(Pc)F]$_n$,(as a Nujol mull) reacted with UF$_6$(a),MoF$_6$(b),NOPF$_6$ (c) and WF$_6$(d).The MF$_6^-$ anion absorptions are marked with an asterisk.

a band at 1060 cm^{-1} which has been assigned to phthalocyanine cations. Therefore by comparison with the above reported studies, the band at 1050-1065 cm^{-1} observed in the present spectra could be also attributed to the formation of $[Al(Pc)F]_n^+$ species. All the absorption bands observed in the spectra of the products and their assignments, where possible, are summarised in table 4:6.

The electronic spectra of the purple solutions formed from the reactions of $[Al(Pc)F]_n$ with MF$_6$ or NOPF$_6$ in the presence of MeCN were compared with that of the blue mixture of $[Al(Pc)F]_n$ in acetonitrile. The comparison showed that when $[Al(Pc)F]_n$ reacted with UF$_6$ or MoF$_6$ the Q band was shifted to longer wavelength (lower energy) and split into two components (Fig. 4:12). The intensities of these components were decreased compared with that of the Q band before the reaction. A shoulder was observed at 540-560 nm in these spectra. The bands in the B region (B1, B2 and B3) were shifted to lower wavelength and their intensities increased compared with those before the reaction. The spectra also showed a new shoulder on the lower energy side of the B1 band.

The electronic spectrum of the purple solution formed from the reaction between $[Al(Pc)F]_n$ and UF$_6$ in MeCN showed several absorption bands in the region 1500-1100 nm (Fig. 4:13). These bands were assigned to a mixture of UF$_6^-$ anion and UF$_5$.NCMe by comparison with $[Tl(MeCN)_5][UF_6]_3$ in MeCN [164], $[AsPh_4][UF_6]$ in MeCN [165] and UF$_5$.NCMe in MeCN [48].

The electronic spectra of the purple solutions formed from the reactions of $[Al(Pc)F]_n$ with NOPF$_6$ and WF$_6$ in the

Table(4:6).Infrared absorptions (cm^{-1}) of [Al(Pc)F]$_n$
reacted with UF$_6$, MoF$_6$, NOPF$_6$ and WF$_6$
in acetonitrile; the samples were examined
as Nujol and Fluorolube mulls.

[Al(Pc)F]$_n$	[Al(Pc)F]$_n$/UF$_6$	[Al(Pc)F]$_n$/MoF$_6$	[Al(Pc)F]$_n$/NOPF$_6$	[Al(Pc)F]$_n$/WF$_6$	Approximate assignment*
1612 m	----	----	----	----	C - C str.
1592 vw	1590 sh	1600 vw	1595 vw	1600 vw	C - C str.
----	1550 b	----	----	----	C - C str.
1500 m	1490 sh	1505 w	1520 w	----	C - N str.
1350 m	----	----	----	----	----
1288 m	1270 vw	----	----	1290 vw	C - H ben.
----	----	----	1245 m	----	----
1195 vw	1195 sh	1190 vw	1180 w	1210 w	----
1168 s	1150 s	1160 vw	1160 vw	1170 vw	C - H ben.
1125 s	----	1125 w	1115 w	1120 w	C - H ben.
1085 s	----	1075 vw	1085 vw	1075 m	C - N str.
----	1060 m	1055 w	1060 vw	----	[Al(Pc)F]$_n^+$
----	----	----	1035 w	----	----
1005 w	1002 w	995 vw	1020 w	995 m	C - C str.
960 m	965 m	965 m	965 m	----	----
902 s	905 vw	902 vw	----	900 m	C - H ben.

str.=streching mode, def.=deformation, s=strong
,m=medium, w=weak, vw=very weak, sh=shoulder and
b=broad.

*Band assignments for [Al(Pc)F]$_n$ were made by
comparison with the reported i.r. spectra of
other metal-phthalocyanine complexes[1,152,
155-157,163,164]; the assignments of MF$_6^-$ or
PF$_6^-$ anions were also made by comparisons with
previous works in which these oxidants were used
[47,150,162].

Table(4:6).Continued

$[Al(Pc)F]_n$	$[Al(Pc)F]_n / UF_6$	$[Al(Pc)F]_n / MoF_6$	$[Al(Pc)F]_n / NOPF_6$	$[Al(Pc)F]_n / WF_6$	APProximate assignment*
870 w	——	——	875 vw	——	C - N ben.
——	——	——	845 b	——	$V'_3 (PF_6^-)$
810 m	——	——	——	805 w	C - H ben.
775 m	790 m	790 vw	780 m	780 vw	C - H ben.
760 s	765 sh	765 vw	——	760 w	——
725 s	735 s	735 s	730 s	730 s	C - H ben.
675 vw	——	——	690 w	——	C-C ring def.
665 vw	——	665 sh	——	670 sh	C-C ring def.
——	——	635 b	——	——	$V_3 (MoF_6^-)$
615 vw	——	——	615 vw	——	C-C ring def.
——	——	——	——	605 b	$V'_3 (WF_6^-)$
595 vw	——	——	——	——	C-C ring def.
575 w	——	——	——	——	C-C ring def.
——	565 b	——	——	——	$V_3 (UF_6^-)$
——	——	——	555 s	——	$V_4 (PF_6^-)$
545 vw	——	——	——	——	C-C ring def.
520 s	520 sh	520 w	495 w	515 w	Al - F str.
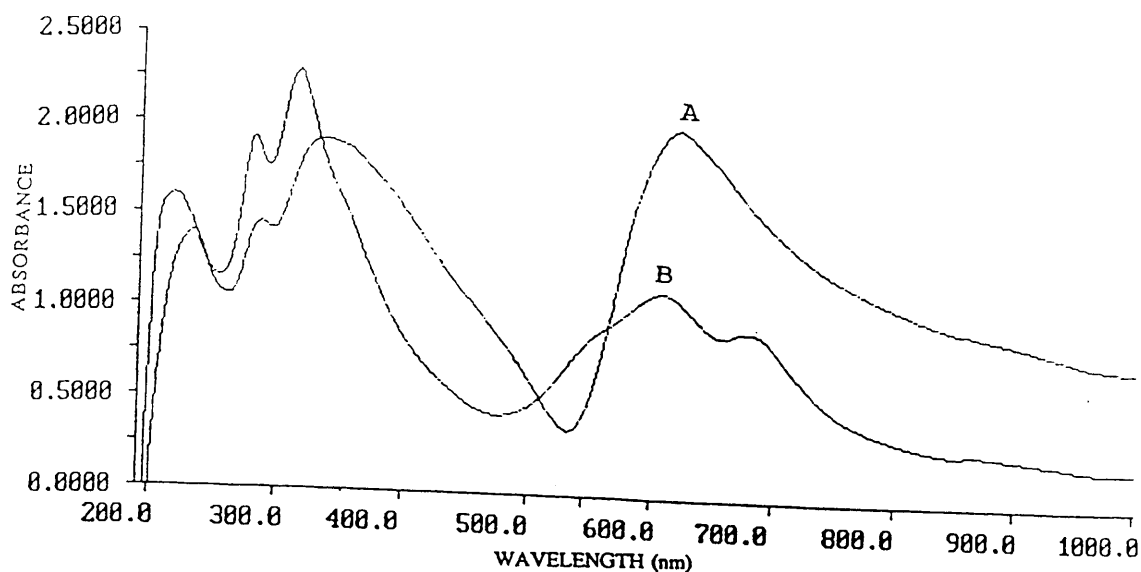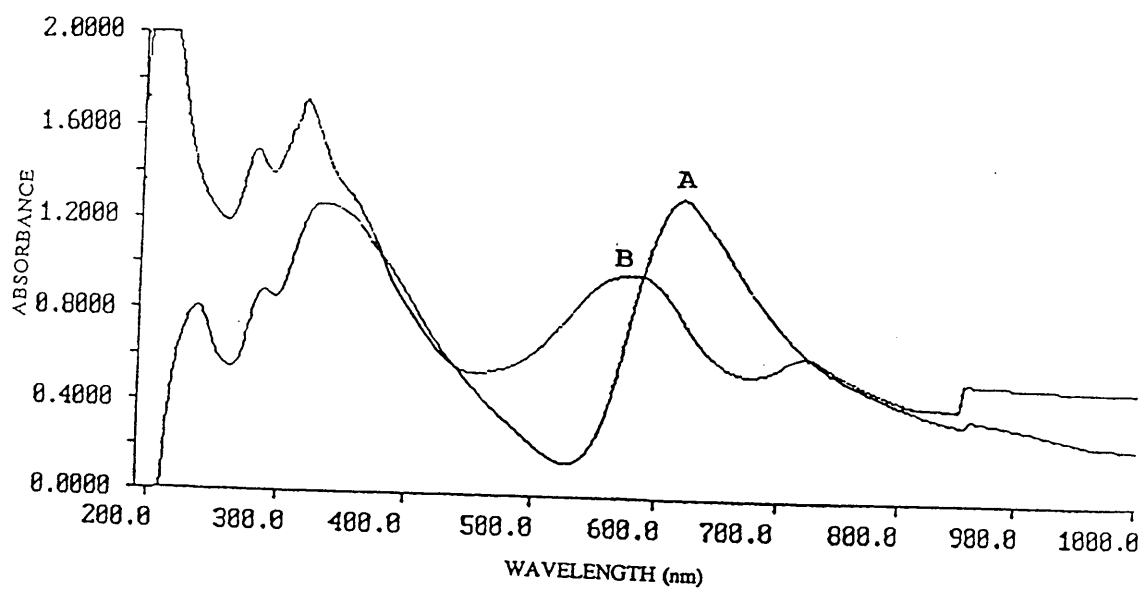
Figure(4:12).Electronic spectra of [Al(Pc)F]$_n$ in MeCN
(1A and 2A) and after the reactions with
UF$_6$ (1B) and MoF$_6$ (2B).
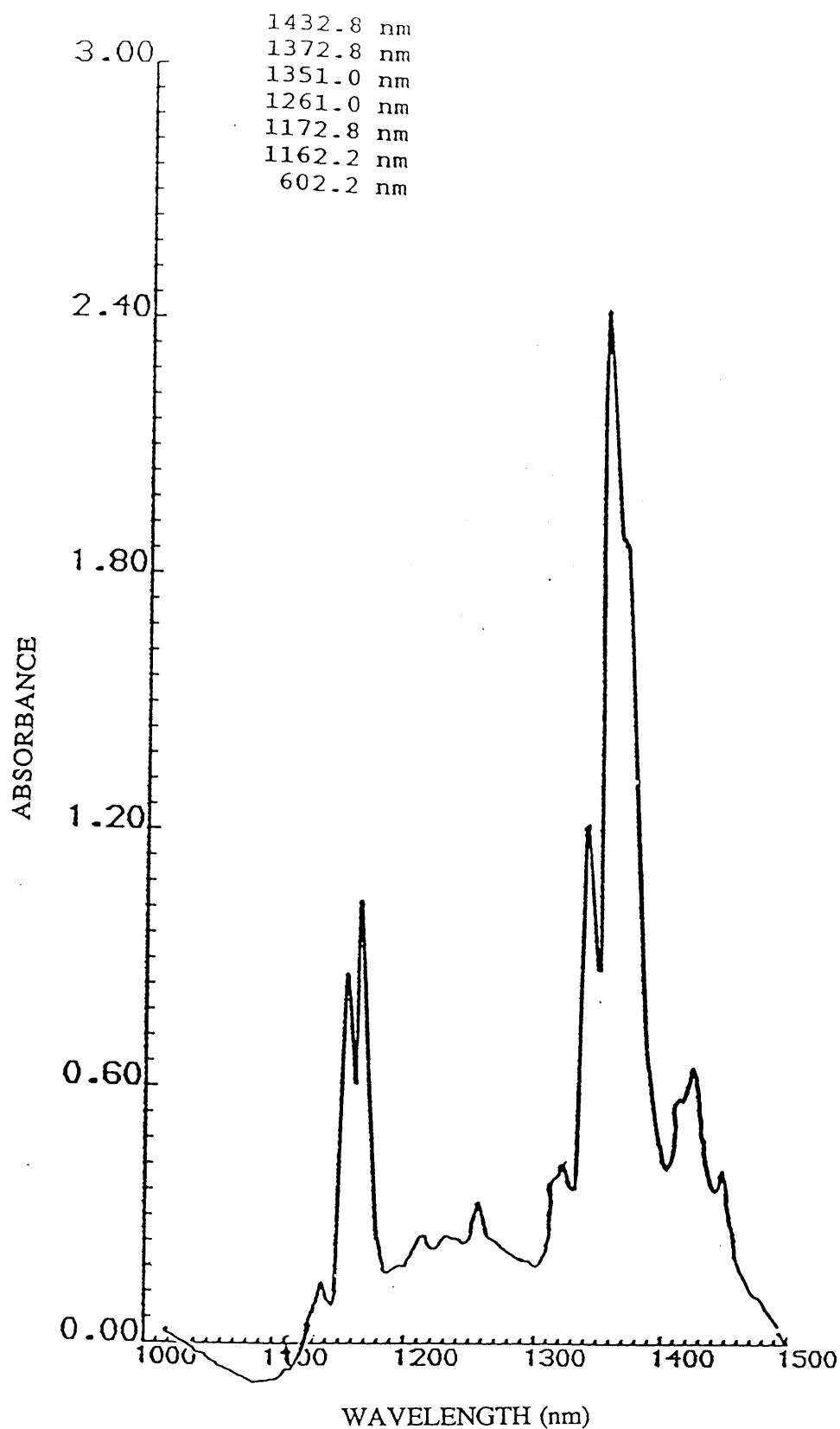
Figure(4:13).Electronic spectra of a mixture of UF$_6^-$

and UF$_5$ in acetonitrile.

presence of MeCN showed that the Q band was shifted to longer wavelength (Fig. 4:14) after the reactions. The intensity of this band appeared to decrease compared with that in the spectrum of $[Al(Pc)F]_n$ in MeCN. In the case of the reaction between $[Al(Pc)F]_n$ and WF_6 the spectrum also showed new bands centred at 965 and 865 nm; the latter band was also found in the spectrum obtained from the reaction with $NOPF_6$. New strong absorption bands near 570-540 nm were also identified in the spectra of $[Al(Pc)F]_n$ after the reactions with $NOPF_6$ and WF_6. Several spectral changes were also observed in the B region of the spectra obtained for the solutions formed from these reactions. The B bands were all shifted to lower wavelength (higher energy) (Fig. 4:14). By comparing the intensities of these bands with those of the B bands in the spectrum of $[Al(Pc)F]_n$ in MeCN, it was found that the intensities of the B2 and B3 bands appeared to increase after the reactions. The intensity of the B1 band was increased when $NOPF_6$ was used as an oxidant and decreased when WF_6 was used as the oxidant. In both reactions, with $NOPF_6$ and WF_6 the spectra showed a new shoulder on the lower energy side of the B1 band (Fig. 4:14).

The absorption bands (λ_{max}) observed in the spectra of unreacted $[Al(Pc)F]_n$, in MeCN and after the reactions with UF_6, MoF_6, $NOPF_6$ and WF_6 are given in table 4:7.
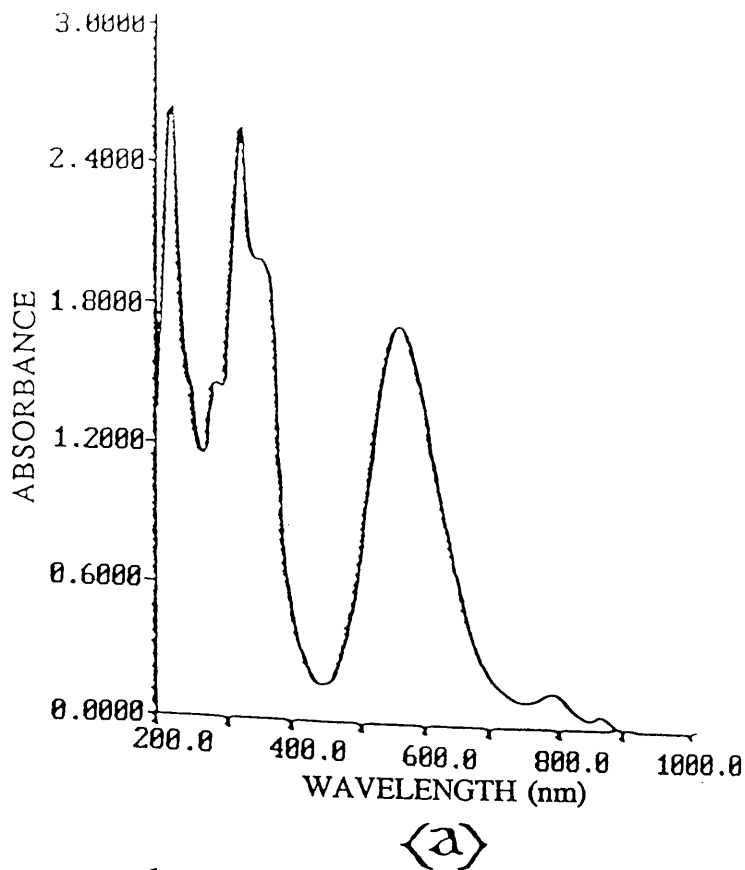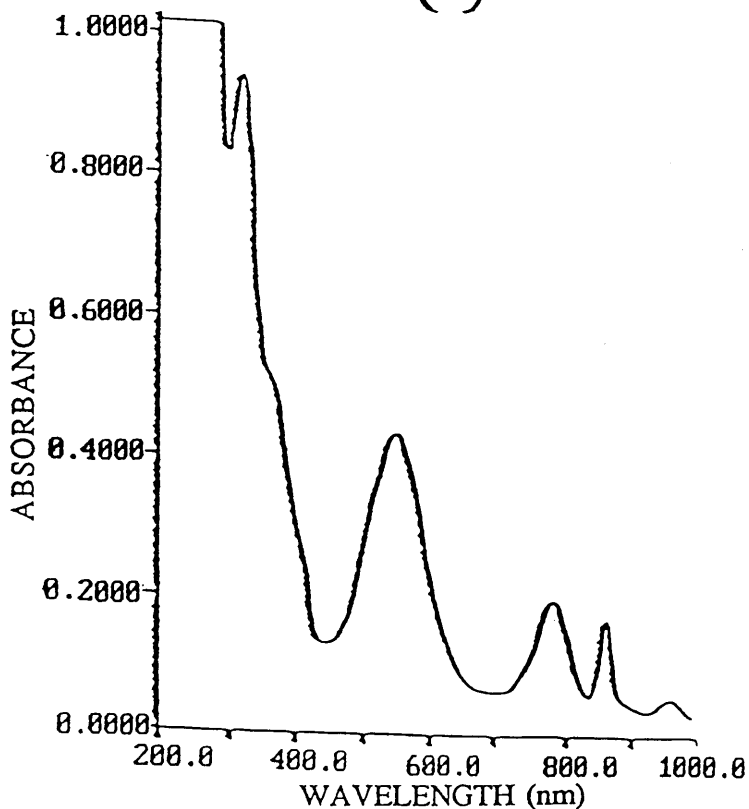
Figure(4:14).Electronic spectra of [Al(Pc)F]$_n$ in MeCN
after the reactions with NOPF$_6$ (a) and
WF$_6$ (b).

Table(4:7).Electronic spectra(λ max,nm) of $[Al(Pc)F]_n$ reacted with UF_6, MoF_6, $NOPF_6$ and WF_6 in the presence of MeCN (6 cm^3) at room temperature.

$[Al(Pc)F]_n$ (nm)	$[Al(Pc)F]_n/UF_6$ (nm)	$[Al(Pc)F]_n/MoF_6$ (nm)	$[Al(Pc)F]_n/NOPF_6$ (nm)	$[Al(Pc)F]_n/WF_6$ (nm)
---	---	---	---	965
---	---	---	865	865
620	685	730	790	785
---	600	585	---	---
---	545 sh	555 sh	560	550
385 sh	355 sh	355 sh	355 sh	365 sh
330	315	320	325	320
285	280	280	280	270*
235	220	205	225	195*

sh=shoulder

*These bands were off scale

B. Thin Film Reactions.

The vibrational spectra of the purple films on KCl substrates resulting from the reactions with MF_6 (M = U, Mo and W) were recorded in the range 4000-400 cm^{-1}. These spectra were compared with those of unreacted $[Al(Pc)F]_n$ films. The comparison showed that the phthalocyanine bands in the region 1600-400 cm^{-1} were broadened and reduced in number after the reactions (Fig. 4:15). The spectra also showed the presence of new broad bands at 655 and 625 cm^{-1} which were tentatively assigned to $v_3(MoF_6^-)$ [149] and $v_3(WF_6^-)$ [47] respectively (Fig. 4:15). A weak absorption band centered at 515 cm^{-1} was observed in the spectrum of the purple film resulting from the reaction with UF_6; this band was tentatively attributed to the presence of UF_6^- anion [149] (Fig. 4:15). All the absorption bands observed in the spectra of the reacted films along with their assignments are listed in table 4:8. Band assignments in tables 4:6 and 4:8 were made by comparison with several reported studies involving other metal-phthalocyanine complexes [1, 139, 150-156, 162, 163, 166].

The electronic spectra of the purple films on silica substrates formed from the reactions with MF_6 oxidants were recorded in the region 1000-185 nm. These spectra were compared with those of $[Al(Pc)F]_n$ films before the reactions. The comparison showed that in all cases the Q band was broadened and shifted to longer wavelength and a new strong band near 610-550 nm had appeared after the reactions (Figure 4:16). A shoulder at 555 nm was observed in the spectrum of the thin film after the reaction with UF_6 (Fig. 4:16). The intensity of the Q band was increased when the
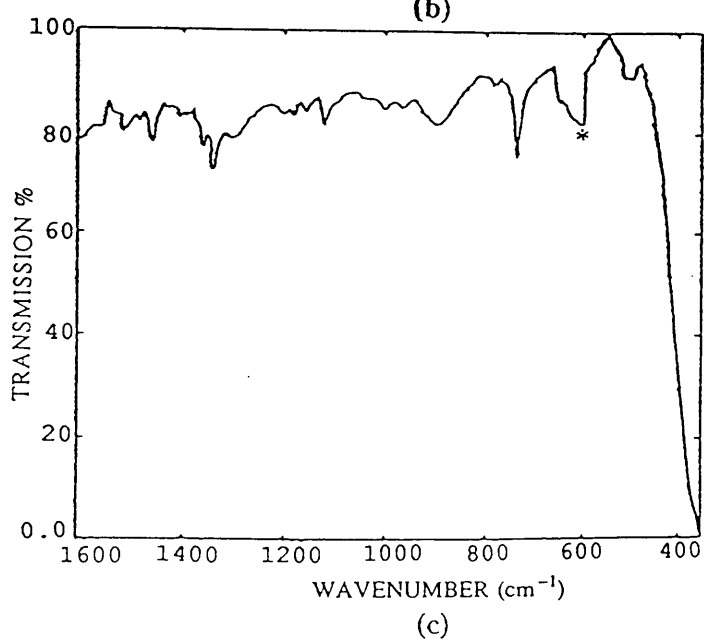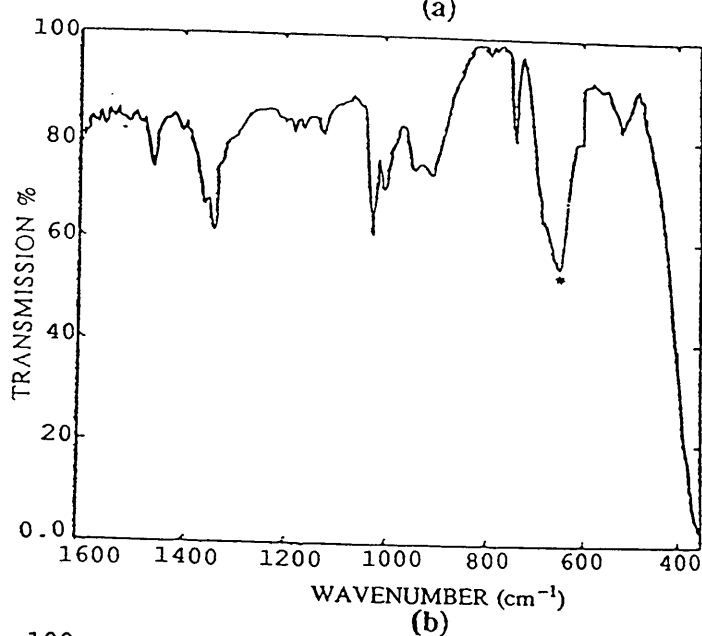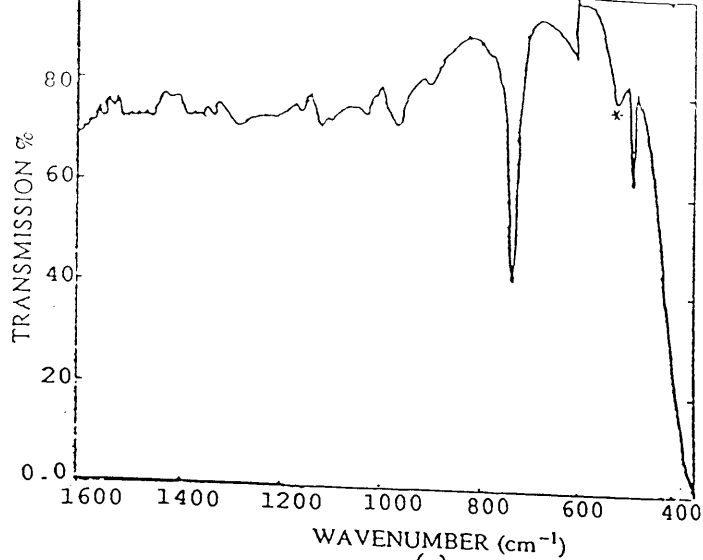
Figure(4:15).Infrared spectra of thin films of $[Al(Pc)F]_n$ deposited on KCI substrates (thickness=90 nm) and reacted with UF_6 (a), MoF_6 (b) and WF_6 (c).The MF_6^- anions are marked with an
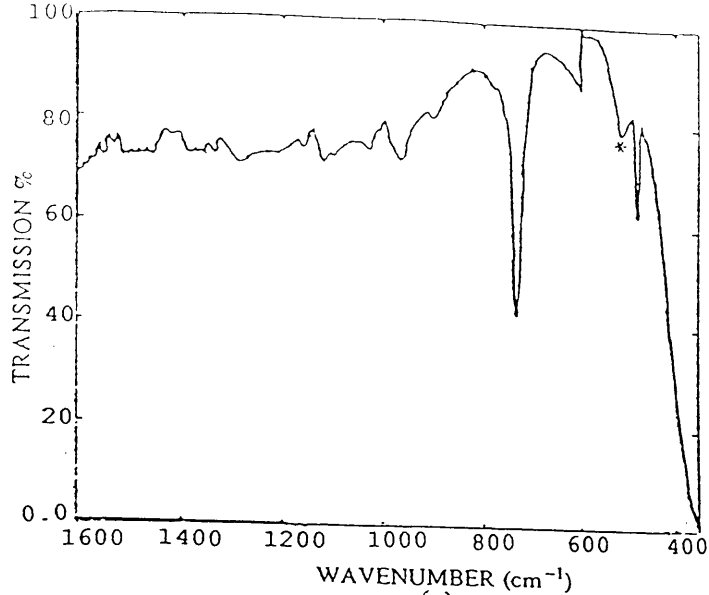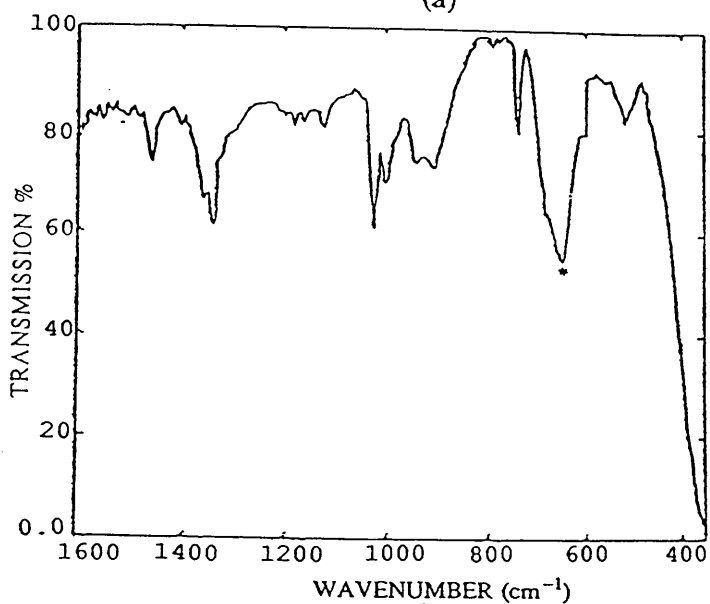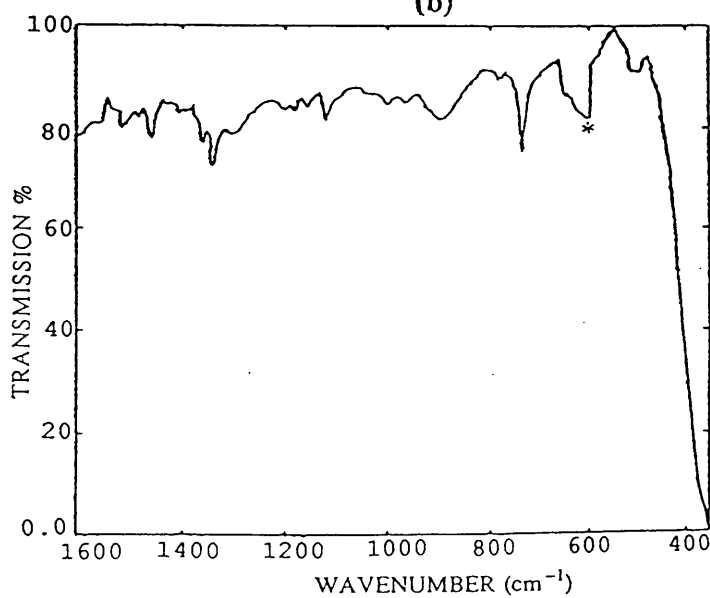
Figure(4:15).Infrared spectra of thin films of $[Al(Pc)F]_n$ deposited on KCl substrates (thickness=90 nm) and reacted with UF_6 (a), MoF_6 (b) and WF_6 (c).The MF_6^- anions are marked with an asterisk.

Table(4:8).Infrared absorptions(cm^{-1}) of thin films of [Al(Pc)F]$_n$ on KCl (thickness=95nm) and exposed to the vapours of UF$_6$, MoF$_6$ and WF$_6$ at room temperature.

[Al(Pc)F]$_n$	[Al(Pc)F]$_n$/UF$_6$	[Al(Pc)F]$_n$	[Al(Pc)F]$_n$/MoF$_6$	[Al(Pc)F]$_n$	[Al(Pc)F]$_n$/WF$_6$	Approximate assignment*
1550 vw	1550 vw	1550 vw	1550 vw	1550 vw	1550 vw	C - C str.
1530 vw	1530 vw					
1510 vw	1510 vw	1510 vw	1510 vw	1510 vw	1510 vw	
1500vw	1500 vw	1500 vw		1500 vw	1500 vw	C - N str.
1480 vw	1480 vw			1475 vw	1480 vw	C - C str.
1465 vw	1470 vw	1455 vw	1450 vw	1450 vw	1460 vw	
				1420 vw		
1400 vw	1390 vw	1390 vw		1400 w		C - N str.
		1355 w	1360 vw	1350 vw	1355 vw	
1335 vw	1335 vw	1340 vw	1345 w	1340 vw	1335 vw	C - C str.
1285 vw	1280 vw	1280 vw		1285 vw		C - H ben.
		1155 vw	1165 vw	1155 vw	1160 vw	C - H ben.

s=strong, m=medium, w=weak, vw=very weak and b=broad

*The bands assigned by comparison with the assignment in table 4:6 (Nujol mull) and with the i.r. spectrum of a thin film of PbPc on NaCl substrate[167].

Table(4:8).Continued

$[Al(Pc)F]_n$	$[Al(Pc)F]_n/UF_6$	$[Al(Pc)F]_n$	$[Al(Pc)F]_n/MoF_6$	$[Al(Pc)F]_n$	$[Al(Pc)F]_n/WF_6$	Approximate assignment*
1120 w	1120 vw	1120 w	1125 vw	1120 m	1125 w	C _ H ben.
1080 vw				1075 vw	1075	C - N str.
			1030 s			
		1005 vw	1005 w			
	965 w					
			930 b			
905 vw		900 vw		900vw	900w	C - H ben.
				760 vw		C - H ben.
735 s	735 s	735 m	740 m	725 m	740 m	C - H ben.
			655 b			$V_3(MoF_6^-)$
					625 b	$V'_3(WF_6^-)$
	515 w					$V_3(UF_6^-)$
		510 w	510 w	510 w	510 w	Al - F str.
480 m	480 m					Al - F str.
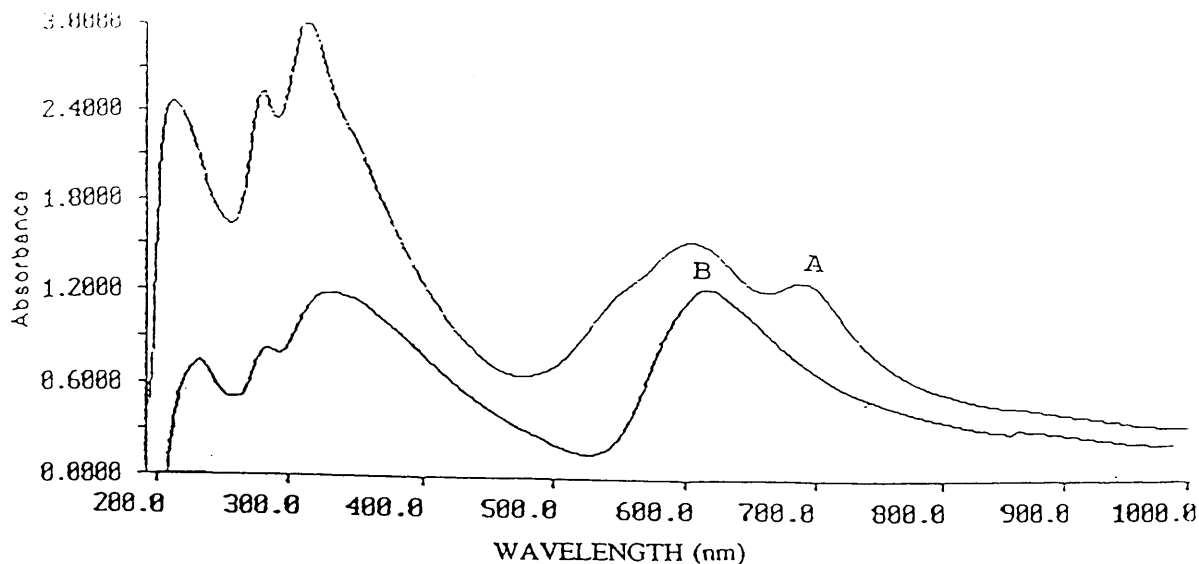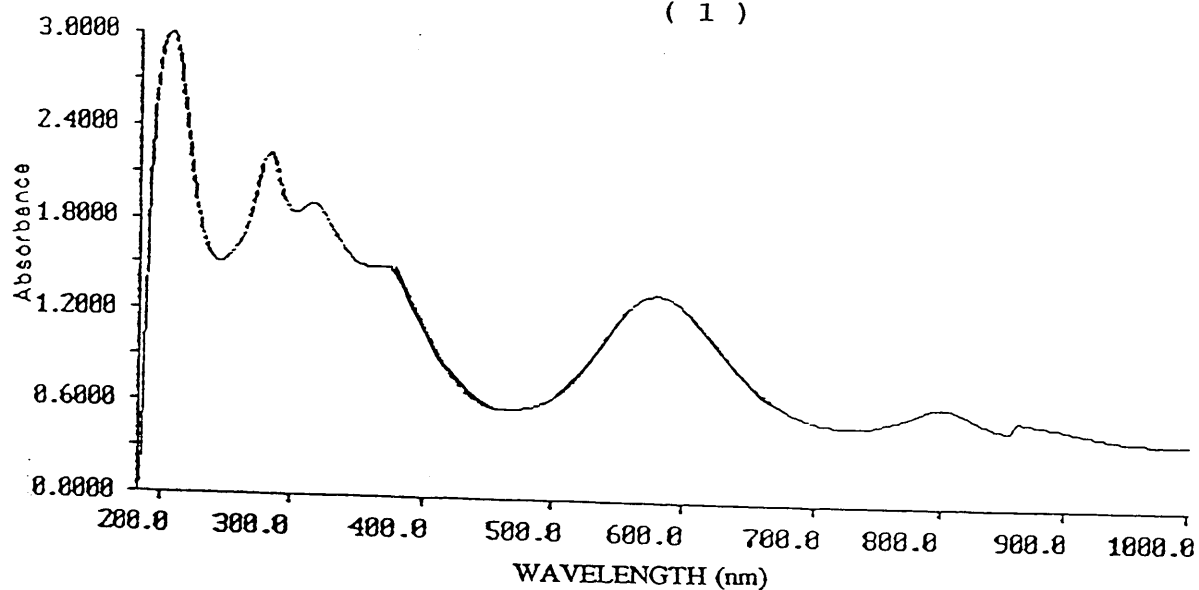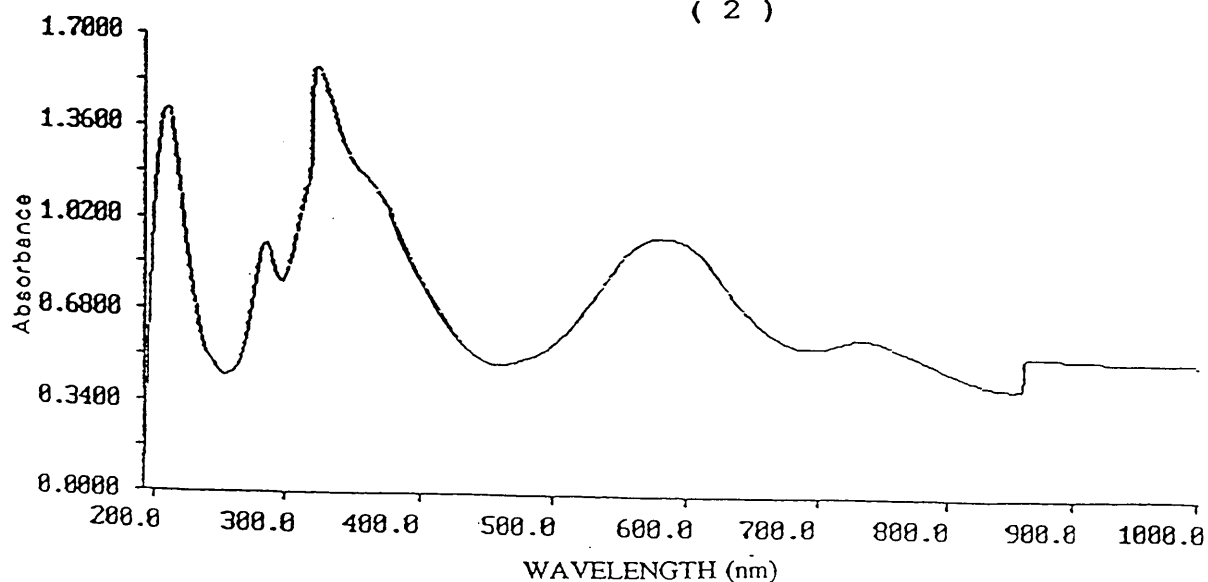
Figure(4:16).Electronic spectra of [Al(Pc)F]$_n$ as a thin
film deposited on silica (thickness=55nm)
(1B) and after the reactions with UF$_6$ (1A)
,MoF$_6$ (2) and WF$_6$ (3).

film reacted with UF_6 while decreased after the reactions with MoF_6 or WF_6. The spectra of the reacted films also indicated that the bands in the B region (B1, B2 and B3) were all shifted to shorter wavelength (Fig. 4:16). The intensities of these bands were increased after the reactions. All the absorption bands observed in the spectra of the purple film formed from the above reactions along with their absorption coefficient values (α) are illustrated in table 4:9. Note that the absorption coefficient values of the bands were estimated by using the following equation (equation 4-2):

$$A = \alpha d \quad \ldots\ldots\ldots\ldots\ldots\ldots\ldots(4\text{-}2)$$

where A = absorbance

   α = absorption coefficient (cm^{-1})

   d = thickness of the film (cm)

The vibrational and electronic spectra of the films obtained from the reactions with MF_6 oxidants were compared with those of the products resulting from similar reactions in the presence of MeCN. The comparisons indicated that in both types of reactions the spectral changes observed were, to some extent, relatively similar.

Table(4:9).Electronic spectra(λmax,nm) and absorption coefficient(α,cm^{-1}) of [Al(Pc)F]$_n$ films (on silica, thickness=55nm) exposed to the vapours of UF$_6$, MoF$_6$ and WF$_6$ at room temperature.

[AL (Pc)F]$_n$		[AL (Pc)F]$_n$/UF$_6$		[AL (Pc)F]$_n$/MoF$_6$		[AL (Pc)F]$_n$/WF$_6$	
λ_{max}	α^*	λ_{max}	α^*	λ_{max}	α^*	λ_{max}	α^*
620	220	690	240	795	120	735	100
---	---	605	280	---	---	---	---
---	---	555 sh	---	570	250	580	170
385	---	360 sh	---	370 sh	---	375 sh	---
330	210	315	580	315	400	320	280
285	140	280	460	280	430	280	170
235	130	210	440	205	540	205	260

sh=shoulder

*The α values (cm^{-1}x10^{-3}) were estimated using equation 4:2.

C. Reactions of [Al(Pc)F]$_n$ with WF$_6$ and NOPF$_6$ in the Absence of Solvent.

(I). Reaction with WF$_6$ Vapour.

The aim of carrying out this reaction was to examine whether or not polycrystalline [Al(Pc)F]$_n$ could interact with WF$_6$ vapour in the absence of a solvent. Attention was devoted to the detection of the spectral changes in the WF$_6$ absorptions after the mixing process of the two reactants.

The vibrational spectrum of WF$_6$ in the gas phase has been reported previously [141, 167]. It has been shown that the spectrum contains twelve absorption bands in the region 1600-400 cm^{-1}. Of these, the intense band centered at 712 cm^{-1} has been assumed to be fundamental (v_3) whereas the remaining bands are overtones. The WF$_6$ molecule is octahedral and so belongs to the point group O$_h$. It has six normal modes of vibration. Of these, only v_3 and v_4 vibrations are infrared active [141].

In the present work the vibrational spectrum of WF$_6$ (96 Torr) was recorded in the region 4000-400 cm^{-1}. The spectrum indicated the fundamental band at 712 cm^{-1} along with seven overtones in the range 1600-400 cm^{-1} (Fig. 4:6).

The difference in the number of bands observed in this spectrum compared with that in the reported spectrum above [167] can be attributed to the higher vapour pressure of WF$_6$ (700 Torr) measured in that study compared with 96 Torr used in the present study.

Three additions of $[Al(Pc)F]_n$ powder were made into the cell containing the frozen WF_6. After each addition the two reactants were allowed to mix at room temperature, shaken for approximately 15 min and the vibrational spectrum of the gaseous products was recorded in the range 4000-400 cm^{-1} (Fig. 4:6). Each spectrum obtained after the additions of $[Al(Pc)F]_n$ powder was compared with that of WF_6 vapour before the reaction. Changes in the transmittance of the overtone bands were the most informative (Fig. 4:6). The transmittance of the overtone bands were significantly decreased compared with those in the spectrum of WF_6 before the reaction. The changes in the intensities of the absorption bands of WF_6 during the additions of $[Al(Pc)F]_n$ indicated that some WF_6 was consumed in the reaction presumably by the $[Al(Pc)F]_n$ powder which changed from blue, before the reaction, to purple. The purple solid product isolated from this reaction was examined by infrared spectroscopy as Nujol and Fluorolube mulls. The spectrum indicated that the phthalocyanine bands in the region 1600-400 cm^{-1} were broadened and reduced in number after the reaction (Fig. 4:6). This spectrum also showed the presence of a new weak absorption band at 625 cm^{-1} which could be assigned to WF_6^- anion. These observations were made by comparing the above spectrum with that of unreacted $[Al(Pc)F]_n$ (Fig. 4:8). The spectrum was also compared with that of the purple solid isolated from the reaction between $[Al(Pc)F]_n$ and WF_6 in the presence of MeCN (Fig. 4:11). This comparison indicated that the spectral changes observed after the reactions were relatively similar in both spectra.

The absorption bands observed in the spectrum of WF_6 vapour along with the changes in their transmittance after

the reaction with three additions of $[Al(Pc)F]_n$ powder are given in table 4:10. Band assignments in this table were made by comparison with other reported studies involving WF_6 in the vapour phase [141, 167]

The purple solid isolated from this reaction was dissolved in acetonitrile (6 cm^3) and an intense purple solution was obtained; the concentration of Al^{III} in this solution was estimated as <u>ca</u> 0.01 mol dm^3. This solution was examined by electronic spectroscopy in the region 1000-185 nm. The spectrum showed that all the absorption bands were off scale due to the high concentration of the solution. Therefore, a diluted solution was obtained by using the manipulations described earlier in section 4:2. The electronic spectrum of this diluted solution (Fig. 4:17) was compared with that obtained for the products isolated from the reaction between $[Al(Pc)F]_n$ and WF_6 in the presence of MeCN (see Fig. 4:14). The comparison indicated that in both spectra the spectral changes involving the Q and B bands were relatively similar. However, the main difference between the two spectra was that the new bands observed in the region 1000-850 in the spectrum obtained from the reaction in the presence of MeCN (see Fig. 4:14) were not found in this spectrum (Fig. 4:17).

(II). Reaction with $NOPF_6$.

The $NOPF_6$ salt was mixed with $[Al(Pc)F]_n$ powder (mole ratio $[Al(Pc)F]_n$:$NOPF_6$ <u>ca</u> 1.0:2.3) in the reaction gas cell. The colour of $[Al(Pc)F]_n$ changed from blue to purple during the mixing process. The vibrational spectrum of the gaseous products formed from the reaction contained several bands in

Table(4:10).Infrared absorptions (cm^{-1}) of WF_6 vapour and the changes in their intensities after the reaction with three additions of $[Al(Pc)F]_n$ powder at room temperature.

WF_6 (cm^{-1})	Transmittance(%) before adding $[Al(Pc)F]_n$	Transmittance(%) after reactions with three additions of $[Al(Pc)F]_n$			Assignment[*]
		Addition 1	Addition 2	Addition 3	
1481	82	62	40	35	$\nu_1 + \nu_3$
1385	89	75	51	44	$\nu_2 + \nu_3$
1290	22	12	12	12	$\nu_1 + \nu_5 + \nu_6$
1130	20	11	11	11	$\nu_2 + \nu_6$
1027	59	71	62	32	$\nu_1 + \nu_4$
928	46	27	18	15	$\nu_2 + \nu_4$
805	94	87	61	54	ν_4
712[a]	---	--	--	--	ν_3

[*]Assignments were made by comparison with the i.r. spectrum of WF_6 vapour reported in previous studies [142,168].

a.This band was too intense to show any transmittance variation

λ_{max} (nm)
790
575
375 sh.
315
280
210

sh. = shoulder
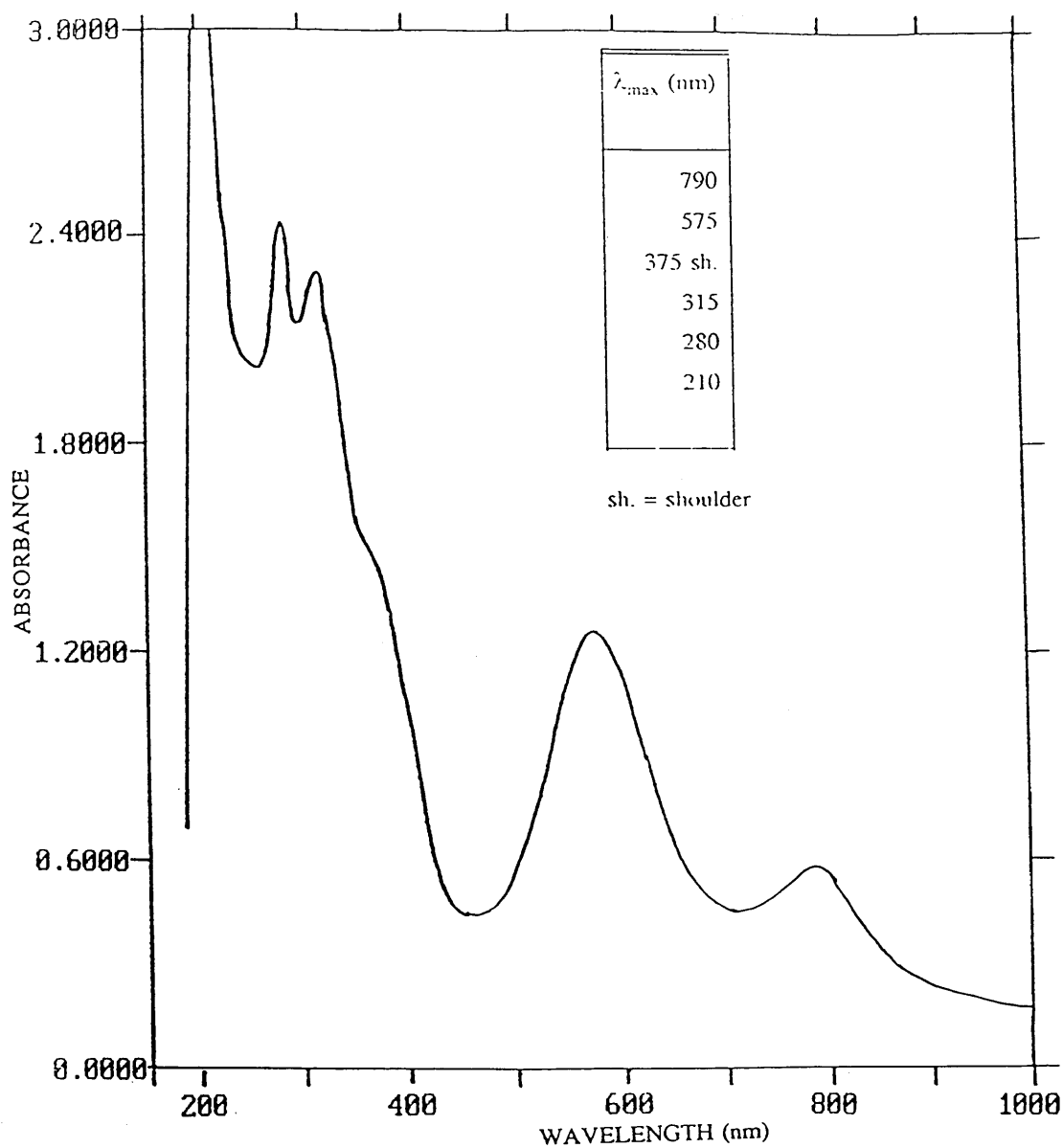
Figure(4:17).Electronic spectrum of the solution (in MeCN) formed by dissolving the solid isolated from the reaction between [Al(Pc)F]$_n$ and WF$_6$ in the absence of a solvent.

the region 3500-800 cm^{-1} (Fig. 4:7). This spectrum was compared with that of pure NO gas from the literature [168]. The comparison indicated the presence of the band at 1875 cm^{-1} which was assigned to the NO gas evolved from the above reaction. Other bands observed in the spectrum were attributed to impurities of NO_2, and N_2O_4 [168] which might have resulted from the presence of trace oxygen or moisture adsorbed on the cell.

The solid products isolated from this reaction were examined as Nujol mull, by infrared spectroscopy in the range 1650 - 400 cm^{-1}. This was compared with that obtained for the products isolated from the reaction between $[Al(Pc)F]_n$ and $NOPF_6$ in the presence of MeCN (Fig. 4:11). The comparison indicated that in both spectra the spectral changes were almost identical.

The purple solid isolated from the above reaction was also dissolved in MeCN (6 cm^3) and an intense purple solution was produced; the concentration of Al^{III} in the solution was estimated as $\underline{ca}$ 0.11 mol dm^{-1}. This solution was diluted without opening the reaction cell by using the dilution method described in section 4:2. The electronic spectrum of the solution after the dilution was recorded in the region 1000-185 nm (Fig. 4:18). This was compared with that obtained for the purple solution formed from the reaction in the presence of MeCN (Fig. 4:14). This comparison indicated that the spectral changes resulted from both types of reactions being almost similar; except that the band at 865 nm observed in the spectrum in figure 4:14 was not found in this spectrum (Fig. 4:18).
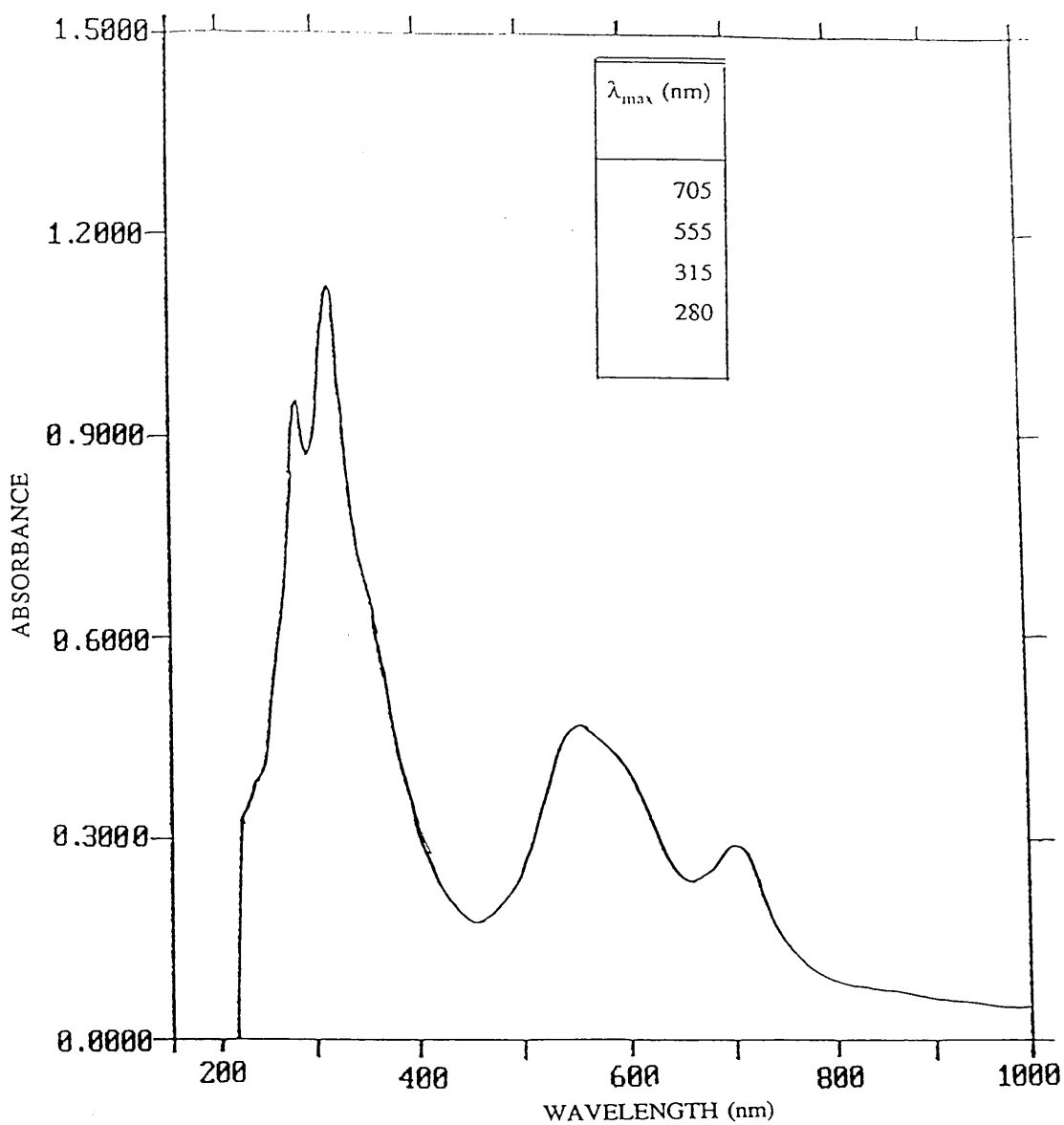
Figure(4:18).Electronic spectrum of the solution (in
MeCN) formed by dissolving the solid
isolated from the reaction between
[Al(Pc)F]$_n$ and NOPF$_6$ in the absence of
a solvent .

4:3:2 <u>Discussion</u>

The results described in section 4:3:1 indicate that reactions occur between the $[Al(Pc)F]_n$ polymer and the oxidants UF_6, MoF_6, WF_6 and NO^+ cation in the presence, or absence, of MeCN at room temperature.   Thin films of the $[Al(Pc)F]_n$ polymer deposited on silica and KCl substrates also react with the vapours of UF_6, MoF_6 and WF_6 at room temperature.   The vibrational and electronic spectra of the products formed provide strong evidence which indicates the oxidation of the $[Al(Pc)F]_n$ polymer.

The most characteristic feature of the vibrational spectra of the products is the presence of new bands assigned to MF_6^- (M = U, Mo or W) and PF_6^- anions (Figs. 4:11 and 4:15).   The observation of these bands suggests that charge transfer from the polymer to the oxidants has occurred. This is supported by the appearance of a new band at 1060 cm^{-1} (which is tentatively assigned to $[Al(Pc)F]_n^+$) in the spectra of the solids (Fig. 4:11).   The broadness in the phthalocyanine bands (some bands are obscured) in the spectra of the products formed from all reactions (see Figs. 4:11 and 4:15) has been also observed in the i.r. spectra of $[Al(Pc)F]_n$ or $[Ga(Pc)F]_n$ polymers oxidised by I_2 [169] and $NOBF_4$ [2].

The observation of gas bubbles during the reaction between $[Al(Pc)F]_n$ and $NOPF_6$ in MeCN and the detection of the band at 1875 cm^{-1} (Fig. 4:7) assigned to NO gas when the reaction was repeated in the absence of a solvent provide more evidence that the polymer is oxidised.   The spectral

changes from the reactions between polycrystalline $[Al(Pc)F]_n$ and $NOPF_6$ salt (Fig. 4:7) or WF_6 vapour (Fig. 4:6 and table 4:10) indicate that oxidation of this polymer is also achieved in the absence of a solvent.

The spectral changes in the electronic spectra after the reactions provide additional evidence. The strong red shift (and in some cases splitting) of the Q band and the weak blue shift of the bands in the B region (see Figs. 4:12 - 4:18 and tables 4:7 and 4:9) are similar to the changes observed from the reactions of the $[Al(Pc)F]_n$ polymer with strong protonic acids (see chapter three). In chapter three it was concluded that these changes can be attributed to the formation of a positive charge on the polymer as a result of the attachment of a proton (or protons) to the phthalocyanine molecules. The spectral changes in the present reactions can be also attributed to the formation of $[Al(Pc)F]_n^+$ species. The strong absorption band near 550 - 610 nm which is present in the spectra of the products from all reactions has also been observed in the spectra of $[Mn(Pc)]$ oxidised by Br_2 or I_2 [163]. This band is assigned as a $\pi - \pi^*$ intramolecular charge transfer [163]. The new absorption bands in the near i.r. region of the spectra obtained for the products from the reactions with $NOPF_6$ or WF_6 in MeCN are possibly due to the formation of monomeric and dimeric species. Similar bands are observed in the spectra of the products formed from the reactions between $[Al(Pc)F]_n$ and CF_3COOH, described in chapter three. Furthermore, these bands have been also reported [150] in many studies involving several metal-phthalocyanine complexes $[M(Pc)]$ (where M = Cu, Ni, Zn, Fe, Mn or Cr) and it has been suggested that they arise from n(aza) -> π^* Pc transitions.

Thus, there is some evidence for depolymerization in these reactions.

In the previously reported studies involving the oxidation of the $[Al(Pc)F]_n$ polymer by diiodine [169] or by $NOBF_4$ [2] it has been suggested that electron transfer from the polymer to the oxidant molecules occurs. Similar suggestion has been made when this polymer was oxidised by AsF_5 [115]. However, the nature of the reaction has not been completely described. The structure and ionization potential of $[Al(Pc)F]_n$ and the structure and electron affinity of the oxidising agent used, all play important roles in the outcome of the reactions. The medium in which the reaction is carried out, for instance the nature of the solvent in the case of solution reactions, is also important. These aspects are discussed below.

In order for complete electron transfer from the $[Al(Pc)F]_n$ polymer to the oxidising agent to occur, it is necessary that the electron affinity of the oxidant and the ionization potential of the polymer are compatible. The ionization potential of the $[Al(Pc)F]_n$ polymer has been reported by Dugay et al [112] as 439 kJ mol^{-1}. For electron transfer to be complete in a homogeneous gas phase reactions the electron affinity of the oxidising agent must be numerically greater than 439 kJ mol^{-1}.

Several methods have been used for the determinations of the electron affinities of UF_6, MoF_6 and WF_6 (see chapter one) and different values have been reported. However, the most recent determinations which are often used in the literature are 502 kJ mol^{-1} for UF_6 [170], 492 kJ mol^{-1} for

MoF$_6$ [171] and 338 kJ mol^{-1} for WF$_6$ [172]. The order of the oxidising power of the above oxidants has been practically established in MeCN as follows UF$_6$>MoF$_6$>NO$^+$>WF$_6$ [50]. Furthermore, from reactions involving the use of these oxidants in the gas phase it has been found that UF$_6$ and MoF$_6$ will oxidize NO to NO$^+$ (examples are given in chapter one).

The inter-ring spacing in the [Al(Pc)F]$_n$ polymer (the distance between two phthalocyanine rings) is 3.66 Å [5]. Hence, if the doping process involves intercalation of the oxidant molecules between the phthalocyanine rings, their diameters must be less than 3.66 Å.

It is clear from the experimental results that the oxidation of the [Al(Pc)F]$_n$ polymer is not simply dependant on the electron affinity and the ionization potential of the oxidant and the polymer respectively. Other additional factors (e.g. the lattice energy of the oxidised product and enthalpy of formation) must play important roles in driving the reactions. The importance of these factors as a driving force for the oxidation reaction has been illustrated by Bartlett [29] in his studies of the oxidising properties of the third transition series hexafluorides. For instance the reaction between PtF$_6$ and simple one-electron reductant such as O$_2$ [29] in the following equation (equation 4-3):

$$O_{2\ (g)} + PtF_{6\ (g)} \longrightarrow O_2^+(PtF_6)^-_{\ (s)} \quad ....(4\text{-}3)$$
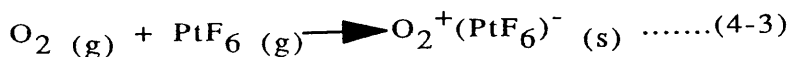
has been described by Bartlett using the following Born-Haber cycle for the product O$_2^+$(PtF$_6$)$^-_{\ (s)}$:

$$O_2 \text{ (g)} \quad + \quad PtF_6 \text{ (g)} \quad \underline{\text{exothermic}} \quad O_2^+(PtF_6)^- \text{ (s)}$$

$$I=1175.7 \qquad E>-652.7 \qquad\qquad U=-523$$

$$O_2^+ \text{ (g)} \quad + \quad PtF_6^- \text{ (g)}$$
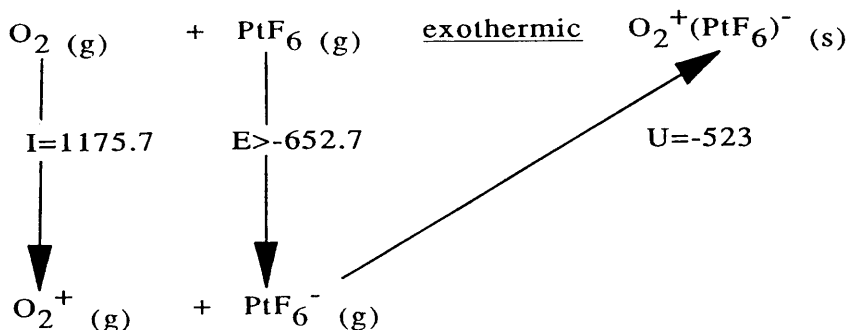
where I, E and U are the ionization potential, electron affinity and lattice energy respectively; all enthalpies in kJ mol^{-1}.

The reactions in the present work can be interpreted in a manner similar to that used by Bartlett [29].

The ionization potential of [Al(Pc)F]$_n$ is stated by Dugay et al [112] to be 439 kJ mol^{-1}. These workers give no details in their study of how the above value was obtained. Furthermore, they did not explain to which of the following reactions (equations 4-4 - 4-7) the term 'ionization potential' refers; for instance is it to:

$$[Al(Pc)F] \text{ (g)} \longrightarrow [Al(Pc)F]^+ \text{ (g)} \quad + \quad e^- \quad .....(4\text{-}4)$$

or to:

$$[Al(Pc)F]_n \text{ (g)} \longrightarrow [Al(Pc)F]_n^+ \text{ (g)} + e^- \quad ....(4\text{-}5)$$

or to:

$$[Al(Pc)F] \text{ (s)} \longrightarrow [Al(Pc)F]^+ \text{ (s)} + e^- \quad ....(4\text{-}6)$$

or to:

$$[Al(Pc)F]_n \text{ (s)} \longrightarrow [Al(Pc)F]_n^+ \text{ (s)} + e^- \quad ....(4\text{-}7)$$
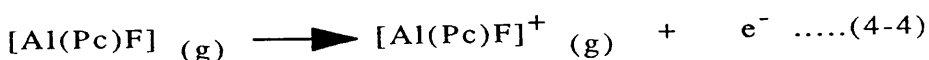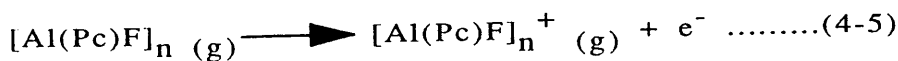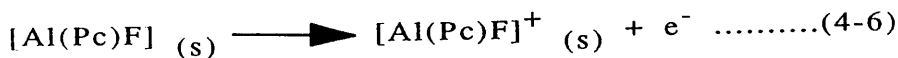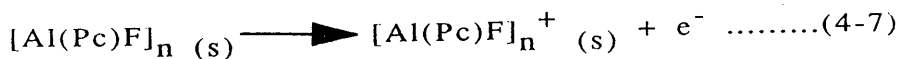
If it refers to the latter (which seems most reasonable) the reactions with the MF_6 (M = U, Mo or W) in the absence of a solvent can be considered as following:

$$[Al(Pc)F]_{n(s)} + YMF_{6(g)} \xrightarrow{\Delta H_{react}} \{[Al(Pc)F]^+[MF_6]^-_y\}_{n(s)}$$

$$- - \cdots \cdots (4-8)$$
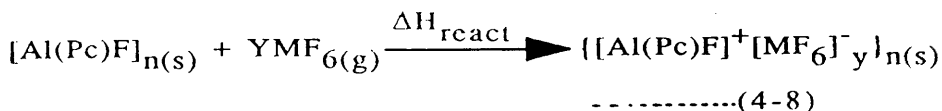
where ΔH_{react} is the enthalpy change of the reaction, n is the number of the polymer units and y is the number of moles of the oxidant. Similarly, the reaction between $[Al(Pc)F]_n$ and $NOPF_6$ can be represented as follows:

$$[Al(Pc)F]_{n(s)} + YNOPF_{6(s)} \xrightarrow{\Delta H_{react}} \{[Al(Pc)F]^+[PF_6]^-_y\}_{n(s)}$$

$$- \cdots \cdots (4-9)$$
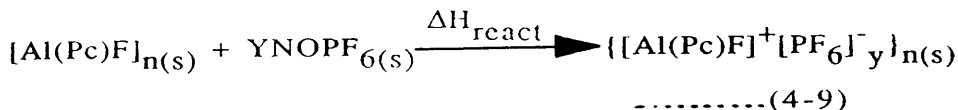
When reactions 4-8 and 4-9 occur we can assume that ΔH_{react} has a negative value (exothermic reaction) and these reactions can be treated by the following Born-Haber cycle:

$$[Al(Pc)F]_{n(s)} + YOx_{(g)} \xrightarrow{\Delta H_{react}} \{[Al(Pc)F]^+[Ox]^-_y\}_{n(s)}$$

$$\downarrow IP \qquad \downarrow EA \qquad \qquad \Delta H^-$$

$$[Al(Pc)F]^+_{n(s)} + YOx^-_{x(g)}$$
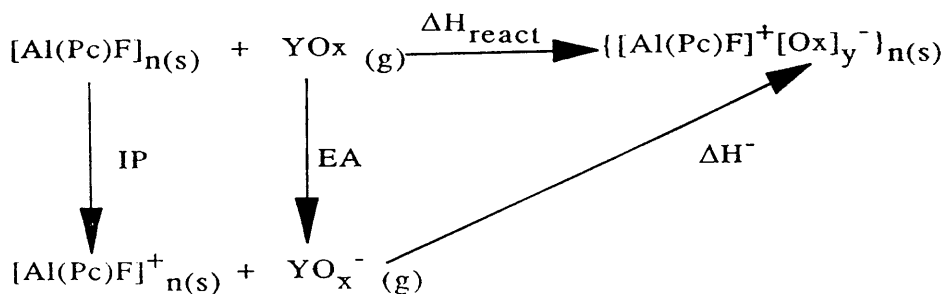
where IP is the ionization potential, EA is electron affinity of the oxidant $Ox(MF_6$ or $NO^+)$ and ΔH^- is an enthalpy term describing the formation of $\{[Al(Pc)F]^+[Ox]^-_y\}_{n(s)}$ and reflecting the electrostatic interaction between $[Al(Pc)F]^+_n$ cations and YOx^- anions.

In the case of the reactions carried out in the presence of MeCN, solvation of the cation by MeCN and ion pairing between $[Al(Pc)F]_n{}^+$ and YOx^- ions replace ΔH^- as the driving force for the reaction to occur.

The M-F bond distances in UF_6, MoF_6 and WF_6 (in the orthorhombic phase) have been reported as 1.990 Å [62], 1.810 Å [23] and 1.818 Å [23] respectively. Using these distances the diameters of the corresponding hexafluoride molecules are estimated as ca 5.170 Å, 4.810 Å and 4.826 Å for UF_6, MoF_6 and WF_6 respectively. The addition of a negative charge to an atom or molecule causes an increase in the diameter and larger anions will be formed. Therefore even if the oxidants UF_6, MoF_6 or WF_6 can be intercalated between the rings of the polymer and form anions, the diameters of the latter are such that considerable distortion of the Pc complex would occur. Similarly the minimum calculated diameter for the $PF_6{}^-$ anion is 4.6 Å [173] and it is too large to be intercalated.

Insertion of octahedral doping molecules, MF_6 is likely to entail an intra chain disorder which can become so large that the eclipsed conformation of the phthalocyanine rings is destroyed. Evidence for distortions in the structure of $[Al(Pc)F]_n$ as a result of doping has been obtained from the study by transmission electron microscopy and is reported in chapter six. The distortion is due to both steric and electronic factors associated with the doping process. The former arising from the dopant molecules attempting to intercalate between the Pc rings, resulting in the pushing of the rings and hence, weakening the Al-F-Al bonds. While the latter arises from the formation of a positive charge on the

rings, thus, reducing the stability of the electronic structure of the polymer. Both of the above factors cause depolymerization of $[Al(Pc)F]_n$. Speculations about the effects of these factors on the structure of the $[Al(Pc)F]_n$ polymer are made in chapter seven.

CHAPTER FIVE

REACTIONS OF THIN FILMS OF [Al(Pc)F]$_n$ WITH THE
HALOGENS, Cl$_2$, Br$_2$ AND I$_2$, AND WITH THE
PENTAFLUORIDES, PF$_5$, AsF$_5$ AND IF$_5$.

5:1 Introduction

Oxidation reactions between monomeric or polymeric metal-phthalocyanine complexes and members of the halogen family have been reported previously. For instance, several [M(Pc)] complexes (where M=Ni, Co, Cu or Zn) have been oxidised by diiodine to give products of the composition [M(Pc)I$_x$] (where $0.5 < x < 3.0$) [174]. Thin films of [Mn(Pc)] have been treated with dibromine or diiodine vapours at room temperature to give oxidised materials of the composition [Mn(Pc)X] (where X=Br or I) [175]. In both of the above reported studies [174,175] it has been mentioned that the central metal atom in the [Mn(Pc)] complexes examined has been oxidised from bivalent to trivalent states; but, however, no evidence for the formation of M(III) cations has been given. Stillman et al [143] have recently studied the oxidation of magnesium-phthalocyanine, [Mg(II)Pc(-2)], by dibromine in a solution of dichloromethane at room temperature. Using electronic spectroscopy, these workers have established that the oxidation occurred on the Pc rings and the products formed consisted of monomeric and dimeric π-cation-radical species of the composition [Mg(II)Pc(-1)]$^{\cdot+}$ and [Mg(II)Pc(-1)]$_2{}^{+2}$ respectively [143]. Complexes of the composition {[M(Pc)F]I$_x$}$_n$ (where M=Al, Ga, Cr or Fe and x is the anion coefficient) have been mentioned earlier (see chapter one). Similar systems such as {[M(Pc)O]I$_x$}$_n$ (where M=Si, Ge or Sn) [115] and other organic conjugated iodine-doped polymers such as [(CH)I$_x$]$_n$ [176] have been also studied.

Diiodine has been used most often in the literature as

an excellent doping agent for metal-phthalocyanine complexes and many other organic conjugated systems. Partial oxidation has been achieved in most cases and the polyiodide counterions which have been identified in the products are usually I_5^- or I_3^- [114]. In some cases, reversal of the iodine incorporation has been reported during pumping or heating (e.g. $\underline{ca}$ 523 K) of the oxidised materials [114,174,175].

However the halogens, and in particular diiodine, are not the only oxidising agents to be used for metal-phthalocyanine complexes. In addition to the systems discussed in chapter four, reactions between $[Al(Pc)F]_n$ and other fluorides such as AsF_5 [116] and IF_5 [117] have been mentioned. The products obtained have been studied by x-ray diffraction, thermogravimetric analysis, infrared spectroscopy and electrical conductivity measurements. These studies [116,117] have shown that partial oxidation was achieved and bands assigned to the AsF_6^- or IF_6^- anions were observed in the i.r. spectra of the products. Furthermore, it has been concluded that the oxidant molecules (AsF_5 or IF_5) lie between the polymer chains and cause a rotation of the Pc rings with respect to each other; heating of the products at temperatures between 423-623K result in loss of AsF_5 or IF_5 [116,117].

In the present work, thin films of $[Al(Pc)F]_n$ polymer deposited on silica have been exposed to the halogens Cl_2, Br_2 and I_2 and to the pentafluorides PF_5, AsF_5 and IF_5. Electronic spectroscopy was used to examine the films after reactions. Films deposited on KCl and reacted with Br_2 were also examined by infrared spectroscopy. In some cases thin

films of $[Al(Pc)F]_n$ deposited on KCl have been exposed to the vapours of Br_2 or I_2 and subsequently examined by transmission electron microscopy; the results are described in chapter six.

5:2 Experimental

Thin films of the $[Al(Pc)F]_n$ polymer were deposited on silica and KCl substrates using the method described in chapter two. The thicknesses of these films were estimated by using equation (2-3) of chapter two; they were approximately 40 nm for the films on silica and 95 nm for those on KCl.

The reactions of these films with the halogens, X_2 (X=Cl, Br or I) and the pentafluorides, AF_5 (A=P, As or I) were carried out in an evacuable reaction gas cell (Fig. 2:3). The experimental manipulations used for each reaction were identical as follows.

The reaction cell containing a P.T.F.E. holder was attached to a vacuum line and evacuated. The cell and the thin film of $[Al(Pc)F]_n$ were trasnferred to the dry box. The film was placed inside the cell in a position suitable for the spectroscopic measurements (i.r. and u.v./visible) by means of the P.T.F.E. holder. The cell containing the film was attached to a reaction manifold on the vacuum line, and re-evacuated. The cell was left pumping for approximately 3 h in order to ensure the removal of any oxygen or moisture which could be present. Single-limb vessels containing the oxidising agents X_2 or AF_5 were attached to the reaction manifold and degassed several times at 77 K. The tap of the cell was closed and the calibrated manifold (201.9 cm^3) was isolated from the pumps and filled with the vapour of the oxidant (Cl_2, Br_2, PF_5, AsF_5 or IF_5) at a measured pressure of 85.5 Torr. The calibrated gas cell (53 cm^3) was then re-

opened to the manifold, filled with the vapour of the oxidant (67.7 Torr, 0.19 mmol) and closed again; the vapour pressure of I_2 (at room temperature) is very small and, hence, it was not possible to measure the pressure used in the gas cell. The excess quantity of the oxidant in the manifold was transferred to its original vessel by vacuum distillation at 77 K. The reaction was allowed to proceed for a further 5 min. The residual oxidant in the cell was collected in an empty vessel (attached to the manifold and evacuated previously) by vacuum distillation at 77 K. The cell was pumped for approximately 30 min, to ensure the removal of any traces of unreacted oxidant adsorbed on the film or SiF_4 which could have resulted from trace hydrolysis in the case of AF_5 oxidants.

The quantities of $[Al(Pc)F]_n$ deposited on silica substrates were determined by weighing the substrates before and after the deposition of the films. The silica substrates which were used for the deposition of the films were identical, and all the films were prepared using an identical preparation method. Hence, all the films used for the reactions with the X_2 or AF_5 oxidants had identical weight of 0.6 mg (0.01 mmol).

The mole ratio $[Al(Pc)F]_n$: X_2 (X=Cl or Br) or $[Al(Pc)F]$: AF_5 (A=P, As or I) present was estimated as 1:19 for all reactions. However, most of the quantity of the oxidant used remained unreacted in the reaction cell and it proved impossible experimentally to determine the combining ratio. All that can be stated is that the reactions were carried out in the presence of a very large excess of the oxidant.

5:3 Results and Discussion

The $[Al(Pc)F]_n$ films deposited on silica substrates and exposed to the vapours of the oxidants were examined by electronic spectroscopy over the range 1000-185 nm. On one occasion a thin film of $[Al(Pc)F]_n$ deposited on a KCl substrate and exposed to Br_2 vapour was examined by vibrational spectroscopy in the region 1800-400 cm^{-1}. In all cases the spectra of the reacted films were compared with those of an unreacted $[Al(Pc)F]_n$ film.

5:3:1 Results

Exposing the $[Al(Pc)F]_n$ films to the vapours of Cl_2, Br_2 or I_2 resulted in a rapid colour change from blue to purple. A similar change in colour was observed after approximately 2 min when the films were exposed to the vapours of PF_5, AsF_5 or IF_5.

The resulting purple films from all reactions showed high stability (as far as the colour is concerned) in vacuo for several weeks. Exposing these films to the atmosphere resulted in a colour change from purple to greenish blue. The time associated with this latter change in the colour varied depending upon which oxidising agent was used. For instance, the greenish-blue colour was observed after few seconds in the case of the films that resulted from the reactions with AF_5 (A=P, As or I), and after approximately one minute in the case of the films resulted from the reactions with Cl_2 or I_2. The purple colour of the films

which resulted from the reaction with Br_2 vapour persisted for approximately 3 min after exposure to moist air before it changed to greenish-blue.

The vibrational spectrum of a thin film of $[Al(Pc)F]_n$ deposited on a KCl substrate contained several absorption bands assigned to the phthalocyanine rings (Fig. 5:1); approximate assignments of some specific bands were described earlier (see chapter four).   After exposure to Br_2 the phthalocyanine bands were broadened and reduced in number (Fig. 5:1).   The most characteristic feature of the spectrum after the reaction was the presence of a very weak absorption band at 1060 cm^{-1}.   This band was also observed in the spectra of the products formed from the reactions between $[Al(Pc)F]_n$ and MF_6 oxidants (where M=U, Mo or W) or the NO^+ cation in the presence of MeCN (see chapter four) and was assigned to the $[Al(Pc)F]_n^+$ cation by comparison with several studies involving other metal phthalocyanine complexes [164,174,177].   Hence, the band at 1060 cm^{-1} observed in the present spectrum could be tentatively attributed to the appearance of a positive charge on the polymer (e.g. $[Al(Pc)F]_n^+$).   Spectra are tabulated in table 5:1.   Band assignments in the table were made by comparison with the work described in chapter four.

The electronic spectra of $[Al(Pc)F]_n$ films exposed to the vapours of X_2 or AF_5 oxidants indicated that several spectral changes which involved the positions and intensities of the Q and B bands had occurred.   These changes are described in sections A and B below.

A. Electronic spectra of thin films of $[Al(Pc)F]_n$ exposed to
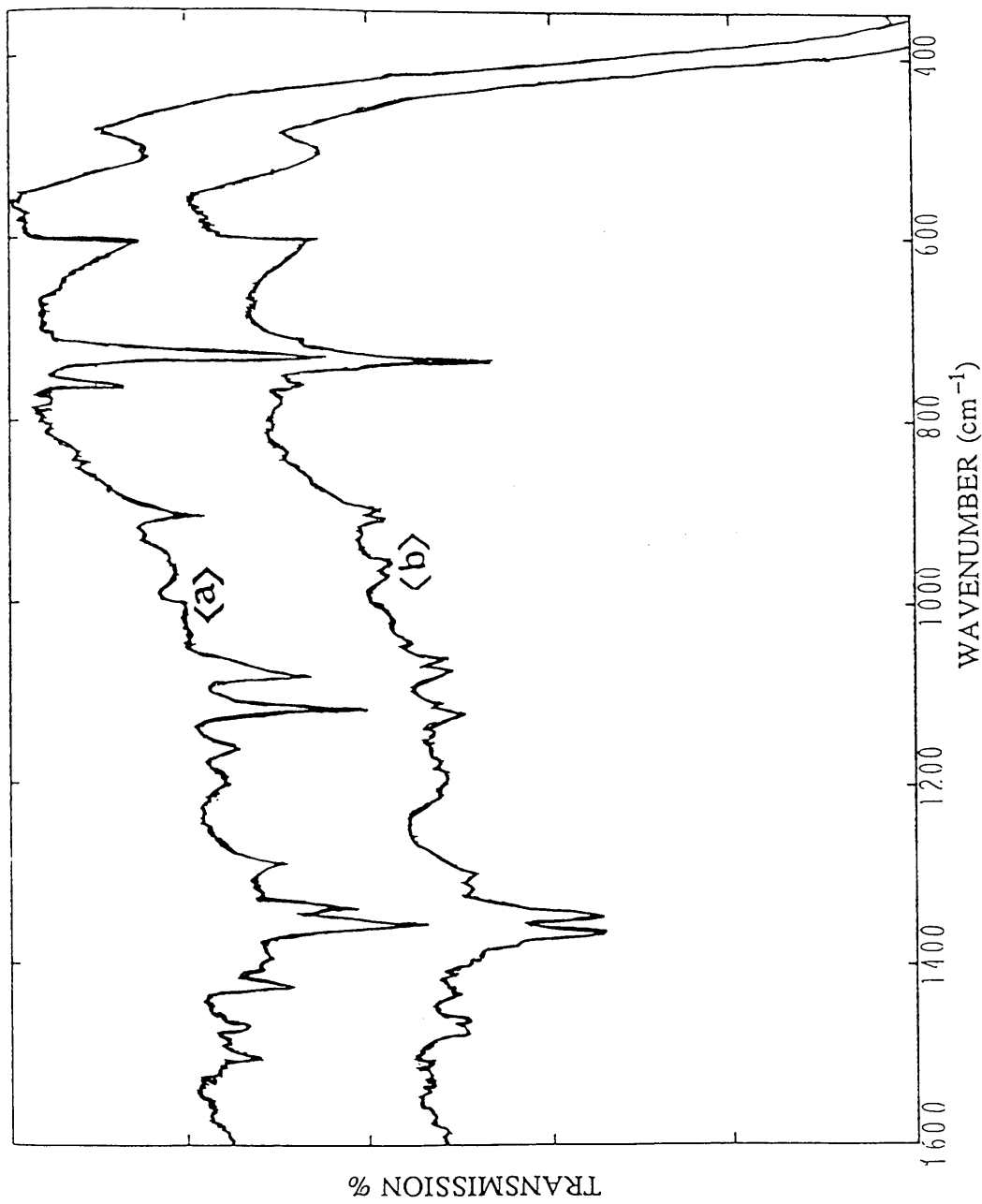
Figure(5:1).Infrared spectra of a thin film of $[Al(Pc)F]_n$ (thickness=95nm) deposited on KCl (A) , and the film after the reaction with Br_2 vapour (B).

Table(5:1).Infrared absorptions (cm^{-1}) of a thin film of $[Al(Pc)F]_n$ (thickness=95nm) on a KCl substrate before and after the reaction with Br_2 vapour at room temperature.

$[Al(Pc)F]_n$	$[Al(Pc)F]_n/Br_2$	Approximate assignment[*]
1500w	1500w	C--N str.
1465w	1460w	--------
1420w	1425w	--------
1350m	1355m	--------
1335m	1335m	C--C str.
1285w	-----	C--H def.
1160w	-----	C--H def.
1120m	1120w	C--H def.
----	1062w	$[Al(Pc)F]_n^+$
1080m	1075w	C--N str.
970b	970w	--------
905w	910w	C--H def.
----	900w	--------
775w	-----	C--H def
760w	760m	--------
725s	735s	C--H def.
510b	510b	Al--F str.

s=strong, m=medium, w=weak, vw=very weak and b=broad.

[*]The bands were assigned by comparison with the work described in chapter four.

the vapours of Cl_2, Br_2 and I_2:

The spectra of the purple films which resulted from the reactions with X_2 (where X = Cl, Br or I) oxidants indicated that, in all cases, the Q band was shifted to longer wavelength (lower energy) and appeared to decrease in intensity after the reactions (Fig. 5:2). The spectra also showed a new broad absorption band which appeared on the high energy side of the Q band after the reactions. An additional shoulder near 570-510 nm was also observed in the spectra of the reacted films (Fig. 5:2).

The B1 band was shifted to shorter wavelength (higher energy) and appeared to decrease in intensity (Fig. 5:2). The shoulder near 360 nm which was observed in the spectrum of the $[Al(Pc)F]_n$ film appeared at longer wavelength. The position of the B2 band remained constant, but its intensity appeared to increase. The B3 band was shifted to shorter wavelength and its intensity appeared to increase when the films were exposed to Cl_2 or Br_2 vapours, while it decreased after the reaction with I_2 vapour (Fig. 5:2). The absorption maxima (λ_{max}) of all bands and their absorption coefficients (α) are given in table 5:2. Note that the α values of the bands in the table were calculated using equation 4-2 of chapter four.
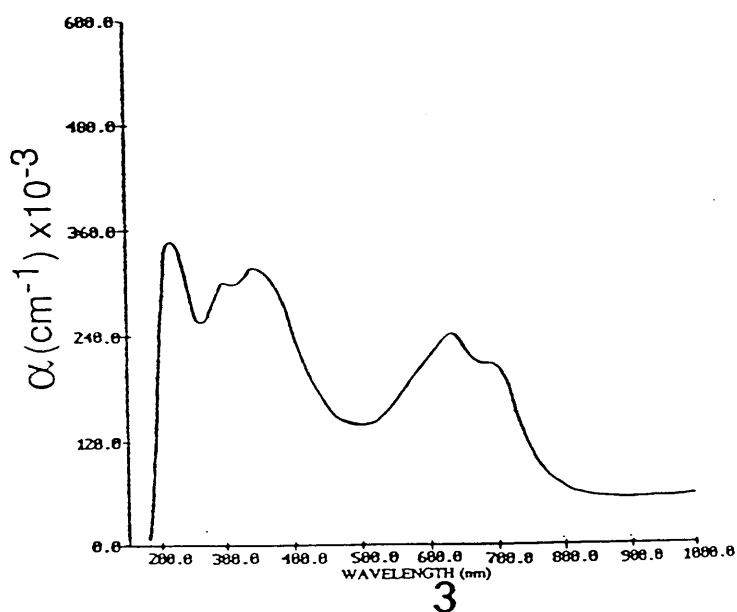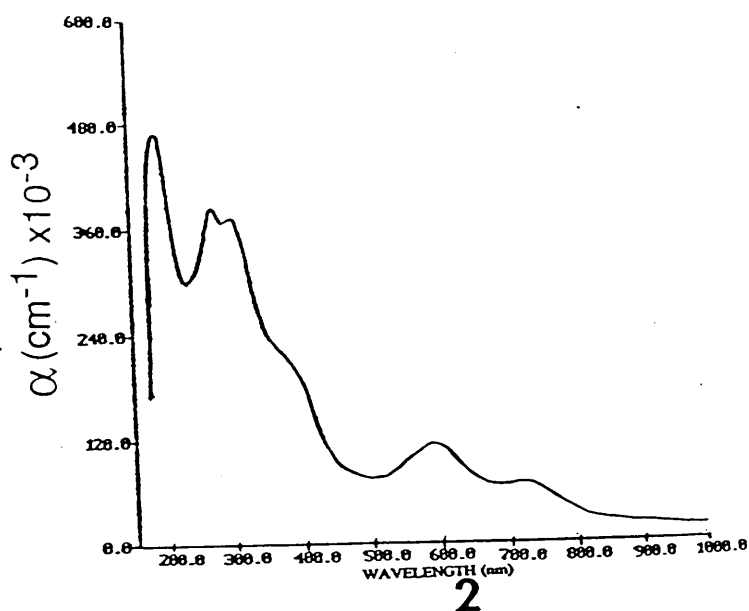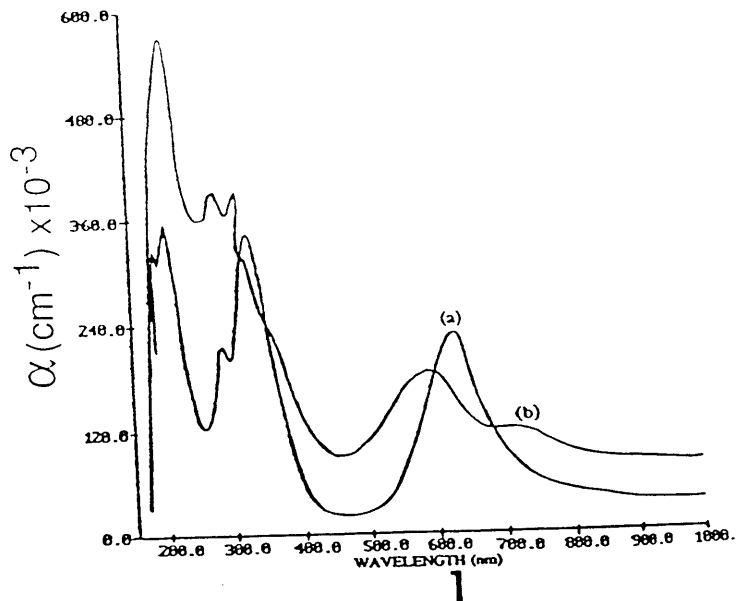
Figure(5:2).Electronic spectra of a thin film of $[Al(Pc)F]_n$ deposited on silica (1A) and reacted with Cl_2 (1B), Br_2 (2) and I_2 (3).

Table(5:2).Electronic spectra(λmax,nm) and absorptions coefficient values (α,cm^{-1}) of thin films of $[Al(Pc)F]_n$ (thickness=40nm) on silica substrates before and after the reactions with Cl_2, Br_2 and I_2 vapours at room temperature.

$[Al(Pc)F]_n$		$[Al(Pc)F]_n/Cl_2$		$[Al(Pc)F]_n/Br_2$		$[Al(Pc)F]_n/I_2$	
λ_{max}	α^*	λ_{max}	α^*	λ_{max}	α^*	λ_{max}	α^*
625	185	740	95	740	45	690	175
---	---	600	145	600	85	620	205
---	---	560sh	---	560sh	---	520sh	---
360sh	---	365sh	---	400sh	---	365sh	---
330	280	325	255	320	275	325	255
285	180	285	310	285	300	285	245
210	295	205	450	200	400	200	280

sh=shoulder

*The α values (cm^{-1}x10^{-3}) were estimated using equation 4:2.

B. Electronic spectra of thin films of $[Al(Pc)F]_n$ exposed to the vapours of PF_5, AsF_5 and IF_5:

The electronic spectra of the films which resulted from the reactions with AF_5 (where A=P, As or I) oxidants indicated that, in all cases, the Q band was shifted to longer wavelength and appeared to decrease in intensity (Fig. 5:3). A new absorption band near 570 nm was observed in the spectra of the films from reactions with PF_5 or IF_5 (Fig. 5:3). The spectrum recorded after the reaction with AsF_5 indicated that new shoulders had appeared on both sides of the Q band, one near 820 nm and another near 620 nm (Fig. 5:3).

The B1 band was shifted to shorter wavelength and appeared to decrease in intensity after all reactions (Fig. 5:3). The shoulder which had been observed near 360 nm in the spectrum of $[Al(Pc)F]_n$ film appeared at longer wavelength after the reacions with PF_5 or IF_5, while its position remained constant after the reaction with AsF_5. The B2 and B3 bands were both shifted to shorter wavelength and appeared to increase in intensity after all reactions (Fig. 5:3). The absorption maxima (λ_{max}) of the bands and their absorption coefficients (α) are given in table 5:3.
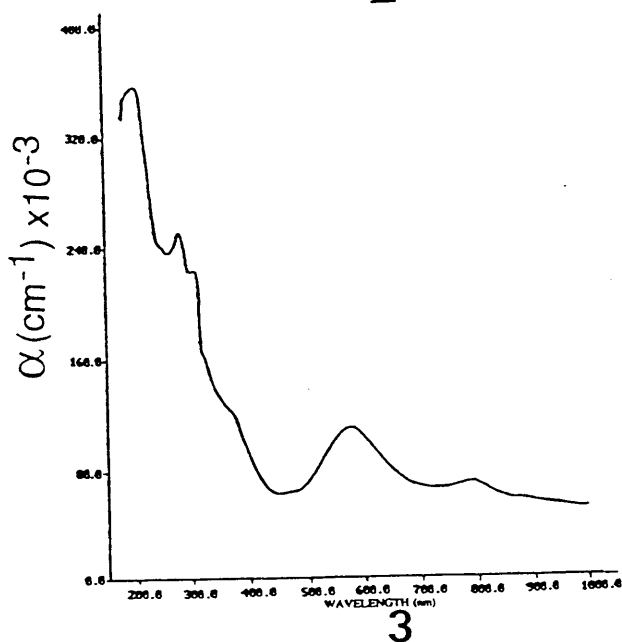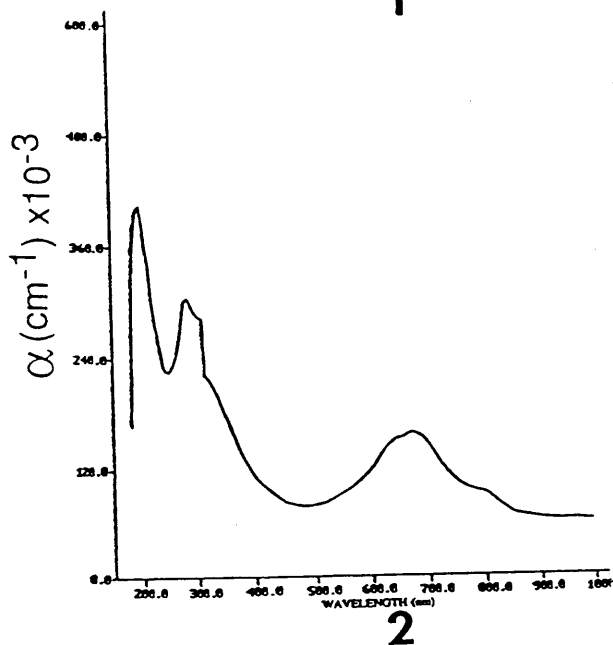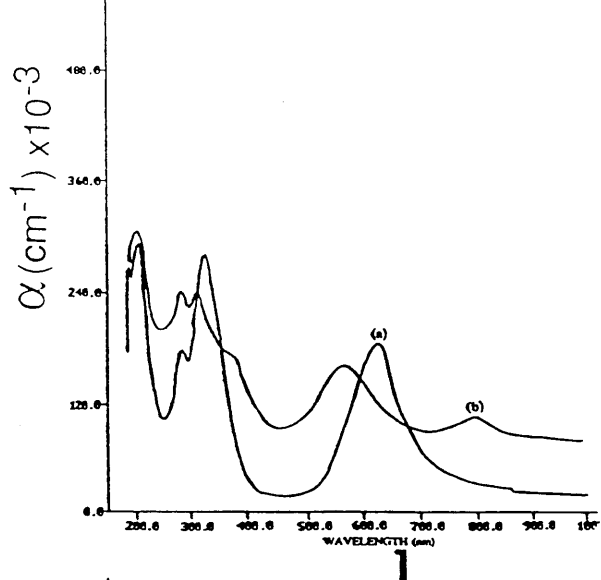
Figure(5:3).Electronic spectra of a thin film of [Al(Pc)F]$_n$ deposited on silica (1A) and reacted with PF$_5$ (1B), AsF$_5$ (2) and IF$_5$ (3).

Table(5:3).Electronic spectra(λmax,nm) and absorptions coefficient values (α,cm^{-1}) of thin films of [Al(Pc)F]$_n$ (thickness=40nm) on silica substrates before and after the reactions with PF$_5$, AsF$_5$ and IF$_5$ vapours at room temperature.

[Al(Pc)F]$_n$		[Al(Pc)F]$_n$/PF$_5$		[Al(Pc)F]$_n$/AsF$_5$		[Al(Pc)F]$_n$/IF$_5$	
λ_{max}	α^*	λ_{max}	α^*	λ_{max}	α^*	λ_{max}	α^*
---	---	---	---	820sh		---	---
625	185	790	105	690	150	790	70
---	---	570	155	620sh	---	570	110
360sh	---	370sh	---	360sh	---	370sh	---
330	280	310	235	310	275	310	200
285	180	280	235	280	295	280	250
210	295	200	300	200	395	200	355

sh=shoulder

*The α values (cm^{-1}x10^{-3}) were estimated using equation 4:2.

5:3:2 <u>Discussion</u>

The changes in the colour and spectra of the $[Al(Pc)F]_n$ films after the exposure to the vapours of X_2 or AF_5 oxidants indicate that some kind of interaction has occurred. These changes are relatively similar to those observed from the reactions described in chapters three and four. Despite there having been many studies in the literature involving the oxidation of $|Al(Pc)F]_n$ (examples are given in chapters three and four and in section 5:1), the electronic spectra of this polymer or the products obtained from its reactions have not been reported. Thus it is necessary to compare the electronic spectra obtained from the reactions in the present study with that from studies reported previously which involve the oxidation of other metal-phthalocyanine complexes by several oxidants; such examples are already mentioned in section 5:1. The spectral changes which have been observed from all these reported studies [14 ,157,174,175] were similar to those observed from the present reactions. In particular the changes involved the Q band and the appearance of the new band near 600-500 nm (after the reactions) which has been assigned to a π-π transition within the phthalocyanine ring [2,3,11,12]. Moreover, in most of these studies [139, 142, 157] the changes in the electronic spectra of the products obtained have been attributed to partial oxidation of the Pc rings. Complete oxidation can be only associated with a complete loss of the Q band in the spectra of the products [140,143]. Hence, on the basis of the above comparison, the spectral changes observed from the present reactions can be, tentatively, attributed to a partial oxidation of the phthalocyanine rings of the $[Al(Pc)F]_n$

polymer. In the case of the reactions with Br_2 or I_2 the anions which should be present in the products are, Br_3^-, and I_3^- or I_5^-. These anions are usually identified in the electronic spectra by their characteristic absorption bands in the region 500-200 nm. This region also features absorption bands assigned to the phthalocyanine rings (e.g. B1, B2 and B3 bands). Thus, when partial oxidation occurs, it can be assumed that the concentrations of these anions are low and, consequently, their absorption bands are weak and, hence, they are possibly obscured by the phthalocyanine bands. Polychloride anions are not well characterised species and it is likely in this case that the counter anion is Cl^-. Chlorination of the benzene rings of the phthalocyanine molecule is also a possibility. It is noteworthy that in all the reported studies from the literature which involve the use of Br_2 or I_2 oxidants (see section 5:1), no direct evidence for the presence of the above anions (Br_3^-, I_3^- or I_5^-) in the electronic spectra of the products formed has been obtained. In most cases the I_3^- and I_5^- anions have been detected in the products by using infrared or Raman spectroscopy [114]. The electronic spectra of the films obtained from the reactions with X_2 or AF_5 oxidants were reproducible and remained unchanged after pumping for approximately 30 min.

Using the halogens, X_2, as oxidants for $[Al(Pc)F]_n$, the first step in this proces can be formally described by the equation (5-1) [7].

$$\tfrac{1}{2}\, X_{2(g)} + e^- \xrightarrow{\;-\Delta H_f^{\ominus}\;} X^-_{(g)} \quad \ldots\ldots\ldots\ldots(5\text{-}1)$$
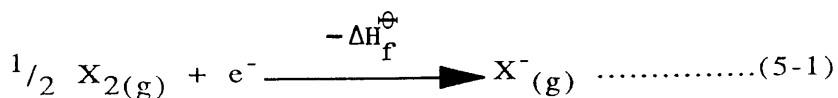
where X = Cl, Br or I and $\Delta H_f^{\ominus}$ is an enthalpy term which represents the sum of half the enthalpy of dissociation of

X_2, $[^1/_2 D(X_2)]$, and the enthalpy of adding an electron to $X_{(g)}$ atom to form the $X^-_{(g)}$ anion, $[-Ea(X,g)]$.

The values of $\Delta H_f^{\ominus}$ in equation (5-1)are reported in the literature [178] as -246.0 kJ mol^{-1} for X = Cl; -249.4 kJ mol^{-1} for X = Br and -227.8 kJ mol^{-1} for X=I. In all cases, these values are less than the ionization potential of $[Al(Pc)F]_n$ (439 kJ mol^{-1}) and hence, the halogens should not be able to oxidise this polymer. However, as described earlier oxidation has occurred. As stated in chapter four other factors concerning the lattice energy of the products formed and the electrostatic interaction between the cations and anions in the products can play important roles in driving these reactions to occur. Furthermore, it has been reported [7] that the maximum bond length in the molecules Cl_2, Br_2 and I_2 are 1.99 Å, 2.28 Å and 2.66 Å respectively, and they are linear molecules. Hence, it is perhaps possible for these molecules to intercalate between the Pc rings of the $[Al(Pc)F]_n$ polymer.

In the case of the pentafluorides PF_5, AsF_5 and IF_5 the oxidation reactions are likely to involve the following process (equation 5-2) [40]:

$$3AF_{5\ (g)} + 2e^- \xrightarrow{\ -\Delta H_f^{\ominus}\ } 2AF_6^- + AF_{3\ (g)} \quad ....(5-2)$$

where A=P, As or I and $\Delta H_f^{\ominus}$ is the enthalpy change associated with the process.
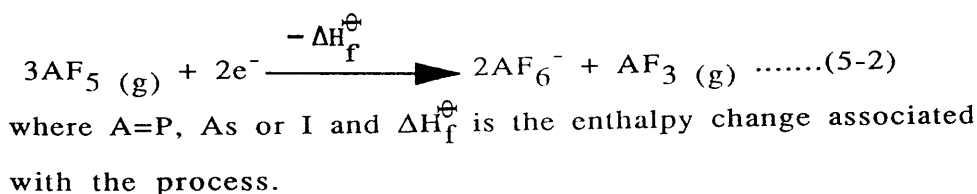
The values of $\Delta H_f^{\ominus}$ in the above equation have been reported in the literature [40] as -686 kJ mol^{-1} for A=P and -1012 kJ mol^{-1} for A=As. Hence these pentafluorides are stronger oxidising agents than the halogens. The enthalpy change ($\Delta H_f^{\ominus}$) associated with the formation of IF_6^- anion in

equation (5-2) has not been reported in the literature. Contrary to the halogens, the values of $\Delta H_f^{\ominus}$ in the case of PF_5 and AsF_5 oxidants are numerically greater than the ionization potential of $[Al(Pc)F]_n$. Similar comments can be tentatively made for IF_5. However, the diameters of the pentafluorides PF_5, AsF_5 and IF_5 are larger than the separation distance between the Pc rings in the polymer. For instance, both AsF_5 and IF_5 molecules have a reported [116, 117] minimum diameter of 4.6 $\overset{o}{A}$; similar value can be expected for the diameter of PF_5. Thus, insertion of these molecules between an inter-ring separation of 3.66 $\overset{o}{A}$ will be difficult without causing distortion in the eclipsed structure of the Pc rings in $[Al(Pc)F]_n$.

Oxidation reactions using IF_5 result in the formation of IF_3 which is unstable with respect to disproportionation [117] and decomposes to give IF_5 and free iodine (equation 5-3).

$$5IF_5 \longrightarrow 3IF_5 + I_2 \quad \dots\dots\dots\dots(5\text{-}3)$$
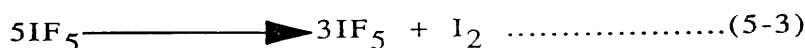
There was no evidence for I_2 liberation during the reaction with $[Al(Pc)F]_n$, but the possibility exists that any I_2 formed could have reacted with the polymer also. Therefore it is not possible to confirm whether or not the reaction in equation (5-3) has occurred in the present investigation.

As stated earlier in this chapter, the spectral changes occurring in the present reactions are relatively similar to those obtained from the reactions described in chapters three and four. A general model for all reactions will be given in chapter seven.

CHAPTER SIX

TRANSMISSION ELECTRON MICROSCOPY STUDY OF THE [Al(Pc)F]$_n$ POLYMER REACTED WITH MoF$_6$, WF$_6$, Br$_2$,I$_2$ AND CF$_3$COOH.

6.1 : <u>Introduction.</u>

<u>Historical Background</u>.

The discovery of the light microscope by Galileo in 1610 offered great help in the investigation of materials not previously observable, and thus provided a great impetus to a number of scientific fields.   From the very first microscope a large number of alterations have been made to improve the resolution.   However the limit of the wavelength of the light used could not be overcome [179].   Therefore the dependence on wavelength limits the theoretical resolution of light microscopes to the region of 200 nm.

It was not until the hypothesis of wave particle duality[180]and its experimental confirmation[181]that a practical method of overcoming this limit became evident. The theory would indicate that an accelerated electron had a wavelength much smaller than that of visible light, and therefore a microscope employing accelerated electrons would have a much greater resolution than that of a light microscope.

An extensive investigation on the electron microscope had been carried out by Knoll and Ruska[182],in fact the initial investigations of imaging by these workers were based on the work of Busch[183]which treated electrons as classical charged particles.

The work of Knoll and Ruska led to the production of the first transmission electron microscope (TEM) in 1931 and the first high resolution instrument was built by the same

pioneers in 1933. This instrument was capable of resolving 50 nm, a great advance on the light microscope. Since then development of microscopes has continued to the present state of technology, which is far beyond the vision of the originators, Knoll and Ruska.

Modern electron microscopes, such as those at Glasgow, are capable of routinely achieving resolution of 0.3 nm. Instruments which employ higher accelerating voltages such as the Cambridge 600 kV microscope [184] can achieve atomic resolution for suitable specimens, and have achieved lattice resolution of less than 0.1 nm [185, 186]. This ability allows the detailed study of structure in many fields, for example see [187], making the electron microscope one of the most important research tools in existence. In recognition of this fact Ruska gained the Nobel prize for physics in 1986.

The history of electron microscopy has been well documented [188-190] and the electron optical theories and development of the instrument have been extensively reviewed [191, 192].

6:2 : <u>Principles of the Electron Microscope</u>.

Transmission electron microscopes are designed to operate in a similar fashion to that of light microscopes. In both systems there is a source of illumination which is focussed onto the sample being examined. The illuminating agent then passes through the sample, interacting with it. The wave exiting from the sample is magnified and projected to produce a magnified image which can then be studied. The differences between the two systems arise from the use of the

beam of electrons as the illumination source in TEM.

The source of illumination must be a source of electrons rather than visible light; because electrons cannot be focussed by glass lenses, magnetic or electrostatic lenses must be used. These are magnetic or electrical fields designed to alter the path of an electron in an analogous fashion to that of the alteration of a ray of light by a glass lens. As the electron beam is not visible it cannot be directly observed and the image must be projected onto a fluorescent screen for examination. Because electrons have a low penetrating power, and can only travel significant distances in a vacuum, it is necessary to have thin samples and the column of the microscope kept under a vacuum of 10^{-3} Pa or less.

The main features of a modern transmission electron microscope are shown schematically in figure 6:1 and the operation in the transmission mode is depicted in figure 6:2.

The source of illumination is the electron gun, in which electrons are generated and focussed into a fine beam. The source of electrons is an electrically heated cathode emitter at a selected negative potential. Owing to its high melting point, low vapour pressure and high mechanical strength tungsten is normally used as the emitter in the form of a hairpin filament [193] An increase in source brightness can be obtained by using special pointed tungsten filaments [194] or from lanthanum hexaboride cathodes [195]

The electrons produced in the gun are then accelerated by the potential difference between the filament and an anode

HT supply

Electron gun

Condensers

Beam alignment stage

Specimen stage

Objective lens

Intermediate lens
(first projector)

(Second) projector lens

Viewing chamber

Recording camera

High vacuum
pumping system
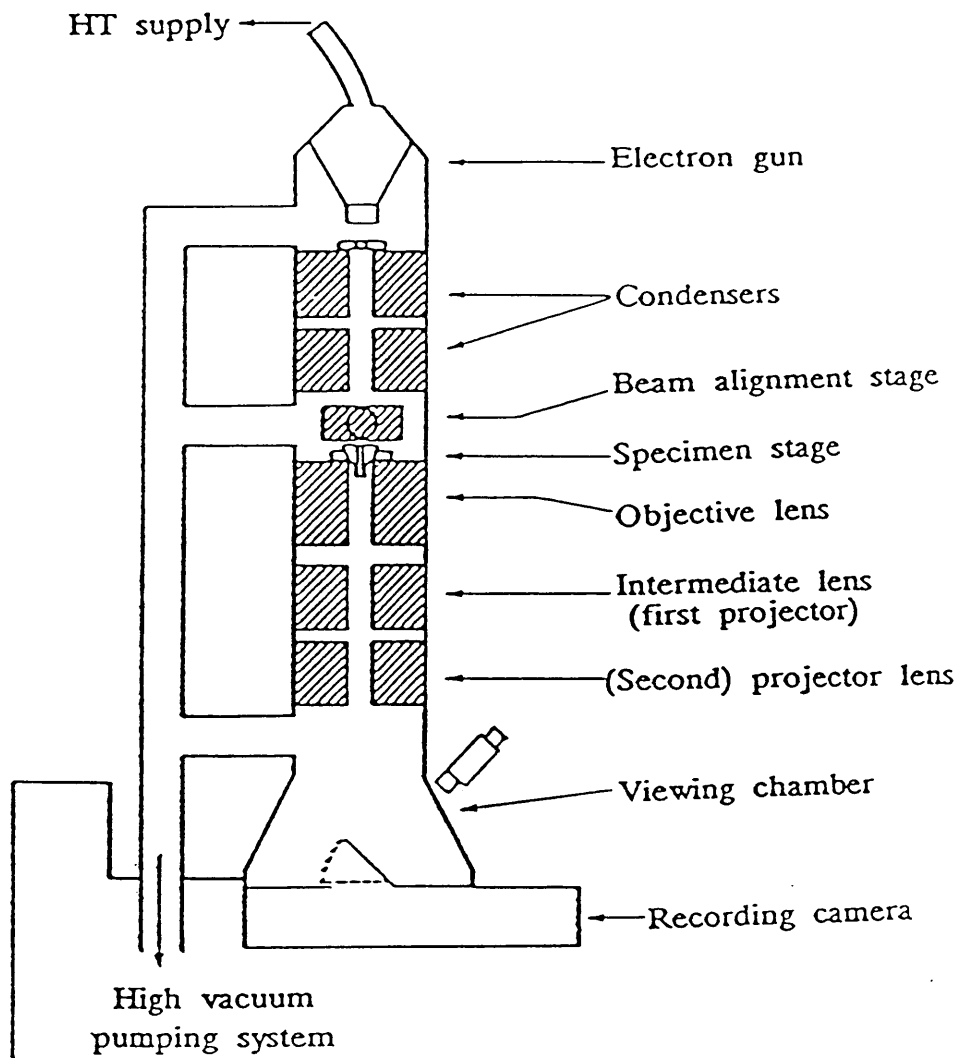
Figure(6:1).Schematic diagram of a transmission
electron microscope.

Electron gun

Condenser lens

Specimen

Objective lens

Objective lens aperture

Field limiting aperture

Intermediate lens

Projector lens

Fluorescent screen
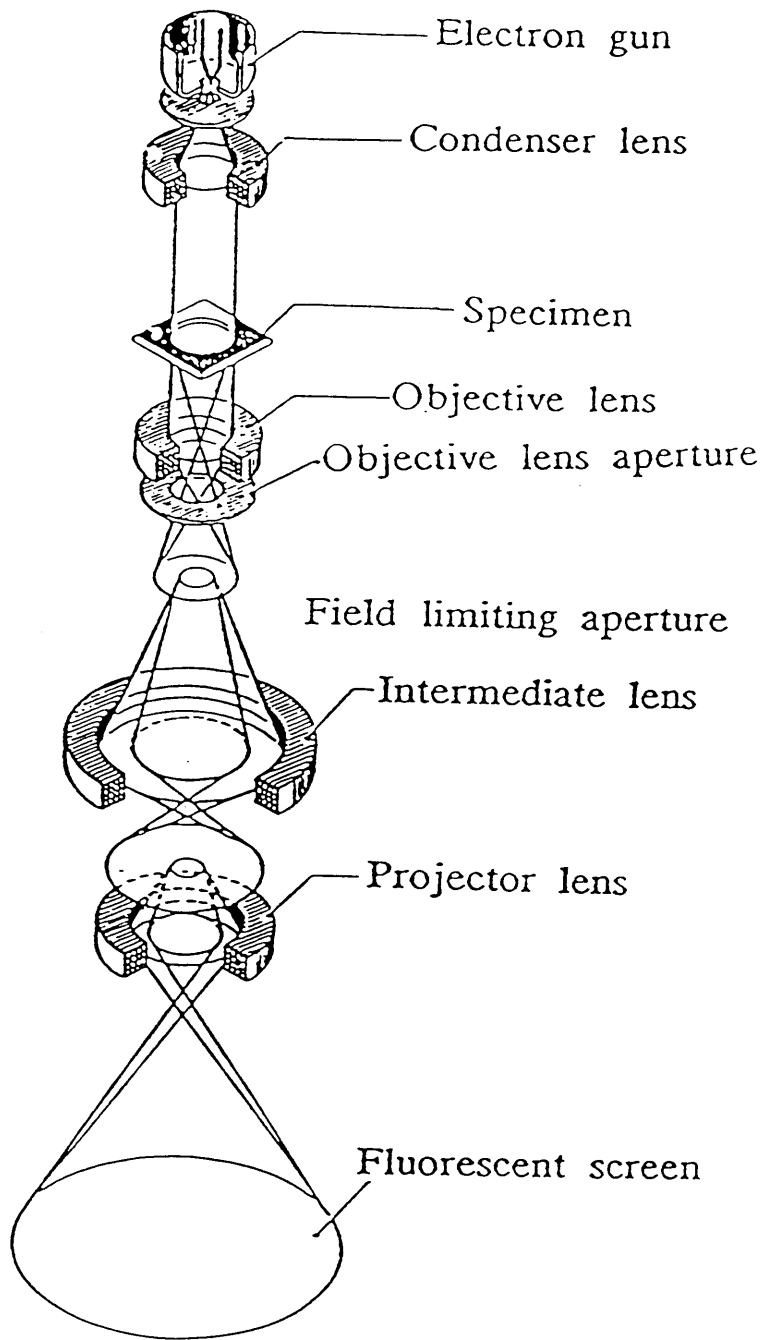
ELECTRON MICROSCOPE IMAGE

Figure(6:2).Operation of the TEM in the transmission mode.

plate kept at earth potential. The beam is then focussed onto the sample by the condenser lens system with a field limiting aperture. A double condenser lens is normally used for high resolution studies. The first lens produces a highly demagnified image of the electron source. This beam of reduced cross section is then projected onto the specimen by the second condenser lens. This system gives a very small minimum spot size, with the advantage of enhanced brightness over a small area. After the beam emerges from the specimen the image is magnified and projected onto a fluorescent screen by a lens system consisting of an objective, intermediate and projector lenses. The image can then be recorded on a photographic plate positioned beneath a movable section of the fluorescent screen. The magnification is determined by the excitation of the intermediate lens, the brightness by control of the excitation of the condenser lens and the focus is controlled by the objective lens.

The objective lens detects, transmits and magnifies the modified electron beam and therefore the performance is critical to the overall performance of the microscope. Light microscopes employ a series of converging and diverging lenses to compensate for individual lens defects. However the nature of electrostatic and electromagnetic lenses is always converging and as such the lens defects cannot be compensated for in the same manner as light microscopes. Therefore high resolution electron microscopes require an objective lens designed and constructed to an extremely high standard. Even with this, the defects still occur and this has a great effect on the performance of the microscope.

The intermediate and projective lenses, although less critical to the overall performance, transmit and further magnify the modified electrons from the objective lens.

The information which can be recovered from TEM is contained in the electrons scattered during the passage through the sample. The information desired is represented by perturbations in the electron waves. Electron optical defects can cause similar perturbations. However if these are suppressed to a lower level than the specimen perturbations then meaningful resolution may result, although the lens aberrations can make interpretation difficult.

6:3 : Interactions of the Electron Beam with the Specimen.

The basis of all information gained from electron microscopy is the interaction of a beam of high energy electrons with the specimen. The possible interactions are summarised in figure 6:3 [125].It can be seen that a number of signals are generated. These signals can be used to obtain information about the specimen. Signals which are of use in TEM are indicated. Other signals are used for scanning electron microscopy and analytical techniques such as energy dispersive spectrometry (EDS), electron energy loss spectrometry (EELS) and several others [196].

The electron microscope is based on the interaction between the electron beam and the electrostatic potential within the specimen (Coulomb interactions). Almost all of the incident electrons pass through (assuming the sample is thin) with only those passing close to atoms being deflected.
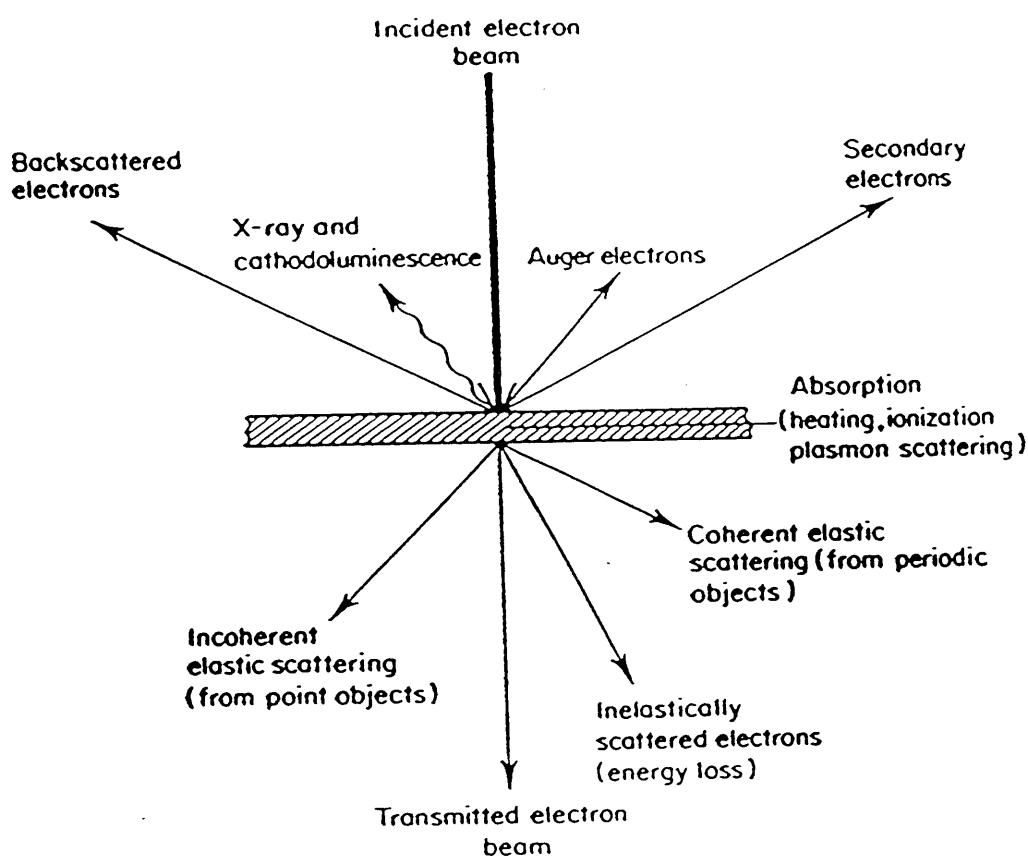
Figure(6:3).Schematic representation of the information
resulting from the interaction of the
electron beam with the specimen.

The two dominant interactions which are of most interest in conventional transmission electron microscopy, are elastic and inelastic scattering. Elastic scattering occurs when the electrons of the probe interact with the nuclei in the specimen and are deflected without loss of energy. The scattering angles are related, in crystalline samples, to the geometry of the crystal lattice and to the electron wavelength. The inelastic scattering occurs when the electrons of the probe interact with the orbital electrons of the specimen and are deflected with a loss of energy.

The elastic scattering of electrons increases when the atomic number of the specimen nuclei increases or with increasing specimen thickness. If elastic scattering occurs at large angles to the optical axis of the incident electron beam, or an aperture is inserted such that the electrons scattered greater than the aperture angle are cut out, then image contrast arises as "mass thickness" contrast or amplitude contrast, or for specimens with a periodic nature "diffraction contrast". In such cases, areas of specimens from which elastically scattered electrons have been removed appear dark in the image.

In inelastic scattering small deflections are imparted to the electrons along with the alteration to their energy and hence their wavelengths. Recombination of these inelastically scattered electrons with similarly altered unscattered electrons results in increased or decreased intensities in the image contrast, depending on the relative phases of the interacting waves. This phenomenon is referred

to as inelastic phase contrast. Elastic phase contrast corresponding can be obtained if the aperture allows transmission of the phase-altered elastically scattered electrons. Amplitude is again increased or decreased to allow recombination of these with the undeviated electrons. If the elastically scattered electrons arise from a periodic structure in the specimen, then a related periodicity in the image may be obtained. This information may only be obtained from periodicities normal to the electron beam. This is the basis of "lattice imaging" in high resolution TEM.

6:4 : <u>Image Formation.</u>

The interaction between the electron beam and the specimen leads to the formation of a transmitted wave at the exit surface of the specimen. This transmitted wave may be interpreted as being the sum of the unscattered waves and a set of scattered waves. The next process of importance is the propagation of this transmitted electron wave along the optical axis of the microscope and the formation of an image.

If the scattered and unscattered beams can be made to recombine, so combining their phase and amplitude, then a lattice image of the planes which are diffracting may be resolved directly (phase contrast). Alternatively amplitude contrast is obtained by deliberately excluding the diffracted beams from the imaging process by use of suitably sized apertures placed in the back focal plane of the objective lens.

6:5 : <u>Lens Aberrations</u>.

The discussion of image formation is theoretically based on an ideal system in which all of the exit wave takes part in the imaging process, and the lens system perfectly reproduces a magnified image of this wave. Practically, however, this is not the case, the lenses are not perfect and these imperfections have a direct effect on the operation of the microscope. The interaction of the incident wave with the sample also scatters some of the electrons. The electrons scattered at large angles (those scattered by small periodicities) will not take part in the imaging process because they will be removed by the apertures, or at extreme values by the microscope column.

The imperfections are lens aberrations which are analogous to those obtained in light optical systems. There are several aberrations which occur, many of which can be reduced or eliminated by careful construction of the lenses. The aberrations which are of greatest importance to the image formation are described in the following.

(I) Spherical aberration:

Because of the nature of electron field geometries and the coincidence of the component electron rays, electrons originating at different points on the object are focussed at slightly different points along the optical axis.

(II) Astigmatism:

This problem is most effective in the objective lens, although the condenser lens system is also affected. This occurs because the focal length of a lens is longer in one

plane direction than another normal plane direction. This can be due to inaccuracies in manufacture, inhomogeneties in the soft iron pole piece or by contamination within the microscope column, causing distorted fields due to charging. The latter can be minimised by maintaining extreme cleanliness on all surfaces, especially aperture, which are exposed to the electron beam.

(III) Chromatic aberration:

The above aberrations are based on problems in the lenses; there are also problems caused by the electron beam. These are basically due to velocity differences within the electron beam, for instance the electrons do not have a uniform energy or velocity. Therefore the lenses have different effects depending on the energy of the electron, that is the focal length depends on the energy of the electron.

The differences in velocity can arise from a number of effects. These are (a) the energy distribution of the electrons emitted from the source, due to different work functions on different crystal faces; (b) instability of the electrical power supply and (c) electron-electron repulsion at the beam cross-over (the Boersch effect).

In practice the use of a low beam current can reduce the Boersch effect and the use of single crystal emitters can reduce the energy distribution of the beam.

6:6 : <u>Coherence</u>.

The term coherence refers to the condition of an illuminating electron wave as it approaches an object. The illumination is said to be coherent if all the waves in the incident beam are in phase with one another, and if recombined after striking an object, are capable of interference with one another. It has been pointed out [197] that the beam coherence could be expressed by the ratio of the incident beam aperture, $2\alpha_c$, at the specimen to the angular aperture of the objective lens, 2α. When $2\alpha_c/2\alpha<<1$, the illumination is coherent; for $2\alpha_c/2\alpha = 1$, incoherent, and intermediate values correspond to partial coherence.

Coherence has effects on the image forming process at the highest resolutions, and it can be improved by the use of small condenser apertures, though a balance has to be achieved between coherence and sufficient illumination intensity, and the use of pointed tungsten filaments or lanthanum hexaboride [198].

6:7 : <u>Limiting Factors</u>.

The discussion above described how the electron optical system can affect the resolution of the microscope. However the aberrations in the magnetic lenses and the coherence effects already mentioned, are not the only factors which can affect the performance of the electron microscope and some of the other limitations are described below.

6:7:1 : <u>Specimen Contamination</u>.

The build-up of amorphous, usually carbonaceous material on the specimen, enhanced by the electron beam, obscures fine structure in the specimen and causes a general loss of clarity. The residual atmosphere inside the column of the microscope will contain atmospheric gases including hydrocarbon compounds. These may have originated from vacuum pumping fluids, vacuum sealing gaskets and any removable parts which are handled by the operator. Under normal conditions there will be a thin layer of hydrocarbon absorbed on all surfaces within the column, including the specimen. Electron bombardment polymerises the surface film and permanently fixes it in place. The depleted surface layer of hydrocarbon is replenished by continued condensation of vapour and by diffusion of freshly condensed material inwards across the surface from the outside of the electron bombarded area. Thus, a permanent deposit grows on the specimen surface whenever it is under examination. The deposit is referred to as "contamination" and its rate of formation as the "contamination rate".

In modern electron microscopes, this problem can be reduced by the attachment of anti-contaminators or by maintaining an extremely high and clean vacuum by the use of dry pumps such as sputter-ion and turbomolecular systems. Anti-contaminators normally take the form of liquid nitrogen cooled jackets around the specimen area, to remove organic and other contaminant vapours by preferential condensation.

6:7:2 : <u>Specimen Stability.</u>

Most materials undergo some form of alteration when bombarded by electrons in the microscope, to the extent that, such alterations affect the integrity of the information sought from the specimen, they are referred to as "radiation damage", but when the effects prove incidental to the information sought they are largely ignored.

Radiation damage affects all types of material in the microscope. The effect of radiation damage in inorganic materials, can totally destroy the structure being examined [199] and as such is prohibitive to their study. Although organic materials are generally more stable, radiation damage still occurs [200]. This damage occurs by one of two mechanisms; (a) "knock-on" displacement where the electron beam interacts with the cores of atoms in the specimen [201] or (b) radiolytic mechanism where the electron beam transfers energy to the electrons in the specimen leading to bond breaking and structure alteration [202].

A large number of techniques have been developed in order to minimise radiation damage. These include the use of image intensifiers and low beam doses [203]; minimum dose systems, which allow focus in other areas of the sample and then the examined area, is brought into the photograph area only long enough to expose the plate [204]. These techniques can also be aided by the use of x-ray film which has a much shorter exposure period [205].

6:7:3 : <u>Mechanical Stability</u>.

Mechanical stability, mainly in the form of residual drift in the specimen stage, can adversely affect the microscope performance, especially during high resolution imaging. This problem can be made worse by high beam doses, causing local heating which in turn produces differential thermal expansion which causes drift.

6:8 : <u>Electron Diffraction</u>.

The diffraction pattern gives information about the crystal structure within the sample and can be used to identify the material. A crystalline specimen will diffract the electron beam strongly, through certain angles according to the Bragg law [206] The diffracted beams, along with the undeviated incident beam are brought to a focus at the back focal plane of the objective lens, to form a diffraction pattern. In normal magnification mode (transmission mode), the intermediate lens is focussed on the first intermediate image (**Fig. 6:2**) whilst for electron diffraction the intermediate lens is focussed on the back focal plane of the objective lens producing a magnified image of the diffraction pattern, which is further magnified by projector lenses and displayed on the screen (**Fig. 6:4**).

It is possible to obtain the diffraction pattern from a particular area of the sample rather than the whole area under illumination. This technique developed by Boersh [207] and Le Poole [208] allows the study and identification of small particles or regions of interest within the sample.

Electron gun

Condenser lens

Specimen

—Objective lens

Field limiting aperture

Intermediate lens

Projector lens

Fluorescent screen
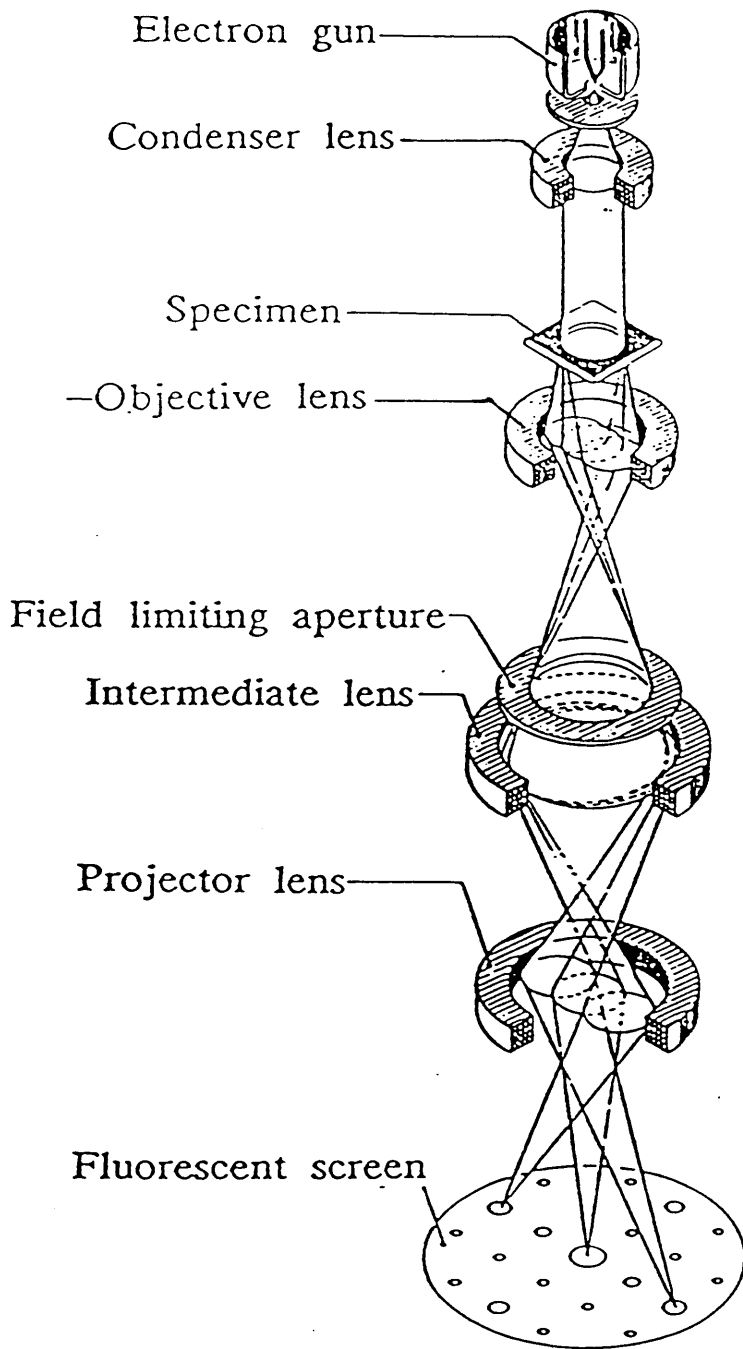
ELECTRON DIFFRACTION PATTERN

Figure(6:4).Operation of the TEM in the diffraction mode.

The interplanar spacing, d, of the crystal lattice can be derived from the electron diffraction pattern (Fig. 6:5) as follows:

$$\tan 2\theta = \frac{D}{2L} \qquad \text{.................. (6-1)}$$

where D is the diameter of a pair of diffraction spots, or of a polycrystalline ring, and L is the effective camera length, which is the equivalent physical distance between the diffraction plane and the final image screen.

The Bragg law for first order diffraction is given by:

$$\lambda = 2d\sin\theta \qquad \text{................... (6-2)}$$

Since the angles through which the electrons are diffracted are small ($<3^\circ$), the approximation,

$$\tan 2\theta \simeq 2\sin\theta \simeq 2\theta \qquad \text{................. (6-3)}$$

can be used, and hence:

$$Dd = 2\lambda L \qquad \text{.................... (6-4)}$$

Since λ is constant ($\lambda = 0.0037$ nm for 100 kV) and L is fixed by the operating condition, thus equation(6-4) can be rewritten as the following:

$$Dd = K \qquad \text{.................... (6-5)}$$

where K is the "camera constant". The camera constant, K, may be found by calibration with a sample of known lattice parameters. In the electron microscope, however, the powder rings are often slightly elliptical due to lens aberrations
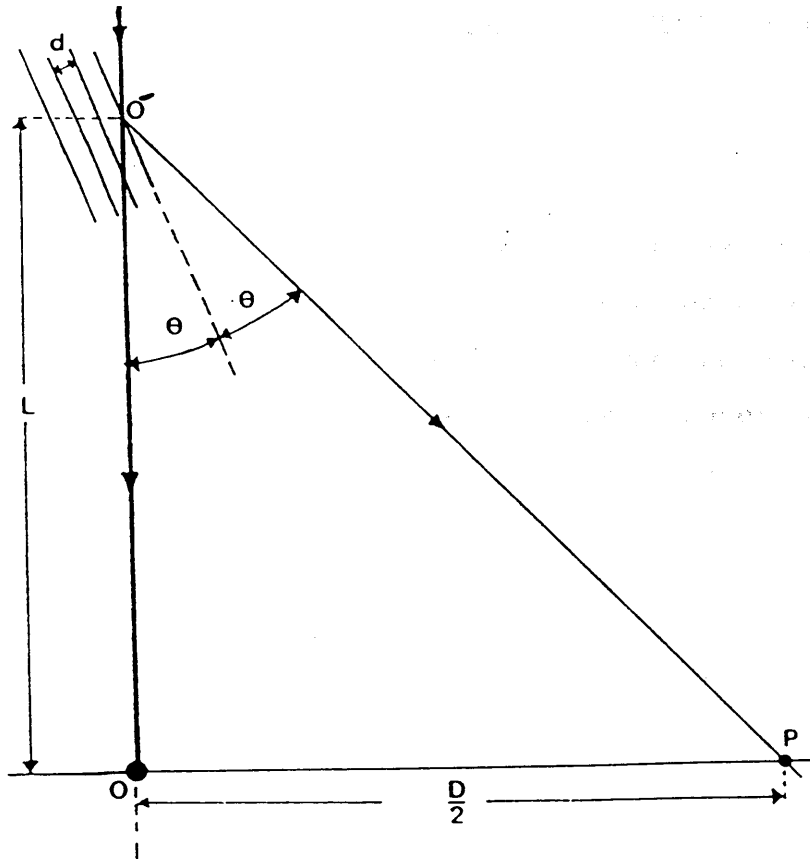
ó:Object lattice planes

p:Diffraction spot

o:Central spot

d:Interplaner spacing

θ:Bragg angle

Figure(6:5).The basic geometry for diffraction. For electron diffraction the angle θ is very small ($<3°$).

and particularly specimen tilt, and L is sensitive to small changes in specimen height, thus the use of an internal standard is therefore strongly recommended.   In the present work, the diffraction pattern of graphite was used as a standard in the calculation of K, which was then used for obtaining lattice spacings for $[Al(Pc)F]_n$ on a KCl substrate.

6!9 : Epitaxial Growth.

An epitaxial layer is one in which an overgrowth is arranged on a substrate so that all of its crystals have the same orientation.   Epitaxy may occur in many systems, for instance certain metals upon alkali halides, silicon upon quartz, alkali halides upon other alkali halides or mica [124].

When the vapour of the overgrowth material meets the face of the substrate, the first stage in the formation of the thin film will be nucleation [125].   This involves the adsorption of sufficient molecules to form a nucleus of s critical size which is stable enough to grow before desorption occurs.   Ueda and Mullin[209] have reported that nucleation tends to occur most readily at a defect in the substrate crystal.   These workers have also established that the formation of stable clusters appears to depend on the rate of deposition, the temperature of the substrate and the energy relationship of the deposition process.

The clusters formed in the nucleation stage may grow by migration of incoming atoms over the surface of the substrate to form islands of overgrowth material which eventually join to form a continuous film.

For epitaxy to be energetically favourable, the lattice spacing of the overgrowth should correspond to a multiple of the lattice spacing of the substrate. The first monolayer of the overgrowth may become distorted to achieve this correspondence, or dislocations may occur between it and the substrate.

The study of epitaxial growth carried out by Frank and van der Merwe [210] showed that the lattice of the overgrowth will deform to fit the substrate, provided the degree of misfit is less than 9%. However, it is still possible to deposit a monolayer at up to 14% misfit, forming a metastable state, provided the temperature is sufficiently low that the overgrowth does not acquire enough activation energy to form dislocations. The degree of misfit was defined [209] as:

$$P_o = \frac{b-a}{a} \qquad \ldots\ldots\ldots\ldots\ldots \text{(6-6)}$$

where a and b are the lattice spacing of substrate and overgrowth respectively. It was also reported [209] that the exact critical misfit would vary according to the substrate and overgrowth materials.

The orientation of the overgrowth also depends on the nature of the substrate and overgrowth. In the case of molecular crystals of planar molecules, the orientation also depends upon the angle which is made by the molecules with their column axis. Crystals may be orientated with their column axes parallel, pendicular, or at an angle to the substrate, depending on the interactions of the crystal with substrate [125].

In the present work, thin films of poly(fluoro-aluminium-phthalocyanine), $[Al(Pc)F]_n$ (Fig. 4:1) on the substrates KCl, silica, and $LiNbO_3$ were prepared and coated with a thin layer of carbon, (see section 2:7 in Chapter 2). The films on KCl substrates were reacted with molybdenum hexafluoride, MoF_6; dibromine, Br_2; diiodine I_2 and trifluoroacetic acid, CF_3COOH. In order to study the structural changes which could be occurring, during these reactions, the films were examined by transmission electron microscopy, before and after the reaction. The films on substrates other than KCl, were not examined because of difficulties in the preparation of specimens suitable for TEM; these difficulties are explained in the experimental section of this chapter.

6:10 : Experimental

Specimens for TEM examination were prepared using the following method:

A carbon coated thin film of $[Al(Pc)F]_n$ on a KCl substrate, was carefully placed in a petri dish containing distilled water. The KCl substrate was dissolved leaving the $[Al(Pc)F]_n$ film supported by the carbon coat floating on the water. Microscope copper and gold grids were used to pick up small pieces of the film which were transferred to a warm oven to dry. Some of these specimens were examined directly by TEM, others were reacted with the oxidants mentioned earlier.

The reactions between the specimens and the oxidants

were carried out using a vacuum system. Therefore an evacuable gas vessel made of Pyrex glass was specially designed for handling the specimens under vacuum, as shown in figure 6:6. All reactions of the $[Al(Pc)F]_n$ specimens with each oxidant were carried out using the same procedure as follows:

The gas vessel was flamed out under vacuum and transferred along with the specimen into the dry box. The vessel was loaded with the specimen inside the box, attached to a vacuum line and re-evacuated. The oxidant (attached to the vacuum line and degassed previously at 77 K) was distilled into the vessel, as vapour, at room temperature. The reaction was allowed to proceed for 5 mins. The vessel was then degassed and left pumping off for approximately 2 h. During the reaction process the original blue colour of the $[Al(Pc)F]_n$ specimen was changed to purple after approximately 2 min. The vessel was opened to the atmosphere and the specimen was loaded into the microscope as quickly as possible and then examined.

The reacted specimens obtained from the above reactions showed different stabilities in the atmosphere, depending on which oxidant was used. For instance, the colour of the specimen formed from the reactions with I_2, MoF_6 and WF_6 changed rapidly from purple to pale green or greenish-yellow respectively when the vessel was opened to the atmosphere. In the case of the specimens obtained from the reactions with Br_2 and CF_3COOH the colour did not change and it was possible to load them into the microscope as purple coloured specimens.

Attempts were made to obtain specimens for TEM
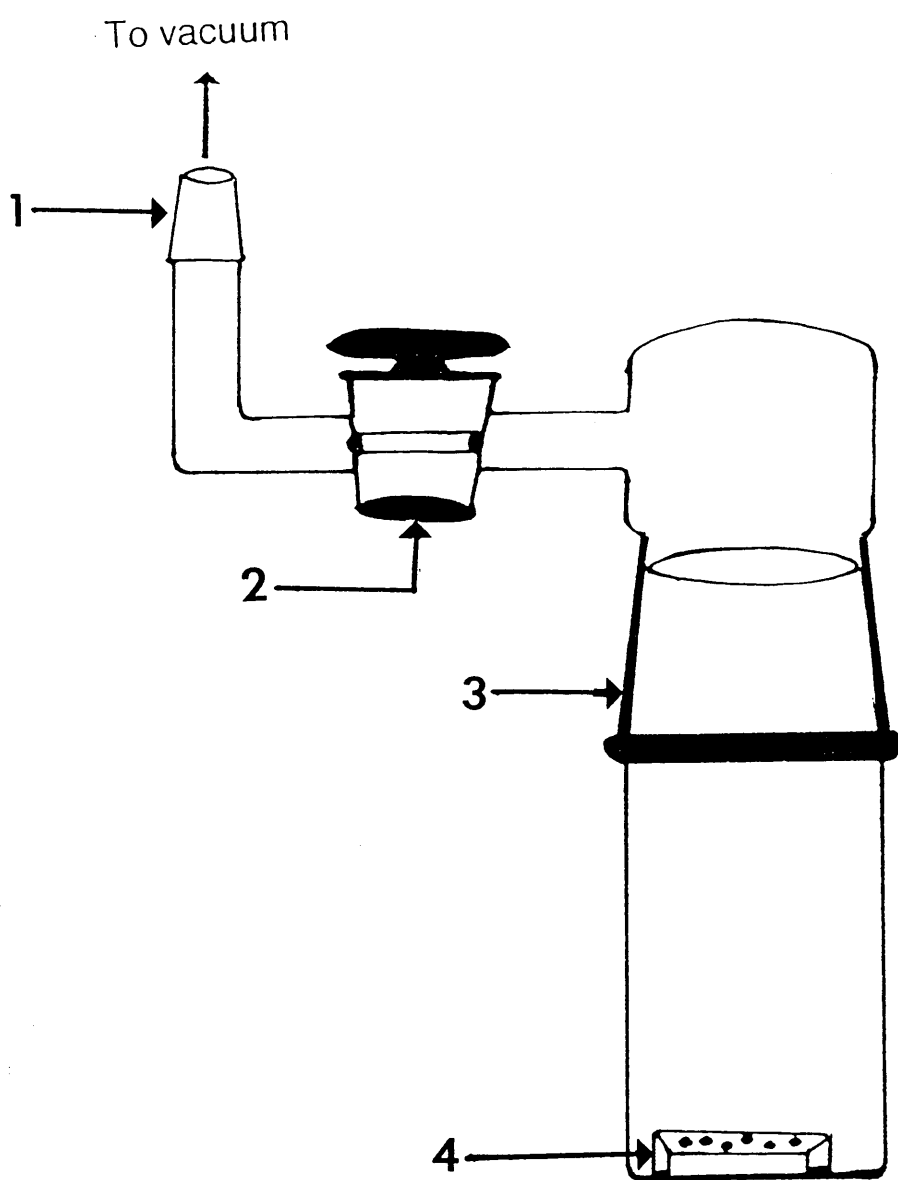
1. B-14 Ground glass cone
2. High vacuum Pyrex tap
3. B-55 socket
4. Copper holder with the specimen on it

Fgure(6:6).An evacuable Pyrex vessel for handling EM
specimen on vacuum line.

examination from the $[Al(Pc)F]_n$ films on silica and $LiNbO_3$ substrates, but this was prevented by the difficulty in peeling the films off these substrates. This problem suggested that some kind of chemical interaction between the substrates (silica and $LiNbO_3$) and the $[Al(Pc)F]_n$ film may have taken place.

6.11 : <u>Results and Discussion</u>.

Previous studies of normally sublimed $[Al(Pc)F]_n$ based on x-ray powder and other techniques [1] have shown that it is made up of acicular crystallites and the molecular chains in these crystallites are parallel to the needle axes of the crystallites. Fryer and Kenney [5] have carried out electron microscopy studies on $[Al(Pc)F]_n$ and $[Si(Pc)O]_n$ polymers sublimed on KCl substrates. In the case of $[Al(Pc)F]_n$, it has been observed that the chains of molecules lie perpendicular to the substrate surface and in parallel with one another. The phthalocyanine rings are held in an eclipsed conformation and are perpendicular to the Al-F back-bones. These workers have concluded that the length of some of the chains in $[Al(Pc)F]_n$ are at least 120-150 $\overset{o}{A}$ long. Since the interring spacing in this polymer is reported as 3.66 $\overset{o}{A}$ [1], these lengths indicate that there are about 33-41 rings in the chains and they have molecular weights of 18000-23000 units. The same workers have provided electron diffraction data for the normally sublimed crystallites on a KCl substrate. This data led to the conclusion that the unit cell of the crystallites is tetragonal with the parameters a=b=13.37 $\overset{o}{A}$ and c=3.6 $\overset{o}{A}$. Diffraction data from the epitaxial crystallites have shown that they have the same

a and b parameters. Thus, it has been concluded that the normal and epitaxial growth processes of $[Al(Pc)F]_n$ on KCl substrate yield the same type of crystal [5].

In the present study, as expected, images of the preparations of sublimed $[Al(Pc)F]_n$ on a KCl substrate ($\simeq$ 493K) showed that the needle axes of some of the crystallites in these preparations are horizontal (i.e. in the film plane) and that the molecules in the crystallites are parallel (plate 1). In several cases, the fringes in the images were discontinuities or breaks (plate 1). Selected area electron diffraction of $[Al(Pc)F]_n$ (plate 1), in which the electron beam was perpendicular to the crystal flake, showed that it consisted of six inner spots, having similar d spacings, which could be indexed in accord with a hexagonal unit cell. The tabulated d-spacings of $[Al(Pc)F]_n$ lattices were calculated from the diffraction pattern in plate 1 using graphite as the standard, and are given in table 6:1. In plate 1, the lattice images appeared like disordered islands. The disorder within the crystalline islands is attributable to the nonpolar, rigid, essentially cylindrical nature of the phthalocyanine molecules. The relatively great uniformity of contrast in the images indicated that the lengths of the molecular chains are fairly constant.

High magnification images of some films showed that they consist of platey crystallites lying horizontally (plate 2). They further showed that the molecules in these crystallites are parallel to each other and are oriented vertically (i.e. perpendicular to the film plane) (plate 2).

Plate 1 - Lattice Images and Electron Diffraction

Pattern of $[Al(Pc)F]_n$.

Magnification = x 80 K

PHOTOGRAPHIC
ENLARGEMENT x 10
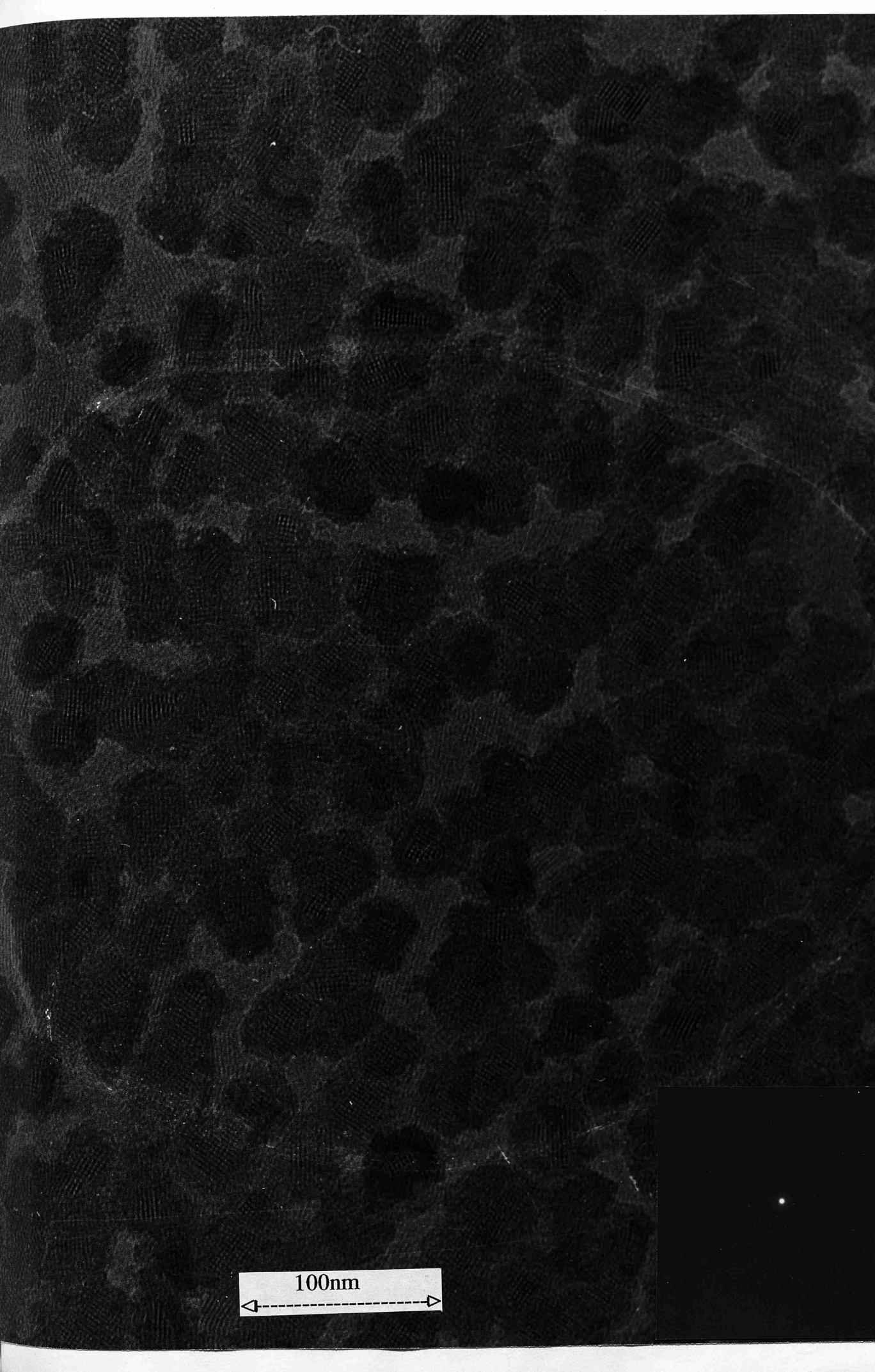
100nm

Table(6:1).Tabulated d-spacing of $[Al(Pc)F]_n$ sublimed
on KCl substrates before and after the
reactions with CF_3COOH and Br_2 vapours.

$[Al(Pc)F]_n$ $d(\overset{o}{A})$	$[Al(Pc)F]_n/CF_3COOH$ $d(\overset{o}{A})$	$[Al(Pc)F]_n/Br_2$ $d(\overset{o}{A})$
10.83	8.96	3.25
4.0	2.28	---
3.17	---	---
1.32	---	---

Plate 2 – Lattice Images and Electron Diffraction

Pattern of $[Al(Pc)F]_n$.

Magnification = x 160 K.
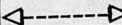
PHOTOGRAPHIC
ENLARGEMENT x7

11.56 Å

10nm
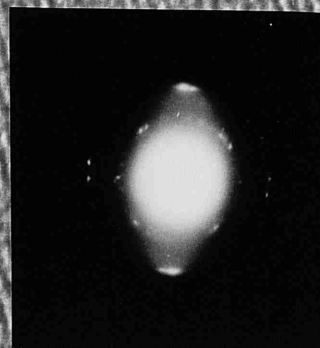
The lattice fringes shown in plate 2, correspond to 11.56 $\overset{o}{A}$ spacing; this value is close to that obtained from the diffraction pattern calculation (table 6:1).

Several micrographs of $[Al(Pc)F]_n$ reacted with CF_3COOH on the copper grids were obtained. In some images the lines between the lattices run parallel to the long axes of the crystals (plate 3). Electron diffraction patterns from the reacted specimen contained spotty and diffused-broad rings (plate 3) indicating a decrease in the crystallinity of $[Al(Pc)F]_n$. The lines of the lattice image in plate 3 are spaced by approximately 10.35 $\overset{o}{A}$.

Images of $[Al(Pc)F]_n$ exposed to bromine vapour on copper grids were shown to be amorphous and in some areas lattice structure could be observed at high magnification (plate 4). The lines in these lattices are spaced by approximately 10.99 $\overset{o}{A}$. Electron diffraction pattern from some images showed a diffused-broad ring (plate 4) which was used in the calculation of the lattice fringes in the image (table 6:1).

The images and diffraction patterns obtained from $[Al(Pc)F]_n$ samples reacted with CF_3COOH and Br_2 were compared with that of the unreacted $[Al(Pc)F]_n$. The comparison showed that the rings in the diffraction pattern were reduced and became broad with the loss of the spot brightness when $[Al(Pc)F]_n$ reacted with CF_3COOH and Br_2. This is possibly attributed to the breaking of the polymer chains and hence a decrease in crystallinity. The traces of lattices appearing in the images of the reacted polymer may correspond to the unreacted crystallites.

Plate 3 - Lattice Images and Electron Diffraction

Pattern of $[Al(Pc)F]_n$ Exposed to

CF_3 COOH Vapour.

Magnification = x 160 K.

PHOTOGRAPHIC

ENLARGEMENT x 7

10.35 Å

50nm

Plate 4 – Lattice Images and Electron Diffraction

Pattern of $[Al(Pc)F]_n$ exposed to

Br_2 vapour.

Magnification = x 160 K.

PHOTOGRAPHIC
ENLARGEMENT x7
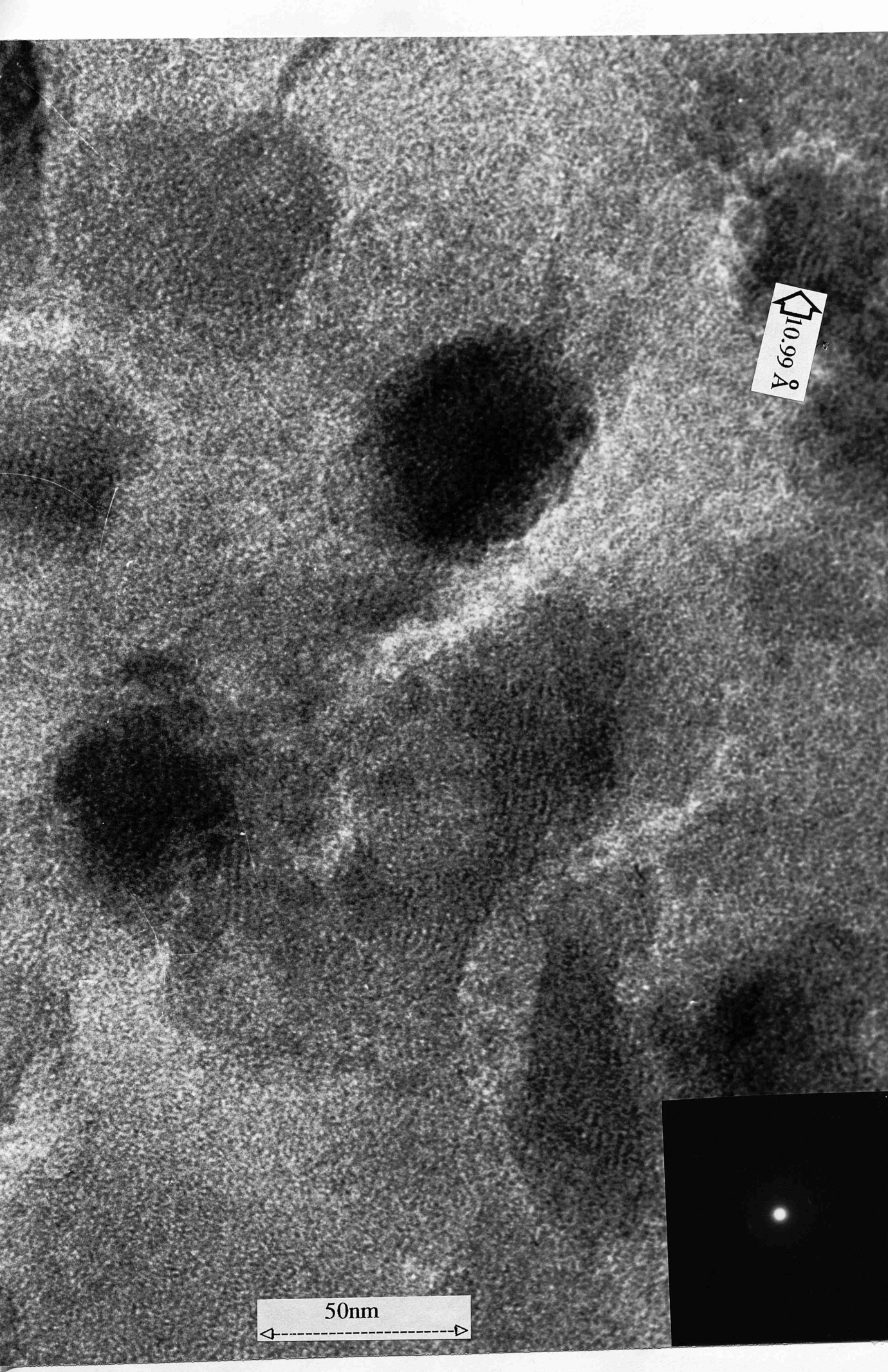
10.99 Å

50nm

In order to collect more structural information about the $|Al(Pc)F|_n$ when it was oxidised with certain oxidants, attempts were made to obtain images of this polymer reacted with MoF_6 and WF_6. These images showed that the lattices of $|Al(Pc)F|_n$ appeared to be completely destroyed. This may not be caused by the insertion of the MoF_6^- and WF_6^- ions but resulting from the hydrolysis of these anions during the preparation of the microscope specimens. This hydrolysis probably caused the lattice to be destroyed. The hydrolysis caused by exposing the specimens to the atmosphere may also have affected the specimen obtained from the reaction with I_2 in which no lattice remained to be observed.

CHAPTER SEVEN

GENERAL REMARKS CONCERNING THE REACTIONS OF

[Al(Pc)F]$_n$ FILMS, CONCLUSIONS AND FUTURE WORK.

7:1 General Remarks

The aim of this chapter is to make a general comparison among the results obtained from the reactions which are described in chapters three, four, five and six.

The products obtained from all reactions had a different colour and different spectra from those of $[Al(Pc)F]_n$. Despite the fact that different reagents, protonic acids and oxidising agents, were used in the reactions with $[Al(Pc)F]_n$, the results from the electronic and vibrational spectra of the products obtained indicate that there are many spectral features in common. In all cases these features are attributed to the formation of a positive charge on the phthalocyanine rings of $[Al(Pc)F]_n$. The rings are protonated and oxidised, respectively, by the acids and the oxidants used but these very different types of reactions apparently produce similar effects on the phthalocyanine rings.

The most common feature in the electronic spectra of all products is the bathochromic shift of the Q band in the visible region. This band also appears to decrease in intensity after the reactions. In most cases the Q band is split into several components. By comparison with other studies involving the oxidation of various metal-phthalocyanine complexes (examples are given in chapters 3-5) these components can be attributed tentatively to the presence of a mixture of reacted and unreacted $[Al(Pc)F]_n$. Therefore, protonation or oxidation are incomplete under the conditions used.

The electronic spectra of the $[Al(Pc)F]_n$ films after exposure to the vapours of the hexafluorides, UF_6, MoF_6 or WF_6, the pentafluorides, PF_5, AsF_5 or IF_5, or the halogens, Cl_2, Br_2, or I_2 are particularly suitable to make comparisons as the reactions were all carried out in a similar fashion under carefully controlled conditions. This comparison indicates that the magnitude of the bathochromic shift of the Q band depends on the identity of the oxidising agent used. It is therefore interesting to enquire whether the magnitude of this shift is related to the oxidising abilities of the oxidants. Estimated enthalpy values for the half-reactions involved (see equations 4-1, 5-1 and 5-2) are tabulated in table 7:1 with the corresponding shift in the Q band observed after each reaction. The oxidants are ranked, from top to bottom in the table, according to their thermodynamic oxidising power as represented by the enthalpy changes $(\Delta H^{\varnothing}{}_f)$ which are associated with the formation of simple anions, reactions being carried out in the gas phase. For the hexafluorides, MF_6 (where M = U, Mo or W), the enthalpy changes associated with the formation of MF_6^- anions (equation 4-1) are equal to the electron affinities (EA) of these oxidants.

It can be seen from table 7:1 that the magnitude of the shift in the Q band is 65 nm when the oxidants are AsF_5, UF_6 and I_2. The magnitude increases to 110-115 nm for WF_6, Cl_2 and Br_2 as the oxidants and to 165-170 nm when MoF_6, PF_5 and IF_5 are used. These observations clearly indicate that there is no simple correlation between the Q band shift and the thermodynamic oxidising ability, although the oxidants can be grouped on the basis of the effect which they have on

Table(7:1).The magnitude of the bathochromic shifts in
the Q band observed in the electronic
spectra of $[Al(Pc)F]_n$ films (on silica)
after reactions with the hexafluorides, UF_6
, MoF_6 or WF_6, with the Pentafluorides, PF_5,
AsF_5 or IF_5 and with the halogens, Cl_2,
Br_2 or I_2 at room temperature.

Oxidising agent[a]	Enthalpy changes[b], $-\Delta H(O_x^-,g)/kJ\ mol^{-1}$	Magnitude of shift[c] in the Q band, $(Q_1-Q_2)/nm$	New spectral absorptions/nm
AsF_5	1012	65	620sh
PF_5	686	165	570
IF_5	---	165	570
UF_6	502	65	555sh
MoF_6	492	170	570
WF_6	338	110	580
Br_2	249.4	115	560sh
Cl_2	246	115	560sh
I_2	227.8	65	520sh

sh=shoulder

a.The oxidant IF_5 is placed below PF_5 because both
oxidants produced an identical shift in the Q band.

b.The numbers in this column represent the enthalpy
changes associated with the formation of anions of
the oxidants.

c.The terms Q_1 and Q_2 represent the λ_{max} of the Q band
before and after the reactions respectively.

the spectrum. Thus, it can be assumed that other factors are important in determining the outcome of a reaction. These may include the size of the oxidant used and the size of the anion formed both in relation to the distance separating the phthalocyanine rings of the $[Al(Pc)F]_n$ polymer. An additional factor is the ability of the oxidant to interact with the polymer prior to oxidation, for instance by adsorption on the surface of the film. All these factors are considered below.

In all cases, insertion of the oxidant molecules (MF_6, AsF_5 or X_2) between the chains or the Pc rings of $[Al(Pc)F]_n$ apparently introduces some disorder into the structure of this polymer. For instance, results from the examination of some samples by TEM indicate that some chains of the polymer are broken and its eclipsed structure is distorted after the reactions (see chapter six). Furthermore, in some cases, evidence for depolymerization of $[Al(Pc)F]_n$ is obtained from the electronic spectra of the products formed from the reactions carried out in the presence of MeCN. These structural changes can be attributed to electronic and steric effects resulting from oxidative intercalation of the $[Al(Pc)F]_n$ polymer. The electronic effect arises from the accumulation of the positive charge on the Pc rings as a result of partial electron transfer from the rings to the oxidant molecules. This leads to polarization of the rings, and consequently, causes disturbance in the organization of their π molecular orbitals. For instance, the relative energy difference between the ground and excited states of these orbitals is changed after the reactions. Steric effects arise when the oxidant molecules attempt to intercalate between the Pc rings by pushing them apart and,

hence, impair the conditions for the π overlap in the phthalocyanine macroring. It has been reported in the literature [101] that in all metal-phthalocyanine complexes this overlap involves the lone pair of electrons on the nitrogen atoms and the π-bond system of the benzene rings in the phthalocyanine molecules (see Figs. 1:6 and 3:10).

As described earlier in chapters four and five, the oxidant vapours (MF_6, AF_5 or X_2) surround the $[Al(Pc)F]_n$ film in the reaction gas cell. The interaction between these molecules and the layers of $[Al(Pc)F]_n$ film on the substrate (e.g. silica or KCl) can be envisaged as follows. Since the $[Al(Pc)F]_n$ polymer is a base (see chapter three) and the oxidants MF_6, AF_5 or X_2 are Lewis acids, it seems likely, that the first step of this interaction involves migration of the oxidising agent molecules to the surface of the film i.e. adsorption. In the second step the adsorbed molecules attempt to migrate into the layers of the film and lie between the polymer chains or perhaps, even between the phthalocyanine rings. However, the ease of diffusion depends on the orientation of the $[Al(Pc)F]_n$ chains on the substrate and it also depends on the size of the oxidant molecule in relation to the 3.66 $\overset{o}{A}$ gap between the Pc rings. During the preparation of a thin film of $[Al(Pc)F]_n$, the crystals may be orientated with their column axis parallel, pendicular or at an angle to the substrate depending on the interactions of these crystals with the substrate used. Using transmission and scanning electron microscopy, Fryer et al [5] have shown that the $[Al(Pc)F]_n$ chains are aligned vertically in a tetragonal array on a KCl substrate, but on mica the chains axis is horizontal. In the present study, attempts to study the structure of $[Al(Pc)F]_n$ films on silica

substrates by transmission electron microscopy have failed due to the experimental difficulties which are described in chapter six. In order to give a better understanding to all speculations made above, a schematic representation of the interaction between the $[Al(Pc)F]_n$ film on silica and the oxidants MF_6, AF_5 and X_2 is given in figure 7:1. Note that the orientation of the $[Al(Pc)F]_n$ chains on silica are considered to be random.

The diameters of MF_6 molecules (M=U, Mo or W) in the vapour state can be estimated using the following equation (equation 7-1):

[length of M-F bond (Å) + van der Waals radius of F atom (Å)]

$$x2 \simeq \text{diameter of } MF_6 \text{ molecule (Å)} \quad ....(7\text{-}1).$$

Molecular diameters estimated are as follows, 6.680 Å for UF_6, 6.320 Å for MoF_6 and 6.336 Å for WF_6 (see chapter four). A similar approach can be also used to estimate the sizes of AF_5 molecules (A=P, As or I) by replacing M-F by A-F in the equation. Thus, the sizes of the molecules PF_5, AsF_5 and IF_5 are found to be 5.85 Å, 6.12 Å and 6.20 Å respectively (see chapter five and Fig. 1:4). The sizes of the halogens, X_2, can be estimated as follows (equation 7-2).

[van der Waals radius of X atom (Å)]x2 $\simeq$ diameter of

$$X_2 \text{ molecule (Å)} \quad ....(7\text{-}2)$$

From the above equation the sizes obtained for Cl_2, Br_2 and I_2 molecules are 3.6 Å, 3.9 Å and 4.3 Å respectively (see chapter five).

These crude estimates indicate that all oxidants, MF_6, AF_5 and X_2, have effective diameters greater than the separation distances, 3.66 Å, between the Pc rings in the $[Al(Pc)F]_n$ polymer. Hence intercalation of these molecules
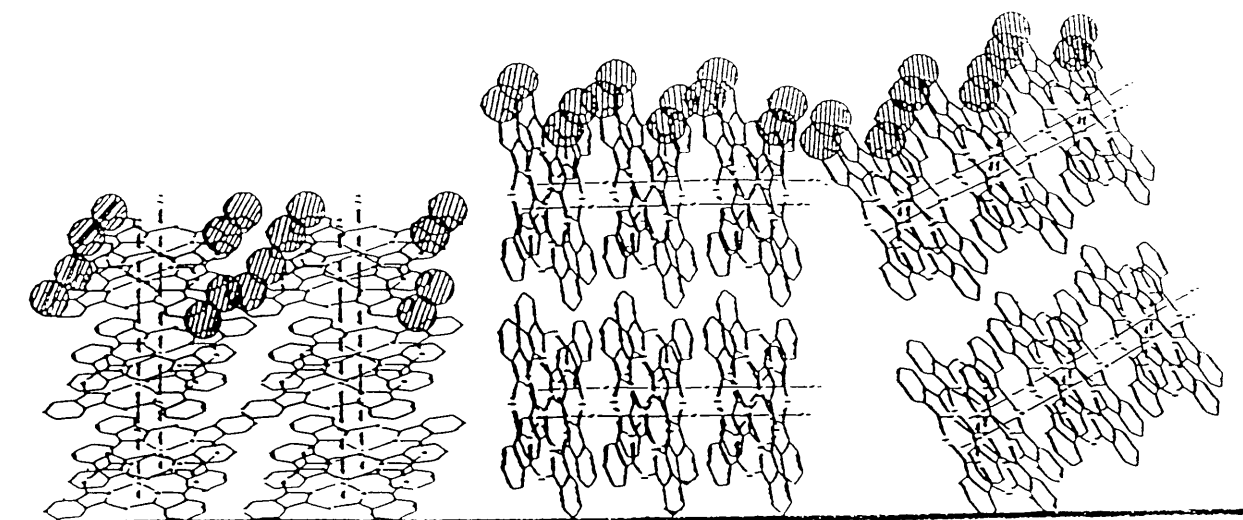
(a)
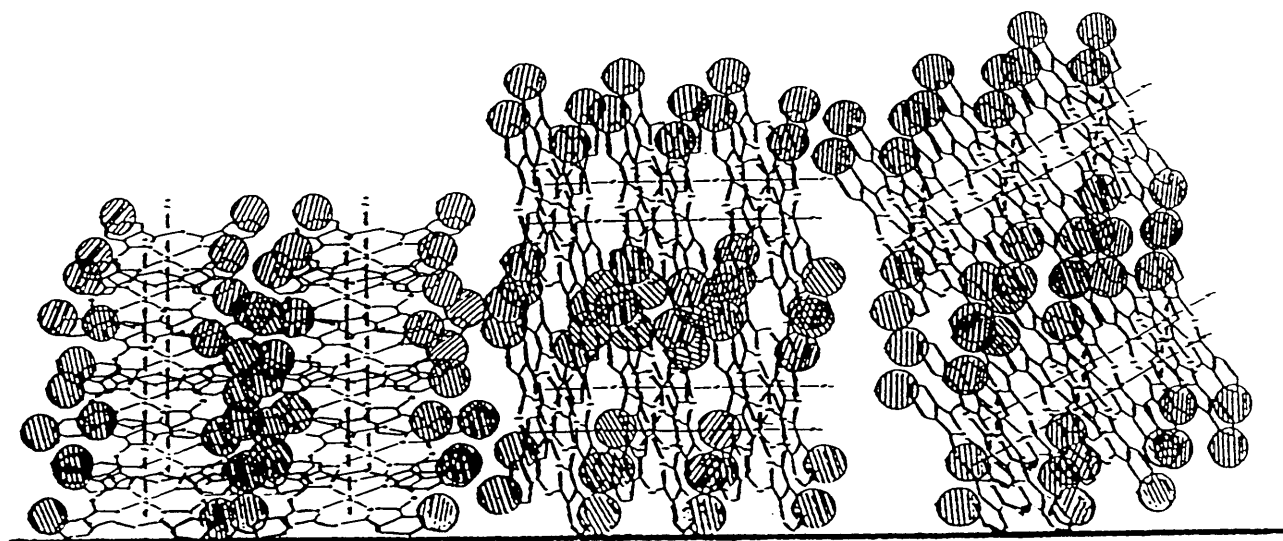
(b)

Figure(7:1).Schematic representation of the interaction
between thin film of [Al(Pc)F]$_n$ on a silica
substrate and the oxidants MF$_6$,AF$_5$ and
X$_2$; the oxidant molecules are adsorbed on
the surface of the film (a) and then they diffuse
into the film (b)·

between the rings is not likely unless it involves distortion of the eclipsed structure of the rings and depolymerization of $[Al(Pc)F]_n$. An exception may be the halogens, X_2, as these molecules are linear and they are, possibly, able to slide between the Pc rings.

7:2 Conclusions and Future Work

In the present study, poly(fluoroaluminium-phthalo-cyanine), $[Al(Pc)F]_n$, was prepared using the preparative method described earlier by Kenney et al [1]. This polymer was partially oxidised by the hexafluorides, UF_6, MoF_6, and WF_6 and by the NO^+ cation at room temperature. The oxidation occurred in the presence of acetonitrile and in the absence of a solvent. In the case of the reactions carried out in the presence of MeCN the mole ratios $[Al(Pc)F]_n:MF_6$ (M=U, Mo or W) and $[Al(Pc)F]_n:NOPF_6$ were estimated to be less than one. The oxidised products were stable _in vacuo_ for several weeks. The MF_6^- and PF_6^- anions were identified by their characteristic absorption bands in the vibrational spectra of the oxidised products. Thin films of $[Al(Pc)F]_n$ with thickness up to approximately 100 nm were prepared by vacuum deposition of the sublimed polymer onto silica, KCl, mica and $LiNbO_3$ substrates. Partial oxidation was also achieved by exposing the films on silica and KCl substrates to the vapours of the hexafluorides, UF_6, MoF_6 and WF_6, the pentafluorides PF_5, AsF_5 and IF_5 and the halogens Cl_2, Br_2 and I_2 at room temperature. In all cases the colour of $[Al(Pc)F]_n$ changed rapidly from blue to purple. The $[Al(Pc)F]_n$ polymer was allowed to react with the strong protonic acids, CF_3SO_3H, H_2SO_4 (various concentrations) and CF_3COOH to give protonated products. The protonation presumably involved the bridging nitrogen atoms of the phthalocyanine rings in the polymer. These results have indicated that the $[Al(Pc)F]_n$ polymer is a base. Unlike pristine $[Al(Pc)F]_n$, the oxidised or protonated products were easily dissolved in acetonitrile and formed dark purple solutions. Results from the examination of all products by

electronic and vibrational spectroscopy and by transmission electron microscopy indicated that both oxidation and protonation reactions induced some changes into the electronic system and structure of the $[Al(Pc)F]_n$ polymer. In some cases, evidence for depolymerization of $[Al(Pc)F]_n$ was obtained from the electronic spectra of the products and from TEM examination. Finally, the present study has demonstrated that the ionization potential of $[Al(Pc)F]_n$ and the electron affinity of the oxidising agent are not the only terms affecting the oxidation and this polymer can be doped by a great variety of oxidants using carefully controlled reaction conditions.

In future work, further electron microscopy must be carried out on the oxidised and protonated products in order to obtain definite results about their lattice structures. Infrared and Raman spectra should be recorded for the products obtained from the reactions with the pentafluorides or the halogens used in the present study in order to identify the nature of the anions formed. It would also prove beneficial to carry out electrical conductivity measurements on the oxidised products.

References.

1. J.P. Linsky, T.R. Paul, R.S. Nohr and M.E. Kenney,
    Inorg. Chem., 19, 1980, 3131.

2. P. Brant. D.C. Weber, S.G. Haupt, R.S. Nohr and K.J. Wynne,
    J. Chem. Soc. Dalton Trans., 1985, 269.

3. R.S. Nohr, P.M. Kuznesof, K.J. Wynne, M.E. Kenney and
    P.G. Siebenman, J.Am. Chem. Soc., 103, 1981, 4371.

4. D. Djurado, A. Hamwi, C. Fabre, D. Avigant and J.C. Cousseins,
    Mat. Res . Bull., 22, 1987, 911.

5. J.R. Fryer and M.E. Kenney, Macromolecules, 21, 1988, 259.

6. K.M. Mackay and R.A. Mackay "Introduction to Modern
    Inorganic Chemistry", International Textbook Co. Ltd.,
    Glasgow, 3rd Edition, 1981.

7. F.A. Cotton and G. Wilkinson, "Advanced Inorganic Chemistry",
    John Wiley & Sons, Inc., New York, 5th Edition, 1988.

8. H.J. Emeléus and A.G. Sharpe, "Modern Aspects of Inorganic
    Chemistry", Routledge & Kegan Paul, London, 4th Edition,
    1973.

9. J.H. Simons, J. Fluorine Chem., 32, 1986, 8.

10. R.B. Heslop and K. Jones, "Inorganic Chemistry, A Guide to
    Advanced Study", Elsevier Scientific Publishing Co.,
    Amsterdam, 1976.

11. D. Price, B. Iddon, and B.J. Wakefield, "Bromine Compounds, Chemistry and Applications", Elsevier Science Publishing Co., Inc., 1988.

12. Z.E. Jolles, "Bromine and Its Compounds", Ernest Benn Ltd., 1966.

13. A.J. Downs and C.J. Adams, "The Chemistry of Chlorine, Bromine, Iodine and Astatine", Pergamon Press, Oxford, 1975.

14. M. Stacy, J.C. Tatlow and A.G. Sharpe, "Advances in Fluorine Chemistry", Butterworth & Co Ltd., London, Vol. 2, 1961.

15. A.J. Rudge, "The Manufacture and Use of Fluorine and Its Compounds", Oxford University Press, 1962.

16. K.O. Christe, Inorg. Chem., 25, 1986, 3723.

17. J.S. Sconce, "Chlorine, Its Manufacture, Properties and Uses", Chapman & Hall Ltd., London 1962.

18. F.A. Cotton, G. Wilkinson and P.L. Gaus, "Basic Inorganic Chemistry", John Wiley & Sons, Inc., Canada, 2nd edition, 1987.

19. A.G. Sharpe, "Inorganic Chemistry", Longman Group Ltd., England, 2nd edition, 1986.

20. K.O. Christe, Inorg. Chem., 11, 1972, 1220.

21. J.C. Tatlow, R.D. Peacock and H.H. Hyman, "Advances in Fluorine Chemistry", Butterworth & Co. Ltd., London, vol. 7, 1973.

22. J.L. Russell and A.W. Jack , J. Inorg. Nucl. Chem.,
    Suppl., 1976, 81.

23. A.J. Edwards, Adv. Inorg. Chem. Radiochem., $\underline{27}$, 1983, 83.

24. V. Gutmann, "Halogen Chemistry", Academic Press, London,
    vol. 3, 1967.

25. J.H. Canterford and R. Colton, "Halides of the Transition
    Metals", Wiley Interscience, London 1968.

26. T.A. O'Donnell, J. Chem. Soc., 1956, 4681.

27. J.J. Katz, G.J. Seaborg and L.R. Morss, "Chemistry of the
    Actinide Elements", Chapman and Hall London, 1986.

28. J.H. Canterford, R. Colton and T.A. O'Donnell, Rev.
    Pure and Appl. Chem., $\underline{17}$, 1967, 123.

29. N. Bartlett, Angew. Chem., Int. Ed. Engl., $\underline{7}$, 1968, 433.

30. J.H. Levy, J.C. Taylor and A.B. Waugh, J. Fluorine
    Chem., $\underline{23}$, 1983, 29.

31. R.N. Compton, P.W. Reinhardt and C.D. Copper, J. Chem.
    Phys., $\underline{68}$, 1978, 2023.

32. J. Burgess, I.H. Haigh, R.D. Peacock and D. Taylor,
    J. Chem. Soc., Dalton Trans., 1974, 1064.

33. H. Dispert and K. Lacmann, Chem. Phys. Letters, $\underline{45}$,
    1977, 311.

34. B.P. Mathur, E.W. Rothe and G.P. Reck, J. Chem. Phys.,
    $\underline{67}$, 1977, 377.

35.   J.L. Beauchamp, J. Chem. Phys., $\underline{64}$, 1976, 929.

36.   L.N. Sidorov, A. Ya. Borshehevsky, E.B. Rundy and

       V.D. Butsky, Chem. Phys., $\underline{71}$, 1982, 145.

37.   A.T. Paytenko, A.V. Gusarov and L.N. Gorokhov, Russ.

       J. Phys. Chem., $\underline{58}$, 1984, 1.

38.   N. Bartlett, E.M. McCarron and B.W. McQuillan, Synth.

       Met., $\underline{1}$, 1980, 221.

39.   P.M. George and J.L. Beauchamp, Chem. Phys., $\underline{36}$,

       1979, 345.

40.   N. Bartlett and B.W. McQuillan in "Intercalation Chemistry",

       M.S. Whittingham and A.J. Jacobson (Eds), Academic Press,

       New York, 1982, P.19.

41.   J.M. Winfield, J. Fluorine Chem., $\underline{33}$, 1986, 159.

42.   R.C. Burns and T.A. O'Donnell, J. Inorg. Nucl. Chem.,

       $\underline{42}$, 1980, 1285.

43.   C. Keller, Chem. Ztg., $\underline{106}$, 1982, 137.

44.   R.C. Burns, T.A. O'Donnell and C.H. Randall, J. Inorg.

       Nucl. Chem., $\underline{43}$, 1981, 1231.

45.   D. Vaknik, D. Davidov and H. Selig, J. Fluorine Chem., $\underline{32}$,

       1986, 345.

46.   T.E. Mallouk, G.L. Rosenthal, G. Muller, R. Brusasco and

       N. Bartlett, Inorg. Chem., $\underline{23}$, 1984, 3167.

47.   A. Prescott, D.W.A.Sharp and J.M. Winfield, J. Chem.

       Soc., Dalton Trans., 1975, 936.

48.   J.A. Berry, R.T. Poole, A. Prescott, D.W.A. Sharp and
      J.M. Winfield, J. Fluorine Chem., 10, 1977, 247.

49.   G.M. Anderson, I.F. Fraser and J.M. Winfield, J.
      Fluorine Chem., 23, 1983, 403.

50.   G.M. Anderson, J. Iqbal, D.W.A.Sharp, J.M. Winfield,
      J.H. Cameron and A.G. McLeod, J. Fluorine Chem., 24,
      1984, 303.

51.   C.J. Barbour, J.H. Cameron and J.M. Winfield, J. Chem.
      Soc., Dalton Trans, 1980, 2001.

52.   G.B. Hargreaves and R.D. Peacock, J. Chem. Soc., 1957,
      4212, ibid, 1958, 3776.

53.   J.R. Geichman, E.A. Smith, S.S. Trond and R.R. Ogle,
      Inorg. Chem., 1, 1962, 661.

54.   N. Bartlett, S.P. Beaton and N. K. Jha, J. Chem. Soc. Chem.
      Commun., 1966, 168.

55.   J. Shamir and J.G. Malm, J. Inorg. Nucl. Chem.,
      Supp. 1., 1976, 107.

56.   J. Emsley and D. Hall, "The Chemistry of Phosphorus",
      Harpe & Row Ltd., London, 1976, P.49.

57.   J.M.S. Henis and C.A. Mabie, J. Chem. Phys., 53,
      1970, 2999.

58.   S. Brownstein, Can. J. Chem., 47, 1969, 605.

59.   T.C. Rhyne and J.G. Dillard, Inorg. Chem., 10, 1971, 730.

60.   F.M. Page and G.C. Goode, "Negative Ions and the Magnetron",
      Wiley Interscience, New York, 1969.

61.   R. Bohra and H.W. Roesky, Adv. Inorg. Chem. Radiochem.,
        28, 1984, 242.

62.   A.F. Wells, "Structural Inorganic Chemistry", Oxford
        University Press, 5th edition, 1984, P. 391.

63.   E.L. Muetterties, T.A. Bither, M.W. Farlow and
        D.D. Coffman, J. Inorg. Nucl. Chem., 16, 1960, 52.

64.   D.M. Byler and D.F. Shriver, Inorg. Chem., 13,
        1974, 2697.

65.   A.C. Baxter, J.H. Cameron, A. McAuley, F.M. McLaren
        and J.M. Winfield, J. Fluorine Chem., 10, 1977, 289.

66.   F.N. Tebbe and E.L. Muetterties, Inorg. Chem., 6,
        1967, 129.

67.   W. Wicker, A.R. Grimmer and L. Kolditz, Z. Chemie, 7,
        1967, 434.

68.   L. Lunazzi and S. Brownstein, J. Magn. Res., 1, 1969,
        119; W.S. Sheldrick, J. Chem. Soc., 1974, 1402.

69.   W. Storzer, D. Schomburg, G.V. Roschenthaler and
        R. Schmutzler, Chem. Ber., 116, 1983, 367.

70.   R.J. Gillespie and A. Whitla, Can. J. Chem., 48, 1970, 657.

71.   N. Bartlett and P.L. Robinson, J. Chem. Soc., 1961, 3417.

72.   W.K.R. Musgrave, Adv. Fluorine Chem., 1, 1960, 1.

73.   J.E. Roberts and G.H. Cady, J. Am. Chem. Soc., 82, 1960,
        354.

74.   G. Oates, J.M. Winfield and O.R. Chambers, J. Chem. Soc.
        Dalton Trans., 1974, 1380.

75.   T.A. O'Donnell, Chem. Soc. Rev., 16, 1987, 1.

76.   D.M. Morrison and R.C. Thompson, Can. J. Chem., 56,
       1978, 985.

77.   E.M. McCarron and N. Bartlett, J. Chem. Soc. Chem. Commun.,
       1980, 404.

78.   T.E. Thompson, E. M. McCarron and N. Bartlett, Synth.
       Met., 3, 1981, 255.

79.   S. Karunanithy and F. Aubke, J. Fluorine Chem., 25,
       1984, 337.

80.   B.J. Hathaway and A.E. Underhill, J. Chem. Soc., 1961
       3091.

81,   B.J. Hathaway, D.G. Holah and A.E. Underhill, J. Chem.
       Soc., 1962, 2444.

82.   S. Arrhenius, Z. Phys. Chem., 1, 1887, 631.

83.   N.J. Brønsted, Rec. Trav. Chim., 42, 1923, 718.

84.   T.M. Lowry, Chem. Ind., 42, 1923, 43.

85.   E.C. Franklin, J. Am. Chem. Soc., 27, 1905, 820.

86.   G.N. Lewis, "Valence and the Structure of Atoms and
       Molecules", The Chemical Catalog. Co., New York, 1923.

87.   G.N. Lewis, J. Am. Chem. Soc., 38, 1916, 762.

88.   I. Langmuir, J. Am. Chem. Soc., 42, 1920, 274.

89.   A.P. Zuur and W.L. Groeneveld, Rec. Trav. Chim., 86,
       1967, 1089.

90.   D.K. Sanyal, D.W.A. Sharp and J.M. Winfield, J. Fluorine
       Chem., 19, 1981/82, 55.

91.   K.J. Saunders, "Organic Polymer Chemistry", Chapman
       and Hall, London, 1973, p. 57.

92.   R.W. Dyson, "Special Polymers", Chapman and Hall,
       New York, 1987, p.18.

93.   J. Ferraris, D.O. Cowan, V.V. Walatka and J.H. Perlstein
       J. Am. Chem. Soc., 95, 1973, 948.

94.   J.H. Peristein, Angew. Chem. Int. Ed. Engl., 16, 1977,
       519.

95.   T.A. Skotheim, "Handbook of Conductive Polymers",
       Marcel Dekker, New York, vol. 1 and vol 2, 1986.

96.   A.O. Patil, A.J. Heeger and F. Wudl, "Optical Properties
       of Conductive Polymers", Chem. Rev, 88, 1988, 183.

97.   M.G. Kanatzidis, "Special Report on Conductive Polymers",
       Chem. Eng. News, 3, 1990, 36.

98.   A.G. MacDiarmid and A. Epstein, J. Chem. Soc. Faraday
       Trans, 5, 1989, 1.

99.   R.P. Linstead, J. Chem. Soc., 1, 1934, 1016.

100.   E.A. Lawton, J. Phys. Chem., 62, 1958, 384.

101.   B.D. Berezin, "Coordination Compounds of Porphyrins and
       Phthalocyanines", John Wiley & Sons Ltd., 1981.

102.   R.P. Linstead and J.M. Robertson, J. Chem. Soc.,
       1936, 1195.

103.   J.M. Robertson and I. Woodward, J. Chem. Soc., 1937, 219.

104.   J.M. Robertson and I. Woodward, J. Chem. Soc., 1940, 36.

105. H.J. Emeléus and A.G. Sharpe, Inorg. Chem. Radiochem, 7, 1965, 30.

106. B.D. Berezin and A.N. Shlyapova, Izv. Vuzov. Khim. Khim. Tekhnol., 12, 1969, 1641.

107. B.D. Berezin and A.N. Shlyapova, Vysokomol. Soed., A-15, 1973, 1675.

108. A.S. Alkopov, T.N. Lomova and B.D. Berezin, Koord. Khimiya, 8, 1976, 985.

109. M. Futamata, S. Higuchi and S. Takahashi, Synth. Met., 30, 1989, 39.

110. J.W. Lin and L.P. Dudek, J. Polym. Sci. Polym. Chem. Ed., 23, 1985, 1589; T.M. Keller and R.F. Gatz, Polym. Commun., 28, 1987, 334.

111. S. Venkatachalam, K.V.C. Rao and P.T. Manoharan, Synth. Met., 26, 1988, 237.

112. M. Dugay and C. Maleysson, Synth. Met., 21, 1987, 255.

113. W.A. Orr and S.C. Dahlberg, J. Am. Chem. Soc., 101, 1979 2875.

114. K.F. Schoch, Jr., B.R. Kundalkar and T.J. Marks, J. Am. Chem. Soc., 101, 1979, 7071.

115. D. Djurado, A. Hamwi and J.C. Cousseins, H. Hidar, C. Fabre and G. Berthet, Synth. Met., 11, 1985, 109.

116. D. Djurado, A. Hamwi, C. Fabre D. Avignant and J.C. Cousseins Synth Met., 16, 1986, 227.

117.   D. Nichols , "Complexes and First Row Transition Elements",

        The Macmillan Press Ltd., London, 1974.

118.   A.B.P. Lever, "Inorganic Electronic Spectroscopy",

        Elsevier, Oxford 1984.

119.   E.A.V. Ebsworth, D.W.H. Rankin and S. Cradock, "Structural

        Methods in Inorganic Chemistry", Blackwell Scientific

        Publications, Oxford, 1987.

120.   H. H. Bauer, G.D. Christian and J.E. O'Reilly, "Instrumental

        Analysis", Allyn and Bacon Inc. London, 1978.

121.   F.A. Cotton, "Chemical Applications of Group Theory",

        Wiley Interscience, 2nd edition, London 1970.

122.   P.K. Harris, "Nuclear Magnetic Resonance Spectroscopy",

        Pitman, London 1983.

123.   J. Mason, "Multinuclear NMR", Plenum Press, New York, 1987.

124.   J.W. Matthews "Epitaxial Growth", Academic Press Inc.,

        New York, Part A and B, 1975.

125.   J.R. Fryer, "The Chemical Applications of Transmission

        Electron Microscopy", Academic Press Inc., London, 1979.

126.   F.H. Moser and A.L. Thomas, "The Phthalocyanines", C.R.C.

        Press, Inc., Florida, vol 1. 1983.

127.   A.M.A. Foad, M.Sc. Thesis, Glasgow University, 1988.

128.   J.M. Winfield, J. Fluorine Chemistry, $\underline{25}$, 1984, 91.

129.   M. Walter and L. Ramalay, Analyt. Chem., $\underline{45}$, 1973, 165.

130.   J.E. Huheey, "Inorganic Chemistry", Harper International, 3rd Edition, London, 1983, p.337.

131.   A.J. Hewitt, J.H. Holloway, R.D. Peacock, J.B. Raynor and I.L. Wilson, J. Chem. Soc., Dalton Trans., 1976, 579.

132.   D.L. Ledson and M.V. Twigg, Inorg. Chem. Acta, 13, 1975, 43.

133.   B.D. Berezin, L.P. Shormanova and R.I. Feldman, Zh. Neorg. Khim., 19, 1974, 1833.

134.   K. Bernauer and S. Fallab, Helv. Chem. Acta, 44, 1961 1287.

135.   A.B.P. Lever, M.R. Hempstead, C.C. Lezonoff, W. Liu, M. Melnik, W.A. Nevin and P. Seymour, Pure and Applied Chem. 58, 1986, 1476.

136.   D.R. Lide, "Handbook of Chemistry and Physics", CRC Press INC., 71st Edition, 1990-1991, p.6.

137.   J.J. Lagowski, "The Chemistry of Non-aqueous Solvents", Academic Press, INC., New York, vol. VB, 1978, p.4.

138.   M. Gouterman, J. Molecular Spectroscopy, 6, 1961, 138.

139.   T. Nyokong, Z. Gasyana and M.J. Stillman, Inorg. Chem., 26, 1987, 1087.

140.   J.J. Lagowski, "The Chemistry of Non-aqueous Solvents", Academic Press, INC, New York, vol. VA, 1978, p.64.

141.   K. Nakamoto, "Infrared Spectra of Inorganic and Coordination Compounds", John Wiley & Sons, INC, New York, 2nd Edition, 1970.

142.   E. Ough, Z. Gasyna and M.J. Stillman, Inorg. Chem., $\underline{30}$,

        1991, 2301.

143.   R.G. Plevey, R.W. Rendell and J.C. Tatlow, J. Fluorine

        Chem., $\underline{21}$, 1982, 159.

144.   V.V. Bardin, A.A. Avramenko, G.G. Furin, G.G. Yakobson,

        V.A. Krasilinkov, P.P. Tushin and A.I. Karelin,

        J. Fluorine Chem., $\underline{28}$, 1985, 37.

145.   F. Mathey and J. Benson, Tetrahedron, $\underline{27}$, 1971, 3965.

146.   A. Haas and Th. Maciej, J. Fluorine Chem., $\underline{20}$, 1982, 581.

147.   G.A. Olah and J. Welch, J. Am. Chem. Soc., $\underline{100}$, 1978,

        5396.

148.   D. Djurado, C.F. Fabre, A. Hamwi and J. Cousseins,

        Synth. Met., $\underline{22}$, 1987, 93.

149.   G.M. Anderson and J.M. Winfield, J. Chem. Soc., Dalton

        Trans, 1986, 337.

150.   A. Melson, "Coordination Chemistry of Macrocyclic Compounds",

        Plenum Press, New York, 1979, p.466

151.   A.B.P. Lever, Adv. Inorg. Chem. Radiochem, $\underline{7}$, 1965, 24.

152.   A.J. McHugh, M. Gouterman and C. Weiss, Theor. Chem. Acta.,

        $\underline{24}$, 1972, 346.

153.   M. Gouterman, "The Porphyrins", Academic Press, New York,

        $\underline{3}$, 1987, p.1.

154.   J.E. Bloor, J. Schlabitz, C.C. Welden and A. Dermerdache,

        Can J. Chem., $\underline{42}$, 1964, 2202.

155.   H.F. Shurvell and L. Pinzuti, Can. J. Chem., 44, 1966, 125.

156.   C.W. Dirk, T. Inabe, K.F. Schoch, Jr., and T.J. Marks, J. Am. Chem. Soc., 105, 1983, 1539.

157.   M. Gouterman, G.H. Wagniere and L.C. Snyder, Jr., J. Mol. Spectrosc., 11, 1963, 2.

158.   C. Weiss, H. Kobayashi and M. Gouterman, J. Mol. Spectrosc., 16, 1965, 415.

159.   P.C. Minor, M. Gouterman and A.B. Lever, Inorg. Chem., 24, 1985, 1894.

160.   E. Ough, T. Nyokong, K.A.M. Creber and M.J. Stillman, Inorg. Chem., 27, 1988, 2724.

161.   G.M. Begun and A.C. Rutenberg, Inorg. Chem., 6, 1967, 2212.

162.   A.G. Vinogradskii, Russian J. Phys. Chem., 57, 1983, 1747.

163.   A.G. Vinogradskii and A.N. Sidorov, Teor. Eksper. Khim., 18, 1982, 118.

164.   J.A. Berry, R.T. Poole, A. Prescott, D.W.A. Sharp and J.M. Winfield, J. Chem. Soc., Dalton Trans., 1976, 272.

165.   M.J. Reisfeld and G.A. Crosby, Inorg. Chem., 14, 1965, 65.

166.   A. Rager, B. Gompf, L. Durselen, H. Mockert, D. Schmeisser and W. Gopel, J. Mol. Electro., 5, 1985, 227.

167.   T.G. Burke, D.F. Smith and A.H. Nielsen, J. Chem. Phys., 20, 1952, 447.

168. K. Fukuda, J. Chem. Phys., 42, 1965, 521.

169. K.J. Wynne and R.S. Nohr, Mol. Cryst. Liq. Cryst., 81, 1982, 243.

170. E.V. Skokan, I.D. Sorokin, M.I. Nikitin, N.S. Chiligarov and L.N. Sidorov, Russ. J. Phys. Chem., 57, 1983, 1745.

171. B.K. Annis and S. Datz., J. Chem. Phys., 66, 1977, 4468.

172. P.M. George and J.L. Beauchamp, Chem. Phys., 36, 1979, 345.

173. A. Jobert, Ph. Touzain and L. Bonnetain, Carbon, 19, 1981, 193.

174. S.W. Pelletier and N.V. Mody, J. Am. Chem. Soc., 100, 1977, 286.

175. A.G. Vinogradskii, Russian J. Phys. Chem., 57, 1983, 11.

176. C.K. Chiang, C.R. Fincher, Jr., Y.W. Park, A.J. Heeger, E.J. Loun, S.C. Gau and A.G. MacDiarmid, Phys. Rev. Lett., 39, 1977, 1098.

177. I.F. Myers, G.W.R. Canham and A.B.P. Lever, Inorg. Chem., 14, 1975, 461.

178. D.A. Johnson, "Some Thermodynamic Aspects of Inorganic Chemistry", Cambridge University Press, Cambridge, 2nd Edition, 1982, p.51.

179. F.A. Jenkins and H.E. White, "Fundamentals of Optics", McGraw-Hill, Tokyo, 4th edition, 1981.

180. L. De Broglie, Phil. Mag., 47, 1924, 446.

181. C. Davison and L.H. Germer, Phys. Rev., 30, 1927, 705; G.P. Thomson and A. Reid, Nature (London), 119, 1927, 890.

182.   M. Knoll and E. Ruska, Ann. der Physik, 12, 1932, 607.

183.   H. Busch, Ann. Phys. (Leipzig), 81, 1926, 974;

       Arch. Elektrotech. (Berlin), 18, 1927,583.

184.   V.E. Cosslett, R.A. Camps, W.O. Saxton, D.J. Smith,

       W.C. Nixon, H. Ahmed, C.J.D. Catto, J.R.A. Cleaver,

       K.C.A. Tims, P.W. Turner and P.M. Ross, Nature (London),

       281, 1979, 49.

185.   J.R. Fryer, Mol. Cryst. Liq. Cryst., 96, 1983. 275.

186.   L.D. Marks and D.J. Smith, J. Microsc. (Oxford), 130, 1983,

       249.

187.   J.R. Fryer and D.J. Smith, J. Microsc. (Oxford), 141, 1984,

       3.

188.   T. Mulvey, Proc. Roy. Microsc. Soc., 2, 1967, 201.

189.   E. Ruska, Microsc. Acta., Suppl., 5, 1980.

190.   P. Goodman, "Fifty Years of Electron Diffraction",

       Reidel, Dordrech, 1981.

191.   P.A. Hawkes, "Electron Optics and the Electron Microscope",

       Academic Press, New York, 1985.

192.   J.M. Cowley, "Introduction to Analytical Electron Microscopy",

       Plenum Press, New York, 1979, p1.

193.   C.E. Hall, "Introduction to Electron Microscopy", McGraw-

       Hill, New York, 2nd edition, 1966.

194.   R.J. Wolfe and D.C. Joy, Electron Microsc. Anal., Inst.

       Phys. Conf. Ser. No. 10, London, 1971, p.34.

195. H. Ahmed, Electron Microsc. Anal. Inst. Phys. Conf., London
     Ser. No. 10, 1971, p.30.

196. D.B. Williams, "Practical Analytical Electron Microscopy
     in Materials Science", Verlag Chemie International,
     Deerfield Beach, 1984.

197. F. Thon, Z. Naturforsch, 21a, 1966, 476.

198. M.E. Barnett, J. Microsc., 102, 1974, 1.

199. F. Holland, J.R. Fryer and T. Baird, Electron Microsc.
     Anal. Inst. Phys. Conf., London, Ser. No. 68, 1983, p.19.

200. R. Sharma, J. Barry and L. Eyring, Ultramicroscopy, 23,
     1987, 453.

201. F. Seitz and J.S. Koehler, Solid State Phys., 2, 1956,
     303.

202. L.W. Hobbs, Ultramicroscopy, 23, 1987, 339.

203. C.A. English and J.A. Venables, Electron Microsc. Anal.
     Inst. Phys. Conf., London, Ser. No. 10, 1971, p.40.

204. R.C. Williams and H.W. Fisher, J. Mol. Biol., 52, 1970, 121.

205. J.R. Fryer, 9th International Congress on Electron Microscopy
     Toronto, vol.1, 1978.

206. P.W. Atkins, "Physical Chemistry", Oxford 4th edition,
     1988.

207. H. Boersch, Annalen der Physik, 27, 1936, 75.

208. J.B. Le Poole, Phillips Tech. Rdsch., 9, 1947, 33.

209. R. Ueda and J.B. Mullin, "Crystal Growth and Characterisation",
     Proceedings of the I.S.S.C.G., 2nd Spring School, Japan, 1974.

210. F.C. Frank and J.H. van der Merwe, Proc.Roy.Soc., A198, 1949,
     276.